



Università degli Studi di Ferrara

DOTTORATO DI RICERCA IN "Farmacologia E Oncologia Molecolare"

CICLO XXVI

COORDINATORE Prof. Antonio Cuneo

Studies on Type- 1 Insulin Like Growth Factor and on Reduced Folate in Cancer

Settore Scientifico Disciplinare Bio/14

Dottorando
Dott. [Ali Edris](#)

Tutore
Prof. [Michele Rubini](#)

(firma)

(firma)

Anni 2013/2014

Part 1:

Phosphorylation of IGF1R as predictive biomarker for response to therapy in colorectal cancer.

Abstract(English)

Insulin-like growth factor-1 receptor (IGF-1R) plays a critical role in regulating cancer cell proliferation, survival and metastasis in the transformed cell. Additionally, chemo-resistance acquisition, a cumbersome problem in advanced colorectal cancer (ACRC) patients. The mechanism of resistance acquisition is found to be attributed to a p-IGF-1R membrane-to-nuclear internalization that cannot be overcome with existing IGF-1R inhibitors. In the present study, intriguingly 48% of cases were positive for p-IGF-1R. p-IGF-1R positive cases had different patterns of staining: peri-nuclear detected in 76%, 11% with nuclear localization and only 13% membrane-apical staining. Furthermore, Tumours with positive p-IGF-1R expression, had higher MMP7 co-expression (59%) compared with negative cases 13%. These findings not only indicate that, IGF-1R could be used as biomarker, but also could allow selection of ACRC patients who can benefit from anti-IGF-1R treatment.

Riassunto

L'Insulin-like factor-1 di crescita recettore (IGF-1R) gioca un ruolo critico nella regolazione della proliferazione delle cellule tumorali, la sopravvivenza e metastasi nella cellula trasformata. Inoltre, l'acquisizione di chemio-resistenza, un problema ingombrante nel carcinoma coloretale avanzato (ACRC) pazienti di cancro. Il meccanismo di acquisizione resistenza è risultato essere attribuito ad una interiorizzazione membrana-a-nucleare p-IGF-1R che non possa essere superato con inibitori IGF-1R esistenti. Nel presente studio, intrigante 48% dei casi erano positivi per p-IGF-1R. I casi positivi p-IGF-1R avevano diversi modelli di colorazione: peri-nucleare rilevata nel 76%, 11% con la localizzazione nucleare e solo il 13% membrana apicale colorati. Inoltre, Tumori con l'espressione positiva p-IGF-1R, ha avuto maggiore MMP7 co-espressione (59%) rispetto ai casi negativi 13%. Questi risultati indicano non solo che, IGF-1R potrebbe essere utilizzato come biomarker, ma potrebbe anche consentire la selezione dei pazienti ACRC che possono trarre beneficio dal trattamento anti-IGF-1R.

Abstract

Anti-folate drugs are widely used in cancer therapies, and folate deficiency is considered to contribute to tumor genesis, but still few is known on the actual role of folates in cell survival and proliferation.

We used a human pro-myelocytic cell line (HL-60) as a model to assess the effect of folinic acid (5FTHF) on survival and proliferation in stringent conditions (deprivation of growth factors or exposure to UV light).

5FTHF has shown to increase transient proliferation in serum-free medium, and delay apoptosis in a dose-dependent fashion. Conversely, 5FTHF has resulted in reducing cell proliferation of cells cultured in medium added with growth factors. A similar phenomenon has been observed in PHA-activated lymphocytes, suggesting a possible effect of 5FTHF in increasing autocrine-driven proliferation. 5FTHF turned out to have no effect on apoptosis induced by growth factors deprivation or by exposure to UV-B or UV-C.

These results suggest a role of 5FTHF in modulating cell proliferation, and this could have an impact in therapies that include administration at high doses.

Riassunto

I farmaci “anti – folat” sono ampiamente usati nelle terapie del cancro e la carenza di “folate” è considerata contribuire alla genesi tumorale , ma ancora pochi sanno il ruolo effettivo di “folate” nella sopravvivenza e la proliferazione cellulare .

Abbiamo utilizzato una linea cellulare pro - mieloide umano (HL - 60) come modello per valutare l'effetto di acido folico (5FTHF) sulla sopravvivenza e la proliferazione in condizioni severe (deprivazione di fattori di crescita o di esposizione a luce UV) .

5FTHF ha dimostrato di aumentare la proliferazione transitoria in terreno privo di siero e ritardare l'apoptosi in modo dose -dipendente . Viceversa , 5FTHF ha portato a ridurre la proliferazione cellulare di cellule coltivate in terreno aggiunti con fattori di crescita . Un fenomeno simile è stato osservato nei linfociti PHA - attivati , suggerendo un possibile effetto di 5FTHF ascendente proliferazione autocrino - driven. 5FTHF no ha effetto sulla apoptosi indotta da fattori di crescita deprivazione o da esposizione a UV - B o UV - C .

Questi risultati suggeriscono un ruolo di 5FTHF nel modulare la proliferazione cellulare e questo potrebbe avere un impatto nelle terapie che comprendono la somministrazione a dosi elevate .

List of figure:

Figure 1.1 shows the structure of IGF- 1	7
Figure 1.2 shows the Sumoylation mechanism by E1-E2 and E1-E2-E3 enzymes	8
Figure 3.1 shows the sequence of antibody production	12
Figure-4.1 colorectal cancer cell line (LoVO and HT-29), chronically treated with oxaliplatin had developed drug resistance	14
Figure 4.2. Activation of IGF-1R/PI3K-AKT pathway, in cells chronically treated with oxaliplatin, is due to increase of MMP7 and IGFBP degradation	17
Figure 4.3 The IGF-1R inhibitor AMG479 combined with sorafenib prevents IRS-1-AKT signaling but not apoptosis in HT-OXAR3 OXL cells lines	18
Figure 4.4 IGF-1R, p-IGF-1R (p-1316) and caveolin-1 are located differently in HT-29 and HTOXAR3 cell lines	20
Figure 4.5: HT-29 and HTOXAR3 cell lines were treated with the IGF-1R monoclonal antibody (AMG479) and an IGF-1R tyrosine kinase inhibitor (AEW541)	22
Figure 1.1 chemical structure of folic acid	30
Figure 3.1 shows UVC induced apoptosis (cell proliferation) using haemocytometer	45
Figure 3.2 shows UVC induced apoptosis (cell survival) using haemocytometer	46
Figure 3.3 shows UVC untreated cells and folic acid doses(cell proliferation)	48
Figure 3.4 UVC untreated cells survival using trypan blue dye exclusion	49
Figure 3.5 shows UVC treated cells with 0.5 minute cell proliferation	50
Figure 3.6 Cells treated with UVC for 0.5 minute (cell survival) using trypan blue exclusion	51
Figure 3.7 shows Cells treated with UVC for 10 minutes(cell proliferation)	52
Figure 3.8 illustrates UVC untreated cell (cell proliferation) using haemocytometer	53
Figure 3.9 shows % UVC untreated cell (cell survival) using trypan blue exclusion	54
Figure 3.10 demonstrates Cells treated with 0.1 minute UVC cell proliferation using haemocytometer	54
Figure 3.11 shows Cells treated with 0.1 minute UVC (cell survival) using trypan blue exclusion	55
Figure 3.12 UVC treated cells for 0.5 minutes cell count using haemocytometer	56
Figure 3.13 UVC treated cells for 0.5 minutes cell viability using trypan blue dye exclusion	56
Figure 3.14 Effects of post-treatment of folic acid and UVC on cell proliferation	57
Figure 3.15 Effects of post-treatment of folic acid and UVC on cell survival	58
Figure 3.16 Effect of pre-treatment of folic acid and UVC on cell proliferation	59

Figure 3.17 Effects of pre-treatment of folic acid and UVC on cell viability	59
Figure 3.18 Effects of folic acid on proliferation of untreated cells	61
Figure 3.19 Effects of folic acid on cell survival of untreated cells	61
Figure 3.20 Effect of UVB and folic acid on cell proliferation with 1 minute UVB exposure	62
Figure 3.21 Effects of UVB and folic acid on cell survival with 1 minute UVB exposure	63
Figure 3.22 Effects of UVB and folic acid on cell proliferation with 10 minute UVB exposure	63
Figure 3.23 Effects of UVB and folic acid on cell survival with 10 minutes UVB exposure	64
Figure 3.24 cell proliferation using haemocytometer	65
Figure 3.25 Cell survival using trypan blue exclusion	66
Figure 3.26 cell proliferation using haemocytometer	67
Figure 3.27 Cell survival using trypan blue exclusion:	68
Figure 3.28 UVB dose exposure HL-60 supplemented with 5FTHF (cell count) using haemocytometer	70
Figure 3.29 UVB dose exposure HL-60 supplemented with 5FTHF (cell survival) using Trypan blue dye exclusion	71
Figure 3.30 shows 5FTHF doses on UVB treated HL-60 cell (cell proliferation) by Haemocytometer:	81
Figure 3.31 shows 5FTHF doses on UVB treated HL-60 cell (cell survival) by (% of Trypan blue dye exclusion):	82
Figure 3.32 shows 5FTHF doses on UVB-treated HL-60 cells(cell proliferation) using haemocytometer	93
Figure 3.33 shows 5FTHF doses on UVB-treated HL-60 cells(cell proliferation)	94
Figure 3.34 5FTHF doses -1 -12 doses kinetics (cell proliferation)	104
Figure 3.35 5FTHF doses -1 -12 doses kinetics (cell survival)	105
Figure 3.36 shows SFM 5FTHF 10x5 vs 50 9-15-days(cell proliferation)	123
Figure 3.37 shows Table shows s SFM 5FTHF 10x5 vs 50 9-15-days (cell survival)	124
Figure 3.38 shows cells proliferation in absence of serum	126
Figure 3.39 shows cell survival in absence of serum	127
Figure 3.40 shows Cell proliferation in presence of 1% serum	128
Figure 3.41 shows cell survival in presence of 1% serum	129
Figure 3.42 shows Table shows - SFM- 5FTHF maximal effective dose (cell proliferation)	130
Figure 3.43 shows SFM- 5FTHF maximal effective dose (cell survival) using trypan blue exclusion	131
Figure 3.45 shows table shows effect of 5FTHF supplemental on HL-60 (cell	132

proliferation)	
Figure 3.46 shows table shows effect of 5FTHF supplemental on HL-60 (cell proliferation)	133
Figure 3.47 illustrate Effect of 5FTHF supplemental on HL-60 (cell survival) using trypan blue exclusion:	133
Figure 3.48 illustrate Effect of 5FTHF supplemental on HL-60 (cell survival) using trypan blue exclusion	134
Figure 3.49 describes Effect of 5FTHF supplemental on cell proliferation using MCF-7 cell	135
Figure 3.50 shows c-Myc inhibition and rescue with 5FTHF(cell proliferation) using haemocytometer	136
Figure 3.51 shows Table shows c-myc inhibition and rescue with 5FTHF Cell survival) using trypan blue dye exclusion:	137
Figure 3.52 describes the mitotic activity	141
Figure 3.53 shows mitotic activity of cells that has been released from the block after 3 hours	142
Figure 3.54 shows mitotic activity of cells that has been released from the block after 5 hours	143

List of tables:

Table 1.1 one- carbon substitution of tetrahydrofolates	31
Table 3.1 shows UVC induced apoptosis (cell proliferation) using haemocytometer	45
Table 3.2 shows UVC induced apoptosis (cell survival) using haemocytometer:	46
Table 3.3 shows UVC untreated cells and folinic acid doses(cell proliferation)	47
Table 3.4 UVC untreated cells survival using trypan blue dye exclusion:	48
Table 3.5 shows UVC treated cells with 0.5 minute cell proliferation	49
Table 3.6 demonstrates Cells treated with UVC for 0.5 minute (cell survival) using trypan blue exclusion:	50
Table 3.7 illustrates Cells treated with UVC for 10 minutes(cell	51

proliferation):

Table 3.8 shows UVC untreated cell (cell proliferation) using haemocytometer: 53

Table 3.9 shows UVC untreated cell (cell survival) using trypan blue dye exclusion 53

Table 3.10 demonstrates Cells treated with 0.1 minute UVC cell proliferation using haemocytometer 54

Table 3.11 shows Cells treated with 0.1 minute UVC (cell survival) using trypan blue exclusion: 55

Table 3.12 UVC treated cells for 0.5 minutes cell count using haemocytometer: 55

Table 3.13 UVC treated cells for 0.5 minutes cell viability using trypan blue dye exclusion 56

Table 3.14 Effects of post treatment of folic acid and UVC on cell proliferation 57

Table 3.15 Effects of post-treatment of folic acid and UVC on cell survival 58

Table 3.16 Effect of pre-treatment of folic acid and UVC on cell proliferation 58

Table 3.17 Effects of pretreatment of folic acid and UVC on cell viability 59

Table 3.18 Effects of folic acid on proliferation of untreated cells 60

Table 3.19 Effects of folic acid on cell survival of untreated cells 61

Table 3.20 Effect of UVB and folic acid on cell proliferation with 1 minute UVB exposure 62

Table 3.21 Effects of UVB and folic acid on cell survival with 1 minute UVB exposure 62

Table 3.22 Effects of UVB and folic acid on cell proliferation with 10 minute UVB exposure 63

Table 3.23 Effects of UVB and folic acid on cell survival with 10 minutes UVB exposure 64

Table 3.24 cell proliferation using haemocytometer: 65

Table 3.25 Cell survival using trypan blue exclusion 65

Table 3.26 cell proliferation using haemocytometer 67

Table 3.27 Cell survival using trypan blue exclusion:	68
Table 3.28 UVB dose exposure HL-60 supplemented with 5FTHF (cell count) using haemocytometer	70
Table 3.29 UVB dose exposure HL-60 supplemented with 5FTHF (cell survival) using Trypan blue dye exclusion	71
Table 3.30 shows 5FTHF doses on UVB treated HL-60 cell (cell proliferation) by Haemocytometer:	80
Table 3.31 shows 5FTHF doses on UVB treated HL-60 cell (cell survival) by (% of Trypan blue dye exclusion):	81
Table 3.32 shows 5FTHF doses on UVB-treated HL-60 cells (cell proliferation) using haemocytometer	92
Table 3.33 shows 5FTHF doses on UVB-treated HL-60 cells (cell proliferation)	93
Table 3.34 5FTHF doses -1 -12 doses kinetics (cell proliferation)	104
Table 3.35 5FTHF doses -1 -12 doses kinetics (cell survival)	104
Table 3.36 shows SFM 5FTHF 10x5 vs 50 9-15 days (cell proliferation)	123
Table 3.37 shows s SFM 5FTHF 10x5 vs 50 9-15-days (cell survival)	124
Table 3.38 shows cells proliferation in absence of serum	126
Table 3.39 cell survival in absence of serum	127
Table 3.40 shows cell proliferation in presence of (1% serum)	128
Table 3.41 shows cell survival in presence of 1% serum)	128
Table 3.42 shows - SFM- 5FTHF maximal effective dose (cell proliferation)	130
Table 3.43 shows SFM- 5FTHF - maximal effective dose (% cell survival) using trypan blue exclusion	130
Table 3.44 shows effect of 5FTHF supplemental on HL- 60 (cell proliferation)	132
Figure 3.45 illustrate Effect of 5FTHF supplemental on HL-60 (cell survival) using trypan blue exclusion	133
Table 3.46 shows effects of 5FTHF supplemental on cell proliferation using MCF-7:	134
effects 3.47 of 5FTHF supplemental on cell proliferation using MCF-7 (cell survival)	135
Table 3.48 c-Myc inhibition and rescue with 5FTHF(cell proliferation) using	136

haemocytometer:

Table 3.49 shows c-myc inhibition and rescue with 5FTHF Cell survival) 137
using trypan blue dye exclusion:

Dedications

To my beloved parents for their constant and requite love and support

To my teacher in science

To my teacher in humanity

To my brothers, friends and colleagues

I can't thank you sufficiently

Acknowledgement

I would like to express my deepest thanks and appreciation to my supervisor prof. Michele Rubini for his valuable, immeasurable advices, massive support and encouragement during the course of my PhD. I am mightily pleased with his indefatigable and tireless hard work, without his diligent task this work would never see the light

I would like to thank Dr. Joan Maurel in Hospital clinic Barcelona (Spain) for collaboration. I would like also to thank prof. Renato Baserga in Thomas Jefferson University Philadelphia (USA) for cooperation.

I am extremely indebted to the all colleagues in Rubini's lab particularly Paola and Elia for their help and cooperation. Also I am grateful to the all staff in Medical Genetic lab namely Sergio, Alessandra, Rita and Barbara who have assisted and helped me with both their technical expertise time special thanks and appreciation to Dr Vincenzo who taught me several techniques and been helpful with me. I would like to thank Dr Luisa Ferrari in hematology department for helping us during FACS analysis

I am so grateful to my sponsor faculty of medical lab sciences and administration of teaching assistants University of Khartoum for financial support particularly prof. Nasereldin

I would like to thank my wonderful friends especially in Cenacolo and Puitinati residence and companions for everything. I can never thank them sufficiently and I love you all.

TABLE OF CONTENTS

Introduction	1
1.1 General overview:	1
1.1.1 Ligands:	1
1.1.2 Insulin like growth factor binding proteins:	1
1.1.3 IGFBP proteases:	2
1.1.4 Insulin like growth factor receptors IGF R:	2
1.1.4.1 IGF-IR Internalization	3
1.1.4.1.1 clathrin mediated endocytosis	3
1.14.1.2 caveolin - dependent endocytosis	4
1.1.4.2 signaling via IGF-1R	4
1.1.4.3 SUMOylation	5
1.1.5 Oxaliplatin:	9
objective	10
3- Material and Methods:	11
3.1 Antibody production:	11
3.2 Immunization protocol and antibodies:	11
4- Results:	13

4.1 Chronic oxaliplatin exposure leads to acquired drug resistance	13
4.2 Activation of IGF-1R/PI3K-AKT pathway in cells chronically treated with OXL is due to increased MMP-7 and IGFBP degradation:	16
4.3 AMG 479 inhibits p-AKT in HT29 and HTOXAR3 cell lines, but induces apoptosis only in HT-29 cell line	16
4.4 IGF-1R, p-IGF-1R and caveolin-1 are located differently in HT-29 and HTOXAR3 cell lines	19
4.5 Phospho-IGF-1R in the nucleus is not inhibited in HTOXAR3 cell line by IGF-1R inhibitors	19
5- Discussion	24
6- Conclusion and Recommendations	27
1- Introduction and Review of literature	29
1.1 Folates:	29
1.1.1 Chemistry and properties:	29
1.1.1 Chemistry and properties:	29
1.1.2 Folinic acid:	31
1.1.3 Folate metabolism	32
1.1.2.1 overview	32
1.2 Cell cycle:	34
1.2.1 The G1→ S transition:	35
1.2.2. S- phase progression	36
1.2.2.1 Phosphorylation of E2F-1	36
1.3 Ultraviolet radiation UV:	37
1.4 c-Myc proteins:	38
1.5 Apoptosis:	39
1.5.1 Overview:	39
1.5.2 Morphology of apoptosis:	39
1.5.3 Molecular mechanism of apoptosis signaling pathways:	40

1.5.3.1 Caspases	41
1.5.3.2 Intrinsic pathway	42
2- Rationale and specific aims:	43
3. Methodology and Results	44
3.1 Cell culture	44
3.2 Irradiation of cells with UVC light:	44
3.3 Trypan Blue dye Exclusion	44
3.2.1 Results:	45
3.4 Effect of Folinic acid on cell proliferation and apoptosis in UV-C treated HL60 cells:	46
3.4.1 Results:	47
3.4.2 Effect of Folinic acid on cell proliferation and apoptosis in UVC treated HL-60 cells	52
3.4.3 Effects of pre and post- treatment and UVC on cell proliferation	56
3.4.3.1 Results	57
3.5 Irradiation of cells with UVB light:	60
3.5.1 Effects of UVB and folinic acid on cell proliferation and apoptosis:	60
3.5.1.1 Result	60
3.5.2 5FTHF doses on UVB-treated HL-60 cells	62
3.5.2.1 Result	62
3.5.3 UVB dose exposure of HL-60 cells treated with 5FTHF (cell count)	66
3.5.3.1 Results...	66
3.5.4 UVB dose exposure of HL-60 cells treated with 5FTHF (cell count)	69
3.6 Cell cycle protocol with propidium iodide PI:	69
3.6.1 Flow cytometric analysis	72
3.5.5 5FTHF doses on UVB treated HL-60	79

3.5.5.1 Results	79
3.5.5.2 PI of stained cells by FACS	82
3.5.6 5FTHF doses on UVB-treated HL-60 cells	91
3.5.6.1 Result	91
3.5.6.2 Flow cytometric analysis	94
3.5.7 Serum free medium(SFM) - 5FTHF doses – 1-12 days kinetics:	103
3.5.7.1 Results	103
3.5.7.2 Flow cytometry analysis	105
3.5.7.2.44 Elaboration of FACS result	120
3.5.8 SFM 5FTHF 10x5 vs 50 9-15 days	122
3.5.8.1 Result	122
3.5.9 PBMC SFM 5FTHF doses 1-12 days	125
3.5.9.1 Peripheral Blood mononuclear cells PBMCs preparation	125
3.5.9.1.1 PBMCs isolation	125
3.5.9.1.2 Cells culture and 5FTHF doses	125
3.5.9.1.2.1 Results	125
3.5.10 SFM 5FTHF maximal effective dose	129
3.5.10.1 Results	129
3.5.11 Effect of 5FTHF supplemental on cell proliferation using HL-60:	131
3.5.11.1 Results	131
3.5.12 Effect of 5FTHF supplemental on cell proliferation using MCF-7 cell:	134
3.5.12.1 Results	134
3.5.13 c-Myc inhibition and rescue with 5FTHF:	135
3.5.13.1 Result	135
3.3.13.2 Flow cytometric analysis	138
3.5.13.3 Mitotic index	140

3.5.13.3.1 Mitotic index of cells treated with c-myc inhibitor and rescue with folinic acid	141
3.5.13.3.1.1 Result:	141
3.5.13.4 synchronization of cells with methotrexate and treatment with c-myc inhibitor	142
3.5.13.4.1 Results:	142
3.5.13.5 Flow cytometric analysis for synchronization of cells with MTX and with 10058	143
3.5.13.5.1 Results:	143
4- Discussion	148
5- Conclusion and recommendations	155
Bibliography	156

List of abbreviations

5-CHO-THF	5-formyltetrahydrofolate
AICD	activation- induced cell death
ALS	acid labile subunit
ATP	Adenosine triphosphate
BHLH-ZIP	basic- helix-loop-helix-leucine zipper
CAV-1	Caveolin-1
CCP	Clathrin coated pits
CCV	clathrin coated vesicles
CPDs	Cyclobutane pyrimidine dimers
DACH	diaminocyclohexane
DHF	Dihydrofolate

DHFR	dihydrofolate reductase
DNA	Deoxyribonucleic acid
DSBs	Double strands breaks
dTMP	deoxythymidylate monophosphate
dUMP	deoxyuridylate monophosphate
ECM	extracellular matrix
ERKs	extracellular- regulated kinases
FAICAR	formylaminoimidazol-4 – carboxamide ribonucleotide
FGAR	formylglycinamide ribonucleotide
FPGS	folyl-poly- γ -glutamate synthetase enzyme
GAR	glycinamide ribonucleotide
GGH	γ - glutamyl hydrolase
Gly	Glycine
IGF R	Insulin like growth factor receptors
IGF	Insulin like growth factor
IGFBP	Insulin like growth factor binding protein
IR	Insulin receptor
IRS-1	Insulin receptor substrate- 1
K	Lysine
LDL	low density lipoprotein
LV	leucovorin
Lys	Lysine

mCRC	metastatic colorectal cancer
MMPs	matrix metalloproteinases
mOS	Median overall survival
MS	methionine synthase
MTX	methotrexate
MVB	multi-vesicular body
NADPH	Nicotinamide adenine dinucleotide phosphate
nIGF-1R	nuclear Insulin like growth factor receptors
PABA	Para-aminobenzoic acid
PARP	Poly ADP ribose polymerase
PBMCs	Peripheral blood mononuclear cells
PHA	Phytohaemagglutinin
PIP3	phosphatidylinositol 3,4,5- triphosphate
PteGlu	Pteroylmonoglutamate
Rb	retinoblastoma
RNA	Ribonucleic acid
ROI	Reactive oxygen intermediate
SHMT	serine hydroxymethyltransferase
SUMO-1	Small ubiquitin like modifier
THF	Tetrahydrofolate
TKR	Tyrosine kinase receptor
Ub	ubiquitin

UDS	Unscheduled DNA synthesis
UVB	Ultraviolet B
UVC	Ultraviolet C

Introduction

1.1 General overview:

The insulin – like growth factor(IGF) system compose of two cognate ligands namely IGF-1 and IGF-2, three cell surface receptors, six IGF binding proteins and binding protein proteases((Baserga et al., 1997; Pollak et al., 2004). The IGF signaling axis plays a fundamental role in normal growth and differentiation, furthermore, badly involved in directing, mediating several aspects of the malignant phenotype in a different variety of human malignancies(Liu et al., 1993; Khandwala et al., 2000; Moschos and Mantzoros, 2002; Bohula et al., 2003).

1.1.1 Ligands:

The ligands IGF-1 and IGF-2 are powerful growth factors that serve a pivotal function in differentiation and development of the organism, tissue regulation and wound healing as well(Heald et al., 2006). Both IGF-1 and IGF-2 are synthesized by liver, particularly by extrahepatic sites encompassing both cancer cells and stromal fibroblasts(Chen et al., 2009). IGFs are single chain polypeptides, consisting of A-, B-, C- and D subunits having strong affinity binding toward IGF-1R existing in C domain. The weak binding affinities of both IGF-1 and IGF-2 for insulin receptor are attributed to the lack of Thr^{A8}, Ile^{A10}, His^{B5} and Tyr^{B16} contact points in the A and B domains of IR(Gauguin et al., 2008). IGF-1 as well as IGF-2 share a 62% identity in amino acid sequence, with 40% identity between IGFs and pro-insulin(Fürstenberger and Senn, 2002). Interestingly, the comparative concentration of IGF-1 and IGF-2 vary in favor of IGF-2 that being five times greater than IGF-1 levels in human fetuses, as well as 3.5 times greater in adult serum(Bennett et al., 1983). nevertheless, Yakar et al.,(2005), found the expression levels of IGF-2 in human are ranged between 2 to 6 fold greater than those of IGF-1, moreover, IGF-2 is implicated in the progression of diverse type of tumours. However, the expression of IGF-2 *per se* is not far enough for malignant transformation.

1.1.2 Insulin like growth factor binding proteins:

The bioactivity and bioavailability of IGFs are modulated via a family of specific strong affinity binding proteins IGFBP-1- IGFBP-6(Bach et al., 2005). IGFBPs range in size between 24 – 40 kDa consisting of three structural subunits namely, N and C terminal domains that are identical containing conserved internal disulfide bonds. Intriguingly, both domains are

engaged in high affinity IGF binding. Paradoxically, the central linker domain, that ain't conserved among the IGFBPs, is found to be mostly structurally disorganized doesn't play a genuine role in IGF binding. Nevertheless, it is a common site of post-translational modification such as glycosylation and phosphorylation(Leon et al., 2013). Nearly 80% of circulation IGF are attached in a ternary complex including IGFBP-3 and abundant acid labile subunit(ALS)(Clemmons, 1998). IGFBPs share same affinities for both IGF-1 and IGF-2, in contrast IGFBPs-5 and 6 link IGF-2 with 10 and 100 fold higher affinity than IGF-1. In essence IGFBP are regulated by diverse proteases(reviewed in Andersson, 2009)

1.1.3 IGFBP proteases:

The matrix metalloproteinases(MMPs) are peptide hydrolases, active at neutral pH, metal ion are prerequisite for their catalytic activity. The MMPs have been well recognized as IGBP protease in the serum of pregnant rodents as well as in fibroblast-conditioned medium(Fowlkes et al., 1994; Fowlkes et al., 1994). MMPs degrade IGFBP releasing IGF thus increasing the bioavailability of IGFs (Miyamoto et al., 2004). MMP-7 is a member of this family, zinc- dependent enzyme produced exclusively by tumor cell, and implicated in many types and stages of cancer. Furthermore, this enzyme promotes and enhances metastasis and tumor growth via different variety of mechanisms e.g. Extra cellular matrix ECM degradation, regulation of angiogenesis remodeling and modulation on innate immunity(Chambers and Matrisian, 1997).

1.1.4 Insulin like growth factor receptors IGF R:

The IGF receptor family contains three transmembrane receptor tyrosine kinase (RTK), that mediates IGF bioactivity. In essence IGF-1R gene is positioned on chromosome 15q26 encoding a single polypeptide of 1367 amino acids that is basically expressed in most cells. Not surprisingly, the IGF-1R share around 70% amino acid homology with insulin receptor, as well as their genes show noticeable homology in terms of size and exon organization (Ullrich et al. 1986). IR has two splice variants: IR-B isoform that regulate glucose uptake and mainly expressed in liver, muscle and adipose tissue, compare to IR-A isoform that expressed by fetal tissues and some tumors, moreover, it avidly links to IGF-II promoting proliferation and survival(Sciacca et al. 2002). IGF-2R is a monomeric transmembrane that devoid of auto signaling activity it functions as a negative regulator of IGF activity by sequestration, endocytosis and degradation of IGF-2(Nolan et al. 1990). IGF-1R as well as IR are produced as single- chain pre-pro-receptors, consist of a 30 residue single

peptide which is cleaved co- translationally. In transit to the membrane, pro-receptors are glycosylated, folded and dimerised under control of chaperone proteins prior sending to the Golgi apparatus. Where the receptors are processed at a tetrabasic Arg-Lys- Arg- Arg furin protease cleavage site generating a (130- 135 kDa) and B(90- 97 kDa)domains of the mature receptor(Ullrich et al. 1986). These gathered into disulphide link tetramers that contains two extracellular α subunits, containing 710 amino acid(aa 1-710), that has in its structure two homologous domains namely L1 and L2 divided by a cysteine rich domain(48%) contains 25 or 27 cysteines in three repeating units and two β subunits containing 627 amino acid residues(aa 711- 1337) distributed among the extracellular domain(196 aa), the transmembrane domain(aa 906- 929), and intracellular region of the β subunit, which *per se* composed of a juxtamembrane domain , tyrosine kinase(TK) domain and C- terminal domain. The juxtamembrane domain contains NPXY motif, that may be important for receptor endocytosis. The catalytic domain contains the ATP binding motif(GXGXXG) that positioned between 976- 981, while the catalytic lysine located at position 1003, which is crucial for Mg-ATP binding.TK domain contains three intrinsic tyrosines, located at positions 1131, 1135 and 1136 is important for receptor autophosphorylation. The C- terminus regions roughly the last amino acid contains many regulatory elements fundamental for IGF-1R function((Adams et al., 2000; Ward and Garrett, 2004; reviewed in Girnita et al., 2013).

1.1.4.1 IGF-1R Internalization :

Binding of IGF ligand to its respective receptor induced autophosphorylation, and triggering compartmentalization of ligand/receptor complexes, resulting in detachment and degradation of ligand in the intracellular endosome/lysosome system, additionally, inactivation, recycling of receptors and termination of signal transduction(Foti et al., 2004; Romanelli et al., 2007). Notwithstanding, receptor endocytosis may also fundamentally, involved in signaling especially through Ras/MAPK pathway to mitogenic endpoint(Jensen and De Meyts 2009). IGF-1R mediate internalization via two canonical way clathrin and caveolin-1(Cav-1)(Martins et al., 2011).

1.1.4.1.1 Clathrin- mediated endocytosis:

In clathrin- mediated endocytosis, when the ligands bind to its receptor, the receptors move within the plasma membrane, bind to adaptor protein AP2 that, recruits clathrin to coat the invaginating pits at the plasma membrane hence called clathrin coated pits(CCP). Coated pits are pinched off thanks to the large GTPase dynamin to form clathrin

coated vesicles(CCV), that travel from the plasma membrane, undergo uncoating, and coalesce to the early endosomal compartment, which act as sorting station. Next the cargo proteins advance towards either the late endosome or the multi-vesicular body(MVB), wherein the ligand is uncoupled from the receptor primarily imputed to low pH environment of MVB, and the receptor is recycled back to the plasma membrane. Alternatively, they can be translocated to the lysosome, wherein they are degraded and destroyed(French et al., 1995; Sehat, 2007; Doherty and McMahon, 2009; Serini et al., 2012). The expeditious elimination of receptors from the cell surface and subsequent delivery to the lysosome is aimed to prevent sustained activation from both the plasma membrane and endocytic vesicles, which may result in cell transformation and tumorigenesis(reviewed in Abella and Park, 2009).

1.1.4.1.2 Caveolin-dependent endocytosis:

Caveolae are subfamily of lipid rafts, that exist in cell surface invaginations. It is well distinguished by its flask shaped morphology(Simons and Toomre, 2000). Caveolin-1(Cav-1) is the basic protein, that form the caveolae(Salani et al., 2010). Furthermore, Caveolar structure and function in signaling and internalization as well depend primarily on Caveolin-1 and cholesterol.Cav-1 function to bind and assemble cholesterol. The N- and C-termini of the caveolae are protruded into the cytoplasm, indicating that they form hairpin shape in the membrane beside their ability to oligomerize, additionally, Caveolin serve as a coat protein(Mukherjee et al., 2006; de Laurentiis et al., 2007). Moreover, Cav-1 may interplay and modulate the bioactivity of various proteins through scaffolding domain implicating it as a regulator of signal transduction(Li et al., 1996; Couet et al., 19997; Razani et al., 2002).

There is a compelling evidence indicating that, the number of caveolae in cell and the level of Caveolin expression are closely related to the amount of cholesterol. The higher amount of free cholesterol in fibroblast, the higher external concentration of low density lipoprotein(LDL) that, resulted in an upregulation of Caveolin mRNA and increased the number of caveola(Fielding et al., 1997). Maggi et al., (2002), described the IGF-1R colocalization with Cav-1 in the lipid rafts enriched fraction on plasma membrane and IGF-1 triggering phosphorylation at the level of tyrosine 14 which subsequently results in the translocation of Cav-1, indicating that IGF-1 could regulate its intracellular signaling pathways by redistribution of Cav-1 on the cell surface, Interestingly one study showed that, tyrosine 14 is the principle substrate of Src kinase(Lee et al., 2000).

1.1.4.2 Signaling via IGF-1R:

The IGF-1R is triggered by IGFs exist in the extracellular milieu, stemmed from paracrine, endocrine or autocrine sources. Activation of IGF-1R results in autophosphorylation on tyrosines 1131, 1135 and 1136 in the kinase subunit ensued by phosphorylation of juxtamembrane tyrosines and carboxy-terminal serines. This is followed by recruitment of specific-docking intermediates e.g. (IRS-1), Shc and 14-3-3 proteins(Baserga et al. 1997; Pollak et al. 2004). Furthermore, in the wake of stimulation with cognate IGFs, the SH2-containing adaptor protein Shc is mobilized to phosphorylated tyrosine residue(Tyr950) in the juxtamembrane region of the IGF-1R, and transduce differentiation signals via the Grb2, Ras, Raf and MAPK pathway(Reiss et al., 2000; Valentinis et al., 2000). IGF-1R protects cancer cells against apoptosis, mainly via the phosphoinositide 3-kinase (PI3K) pathway, as once IRS-1 is phosphorylated by the activated IGF-1R, PI3K is activated by linking to IRS-1 through its regulatory subunit(Baserga et al., 1997). This interaction results in the levels of phosphatidylinositol 3,4,5-triphosphate (PIP3), to increase, and subsequently leads to mobilization and activation of phosphoinositide-dependent kinase- along with AKT/protein kinase B. Activation of AKT causes expression of anti-apoptotic proteins, namely Bcl-2, Bcl-x and NF- κ B (Brazil et al. 2004). Additionally, IGF mediates the activation of extracellular-regulated kinases(ERKs), p38 and MAPK through 14-3-3-dependent mitochondrial compartmentalization of RAF(Peruzzi et al. 1999).

IGF-1R over expression is notoriously associated with increased predilection for invasion and metastasis that, mediated by myriad signaling intermediates influencing invasive capacity. Not surprisingly, IGF-instigated phosphorylation of IRS-1 can impact the interaction between E-cadherin and β -catenin, promoting and enhancing β -catenin transcriptional activity and disassociating E-cadherin from the actin cytoskeleton (Playford et al. 2000)

The IGF-1R is found to be overexpressed in tumors, such as colon cancer, melanoma, pancreas, prostate and kidney((Hellowell et al., 2002; reviewed in Bohula et al. 2003a).

1.1.4.3 SUMOylation:

Is a post translational modification whereby protein function is regulated. It involves covalent binding of ubiquitin(Ub) and ubiquitin-like(Ubl) modifiers to target proteins, it forms a crucial step in cellular process such as differentiation, apoptosis, cell cycle and stress response(reviewed in Tozluog et al., 2010). SUMO-1(Small ubiquitin like

modifier), is a one member of the Ubl superfamily that linked to its target proteins and exist in mammal with different names(reviewed in Tozluog et al., 2010). Sehat et al., (2010), reported accumulation of IGF1R in the nucleus after undergoing SUMOylation. Intriguingly, nuclear IGF-R(nIGF-1R) was demonstrated to attach to putative enhancer site within the genomic DNA increasing the transcription. Interestingly, SUMOylation took place at three evolutionarily conservative lysine residues(K1025, K1100 and K1120) of the β domain of the receptor, accordingly, when these lysines were mutated the IGF-1R nuclear translocation and transcription activation were failed to materialize(Sehat et al., 2010).

The SUMOylation cascade is initiated by activating immature SUMO protein which cleaved by protease enzyme, and resulting in exposing C- terminal diglycine motif that is necessary for optimal adenylation by a heterodimeric SUMO E1 enzyme(also known as Aous1/Uba2), and hence get activated. Next SUMO activated by SUMO activating enzyme SAE-1 or E1, through attacking adenylate via a conserved Cys within E1 enzyme forming an E1- SUMO thioester. Then activated SUMO is subsequently transferred to specific conjugation SUMO F2(also known as Ubc9) enzyme, that consequently establishing E2-SUMO thioester. Two alternative pathways can take place as final step, either E2 can straight away transfer SUMO to lysine residue in targeted substrate, or SUMO ligase E3(also known as RanBP2), may join the complex, increasing the E2 catalytic activity, and transferring SUMO to its targeted substrates(reviewed in Sehat et al., 2010; Tozluog[~] lu et al., 2010; Gareau and Lima, 2010)

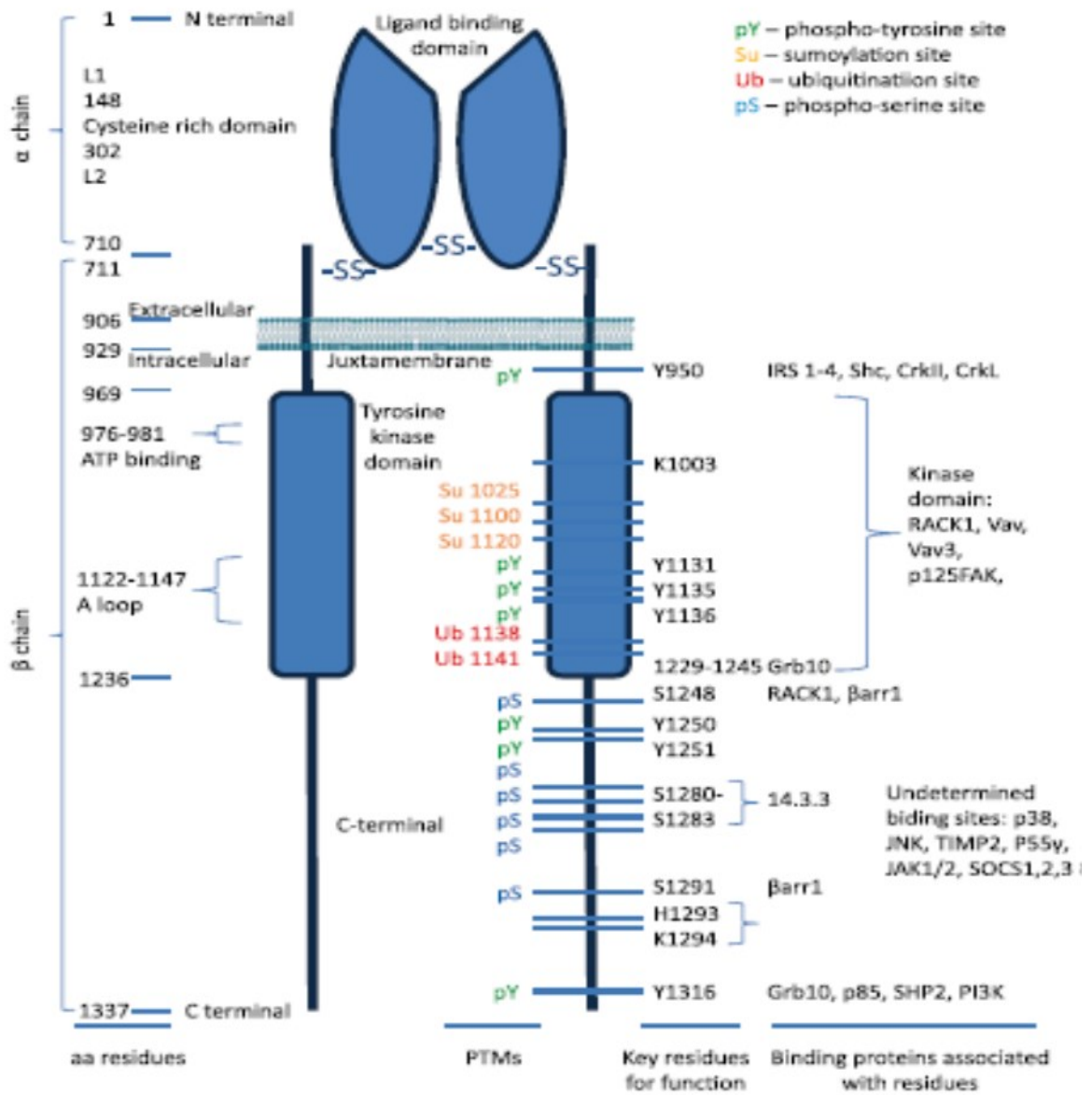


Figure 1.1 shows the structure of IGF- 1R reproduced from (Girnit, L et al., 2013)

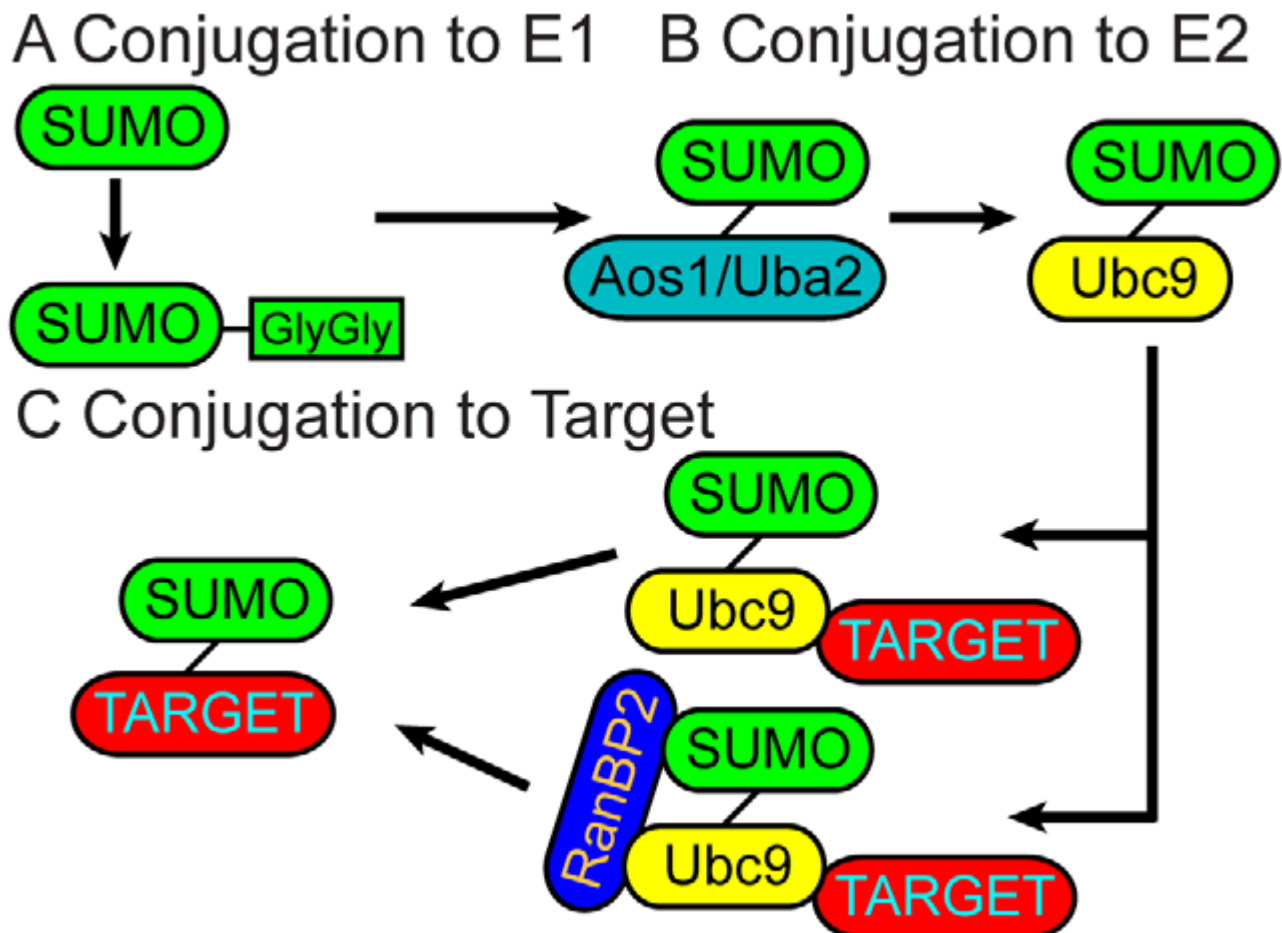


Figure 1.2 shows the Sumoylation mechanism by E1-E2 and E1-E2-E3 enzymes. (A) Produced as an inactive precursor, the SUMO protein is cleaved, exposing its Gly-Gly motif, and gets activated. (B) Active SUMO is transferred by E1 enzyme Aos1/Uba2 heterodimer to the E2 enzyme Ubc9. (C) Two alternative pathways can follow as the third step. Ubc9 can directly transfer SUMO to specific targets (top). Alternatively RanBP2, an E3 enzyme, can also join the complex, increasing the Ubc9 (reproduced from Tozluoglu M et al., 2010).

1.1.5 Oxaliplatin:

Oxaliplatin(*trans*-L-1,2 diaminocyclohexane oxalatoplatinum), is a platinum complex in which diaminocyclohexane(DACH) is the carrier ligand(Pelley, 2001). Oxaliplatin is a third generation platinum compound, and is the first efficacious platinum- based compound used to treat colorectal cancer(Meyerhardt and Mayer, 2005). Oxaliplatin exerts its cytotoxic effect via effectual damaging and inhibiting DNA synthesis probably by forming adducts, commonly the intrastrand linkage of two adjacent guanines by N7 that are too difficult to repair(Schmidt and Chaney, 1993; reviewed in Desoize and Madoulet, 2002). Oxaliplatin has synergistic effects when in a cocktail containing 5-fluorouracil and leucovorin (FOLFOX) for treating advanced colorectal cancer, with response rates >50% and median survival approaching 2 years(Alberts et al., 2005; Cassidy et al., 2004). However, resistance to chemotherapy is the lingering problem that encounter effective treatment of cancer, since sizeable of colorectal cancer patients developed resistance against oxaliplatin. Oxaliplatin-resistant cells are distinguished by low cellular oxaliplatin, accumulation and reduced DNA adducts, additionally, elevation of intracellular glutathione, mediated by gamma-glutamyl transpeptidase and altered in apoptotic pathway namely mitochondrial-mediated apoptosis(Mishima et al., 2002; Gourdier et al., 2002).

2- Objective

Relationship between the expression and cellular localization of IGF-1R and resistance to chemotherapy.

3- Material and Methods:

3.1 Antibody production:

the peptides were prepared by solid-phase synthesis using Fmoc strategy on a 430A peptide synthesizer (Applied Biosystems, Foster City, CA) and a 9050 Pepsynthesizer Plus (Perseptive Biosystems, Cambridge, MA). A 4-fold excess of Na-Fmoc amino acid, O-benzotriazol-1-yl- N,N,N9,N9-tetramethyluronium hexafluorophosphate, and 1-hydroxybenzotriazole and a 10-fold excess of diisopropylethylamine were used in every coupling reaction step. Elimination of the NH₂- terminal Fmoc group was accomplished by 20% piperidine in N,Ndimethylformamide. The cleavage of peptides from the resin was carried out with reagent K for 2 h at room temperature with gentle stirring. Crude peptides were precipitated in ice-cold methyl-t- butyl ether, centrifuged, and lyophilized. Crude peptides were then purified by preparative reverse-phase HPLC using a Dynamax-300Å C18 column (25 cm 3 21.4 mm, inner diameter) with a flow rate of 9 ml/min and two solvent systems of 0.1% trifluoroacetic acid/H₂O and 0.1% trifluoroacetic acid/acetonitrile. The fractions containing the appropriate peptide were pooled together and lyophilized. The purity of the final products was assessed by analytical reverse-phase HPLC, capillary electrophoresis, and matrix-assisted laser desorption/ionization time-of-flight mass spectrometry. Pep922 was a 19-amino-acid peptide corresponding to the C-terminus residues 1319–1337 of the human IGF-IR (numbering of Ullrich et al., 1986). Pep1046 was a 28-amino-acid peptide corresponding to residues 1310-1337 of the human IGF-IR, including a phosphotyrosyl residue at position 1316. Its sequence is NH₂-FDERQPpYAHMNGGRKNERALPLPQSSTC-COOH (Rubini et al., 1999).

3.2 Immunization protocol and antibodies:

Peptides were dissolved in 0.1 M sodium phosphate buffer (pH 7.0) and coupled to activated keyhole limped hemocyanin (Pierce) by glutaraldehyde. Immunogens were diluted 1:1 with complete (first shot) or incomplete (subsequent shots) Freund's adjuvant and injected intradermally in rabbits at 4-week intervals. The anti-peptide serum antibody level was

monitored by ELISA. To get rid of unwanted anti-C terminus antibodies, anti-pep1046 serum was cleared by reverse immunoaffinity purification using pep922-bound Sepharose. The antibody against pep1046 is hereafter referred to as anti-pY1316(Rubini et al., 1999).

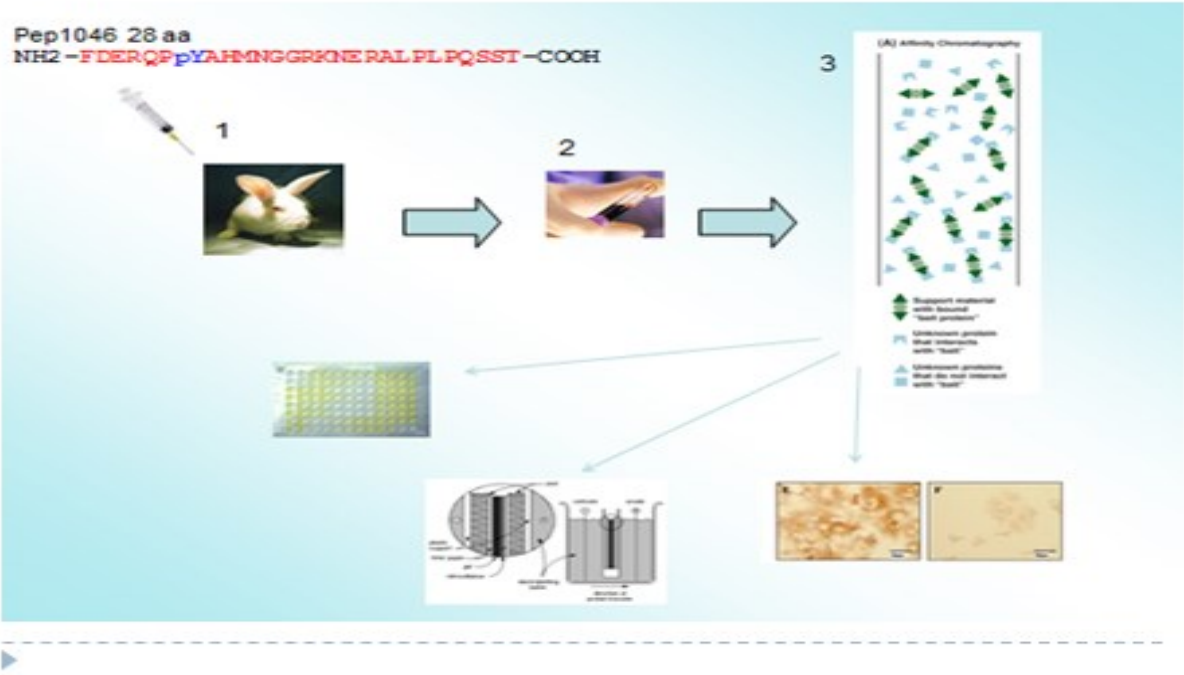


Figure 3.1 shows the sequence of antibody production

4- Results:

A study conducted in collaboration with Codony-Servat and Maurel et al to detect the localization of p-IGF-1R and resistance to oxaliplatin using our antibody(anti-pY1316).

4.1 Chronic oxaliplatin exposure leads to acquired drug resistance

To investigate if chronic OXL treatment could result in acquiring drug resistance, a panel of two colorectal cancer cell lines (LoVo and HT-29) were chronically treated with increasing concentrations of OXL. Sensitivity of the basal LoVo cell line was 10-fold that of LoVOXAR3, 29-fold that of HT-29, and 120-fold that of HTOXAR3 (**Fig 4.1**). To analyze the OXL-induced apoptosis at 24 hours, Fas expression and caspase 8 cleavage (extrinsic pathway) were induced by OXL in LoVo (0.2 μ M) and LoVOXAR3 (20 μ M). No changes in these proteins were observed in HT-29 and HTOXAR3. Bcl-2 decreased in LoVo cells with 2 μ M of OXL and in LoVOXAR3 with 20 μ M of OXL. Bax increased with 0.2 mM of OXL, but 20 mM of OXL was needed to increase Bax in LoVOXAR3. Bax increased in HT-29 (2 μ M) but was not induced in HTOXAR3 despite high 50 μ M doses. Bcl-2 decreased in HT-29 at doses of 2 mM, while 20mM doses were needed for HTOXAR3 cells (**Figure 4.1 A**). These results show that the oxaliplatin-resistant cell lines exhibit more resistance to apoptosis induced by oxaliplatin than parental cell lines. The extrinsic pathway is only implicated in the LoVo cell model.

To further characterize the properties of LoVo and HT-29, they investigated the effects of chronic OXL exposure in the IGF-1R pathway. they observed an increased expression of caveolin-1 in LoVOXAR3 and HTOXA3R cell lines compared with the parental ones. A specific difference between HT-29 and HTOXAR3 was increased expression and activation of IGF-1R in the latter (**Figure 4.1B**). LoVo cell lines express very low levels of MMP-7. HT-29 expressed MMP-7 but at a lower level than HTOXAR3. they found high levels of IGFBP-3 in LoVo and lower but still detectable levels in LoVOXAR3 cells. IGFBP-3 was not detected in

HT-29 cell lines. IGFBP-2 was also highly expressed in LoVo and was detected, with significantly lower expression, in LoVOXAR3 and HT-29, but not in HTOXAR3 cell line (Figure 4.1C).

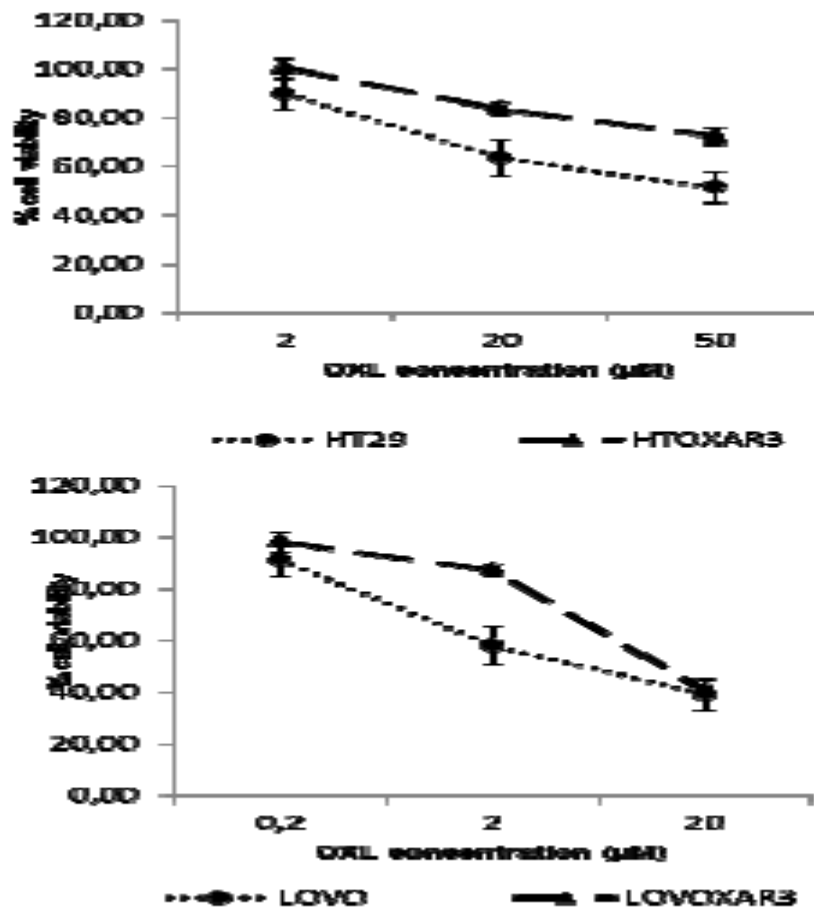


Figure 4.1 colorectal cancer cell line (LoVO and HT-29), chronically treated with oxaliplatin had developed drug resistance

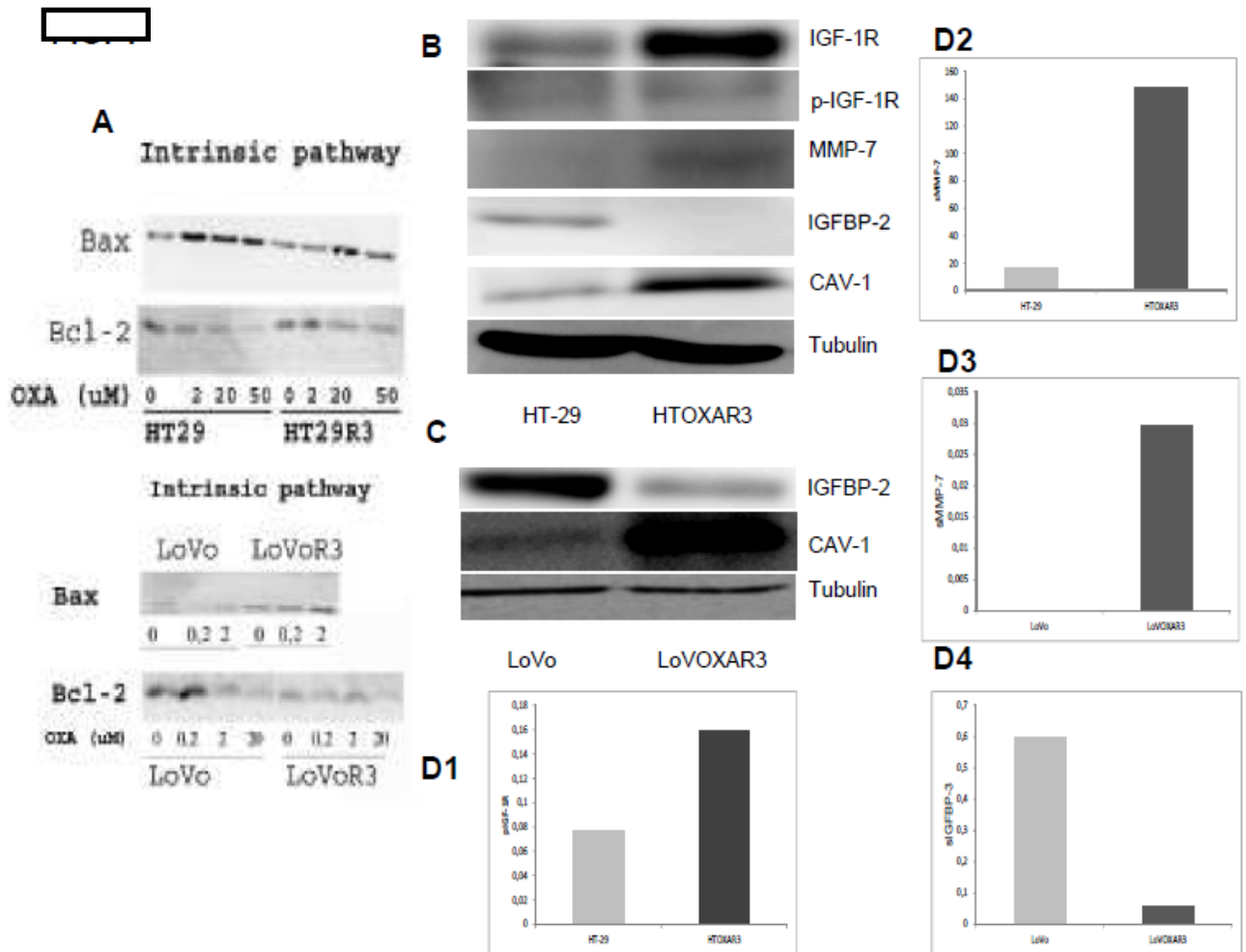


Figure 4.1 Colorectal cancer cell lines (LoVo and HT-29) chronically treated with oxaliplatin develop drug resistance.

A) Apoptosis induction after oxaliplatin inhibition at different doses (0.2, 2, 20 and 50) of parental and chronically treated cell lines was assessed.

B and C) Levels of IGF-1R, p-IGF-1R, MMP7, IGFBP-2 and caveolin-1 expression were determined by Western-blot in parental and resistant cell lines

D1-D4) p-IGF-1R, MMP7 and IGFBP-3 expression was determined in cell lines by ELISA

4.2 Activation of IGF-1R/PI3K-AKT pathway in cells chronically treated with OXL is due to increased MMP-7 and IGFBP degradation:

OXL caused an increase of MMP-7 in LoVOXAR3, HT-29 and HTOXAR3 (Figure 4.2A). In the parental HT-29, a marked decrease of IGFBP-2 expression was seen at 24hours (h)after 20 μ M OXL exposure. Expression of IGFBP-2 was not detected in HTOXAR3. p-IRS-1 and p-AKT were inhibited in HT-29 at 20 μ M concentration after 5' of treatment and remained inhibited until 60'. This effect was not observed in the HTOXAR3 cell line (Figure 4.2B). They evaluated changes at 24h of p-MAPK and p-AKT after exposure to increasing OXL concentration (0.2, 2, 20 and 50 μ mol/L). Phospho-AKT and p-MAPK were inhibited in Lovo cell lines after OXL treatment at doses as low as 0.2 μ M at 24 hours. This effect was not observed in HT-29 and HTOXAR3 despite the administration of high (50 mM) doses of OXL (Figure 2C). Interestingly, a clear decrease in p-AKT was noted in HT-29 but not in HTOXAR3 at 1 hour after OXL exposure (Figure 4.2D).

4.3 AMG 479 inhibits p-AKT in HT29 and HTOXAR3 cell lines, but induces apoptosis only in HT-29 cell line

When MMP-7 was silenced in HTOXAR3 there was a partial reversion in OXL resistance, but not at the level of HT-29, suggesting that mechanisms in addition to MMP-7 could contribute to OXL resistance acquisition in HTOXAR3 cells (Figure 4.3A).

In vitro proliferation after 72 h exposure to individual drugs or a combination of them was assessed by MTT assay. Oxaliplatin primarily affects the HT-29 cell line. Sorafenib affects both HT-29 and HTOXAR3 cell lines equally, while panitumumab did not affect cell proliferation. AMG479 inhibited cell proliferation notably, and especially in HTOXAR3 cells. The effect of the combination of AMG479 plus sorafenib and oxaliplatin induced a maximum cytotoxicity in both cell lines (Figure 4.3B).

To investigate the effects of their drug in AKT and IRS-1 phosphorylation inhibition, they treated HT-29 and HTOXAR3 cells with AMG479, a monoclonal antibody against IGF-1R and TIMP-1, a MMP inhibitor. they observed that AMG479 and TIMP-1 inhibited p-IRS and p-AKT after IGF-1 stimuli. When they combined AMG479, TIMP-1

and sorafenib, they observed that p-IRS-1 and p-AKT inhibition was induced principally by AMG479. When they studied apoptosis they observed that the triplet combination of TIMP-1, AMG479 and sorafenib induced maximum apoptosis (in terms of PARP and caspase 3 cleavage) in the HT29 cell line, but did not show effects in the HTOXAR3 cell line (Figure 4.3C).

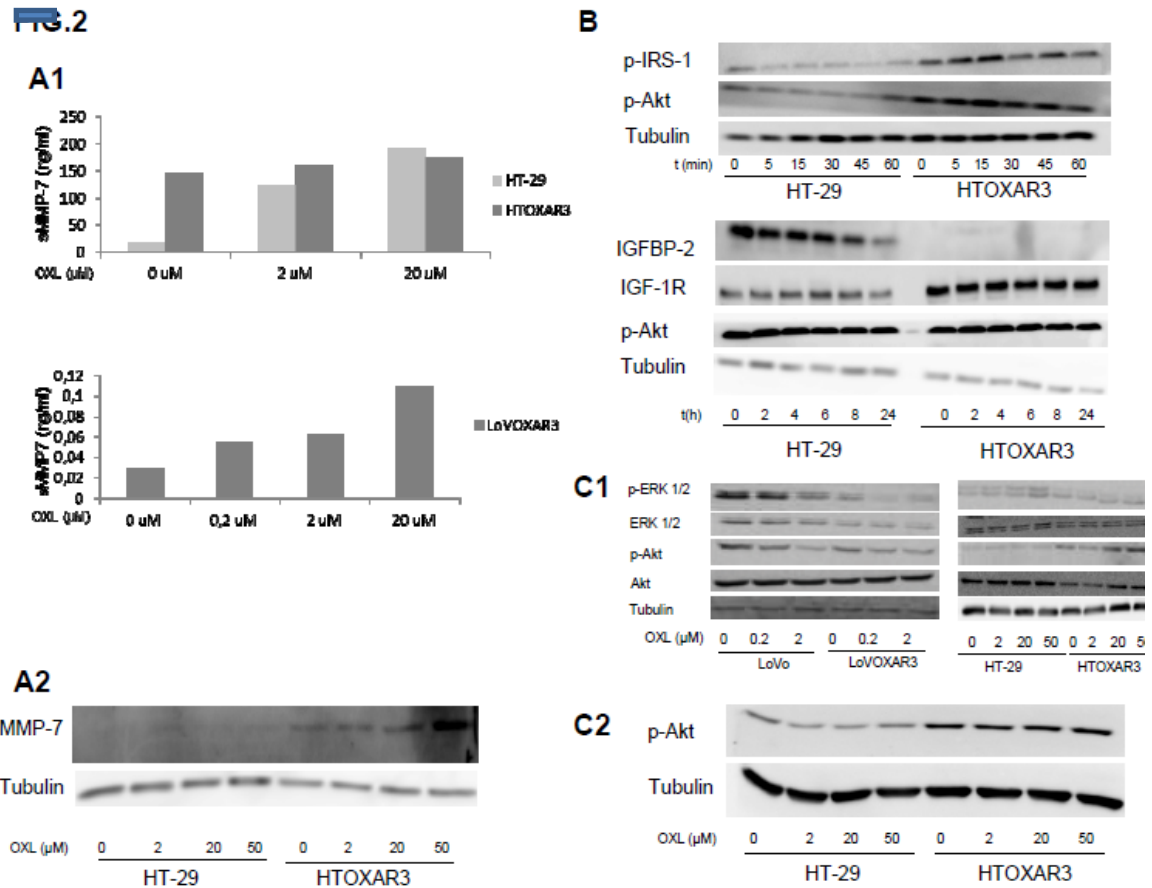


Figure 4.2. Activation of IGF-1R/PI3K-AKT pathway, in cells chronically treated with oxaliplatin, is due to increase of MMP7 and IGFBP degradation

(A) LoVo, LoVOXAR3, HT-29 and HTOXAR3 cells were treated with increased doses of OXL. MMP7 levels were analysed by ELISA method and WB after 48h after therapy.

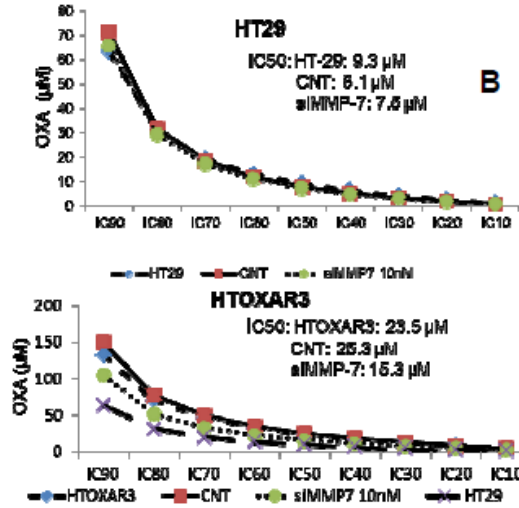
(B) HT-29 and HTOXAR3 cells were treated with OXL (20mM) and collected at indicated times. P-IRS-1, p-AKT, IGFBP-2 and IGF1R expression was assessed by western blot.

(C) Downstream effects on p-MAPK and p-AKT after different doses of OXL treatment (0.2, 2 and 20 mM) in LoVo, LoVOXAR3, HT-29 and HTOXAR3 cell lines.

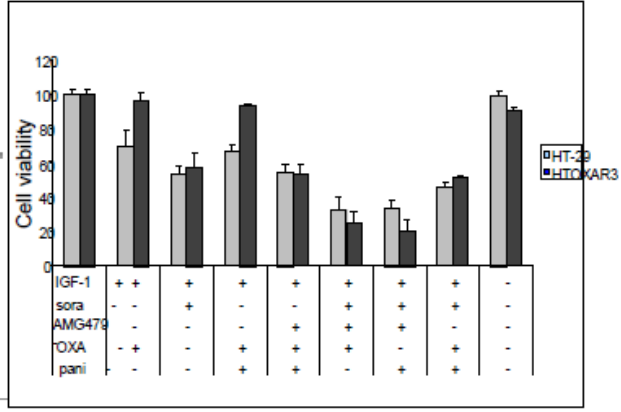
D) HT-29 and HTOXAR3 cells were treated with OXL (20mM) and phospho-AKT inhibition was analyzed at 1 hour after therapy.

FIG.3

A



B



C

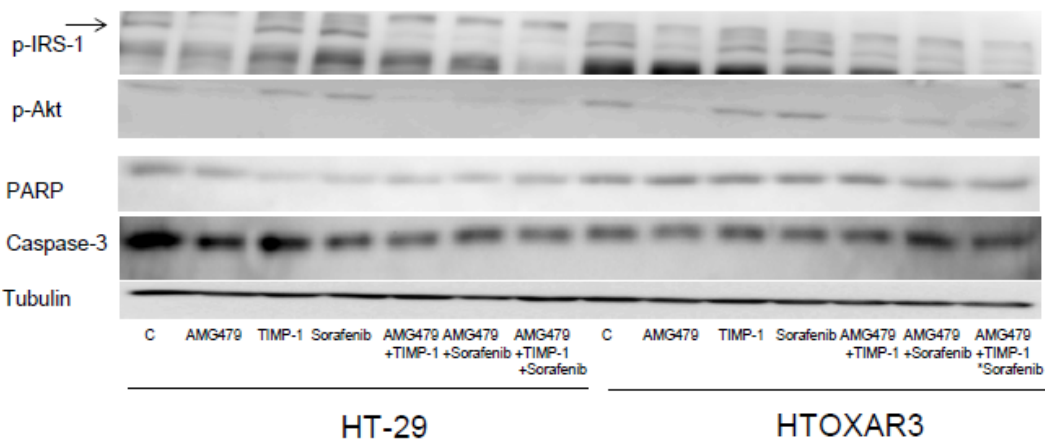


Figure 4.3 The IGF-1R inhibitor AMG479 combined with sorafenib prevents IRS-1-AKT signaling but not apoptosis in HT-OXAR3 OXL cells lines

- A) MMP7 was silenced and the effect on OXL-resistance was evaluated by MTT.
- B) Cytotoxic effects in parental HT-29 cell line and the resistant HT-OXAR3 cell line were analyzed after IGF-1 stimuli with oxaliplatin (5mM), panitumumab, (1mM), sorafenib 2 (mM), and AMG479 (5mM), and different combinations of these drugs.

C) Phosphorylation of IRS-1 and AKT were assessed in parental HT-29 and resistant HT-OXR3 cells treated with AMG479, TIMP-1 and sorafenib.

D) Effects on apoptosis (PARP and caspase 3) at 48 hours, in parental HT-29 cell line and the resistant HT-OXR3 cell line were analyzed after sorafenib, TIMP-1 and AMG479.

4.4 IGF-1R, p-IGF-1R and caveolin-1 are located differently in HT-29 and HTOXAR3 cell lines

It has been observed that IGF-1R was located in the nucleus in HTOXAR3 cells but this wasn't detected in HT-29 cell line (Fig 4.4A). By confocal microscopy they observed that IGF-1R membrane expression was more intensive in HTOXAR3. they also studied caveolin-1 as a possible protein implicated in the internalization of IGF-1R. Caveolin-1 is located mainly in the cytoplasm of HT-29 but in a sparse manner. In HTOXAR3 cells, caveolin-1 was abundantly located in the peri-nuclear area. In HTOXAR3 there is a fraction of cells clearly showing p-IGF-1R expression and activation in the nucleus, but this nuclear pattern was not observed in the parental cell line (Figure 4.4B and Fig 4.4

A tissue block of HT-29 and HTOXAR3 cell lines were performed to study cells characteristics with conventional immunohistochemistry. Differences were observed in the percentage of positive cells, being higher in HTOXAR3 (90%) compared to the parental cell line (30%). There were no major differences in the intensity of MMP7 expression between HT-29 and HTOXAR3 cell lines, with both cell lines showing strong cytoplasm expression. It has been observed that HTOXAR3 expressed p-IGF-1R in moderate-to-intense membrane and dot-like peri-nuclear patterns, compared to HT-29 cell lines, which also express p-IGF-1R as membrane and in the form of dot-like peri-nuclear patterns, but with a weak intensity. These immunohistochemical results confirmed the data obtained with confocal microscopy. (Fig 4.4C)

4.5 Phospho-IGF-1R in the nucleus is not inhibited in HTOXAR3 cell line by IGF-1R inhibitors

To further extend our findings, we examined by confocal microscopy the capacity of the tyrosine kinase inhibitor of IGF-1R AMG479 and AEW541 in HT-29 and HTOXAR3 cell lines to avoid nuclear translocation of IGF-1R. In HT-29 and HTOXAR cell lines, IGF-1R was inhibited in the membrane (Figure 5A and Supl. Fig 4.5). P-AKT was inhibited with and

without IGF-1 stimuli after AMG479 inhibition (Figure 4.5B). Despite p-IGF-1R membrane inhibition, p-IGF-1R was also located and remained in the nuclear area in the HTOXAR3 cell line (Figure 4.5C).

From November 2010 to December 2011, 113 consecutive mCRC patients were screened in 24 Spanish Hospitals in the ongoing prospective PULSE trial (NCT0128833) for p-IGF-1R (p-1316) MMP7 expression. Patients defined as DP should express MMP-7 (++ or +++ intensity in >66% of tumour cells) and p-IGF-1R (++ or +++ intensity in >66% of tumour cells); 48% of cases were positive for p-IGF-1R. Phospho-IGF-1R positive cases had different patterns of staining: peri-nuclear in 76%, 11% nuclear and only 13% membrane-apical staining. We found that tumours with positive p-IGF-1R expression, independently of the pattern of staining, had higher MMP7 co-expression (59%) compared with negative cases (13%, $p < 0.0001$) (Figure 6).

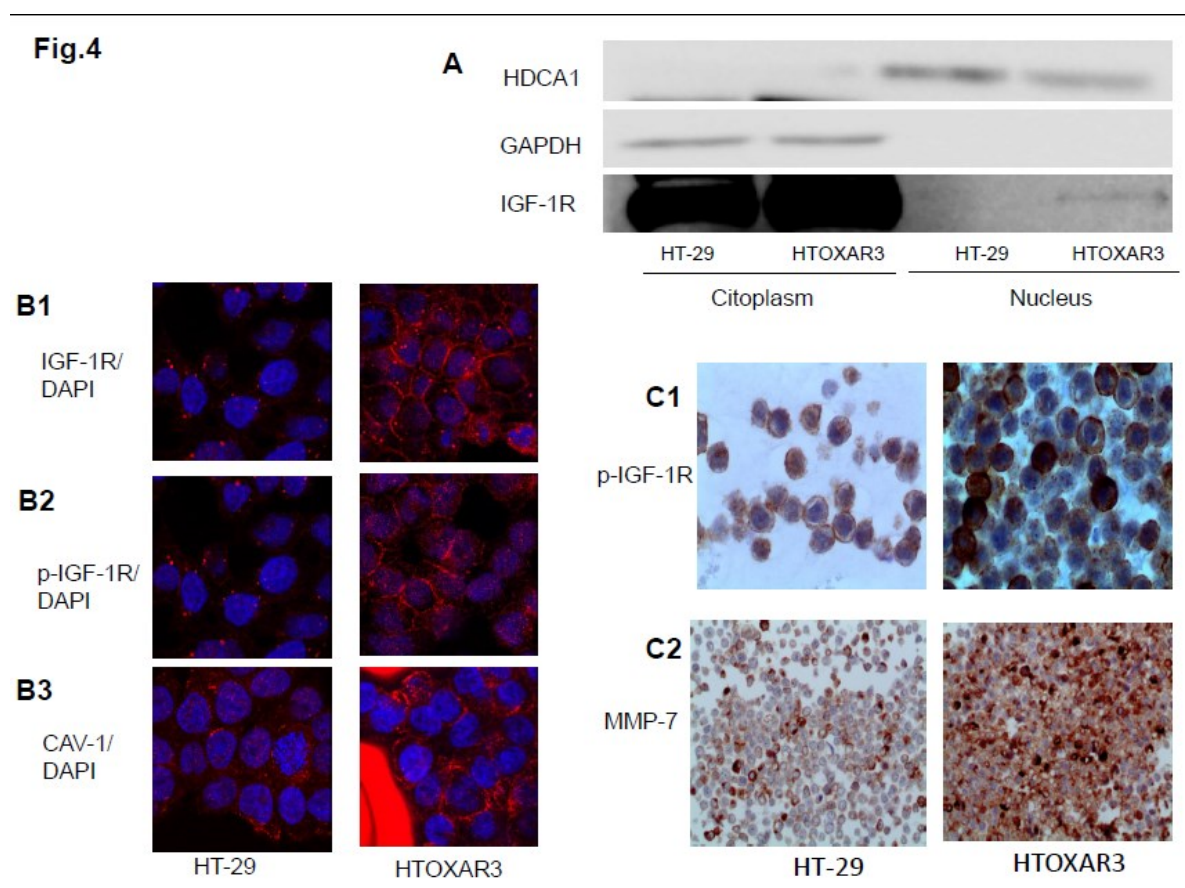


Figure 4.4 IGF-1R, p-IGF-1R (p-1316) and caveolin-1 are located differently in HT-29 and HTOXAR3 cell lines

(A). IGF-1R expression in the cytoplasm and in the nucleus was assessed by Western blot

(B1) Location of IGF-1R was assessed in the resistant HTOXAR3 and the parental HT-29 cell line with confocal microscope

(B2) Location of p-IGF-1R was assessed in the resistant HTOXAR3 and the parental HT-29 cell line with confocal microscope.

(B3) Location of caveolin-1 was assessed in the resistant HTOXAR3 and the parental HT-29 cell line with confocal microscope.

(C1) Location of p-IGF-1R in HT-29 and HTOXAR cell lines with a cell tissue block

(C2) Location of MMP7 in HT-29 and HTOXAR cell lines with a cell tissue block

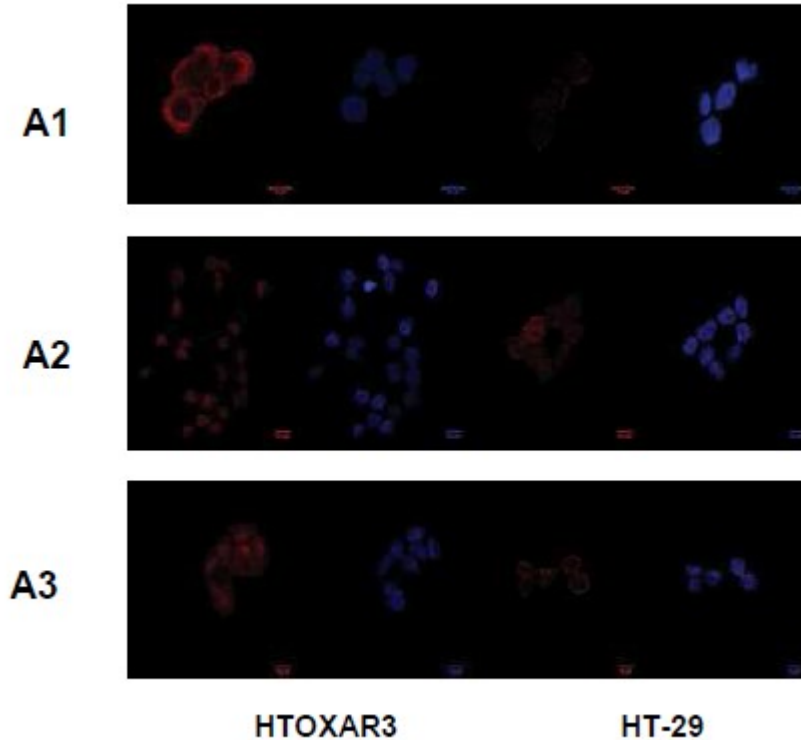


Figure 4.4 IGF-1R, p-IGF-1R (p-1316) and caveolin-1 are located differently in HT-29 and HTOXAR3 cell lines

(A1) Location of caveolin-1 was assessed in the resistant HTOXAR3 and the parental HT-29 cell line with confocal microscope

(B2) Location of p-IGF-1R was assessed in the resistant HTOXAR3 and the parental HT-29 cell line with confocal microscope.

(B3) Location of IGF-1R was assessed in the resistant HTOXAR3 and the parental HT-29 cell line with confocal microscope.

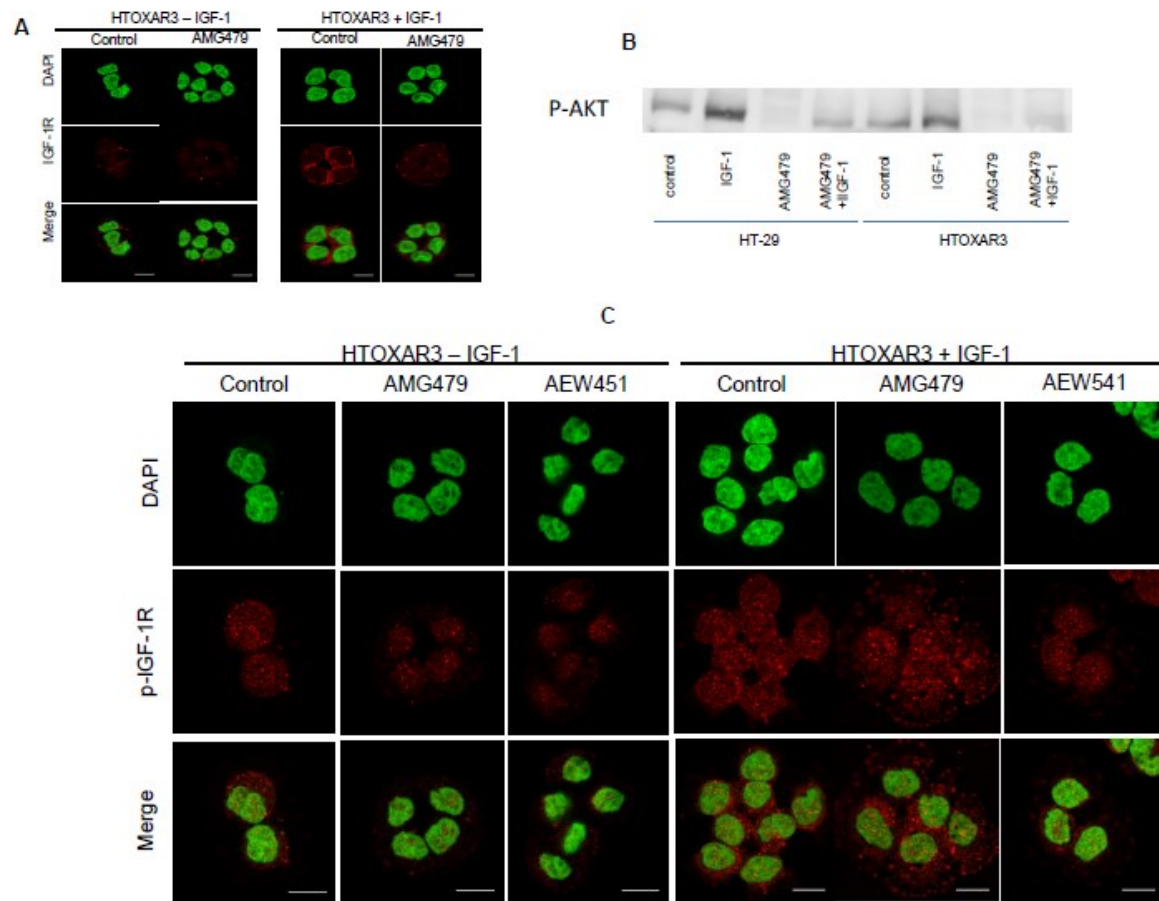


Figure 4.5: HT-29 and HTOXAR3 cell lines were treated with the IGF-1R monoclonal antibody (AMG479) and an IGF-1R tyrosine kinase inhibitor (AEW541). Changes in IGF-1R and p-IGF-1R (1316) were assessed with confocal microscopy.

A: IGF-1R expression with and without IGF-1 stimuli in HTOXAR cell lines after AMG479 treatment.

B: p-AKT expression with IGF-1 stimuli with and without IGF-1 stimuli in HT-29 and HTOXAR cell lines after AMG479 treatment.

C: p-IGF-1R (1316) expression with and without IGF-1 stimuli in HTOXAR cell line after AMG479 and AEW541 treatments.

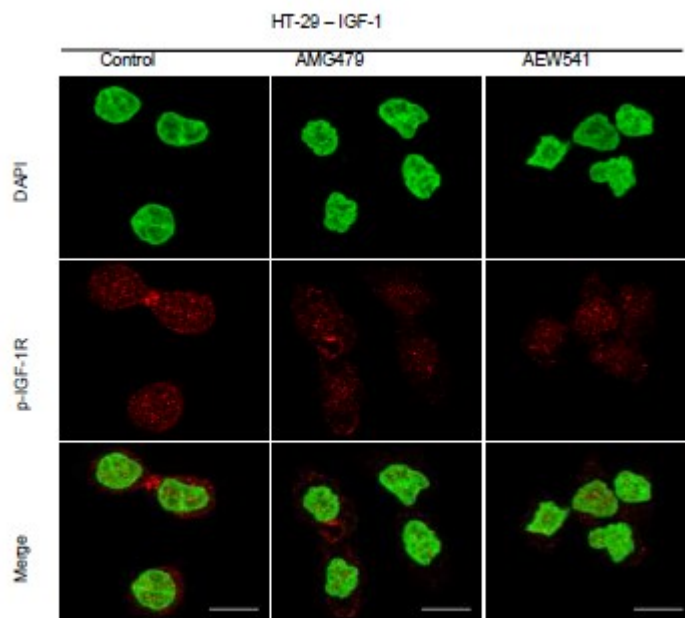


Figure 4.5 (supl): HT-29 cell line was treated with the IGF-1R monoclonal antibody (AMG479) and an IGF-1R tyrosine kinase inhibitor (AEW541). Changes of p-IGF-1R (1316) were assessed with confocal microscopy.

5- Discussion

Acquisition of drug resistance is the main hindrance to effective treatment. In spite of Discovery of a new therapies in colorectal cancer, nearly all patients become chemo-resistant. The present study focused on whether the status of IGF-1R signaling, known to be involved in colorectal cancer progression and growth, contributes to OXL-resistance. The study presents two major findings that might represent a previously uncharacterized mechanism of IGF-1R-related acquired resistance. First, increase of MMP7 in HTOXAR3 contributes to IGF-1R activation and OXL-resistance. Second, HTOXAR3 cell line showed constitutive activated IGF-1R, in part located in the nuclear area, compared with HT-29 and this location probably contributes to IGF-1R resistance.

In LoVo cell lines, AKT phosphorylation was repressed after low OXL exposure and this effect was durable (>24h). In HT-29, although p-AKT inhibition was observed at 1 hour with high doses of OXL, this effect was not sustained at 24 hours. The levels of MMP7 obtained in HT-29 after 24h OXL-exposure were similar to the basal levels in HTOXAR3 and to those achieved by Miyamoto et al., (2004), in HT-29 when 200 ng/mL MMP7, was added to artificially engage p-IGF-1R (8). In the HT-29 cell line, MMP7 increased at 24 hours after OXL treatment, achieving levels similar to those observed in HTOXAR3. hypothesizing that IGFBP-2 degradation can be due to increased MMP7. These very high levels of MMP7 are

then able to activate IRS-1/AKT pathway and preclude the effect of OXL. The study describes that this mechanism of IGF-1R activation by MMP7 is acquired after chronic OXL exposure. Since MMP7 silencing can reverse OXL-resistance in HTOXAR3, at least partially, MMP7 appears to play a crucial role in OXL-acquired resistance. These results are in accordance with published data by Hörndler et al., (2011), showing that this specific pattern (MMP7+/p-IGF-1R+) reflects a subset of patients who are clinically resistant to irinotecan and cetuximab.

IGF-1 regulates caveolin-1 and IRS-1 interplay in caveolae (Panetta et al., 2004). The mechanism by which caveolin-1 expression is increased in OXL-resistant cells (LoVOXAR3 and HTOXAR3) remains unexplained. Several reports indicate that in chemoresistant colorectal cancer cell lines, caveolin-1 expression is increased (Bender et al., 2000), probably as a consequence of detachment (i.e., due to low levels of IGFs) and an ability of tumour cells to survive in the absence of ECM-derived signaling (Ravid et al., 2005). Gallego et al., (2009) has also reported that patients with ACRC treated with chemotherapy show lower levels of IGF-1 and IGFBP-3 at tumour progression, concomitant with increased MMP7.

Two types of IGF-1R induction mechanisms have been recently described. An acute induction (as rapid as 48h) has been described with erlotinib in cell lines addicted to EGFR/AKT pathway (Sharma et al., 2010). Interestingly, the cell subpopulation with EGFR TKI tolerance also exhibits reduced sensitivity to cisplatin. additionally, IGF-1R could be induced with AKT inhibitors in HER-2/AKT dependent cell lines, and also in cell lines lacking HER-2 amplification but AKT-dependent, resulting in FOXO-dependent nuclear translocation and RTK driven signaling (Chandarlapaty et al., 2011). A second mechanism of IGF-1R induction in RAF-MEK dependent cells is mediated by down-regulation of IGFBP and a PI3K-AKT switch after chronic treatment with BRAF inhibitors (Villanueva et al., 2010). A third mechanism that occurs in colorectal cells tolerant to chronic OXL as a consequence of MMP7 increase and suggest IGF-1R/IRS-1/AKT engagement. A similar IGF-1R/IRS-1/AKT induction has been shown by IGFBP down-regulation after chronic erlotinib treatment (Guix et al., 2008). All these data suggest that IGF-1R induction and activation is a mechanism widely used by different types of tumours to acquire multi-drug resistance.

Simultaneous treatment with sorafenib and AMG479 induces maximum cytotoxic effects and AKT inhibition, but there was a modest apoptotic effect in HTOXAR3, suggesting

apoptotic-resistant pathways which are at least partially AKT independent. Therefore we assessed whether apoptotic resistance could be due to differences in p-IGF-1R location, observing that despite membrane p-IGF-1R inhibition with AMG479 and AEW541 in HT-29 and HTOXAR3 cell lines, there is a persistence of p-IGF-1R in the nucleus in the latter, speculating that phosphorylated IGF-1R in HTOXAR3, concomitantly with caveolin-1 increment could induce SUMOylation (Deng et al., 2011), allowing the translocation of part of the p-IGF-1R to the nucleus (Sehat et al., 2010). It has been reported recently that IGF-1R could work as a transcriptional enhancer in the nucleus by means of direct interaction with chromatin (Aleksic et al., 2010) and therefore mediate IGF-1R resistance in the nucleus by an AKT-independent pathway (Kulik and Weber, 1998; Remacle-Bonnet et al., 2007).

The data presented provide a strong rationale to explain why anti-IGF-1R compounds have low efficacy in chemo-resistant patients (Reidy et al., 2010; Eng et al., 2011; Watkins et al., 2011). Meaningfully, some colorectal cancer patients show initially p-IGF-1R in the nucleus, suggesting that a subset of colorectal cancer patients could be coherently resistant to anti-IGF-1R compounds and OXL (Cuatrecasas et al., 2011).

Matrilysin (MMP7) is known to activate pIGF-1R through IGFBP-3 degradation, and consequent releasing of IGF-1. In ACRC patients the co-expression of MMP7 and pIGF-1R (double positivity, DP) has been shown to correlate with poor prognosis in KRAS-WT patients treated with anti-EGFR (Cetuximab) in retrospective analyses (Hörndler et al., 2011). We recently performed a prospective clinical trial to validate those findings. Screening 196 mCRC patients treated with anti-EGFR (Panitumumab) in 24 Centers in Spain came out with a response rate of 56% in non-DP and of 67.6% in DP patients ($p=0.18$) and median PFS (95% CI) was 7.1 months (5.1-9.6) in non-DP and mPFS 9.9 months (8.1-15, $p=0.19$) in DP patients. Median overall survival (mOS) was 28.1 months (25.6-30) in non-DP patients vs 19.9 months (16.1-27.6, $p=0.004$). The multivariate (PS, LDH, age and sex) adjusted HR for mortality was 2.81 (1.33-5.96, $p=0.0069$). The results of this prospective study validates MMP7/pIGF1R as a novel strong prognostic biomarker in ACRC-KRAS-WT patients, treated in first-line with FOLFOX-6 plus anti-EGFR.

Overall, these results suggest that our anti-pIGR1R antibody could be considered a biomarker of response to immunotherapy in patients with ACRC.

6- Conclusion and Recommendations

These results have provided a full functional description of MMP7 and IGF-1R roles and interactions on the acquired resistance after chronic OXL exposure. Accordingly, nuclear IGF-1R location may contribute to intrinsic and acquired resistance to both OXL and anti-IGF-1R therapies. As this specific resistant pattern can be optimally evaluated by immunohistochemistry, with a specific antibody (IGF-1R-p-1316) (Rubini et al., 1999), we believe that our findings may allow potential new strategies to select patients with ACRC who are sensitive to chemotherapy and anti-IGF-1R compounds.

Part 2:

Effect of folic acid on proliferation and survival of HL-60 pro-myelocytic cells

1- Introduction and Review of literature

1.1 Folates:

1.1.1 Chemistry and properties:

Folate, commonly known as vitamin B9 is a water soluble vitamin, existed naturally in a wide variety of foods such as green vegetables, and encompasses a large family of compounds with same chemical structures and nutritional properties(Gropper et al ., 2005). Folate, mediates the transport of one- carbon moieties crucial for the *de novo* biosynthesis of purine and thymidylate, and thus is a fundamental factor for DNA synthesis, replication, repair, methylation reaction and deficiency of vitamin which has been shown to play a major role in the causation of various disorders including anemia, atherosclerosis, adverse pregnancy outcomes, and cancer(Kim, 2007). It's demonstration was dated back to 1931 by Lucy Willis who noticed that, extracts of liver and yeast when administered orally, were found to be effective in treating tropical macrocytic anemia(Willis, 1931; Shane, 1995). Subsequently, the specific nutritional factor in charge of the observed therapeutic benefit was isolated from liver extracts and the chemical structure was established to be N-[4-{{(2-amino-4-hydroxy-6-pteridiny)l)methyl]amino}bonzoyl]glutamic acid. Moreover, the name pteroylglutamic acid' was being proposed by the discovering scientist(Angier et al., 1946). the name folic acid was

concurrently proposed for nutritional factor with the similar nutritional properties that, had been isolated from spinach, with the word ‘ folic’ derived appropriately from Latin- *folium*(leaf)(Mitchel et al., 1941). The chemical structure of folic acid consists of three distinct components: para-aminobenzoic acid (PABA) is attached at one end to a 2-amino-4-hydroxy-pteridine (pteridin) moiety via a methylene group, and at the other end to one L-glutamic acid (glutamate) residue via a peptide bond(Shane, 1995).

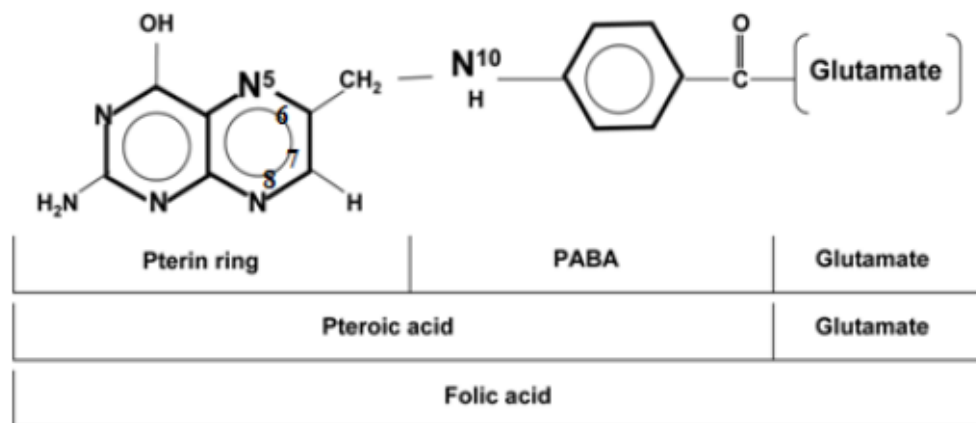


Figure 1.1 chemical structure of folic acid (pteroylmonoglutamate abbreviated as PteGlu). Folic acid consists of three distinct components: the pterine or (pteridine) ring, which is conjugated to PABA(para- aminobenzoic acid by a methylene bridge which together are called pteric acid , which is in turn joined to glutamic acid (glutamate) residue via a peptide bond reproduced from (Kim, 2007).

Folic acid is simply considered as parent structure of this large extended vitamin family existed as a stable, synthetic analogue that is found not only in supplement, but also added in fortified food. The term folate designate to the naturally occurring type of vitamin that is basically differ from folic acid in the oxidation rate of pteridine ring. Tetrahydrofolate THF is constituted of pteridine core ring system (2- amino- 4- hydroxyl – pteridine) that is linked in one side to p – aminobenzoic acid (also known as pteric acid) via a methylene bridge from the C – 6 position of pyrazine ring, therefore, forming tetrahydroptericoic acid. An additional link joins glutamate to the p- aminobenzoic acid with 1 to 9 residues. The pyrazine ring is completely reduced at the 5, 6, 7 and 8 positions forming the biologically active form, referred to as 5,6, 7,8 – tetrahydrofolate(THF). Dihydrofolate(DHF) is formed through two

consecutive reduction of 7 and 8 positions, using two molecules of Nicotinamide adenine dinucleotide phosphate(NADPH). Several other bioactive compound derive from this basic structure(Donnelly, 2001). Additionally, natural occurring forms of folate differ based upon the one carbon units attached at the N- 5 and / or N- 10 positions of THF(**table 1.1**) (Gropper et al ., 2005). In terms of stability, the reduced forms of folates depend upon the substituent of one- carbon. Nonetheless, reduced folates are categorically less stable compared to folic acid(Shane, 1995).

Table 1.1 one- carbon substitution of tetrahydrofolates

Folate derivative	One- carbon substitution
5- FormylTHF	-CHO
5, 10- MethenylTHF	=CH
5, 10 MethyleneTHF	=CH ₂
5- MethylTHF	-CH ₃
10- FormylTHF	-CHO
5- FormininoTHF	-CH=NH

1.1.2 Folinic acid:

Folinic acid, 5-formyltetrahydrofolate (5-CHO-THF), also known as leucovorin(LV) is usually responsible of 3- 10% of total intracellular folate in mammalian cells. Nevertheless its metabolic function in cells has not been fully elucidated(Stover and Schirch, 1990). Folinic acid is formed from 5,10-methenyltetrahydrofolate (5,10-CH=THF) by a hydrolytic reaction catalyzed by serine hydroxymethyltransferase(SHMT) and whereby serine interconverted into glycine(Stover and Schirch, 1990; Holmes, and Appling, 2002).Moreover, spontaneous chemical hydrolysis of 5,10-CH=THF might be a minor extra source(Baggott, 2000). 5-CHO-THF is not only considered as the most stable naturally occurring folate, but also the most enigmatic, as it is solely doesn't serve as a cofactor in one- carbon metabolism. 5-CHO-THF in place is a potent inhibitor of SHMT and many other folates dependent-

enzymes in vitro(Stover and Schirch, 1993; Roje., 2002). Furthermore, methyltetrahydrofolate synthase(MTHFS) is only enzyme known to metabolize 5- CHO-THF, by catalyzing the ATP-dependent and irreversible conversion of 5-CHO- THF into 5,10- CH=THF. MTHFS is found in the cytoplasm of the rabbit liver, whereas human liver accommodates about 85% of the MTHFS activity in the cytoplasm and 15% in the mitochondria(Maras et al., 1994; Bertrand et al., 1995). The joined enzymatic activities of MTHFS and SHMT make up the futile cycle that not only may reduce cellular 5- CHO-THF but also regulate SHMT activity(Stover and Schirch, 1993). The cytoplasmic one- carbon metabolism is accounted for the synthesis of purine, thymidylate, methionine and many subsequent S- adenosylmethionine dependent methylation reaction. Moreover, there is growing evidence that mitochondrial folate metabolism is mainly accountable for the production of formate hence mitochondrial derived formate is the source of one- carbon units requisite for cytoplasmic folate – dependent anabolic reactions(Appling, 1991). The key source of one- carbon units in the form of formate are produced from serine in a reaction catalyzed via mSHMT, nonetheless, formate can be generated in the mitochondria through glycine in cells which contain GCS(Cowin, 1996).the role played by mitochondria in generating one- carbon units for cytoplasmic folate indicates that cSHMT may not serve a chief role in the generation of one- carbon units. However, there is a mass of evidence indicating that cSHMT is not a resourceful of one- carbon units for cytoplasmic metabolism. Interestingly, a study by Narkewicz et al.,(1996) on Chinese hamster cells(CHO) which lack mSHMT activity have revealed that (CHO) cells deprived in mSHMT activity amass 15- fold increased intracellular serine concentrations over wild type CHO cells. Not surprisingly, CHO deficient mSHMT activity are auxotrophic for glycine. In spite of accumulation of intracellular serine, the net metabolic flux via cSHMT enzyme in CHO cells deprived in mSHMT activity is in the direction of serine synthesis. Accordingly, the prime role of cSHMT may not only be to generate glycine or one- carbon units but also instead may have other metabolic functions including the synthesis of 5- CHO- THF(Girgis et al., 1997).

1.1.3 Folate metabolism

1.1.3.1 Overview:

Folate is primarily transported into the cell in form of monoglutamate. Cellular folate leak out is prevented through polyglutamylaton, an energy dependent reaction whereby up to 9 glutamate units are added to the γ - carboxyl group of the glutamate tail, a reaction catalyzed by the folyl-poly- γ -glutamate synthetase enzyme(FPGS)(Shane, 1989). The activity of FPGS

has been well- characterized in many cells, and it shows affinity for THF as the primary folate substrate for polyglutamylation. Since the prime folate obtained from the diet are naturally occurring 5- methylTHF and synthetic folic acid, the cellular enzymes capable of converting these folate forms to THF, namely, methionine synthase(MS) and dihydrofolate reductase(DHFR), are seen as rate limiting for cellular folate accumulation(Lucock, 2000). The FPGS activity is antagonized by the lysosomal activity of γ - glutamyl hydrolase(GGH)(also referred to as folylypoly- γ -glutamate carboxypeptidase) which catalyzes the hydrolysis of these terminal γ -glutamyl residues from polyglutamylated folates(Ifergan et al., 2008). Intracellularly, five major folate- dependent one- carbon transfer reactions have been fully characterized: the interconversion of serine to glycine, the degradation of histidine, the synthesis of thymidylate, methionine and purine nucleotides. Additionally, the methyl or formyl groups contributed by the dietary intake of 5- methyl THF and 5- formylTHF, the one- carbon units utilized in folate- dependent one- carbon metabolism are mainly derived from the β - carbon of serine which is converted to glycine via the enzyme serinehydroxymethyltransferase(SHMT), as it moves the β - carbon group to a THF cofactor creating 5,10- methylenetetrahydrofolate(5,10- methylene THF). The formimino group resulted from the breakdown of histidine, the carbon moiety generated by glycine decarboxylase in mitochondrial degradation of glycine, the methyl moiety produced in the catabolism of choline to first sarcosine then finally to glycine, and cellular formate have all been found as an additional sources of one- carbon units(Lucock, 2000). Folates play a major role in the biosynthesis of pyrimidine and purine nucleotides, fundamental in the new synthesis of DNA and RNA as well as in the repair of damaged DNA. In purine biosynthesis, two one- carbon units from 10- formyl THF are placed in the first place to glycinamide ribonucleotide(GAR) via GAR transformylase enzyme forming N- formylglycinamide ribonucleotide(FGAR), and latter to aminoimidazol-4 – carboxamide ribonucleotide(AICAR) through AICAR transformylase enzyme forming N- formylaminoimidazol-4 – carboxamide ribonucleotide(FAICAR).the transferred formate moiety become carbons 8 and 2 of the purine ring. In the biosynthesis of pyrimidine, the methyl moiety of 5, 10- methylene THF is transported unto deoxyuridylate monophosphate(dUMP) forming deoxythymidylate monophosphate(dTMP) and dihydrofolate(DHF) in a reductive methylation interaction catalyzed by thymidylate synthase(TS) enzyme. DHF is reduced back unto THF via DHFR enzyme, moreover, the cofactor reduced Nicotinamide adenine dinucleotide phosphate(NADPH)(Kompis and Islam, 2005).not surprisingly, folates serve paramount

important biological function in the remethylation of homocysteine(Hcy) to form methionine, which is afterward converted unto S- adenosylmethionine(SAM), the sole methyl donor for all intracellular methylation reactions including DNA, RNA, protein, lipids and toxins. In remethylation of Hcy, firstly, 5,10- methylene THF is reduced to 5- methyl THF in an irreversible reaction catalyzed by methylenetetrahydrofolate reductase enzyme(MTHFR)(Green et al., 1988). 5- methyl THF transfers methyl group to Hcy creating methionine and THF via MS enzyme using B₁₂ as cofactor(Stokstad and Koch, 1967).

The biological functions played by different type of folate species need sophisticated interconversion cycles catalyzed by many different enzymes. Since these cycles intersect many pathways, it is fully appreciated that the interconversion of folate species used as a mechanism whereby aspects of metabolism are regulated. In proliferating cells, DNA synthesis is pretty important, moreover expression of the enzyme TS peaks during the Stationary phase of the cell cycle indicate an adequate supply of thymidylate. Increased thymidylate synthesis leads to elevated concentrations of DHF, which has been found to be an allosteric inhibitor of the MTHFR enzyme. Inhibition of MTHFR ensures that intracellular pools of 5,10- methylene THF are used in purine and pyrimidine synthesis rather than committed toward methionine formation(Matthews and Baugh, 1980). signaling plentiful methylation capacity, inhibiting MTHFR and therefore, the formation of 5- methyl THF. In reverse, increased levels of 5- methyl THF, ensuring decreased levels of SAM thus reducing methylation capacity, have been known to inhibit several non- critical methyltransferase enzymes, therefore conserving limited SAM for essential methylation reaction(Wagner et al., 1985; Lucock, 2000). As had already known the complex metabolism, regulation and interconversion of folate species in concert with the crucial roles that, played by folates in biosynthetic reactions. It is well evident that, folate nutrition is intimately linked to human health and disease.

1.2 Cell cycle:

Four phases have been well defined in eukaryotic cell division cycle: gap 1(G₁) during which the cell conducts a series of checks before entering the (S) phase, DNA stationary phase (S), where DNA synthesis is occurred), gap 2(G₂), similarly the cell check its readiness to proceed to mitosis and mitotic phase(M), is when the cell actually divides(Howard and Pelc, 1953).passing through the cell cycle is tightly controlled and neatly coordinated by a large family of cyclin dependent kinases(cdk), heterodimer complexes

containing internal catalytic kinase domain beside a regulatory cyclin domain and subsequently, forming a family divided into two groups based upon their roles in cell cycle progression and transcriptional regulation (Meyerson et al., 1992; Sausville, 2002). Members of the first group comprise the core part of the cell cycle machinery, which include cyclin D-dependent kinases 4 and 6 and cyclin E- cdk2 complexes as well, which sequentially activate the retinoblastoma protein (Rb), to facilitate the G1→S transition. Cyclin kinases are choreographed and activated by binding to their respective cyclin proteins (Sherr, 1994; Morgan, 1995). Regulated via phosphorylation, controlled by cdk- activating kinases (CAK; cyclin H/cdk7/ MAT1), and inhibited via cdk inhibitors by their association with cyclins and endogenous Cip/Kip or INK4 (inhibitor of cdk4) inhibitors (Solomon, 1993; Hengst et al., 1994; Reed et al., 1994; Sherr and Roberts, 1995; Harper and Elledge, 1998). The cdks finely regulate biochemical pathways, or checkpoints, which combine mitogenic and growth inhibitory signals and track chromosome integrity (Murray, 1992; Hartwell, 1992). The cyclins serve a paramount regulatory role in this process as they are synthesized and catabolized over relatively short periods of time at sharply defined points of the cell cycle (Reed, 1992; Sherr, 1993). Intriguingly, cyclin A- dependent kinases 2, 1 along with cyclin B- cdk1 complexes are a prerequisite for orderly progression and passing through G1 into S and the G2→M transition, respectively (Pines, 1991; Sherr, 1994). In cancer cells, both altered expression of cdk and their modulators as well as overexpression of cyclins and loss of expression of cdk inhibitors, subsequently, deregulated cdk activity, providing a selective growth advantage (Sherr, 1996; Hall and Peters, 1996). Paradoxically, cdks governing the transitions between cell cycle phases transcriptional cdks, containing cyclin H-csk7, and cyclin T- cdk99pTEFb), promoting initiation and elongation of nascent RNA transcript via phosphorylating the carboxy-terminal domain (CTD) of RNA polymerase II (Prelich, 2002; Palancade and Bensaude, 2003).

On one hand at the cellular level, each single cell must go through the cell cycle in a tidily and well controlled fashion where the multiple steps connected with each other must be successfully and efficiently completed prior to the next. On the other hand, at the tissue level, there is experimental as well as clinical data suggesting similar progression through the cell cycles in specific organ entering S- phase and mitosis at specific times of the day (Scheving, 1984).

1.2.1 The G1→ S transition:

The retinoblastoma susceptibility protein(Rb), plays a pivotal role in the G1→ S transition. As in its hypophosphorylated state, Rb abrogates progression from G1→S by interacting with E2F transcription family members. This reaction blocks the transcriptional activation of E2F, furthermore, actively inhibits transcription via recruiting histone deacetylases to the promoters of genes required for entering S- phase(Weinberg, 1995; Harbour and Dean, 2000). During cell cycle progression, Rb is inactivated through sequential phosphorylation directed by cyclin D- dependent kinases^{4,6} and cyclin E- cdk2 complexes. In response to mitogenic stimulation cells produce D- type cyclin which merge with cdk⁴ and ⁶, a process that necessitates contribution of a cip/kip family member. Cip/ kip family members are not only promote activity of cyclin D-dependent kinases, but also are potent inhibitors of cdk2(Lundberg and Weinberg, 1998; Harbour et al., 1999; Sherr and Roberts, 1999). Accordingly, cyclin D- dependent kinases promote G1 progression through phosphorylating Rb, then relieving transcriptional inhibition via the Rb- E2F complex, moreover, by sequestering Cip/Kip proteins, promoting activation of cyclin E- cdk2, which directed Rb phosphorylation dissociates the binding of Rb to E2F, letting on E2F activation, as well as transcription of genes requisite for S- phase entry and furtherance including cyclin E *per se*(Botz et al., 1996; Geng et al., 1996). Much as Rb is the main target of cyclin D- dependent kinases, cyclin E- cdk2 activates other targets, including p27^{kip1}(Sheaff et al., 1997; Vlach et al., 1997).conjointly, G1 progression is regulated by members of the INK4 family, act as specific inhibitors of cdk⁴ and ⁶. p16 INK4A amasses as long as cells age inducing G1 arrest during senescence by assembling with cdk⁴ and ⁶ promoting freeing D- type cyclins. subsequently, damaging of D- cyclins and the redistribution of Cip/Kip proteins to cdk2 contributes to G1 arrest(Jiang et al., 1998; Sherr, and Roberts, 1999).

1.2.2. S- phase progression:

Following phosphorylation of Rb, directed by cdk during G1, E2F restored its activity, and later freed to bound its heterodimeric partner, DP-1, mediates, transcription of genes needed for S phase. This transcription is temporarily activated. Tidily and orderly S- phase succession necessitates the downregulation of E2F-1 activity, partly, achieved by cdk-mediated phosphorylation(Krek et al., 1994; Dynlacht et al., 1994; Xu et al., 1994; Kitagawa et al., 1995). Repression of cdk activity during S Phase leads to inappropriately persistent E2F, known to cause S- phase delay and apoptosis as well.E2F-1- induced apoptosis can happened due to both p53- dependent and p53- independent mechanisms. The very latter involving the

activities of E2F-1 transcriptional targets, such as p 73, Apaf-1, caspase 3; inhibition of Mcl-1; or the capacity of E2F-1 to interact with death receptor and nuclear factor- kappa B(NF-κB) pathways(Phillips et al., 1999; Phillips and Vousden, 2001; Croxton et al., 2002).

1.2.2.1 Phosphorylation of E2F-1:

E2F-1 is phosphorylated by several cdk holoenzyme during S and G2 phases, furthermore, they take part in the appropriately timed neutralization of its activity. Cyclin A-cdk2 stably interacts with N- terminus of E2F-1, and mediates the phosphorylation of E2F-1 (most likely at Ser³⁰⁷), and DP-1 as well, which represses the DNA binding activity of the dimer(Krek et al., 1994; Kitagawa et al., 1995). Phosphorylation by cyclin A-cdk1 at Ser375 may well promote the formation of Rb-E2F-1 complexes, contributing to the turning off of E2F-1 activity late in cell cycle. In such a way that, repression of cdk1 would allow the persistence of E2F-1 release of Rb(Chen et al., 1999). Ultimately, the activity of kinase is associated with general RNA polymerase transcription factor IIH(TFIIH) multisubunit protein complex, cyclin H-cdk7/MAT-1, activates E2F-1 at Ser⁴⁰⁸ and Thr⁴³³, precondition for ubiquitination and degradation. Mutation of these regions to alanine greatly enhances E2F-1 stability(Vandel and Kouzarides, 1999). The targeting of E2F-1 phosphorylation through cdk repression may selectively, result in death among transformed cells. The disrupted cyclin D-cdk4/6- INK4- Rb pathway in tumour cell brings about high level of E2F-1 activity. A small reduction in cdk activity during S phase may result in persistence of E2F activity, which has minimal effect on normal cells, however it may leave transformed cells with unsuitably persistent E2F activity at a high level enough to excel the threshold necessary to induce apoptosis(Chen et al., 1999).

1.3 Ultraviolet radiation UV:

UV radiation is a non – ionizing form of radiation, located in a region of electromagnetic spectrum ranging between 100 nm to 400 nm wavelength. UV radiation is arbitrarily categorized into UV- A(315 nm to 400 nm), UV- B(280 nm to 315 nm) and UV- C(100 nm to 280 nm)(Jo, 2005). Recently, according to the International Agency for the Research on Cancer, both UV-A and UV-B has been classified as a class I carcinogen(El Ghissassi et al., 2009). Possibly, the middle wavelengths of UVB radiation are considered as the most important for cytotoxicity(Ichihashi et al., 2003). Whereas, UVC a highly energetic radiation is irrelevant from a public health perspective, as essentially all of it is absorbed by atmospheric ozone. However, studies on UVC radiation can be conducted using economic

germicide lights that emits chiefly at 254 nm, close the maximum for DNA absorption(Ichihashi et al., 2003).

Cellular DNA is the prime target of UV radiation. Since the energy of UV light had been absorbed by a DNA double bond in pyrimidine bases(thymine and cytosine), brings about bond opening and subsequent reactivity with adjacent molecules. Unfortunately, if the neighboring base is another pyrimidine, a newly covalent bond establishes between them leading to the four membered cyclobutane ring of the pyrimidine dimer. Additionally, a single bond may establish between two carbon atoms on the cyclobutane ring leading to the so called "6-4(T-C) photoproduct(Lindahl and Wood, 1999; Sinha and Haider, 2002; Dunkern and Kaina, 2002; Sancar et al., 2004;). Although the same lesions are caused by UVB radiation they account for about half the cytotoxicity, with the most of the rest attributed to oxidative damage to DNA along with other cellular targets. UVB and UVA generate considerable levels of reactive oxygen species(ROS), such as peroxides, singlet oxygen and transient hydroxyl radicals. damage induced by UVA radiation is mainly ascribed oxidative damage with generation of only insignificant levels of photoproducts such as pyrimidine dimers(Tyrrell and Pidoux, 1986; Ichihashi et al., 2003).

1.4 c-Myc proteins:

The Myc proteins are a basic- helix-loop-helix-leucine zipper(BHLH-ZIP) transcriptional factor playing paramount roles in cell growth as well as proliferation, thanks to their capacity to down-regulate or upregulate genes expression, that collectively induce cellular transformation. Additionally, cell cycle regulation. Accordingly, Mutation, amplification, or activation of the Myc oncogene family is the most frequent events associated with cancer(Lüscher and Larsson, 1999; Fernandez et al., 2003; Levens, 2003; Adhikary and Eilers, 2005; Eilers and Eisenman, 2008). Furthermore, c-Myc is much often activated in acute myeloid leukemia(AML), playing pivotal role in the genesis of leukemia(Hoffman et al., 2002; Renneville et al., 2008). Nevertheless, the expression of c-Myc protein in normal cells correlates with cell growth, whereas expression is deficient in quiescent cells but is rapidly induced upon the supplementation with growth factor. Interestingly, the half-life of c-Myc is as short as 20-30 minutes indicating that, its level perturbations dynamically upon a broad range of cellular activities. Moreover, the expression peaks 3-4 h following growth factor stimulation, and lower level found in cycling cell. Growth factor withdrawal at any point in cell cycle leads to prompt down regulation(reviewed in Mateyak et al., 1997; Chan et al.,

2004). Furthermore, Mateyak et al.,(1997), reported that c-Myc in rat fibroblast caused a distinct prolongation of cell doubling time, proposing a fundamental role c-Myc in regulating cell proliferation.

To exert its function it is necessary that, Myc heterodimerize with its respective partner Max, a stable and constitutively expressed ubiquitous protein. Myc and Max bind through their canonical BHLH-ZIP subunits, and consequently bind to E box DNA sequences containing the core consensus sequence CACGTG(reviewed in Grandori et al., 2000; Amati et al., 2001). Inhibition of c-Myc could be accomplished via the DNA binding activity of c-Myc by disruption of c-Myc/Max heterodimerization(Dang, 1999). 10058-F4 is small molecule c-Myc inhibitor. Mediates its function by preventing the binding of c-Myc/ Max dimer, and resulting in inhibiting proliferation, cell cycle arrest and inducing apoptosis via mitochondrial pathway. Moreover it found to induce myeloid differentiation(Huang et al., 2006).

1.5 Apoptosis:

1.5.1 Overview:

Apoptosis not only is an important process , but also is tightly regulated and controlled forms of cell death, presumably genetically programmed hence called programmed cell death that, takes place under different variety of physiological and pathological conditions. Historically, the term apoptosis is dated back to 1972 when Kerr, Wyllie and Currie described a morphologically definite form of cell death, albeit specific types of apoptosis had been explicitly described many years before(Kerr et al., 1972; Paweletz, 2001; Kerr, 2002). Our knowledge of the detailed mechanisms entailed in the process of apoptosis in mammalian cells is well known, thanks to the exhaustive investigation of programmed cell death that occurs during the development of nematode *Caenorhabditis elegans*(Horvitz, 1999). Intriguingly, in this organism 1090 of somatic cells are generated during the formation of adult worm. Among which 131 of these cells undergo apoptosis. These 131 cells die at specific points during the developmental process, which is fundamentally invariable between worms, displaying the astonishing accuracy and control in this system. Apoptosis has long since been recognized and accepted as a characteristic and important way of programmed cell death that, involves the genetically determined elimination of cell. Nonetheless, it is noteworthy that, other forms of apoptosis has been described, and other forms may yet be discovered(Formigli et al., 2000; Sperandio et al., 2000; Debnath et al., 2005) Apoptosis has been

acknowledged to be of paramount importance for embryonic development, tissue homeostasis, neurodegeneration, autoimmune diseases, AIDS, carcinogenesis, cancer progression and murdering of cancer cells induced by chemotherapeutic drugs(Wyllie, 1980; Cohen, 1991; Ameisen, 1994; Kerr et al., 1994; Friesen et al., 1996; Gehri et al., 1996; Kusiak et al., 1996; Jacobson et al., 1997).

1.5.2 Morphology of apoptosis:

Both light and electron microscopy have identified different diverse morphological changes that occur during apoptosis(Hacker, 2000). Morphologically, apoptosis initially characterized by a change in the refractive index of the cell later ensued by cytoplasmic shrinkage and nuclear condensation. The cell membranes starts showing blebs or spikes(protrusions of the cell membrane), depending upon cell types. And at the last, these protrusions pinch off from the dying cells to form “ apoptotic bodies” furthermore, apoptotic cells stop maintaining phospholipid asymmetry in the cell membranes, and thus Phosphatidylserine externalized to the cell surface(Hengartner, 1997; Williamson, 2000).The mitochondrial outer membrane (MOM) undergoes changes which include loss of its electrochemical gradient, perhaps by forming pores in MOM, moreover, substances such as cytochrome c leak from MOM into the cytoplasm. Finally, a nearby cells or macrophages engulf apoptotic bodies and dying cells. The apoptotic bodies does not initiate an inflammatory response, and only individual cells are affected by apoptosis in vivo. These morphological changes are attributed to a distinctive molecular and biomedical events occurring in an apoptotic cells, most remarkably, the activation of lysosomal proteolytic enzymes which in the course of time mediate the cleavage of DNA into oligonucleosomal fragments and the cleavage of a multitude of specific protein substrate, which establish the unity, integrity and shape of the cytoplasm or organelles(Saraste, 2000). Not surprisingly, the events of apoptosis are diametrically different from necrosis. The cytoplasm and mitochondria of necrotic cells balloon out, and ultimately the cells and many of its organelles lyse. There is no apoptotic body formation, and often necrosis affects groups of neighboring cells. The necrotic cell remnants are phagocytosed by macrophages, and inflammatory responses are provoked in vivo(Leist and Jäättelä, 2001).

1.5.3 Molecular mechanism of apoptosis signaling pathways:

Apoptosis is a complex, multifaceted and highly efficient cell death program which requires interaction of multiple factors. The constituents of the apoptotic signaling plexus are

genetically encoded, moreover, are considered to be usually in place in nucleated cells ready to be triggered by death inducing stimulus (Ishizaki, 1995; Weil, 1996). Apoptosis can be caused and triggered by diverse type of stimuli from either outside or inside the cell, e.g. treatment with cytotoxic or irradiation, by deficient of survival signal, incongruous cell cycle signaling or by developmental death signal, by ligation of cell surface receptors, by DNA damage. Much knowledge of cell death has stemmed from genetic studies in the nematode *C. elegans* whereby several genes have been discovered ([Hengartner, 1999]). The proximate cause of apoptosis in *C. elegans* is the stimulation of cysteine protease ced-3 (is the single *C. elegans* member of a family of the caspases) that is directed by its oligomerization at the activation protein ced-4 (analogy to the mammalian apoptotic protease activating factor 1, Apaf-1), leading to the activity of ced-3/ ced-4 complex which is controlled by apoptosis inhibitor ced-9 as well as apoptosis inducer egl-1. ced-9 and egl-1 are members of the Bcl-2 family of pro- or antiapoptotic proteins (Richardson, 2002).

1.5.3.1 Caspases:

The name caspases is an acronym for cysteine – dependent aspartate- specific protease; their catalytical action depends upon a crucial cysteine residue inside a highly conserved pentapeptide sequence QACRG active site, and the caspases distinctively split their cellular substrate after Aspartic acid residues. They function by attacking cytoskeletal as well as nuclear proteins important for retaining cell architecture, and enzymes entailed in metabolism and repair. Hitherto 7 different caspases have been discovered in *Drosophila*, and 14 different members have been defined in mammals. Additionally caspase -11 and caspase -12 solely identified in the mouse (Gorman et al., 1998; Denault, 2002; Richardson, 2002). Based on its function, caspases have been categorized into two groups: upstream, apical or initiator caspases such as -2, -8, -9 and -10, and downstream, effector or executioner such as caspases -3, -6, and -7 (Ashkenazi and Dixit, 1998; Nicholson, 1999). Caspases are synthesized as inactive pro-enzymes whose activation is set off through vast array of internal and external stimuli (reviewed in Li and Yuan, 2008). It wasn't until receipt apoptotic stimuli, cells energize and activate apical caspases which in turn and in proteolytic cascade cleave and actuate the executioner caspases. After becoming active, executioner caspases proteolytically split a variety of substrate resulting in the destruction of dying cell (Fischer et al., 2003). Structurally, active caspases have a highly conserved homodimeric structure stemming from the combination of two identical monomer catalytic domains. Each catalytic domain comprising

of one active site that contains one large(20 k Da) as well as one small(10 k Da) domains. Upon maturation, pro-caspases(latent zymogens) are proteolytically processed at the cleavage site positioned between the large and the small domains. During caspase activation, both the small and large subunits assemble, forming a heterodimer with both subunits contributing important residues for substrate binding and catalytic activities as well (Nicholson and Thornberry, 1997; Gupta, 2000). Furthermore, the apical caspases are distinguished by long pro-subunit that act as platform for recruiting activated adaptor proteins. The pro-domain of both caspase -2 and 9 possess a caspase recruitment domain(CARD),compared to caspase -8 and -10 embody two tandem repeats of the death effector domain(DED). In each case, these subunits interact homotypically with adaptors that promote caspase activation via a mechanism of introduced propinquity, wherein the close juxtaposition of two caspases results in the formation of an active caspase tetramer. Activation and initiation of caspases may transpire through either an extrinsic or an intrinsic pathway(reviewed in Danial and Korsmeyer, 2004).

Intrinsic pathways are initiated by procaspase-9 which is triggered downstream of mitochondrial proapoptotic events at apoptosome, a cytosolic death signaling protein complex that is formed on the release of cytochrome c from mitochondria. In that event, procaspase-9 molecule dimerizes at the Apaf-1 scaffold that triggers the activation of caspase -9(Salvesen and Renatus , 2002b; Denault, 2002). Once the apical caspases have been triggered, they proteolytically and hierarchically activate the executioner procaspase-3, -6 and -7 which subsequently cleave a specific set of protein substrates, including pro-caspases themselves, leading to the mediation and amplification of the death cue and finally in the execution of cell death with all the morphological and biochemical characteristics usually observed [Earnshaw, 1999].

Extrinsic pathways are directed by procaspase-8 that is recruited by its DED to the death inducing signaling complex(DISC), a membrane receptor complex formed consequently the ligation of the tumor necrosis factor receptor(TNFR) family. Once bound to DISC, several pro-caspase-8 molecules are in close proximity to each other and are assumed to activate each other accordingly via autoproteolysis(Sartorius et al., 2001; Denault, 2002).

1.5.3.2 Intrinsic pathway:

DNA damage inevitably, result in either upregulation of Bax or downregulation of Bcl-2 that subsequently permeabilize the mitochondria to liberate pro-apoptotic factors for

instance cytochrome c, a well-known trigger of pro-caspase-9 activation, ensuing by downstream apoptotic effectors(Crompton, 2000). Nonetheless, it has been proved that in response to DNA damage, activation of caspase-2 is prerequisite ahead mitochondria permeabilization and release of cytochrome-c(Guo et al., 2002; Lassus et al., 2002; Vakifahmetoglu et al., 2006). After freeing cytochrome-c, it attaches to apoptotic protease activating factor Apaf-1 forming apoptosome(multi protein complex), in nucleotide dATP/ATP dependent manner(Zou et al., 1999). Afterward the apoptosome recruits pro-caspase-9 forming an active holoenzyme, that additionally activates downstream effector caspases namely caspase-3 and -7 and then results in programmed cell death(Jiang and Wang, 2004).

2- Rationale and specific aims:

Folate bioavailability could paradoxically influence the response of cells to UV-light exposure, as well as to anti-folate cancer drugs, both in terms of inhibiting proliferation, and in terms of prolonging cell survival (escape from apoptosis). Folate depletion could result in uracil misincorporation, that could activate *onco- protein* such as c-Myc which augur bad for carcinogenesis. While excessive folate administration not only may reinvigorate and revive cells, but also may adversely act against treatment. Fortunately c-Myc activity can be abolished by using antic-Myc 10058-F4. However this might affect normal cells that express small amount of this protein Intriguingly it has been published that, SHMT can bypass the effect of c-Myc. Furthermore, cSHMT catalyzes the hydrolysis of 5,10 methenyl THF to folinic acid which is canonical in reversing the effects of antifolate drugs, additionally, the chemopreventive function of folic acid which 100 time less stronger than folinic acid maybe linked to its capacity to down-regulate IGF-1R level. Accordingly we would like to use folinic acid hoping that it might mimic the role played by SHMT.

The present project is aimed to use a human pro-myelocytic cell line (HL-60) and PHA-activated human Lymphocytes to test the effect of folates (folinic acid) on the response to UV-light, serum free medium, presence of growth factor and anti c-Myc

Different doses of folates and UV exposure will be tested and relative kinetics of proliferation and apoptosis will be recorded. The distribution of cells in the cell cycle phases will be monitored by PI incorporation and flow cytometry analysis.

3. Methodology and Results

3.1 Cell culture:

The established cell line of transformed human promyelocyte leukemic cell line (HL- 60), a kind gift from Dr Paola Secchiero from (Human anatomy unit, university of Ferrara),it is round mononuclear cell, with microvilli. Moreover, it is well known that HL-60 was found rapidly undergoes apoptosis after a short periods of UV exposure(Martin and Cotter, 1991), was routinely cultured in Iscove's Modified Dulbecco's Medium(Gibco Life technologies), supplemented with 5% fetal bovine serum(Gibco Life technologies), and kept at 37° C in an atmosphere of 95% air and 5% CO₂.

3.2 Irradiation of cells with UVC light:

Prior to treatment with UVC, cells were maintained in serum starved Iscove medium , then plated in six petri dishes(Becton Dickinson USA), at density $4 \times 10^6/4\text{ml}$ for each. Next day each plate was placed uncovered in UV stratalinker(stratagene model 1800: 8 watts each) under a UV bulb emitting chiefly 254-nm for different time 0(untreated), 0.1, 0.5,

1, 5, and 10 minutes. Then incubated at 37° C in an atmosphere of 95% air and 5% CO₂ for 2 hours. After that cells were harvested(day 0) and the plate supplemented with 500 µl fetal bovine serum. Then cells were harvested after 1, 2, 3, 6 and 7 days whereby cell count and cell viability as well were checked using haemocytometer and trypan blue dye exclusion.

3.3 Trypan Blue dye Exclusion:

10µl of the cell suspension was then added to 10µl of trypan blue(Sigma, Dorset, UK). 10µl of this mix were aliquoted and loaded into the haemocytometer. To assess the concentration of HL-60 and PBMCs, the live cells (white cells) were counted in two diagonal quadrants in both sides and divided by 105 to give the number of cells per ml of cell suspension. The number of blue cells (dead cells) was also counted in two diagonal quadrants. The % viability was calculated by the following equation:

$$\text{Viability \%} = \frac{\text{number of white cells}}{\text{number of total cell (white and blue)}} \times 100$$

3.2.1 Results:

Not surprisingly, cells thrive, flourish and proliferate in presence of fetal bovine serum since its rich in growth factor(p>0.05). Accordingly, UVC untreated cells have nearly quadruple its number by day 3, and after that its number steadily began to level off and decline. meanwhile cells that have been treated for short dose undergo transient arrest as it had halted proliferating for a while then re-entered cell cycle and restore back its proliferative capacity by day 6, no significant difference between UVC untreated cells and that treated with short dose(p<0.05). Whereas cells that subjected to a relatively short and high doses of UVC have resulted in initial cell cycle arrest hence cells nimbly underwent apoptosis en masse as no much difference between two doses(p<0.05) depicted in table and figure

Table 3.1 shows – **UVC induced apoptosis (cell proliferation) using haemocytometer:**

time	0	1	2	3	6	7
0 min	1.565	1.97	2.595	4.125	3.525	0.2115
0.1 min	1.545	0.725	0.46	0.36	1.085	2.17
0.5 min	1.525	0.68	0.255	0.1	0.02	0
1 min	1.45	0.57	0.135	0.05	0.005	0

5 min	0.83	0.2	0.015	0.01	0	0
10 min	0.29	0.015	0.0125	0.005	0	0

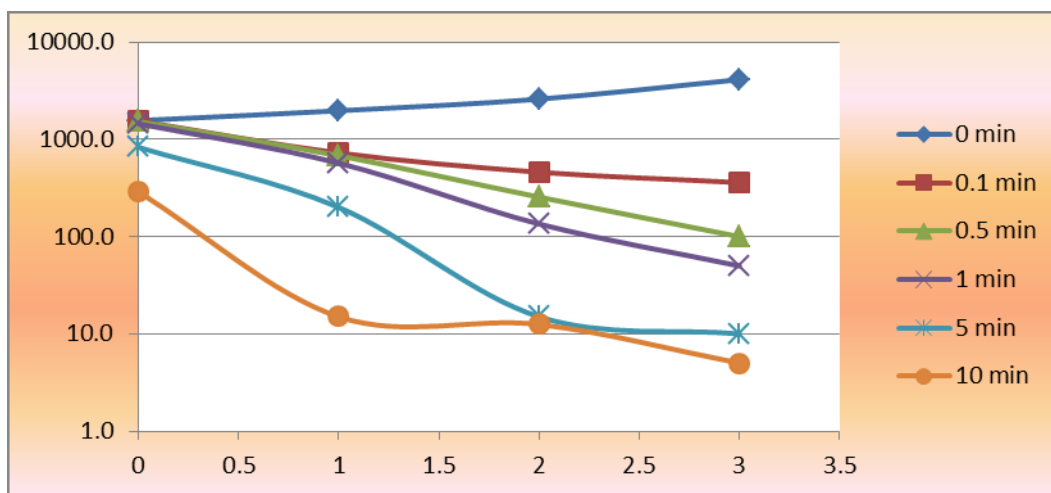


Figure 3.1 shows **UVC induced apoptosis (cell proliferation) using haemocytometer:**

Table 3.2 shows **UVC induced apoptosis (cell survival) using haemocytometer:**

time	0	1	2	3	6	7
0 min	82	87	88.1	94	72	41.9
0.1 min	77	44	23.5	14	30.7	52.2
0.5 min	71.1	33.4	12	4.3	0.77	0.0
1 min	69	26.5	6.7	2.2	0,27	0.0
5 min	61.9	13.8	0.97	0.5	0.0	0.0
10 min	28.5	0.9	0.4	0.4	0.0	0.0

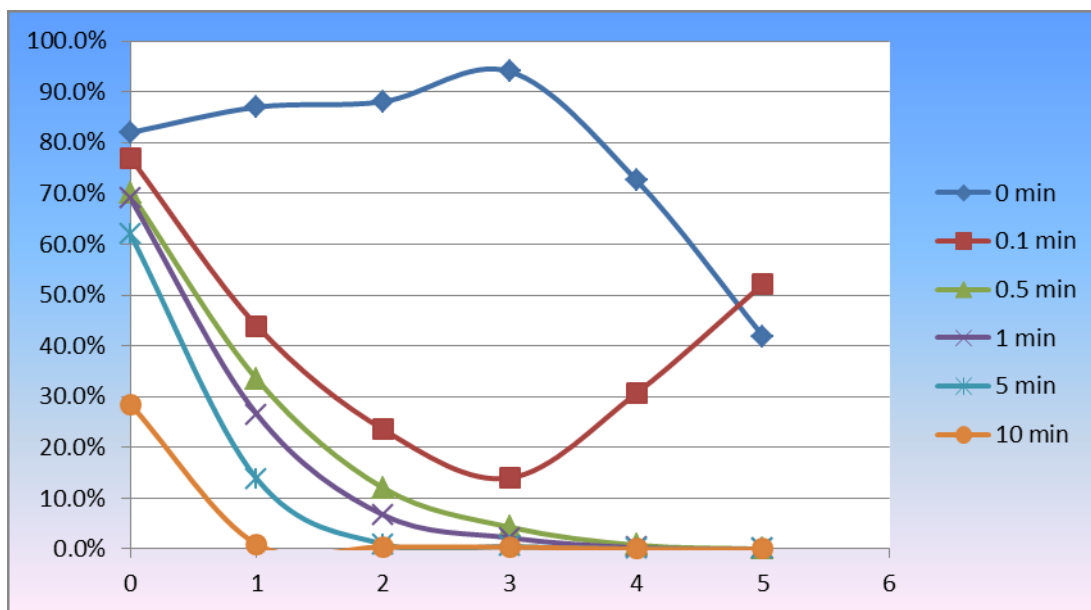


Figure 3.2 shows UVC induced apoptosis (cell survival) using haemocytometer:

3.4 Effect of Folinic acid on cell proliferation and apoptosis in UV-C treated HL60 cells:

To study the effect of Folinic acid on cell proliferation and apoptosis in UV-C treated HL60 cells, therefore before treating cells with UVC, serum was eliminated, and cells were washed twice in PBS, then resuspended and seeded in Iscove's modified Dulbecco's serum free medium, plated in different dishes at concentration of 1×10^6 cells/ml and incubated overnight. Next day supplemented with increasing doses of 5-formyltetrahydrofolate (Sigma) in a dose-dependent manner namely 0, 10, 25, 100 and 400 $\mu\text{g/ml}$ respectively, and then placed uncovered in UV stratalinker (stratagene model 1800: 8 watts each) under a UV bulb emitting chiefly 254-nm. Cells subjected to escalating single dose of UVC radiation namely 0 minute, 0.5 minute and 10 minutes. Cells were harvested after 2h, 2 and 6 days, where both cell count and cell viability were performed.

3.4.1 Results:

In the present study folinic acid used to reverse the cytotoxic effect that, induced by UVC, the results show that, regarding UVC untreated cells, folinic acid induce cell proliferation in absence of growth factors by certain point then cell numbers spontaneously began declining to fall behind the baseline by day 6. The voluminous proliferation in a dose dependent manner. Folinic acid has a minimal effect against cytotoxicity induced by UVC ($p < 0.05$), as cells that subjected for relatively short and long doses underwent apoptosis en masse by day 6. Supplementing cells with supraphysiologic dose (400 $\mu\text{g/ml}$) of folinic

acid which statistically significant in sustaining and rescuing cells a bit, but it hasn't far enough enabling cells to restore its proliferation potentiality($p < 0.05$), as described in table and figure

Table 3.3 shows UVC untreated cells and folic acid doses(cell proliferation)

5-FTHF	0	2	6
0 $\mu\text{g/ml}$	1.585	1.775	0.64
10 $\mu\text{g/ml}$	1.43	1.89	1.025
25 $\mu\text{g/ml}$	1.86	2.695	0.69
100 $\mu\text{g/ml}$	1.345	2.06	0.63
400 $\mu\text{g/ml}$	1.545	2.98	3.025

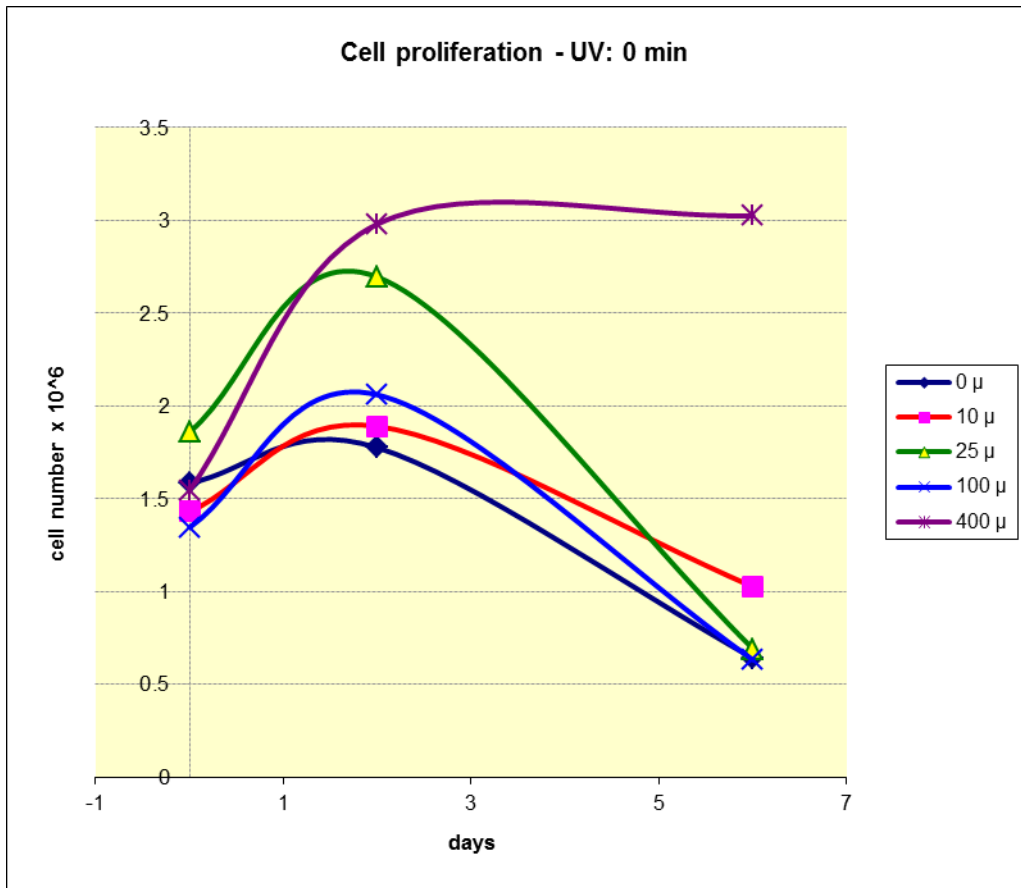


Figure 3.3 shows UVC untreated cells and folinic acid doses(cell proliferation)

Table 3.4 UVC untreated cells survival using trypan blue dye exclusion:

5-FTHF	0	2	6
0 μg/ml	0.9	0.82	0.19
10 μg/ml	0.925	0.87	0.27
25 μg/ml	0.93	0.86	0.19
100 μg/ml	0.94	0.9	0.2
400 μg/ml	0.93	0.91	0.56

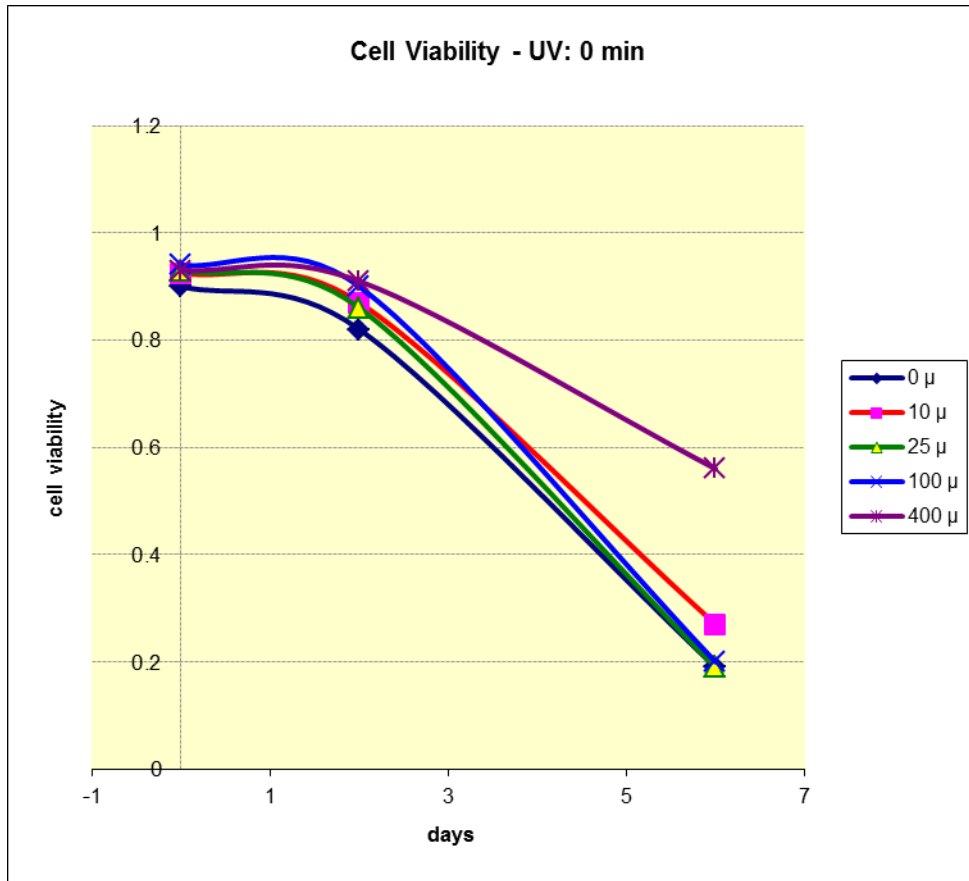


Figure 3.4 Table UVC untreated cells survival using trypan blue dye exclusion:

Table 3.5 shows UVC treated cells with 0.5 minute cell proliferation:

5-FTHF	0	2	6
0 μg/ml	1.05	0.01	0
10 μg/ml	1.22	0.015	0
25 μg/ml	1.34	0.02	0
100 μg/ml	1.44	0.04	0
400 μg/ml	1.285	0.155	0.01

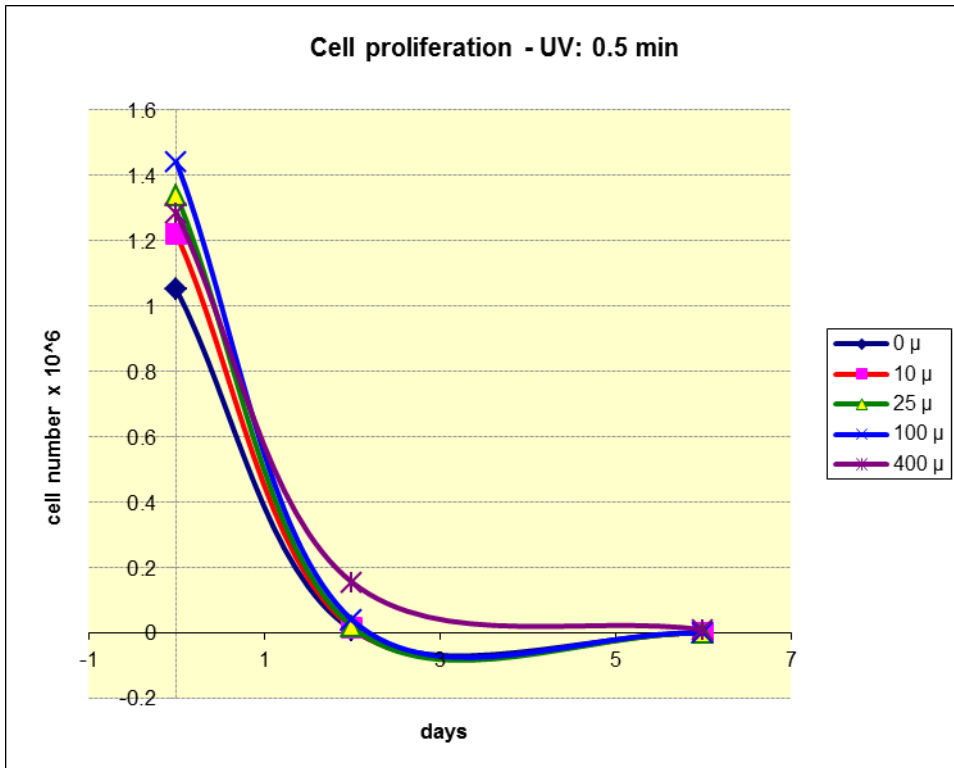


Figure 3.5 shows UVC treated cells with 0.5 minute cell proliferation

Table 3.6 demonstrates Cells treated with UVC for 0.5 minute (cell survival) using trypan blue exclusion:

5-FTHF	0	2	6
0 μg/ml	0.4	0.004	0
10 μg/ml	0.512	0.006	0
25 μg/ml	0.48	0.009	0
100 μg/ml	0.45	0.02	0
400 μg/ml	0.45	0.073	0.004

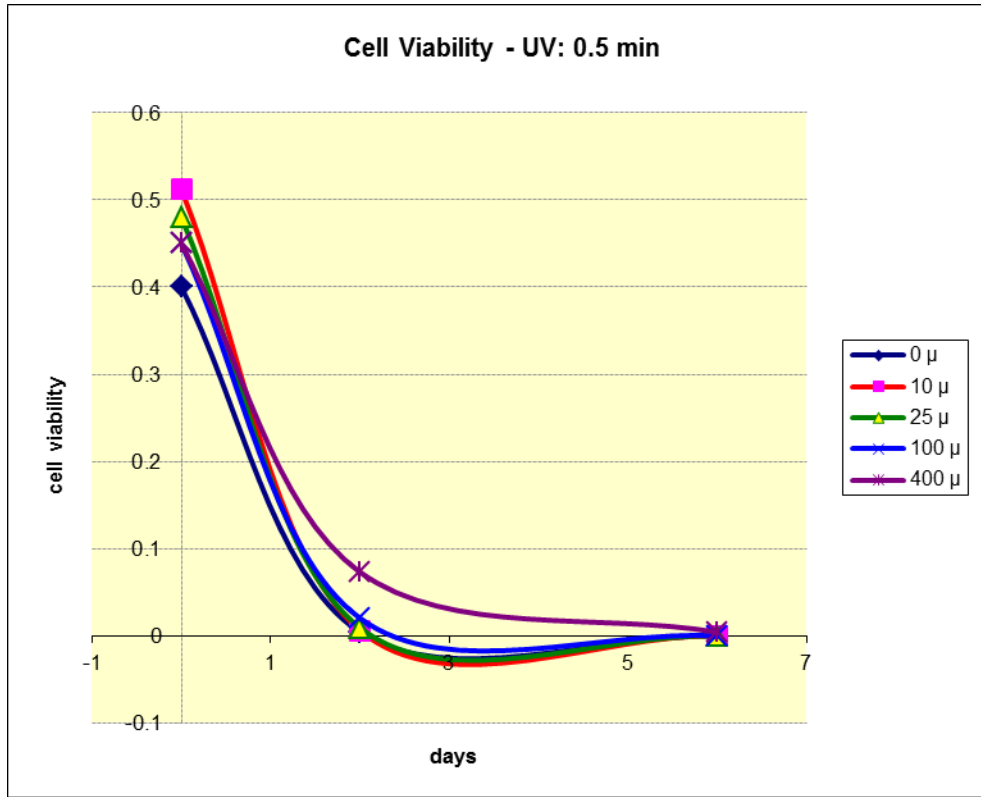


Figure 3.6 Cells treated with UVC for 0.5 minute (cell survival) using trypan blue exclusion

Table 3.7 illustrates Cells treated with UVC for 10 minutes(cell proliferation):

5FTHF	0	2	6
0 μg/ml	0.165	0	0
10 μg/ml	0.32	0.01	0
25 μg/ml	0.75	0.015	0
100 μg/ml	0.11	0.02	0
400 μg/ml	0.92	0.05	0.005

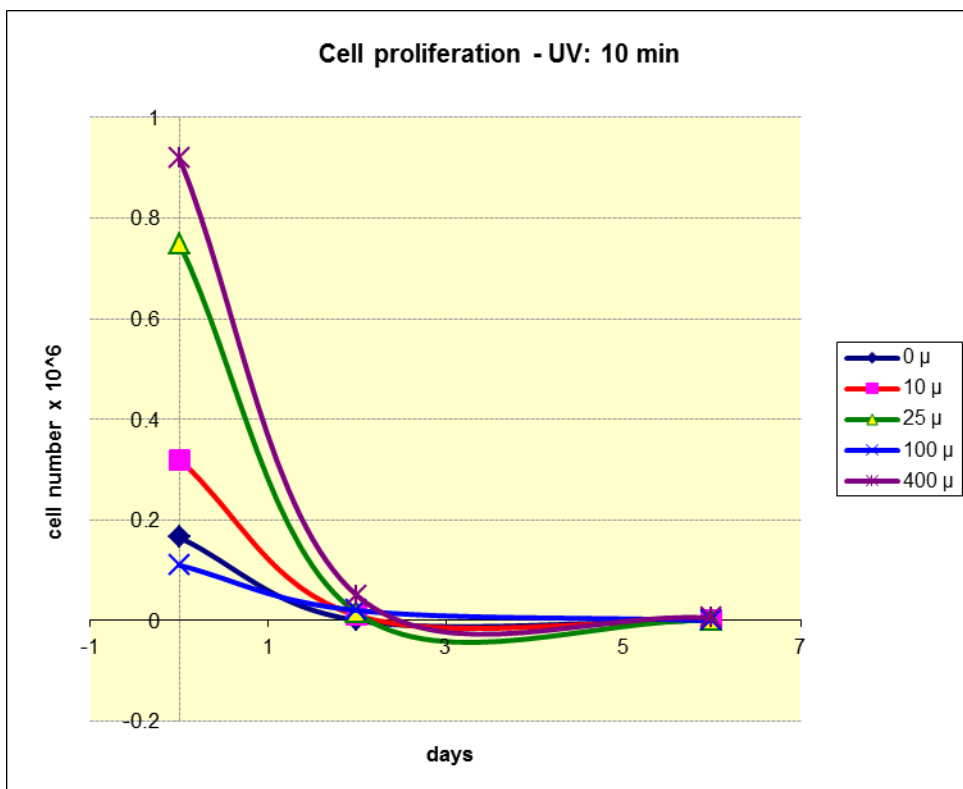


Figure 3.7 shows Cells treated with UVC for 10 minutes(cell proliferation):

3.4.2 Effect of Folinic acid on cell proliferation and apoptosis in UVC treated HL-60 cells

Cells were starved in Iscove serum free medium overnight. Next day supplemented with increasing doses of folinic acid namely 0, 100 and 400 $\mu\text{g/ml}$. thereafter exposed to different doses of UVC specifically, 0.1 minute and 0.5 minute. Additionally we use UVC untreated cells as control. Cells were harvested after 2hour, 3, 4 and 6 days post-radiation where cell count and viability were performed.

3.4.2.1 Result:

Concerning UVC untreated cells folinic acid induced exponential proliferation that culminates by day 3, and then cells began levelling off its number. Whereas in UVC treated cells folinic acid significantly($p > 0.05$), sustains cells survival and viability as much as 6 days as in our case. But doesn't go far enough in restoring back the machinery of cell proliferation as illustrated in table 3.8 and figure 3.8.

Table 3.8 shows **UVC untreated cell (cell proliferation) using haemocytometer:**

5FH7F	0	3	4	6
0 $\mu\text{g/ml}$	0.805	0.815	0.72	0.401
100 $\mu\text{g/ml}$	0.75	1.165	1.005	0.815
400 $\mu\text{g/ml}$	0.815	1.355	1.22	1.245

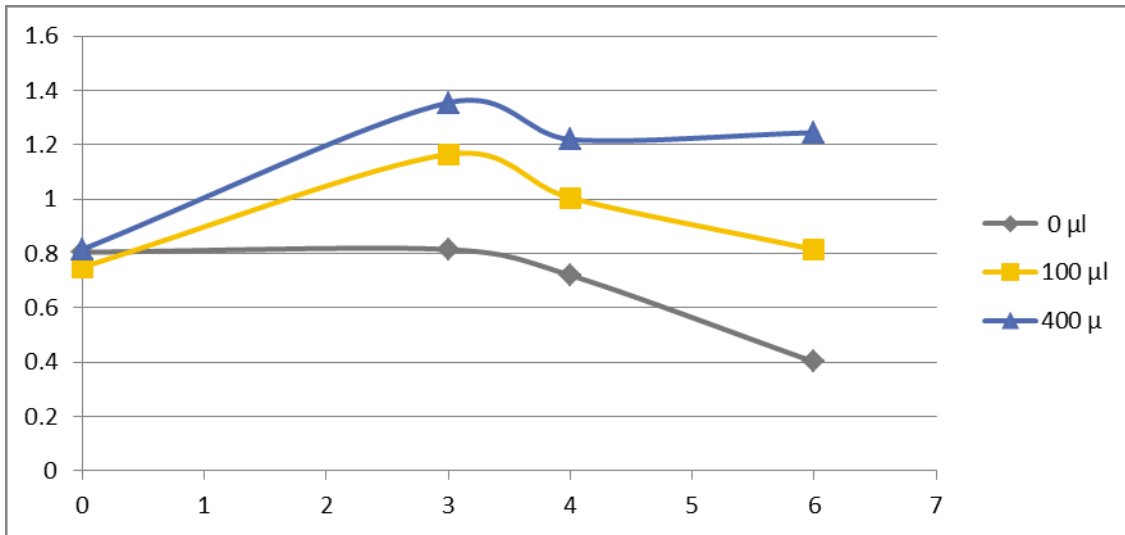


Figure 3.8 illustrates UVC untreated cell (cell proliferation) using haemocytometer

Table 3.9 shows **UVC untreated cell (cell survival) using trypan blue dye exclusion:**

5FH7F	0	3	4	6
0 $\mu\text{g/ml}$	0.8	0.608	0.54	0.22
100 $\mu\text{g/ml}$	0.9	0.789	0.69	0.406
400 $\mu\text{g/ml}$	0.89	0.797	0.664	0.526

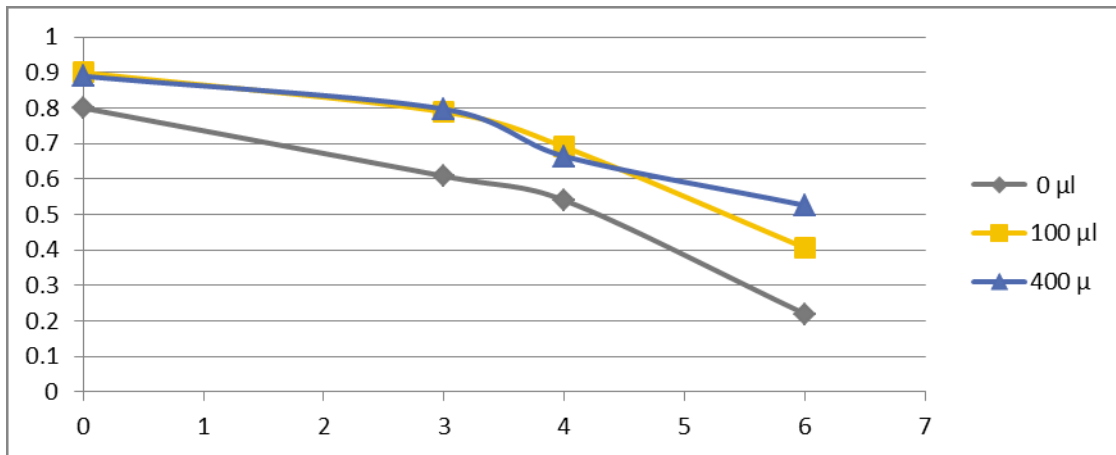


Figure 3.9 shows UVC untreated cell (cell survival) using trypan blue exclusion

Table 3.10 demonstrates Cells treated with 0.1 minute UVC cell proliferation using haemocytometer

5FTHF	0	3	4	6
0 μg/ml	0.685	0.02	0	0
100 μg/ml	0.8	0.075	0.1	0.02
400 μg/ml	0.7	0.14	0.115	0.035

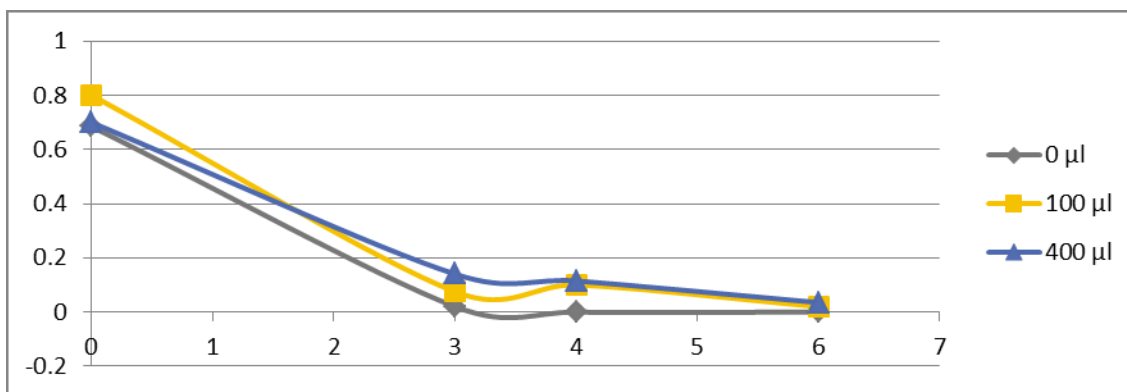


Figure 3.10 demonstrates Cells treated with 0.1 minute UVC cell proliferation using haemocytometer

Table 3.11 shows % Cells treated with 0.1 minute UVC (cell survival) using trypan blue exclusion:

5FTHF	0	3	4	6
0 µg/ml	0.67	0.0143	0	0
100 µg/ml	0.75	0.04	0.063	0
400 µg/ml	0.84	0.107	0.086	0.027

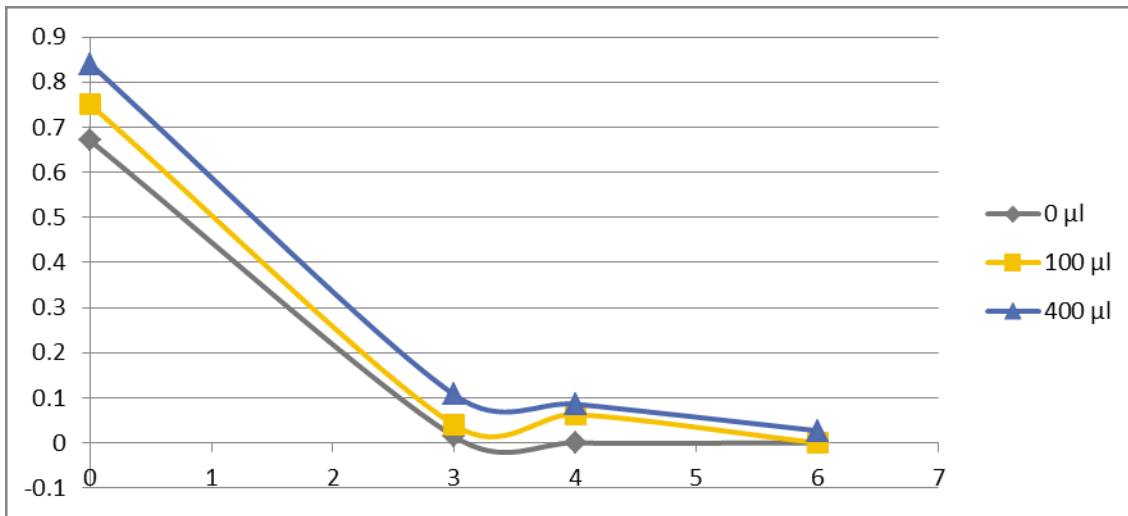


Figure 3.11 shows % Cells treated with 0.1 minute UVC (cell survival) using trypan blue exclusion:

Table 3.12 UVC treated cells for 0.5 minutes cell count using haemocytometer:

5FTHF	0	3	4	6
0 µg/ml	0.62	0	0	0
100 µg/ml	0.67	0.005	0.005	0
400 µg/ml	0.55	0.015	0.01	0.005

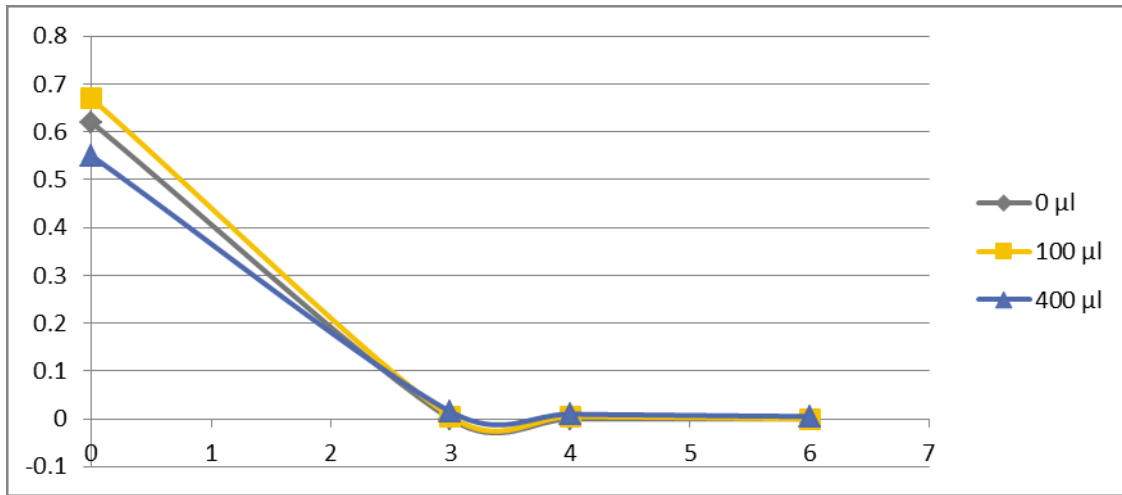


Figure 3.12 UVC treated cells for 0.5 minutes cell count using haemocytometer

Table 3.13 UVC treated cells for 0.5 minutes cell viability using trypan blue dye exclusion

5FTHF	0	3	4	6
0 µg/ml	0.558	0	0	0
100 µg/ml	0.65	0.004	0.004	0
400 µg/ml	0.58	0.0106	0.007	0.0029

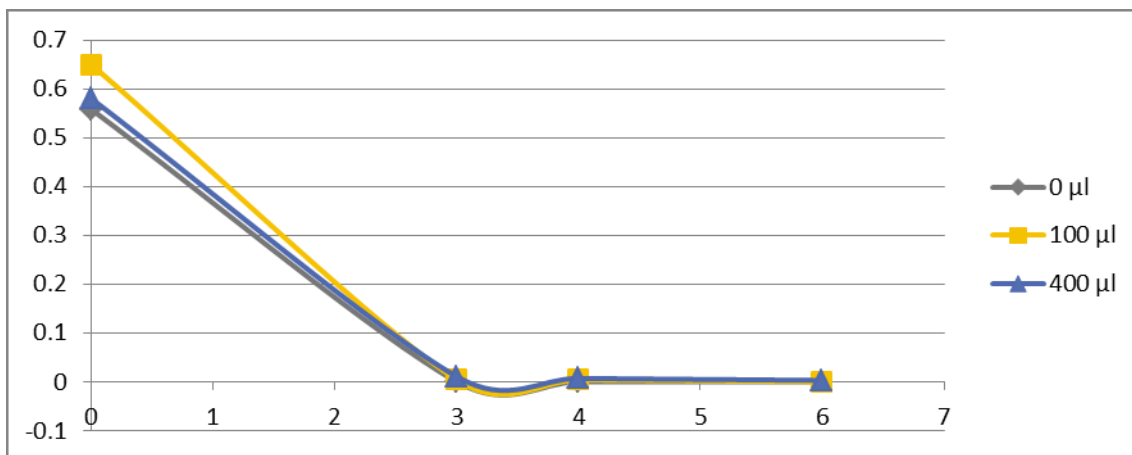


Figure 3.13 UVC treated cells for 0.5 minutes cell viability using trypan blue dye exclusion

3.4.3 Effects of pre and post- treatment and UVC on cell proliferation

One group of Cells were serum- starved in Iscove medium overnight. Next day supplemented with different doses of folic acid namely 0, 100 and 400 µg/ml and

immediately after that exposed to UVC light for 0.5 minute. While the other group starved overnight, exposed to UVC light then latter supplemented with same doses of folic acid. Cells were harvested after 2h, 3, 4, and 6 day post- radiation.

3.4.3.1 Result:

In reality no remarkable differences between pre and post folic acid treatment. Since both groups underwent apoptosis en masse after exposing to relatively short doses of UVC. furthermore, there no significant difference between pre and post- treatment($p < 0.05$). as depicted in table and figure

Table 3.14 Effects of post treatment of folic acid and UVC on cell proliferation

5FTHF	0	3	4	6
0µg/ml	0.955	0	0	0
100 µg/ml	1.165	0.01	0.005	0
400 µg/ml	1.215	0.025	0.01	0

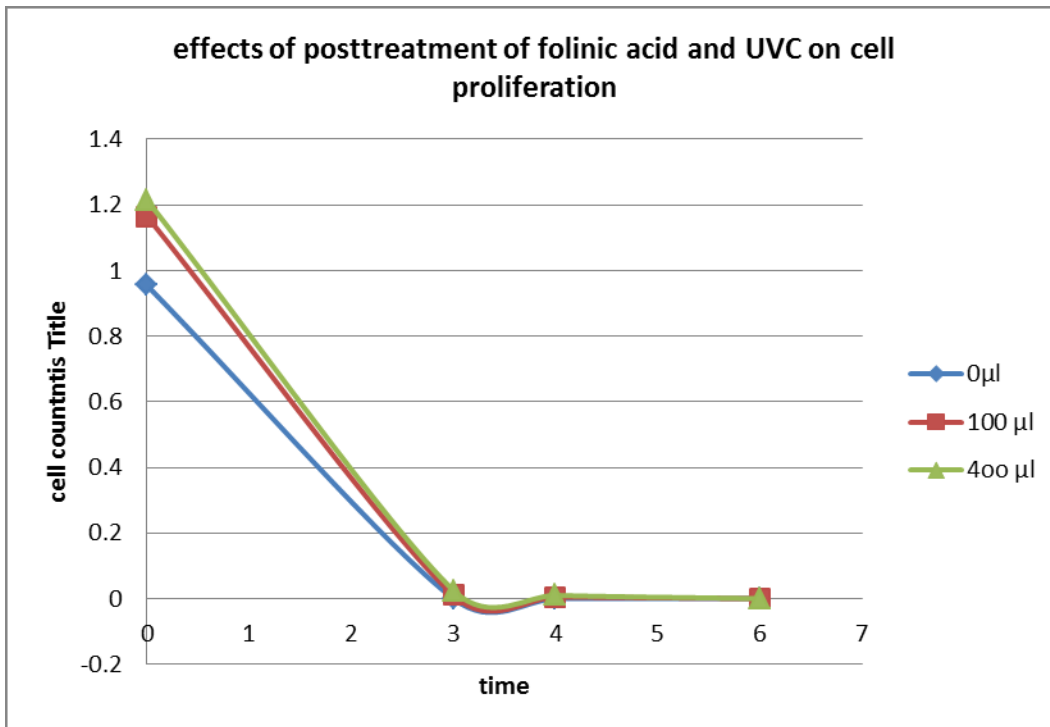


Figure 3.14 Effects of post-treatment of folic acid and UVC on cell proliferation

Table 3.15 Effects of post-treatment of folic acid and UVC on cell survival

5FTHF	0	3	4	6
0µg/ml	0.547	0	0	0
100 µg/ml	0.677	0.0061	0.003	0
400 µg/ml	0.764	0.015	0.0057	0

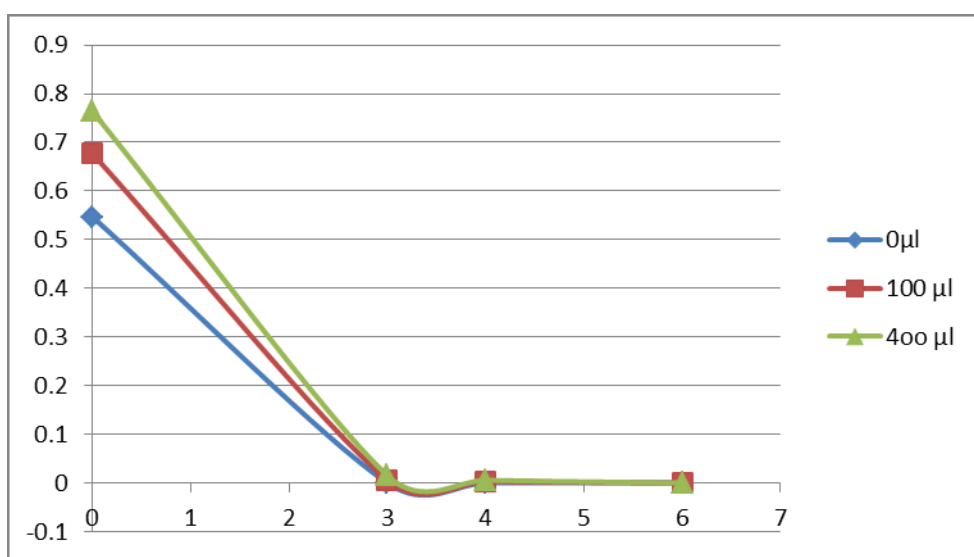


Figure 3.15 Effects of post-treatment of folic acid and UVC on cell survival

Table 3.16 Effect of pre-treatment of folic acid and UVC on cell proliferation

5FTHF	0	3	4	6
0µg/ml	0.985	0	0	0
100 µg/ml	1.4	0.005	0	0
400 µg/ml	1.015	0.01	0.005	0

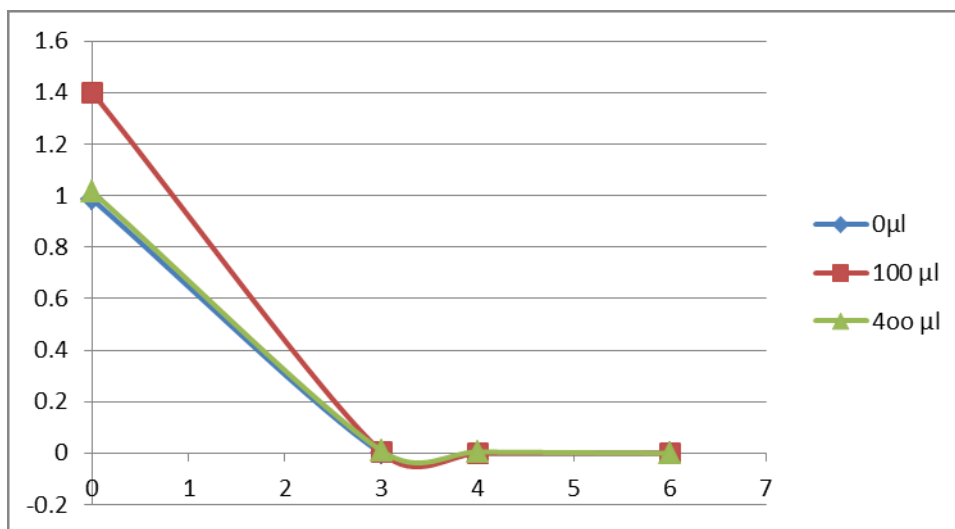


Figure 3.16 Effect of pre-treatment of folic acid and UVC on cell proliferation

Table 3.17 Effects of pre-treatment of folic acid and UVC on cell viability

5FTHF	0	3	4	6
0µg/ml	0.586	0	0	0
100 µg/ml	0.729	0.0027	0	0
400 µg/ml	0.76	0.0062	0.0026	0

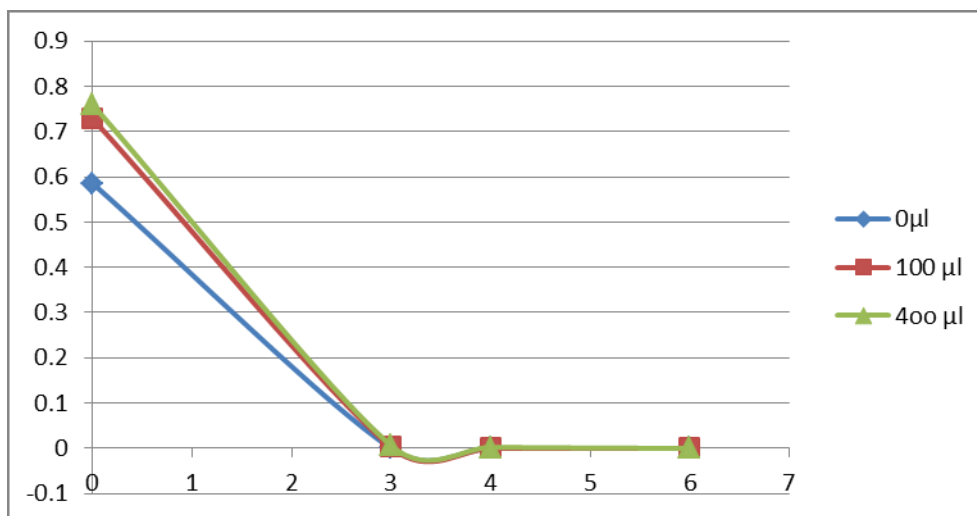


Figure 3.17 Effects of pre-treatment of folic acid and UVC on cell viability

3.5 Irradiation of cells with UVB light:

cells were exposed to UVB (dose 72 J/cm², wavelength 312 nm, Transilluminator UV geneTM, Bio- Rad laboratories, Hercules USA in a dose- dependent manner for three different times namely, 0 minute, 1 minute and 10 minutes at room temperature, at 1 cm distance.

3.5.1 Effects of UVB and folic acid on cell proliferation and apoptosis:

Cells were starved overnight in Iscove serum free medium. Next day before the culture being prepared, cell count and cell viability were checked. Thereafter 5x 10⁶/ 5ml of cells were being aliquoted in(35x 100 mm) dishes. Then supplemented with/no two different doses of folic acid namely 0, 100 and 400 µg/ml, after that exposed to different doses of UVB namely for 1 minute and 10 minutes, in addition to control cells. Cells were harvested after 2h, 3, 4 and 6 day post- irradiation where cell count and cell viability were performed.

3.5.1.1 Result:

Folic acid is instrumental in inducing exponential cell proliferation as seen in case of UVB untreated cell. Cells steadily replicate and doubled its number that reached its peak by day 3, then started dwindling. Needless to say, cell proliferation and cell survival as well are nearly dose dependence(p>0.05). In reference to UVB cells that, treated for short period (1minute), there are inconspicuous decrease in cell number compared to UVB untreated cells. With regard to UVB cells that relatively, treated high dose(10 minutes), Folic acid deficient cells underwent apoptosis en masse and vanished by day3, whereas folic acid supplemental cell levelled off and underwent apoptosis by day 6. the dose at 100 µg/ml was found to protect HI-60 after 1 minutes

Table 3.18 Effects of folic acid on proliferation of untreated cells

5FTHF	0	3	4	6
0µg/ml	1.55	2.13	1.93	1.275
100 µg/ml	1.49	2.555	2.04	1.625
400 µg/ml	1.25	2.455	2.01	1.71

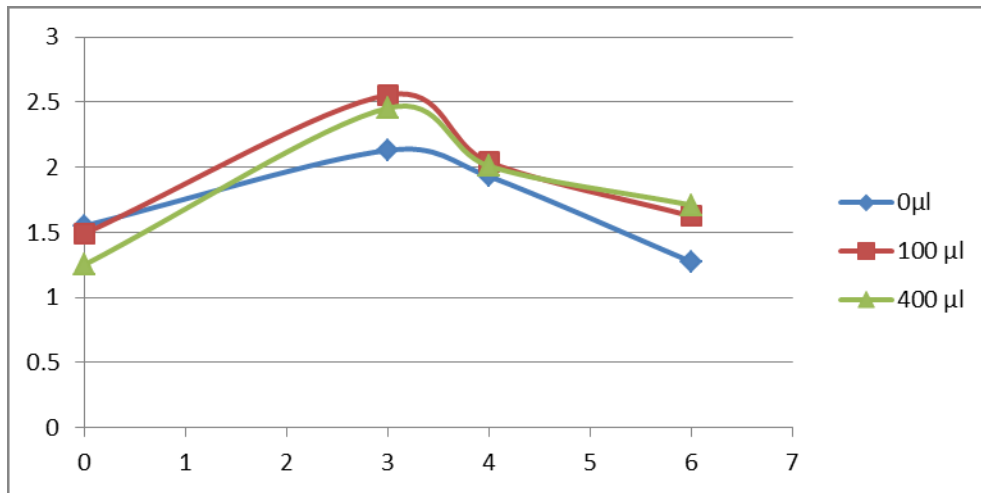


Figure 3.18 Effects of folic acid on proliferation of untreated cells

Table 3.19 Effects of folic acid on cell survival of untreated cells

5FTHF	0	3	4	6
0 μg/ml	0.85	0.733	0.57	0.38
100 μg/ml	0.88	0.825	0.67	0.412
400 μg/ml	0.92	0.85	0.702	0.412

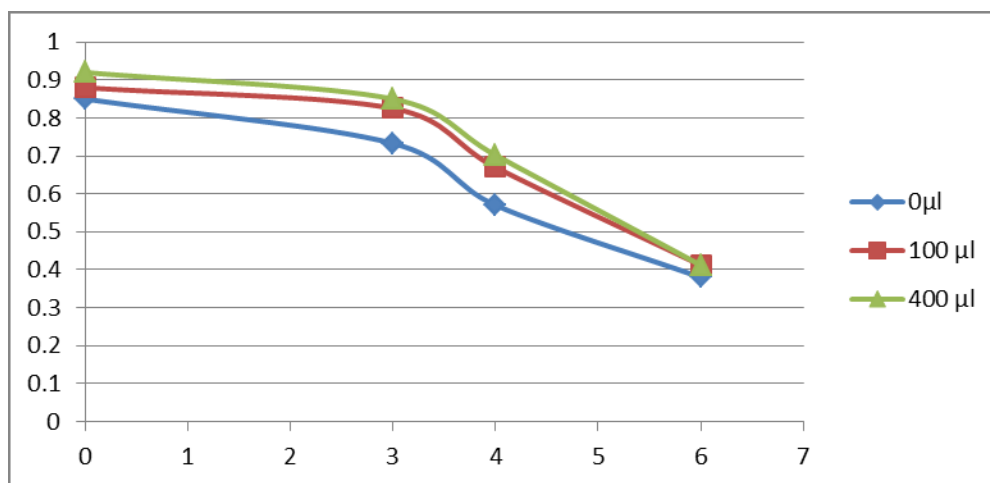


Figure 3.19 Effects of folic acid on cell survival of untreated cells

Table 3.20 Effect of UVB and folic acid on cell proliferation with 1 minute UVB exposure

5FTHF	0	3	4	6
0µg/ml	1.4	1.025	0.78	0.256
100 µg/ml	1.48	1.61	1.35	0.39
400 µg/ml	1.54	1.52	1.085	0.275

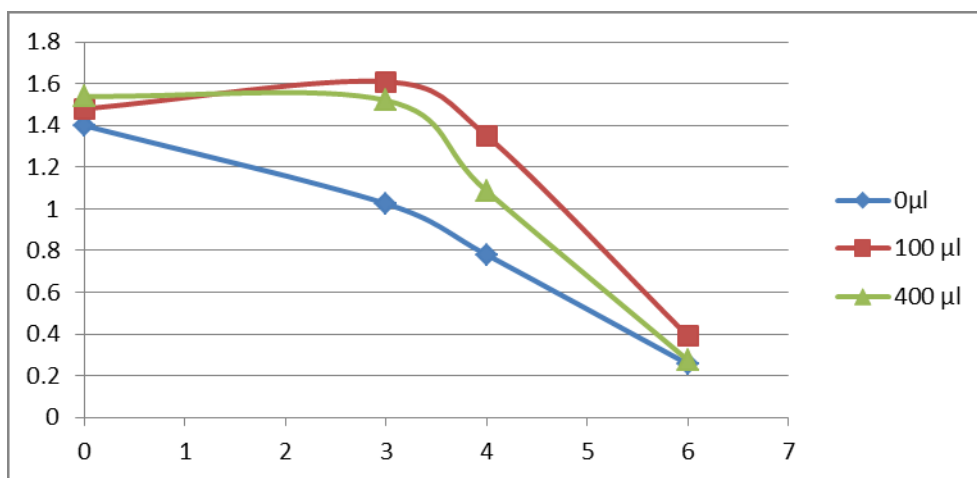


Figure 3.20 Effect of UVB and folic acid on cell proliferation with 1 minute UVB exposure

Table 3.21 Effects of UVB and folic acid on cell survival with 1 minute UVB exposure

5FTHF	0	3	4	6
0µg/ml	0.8	0.48	0.25	0.068
100 µg/ml	0.82	0.62	0.463	0.123
400 µg/ml	0.846	0.62	0.432	0.094

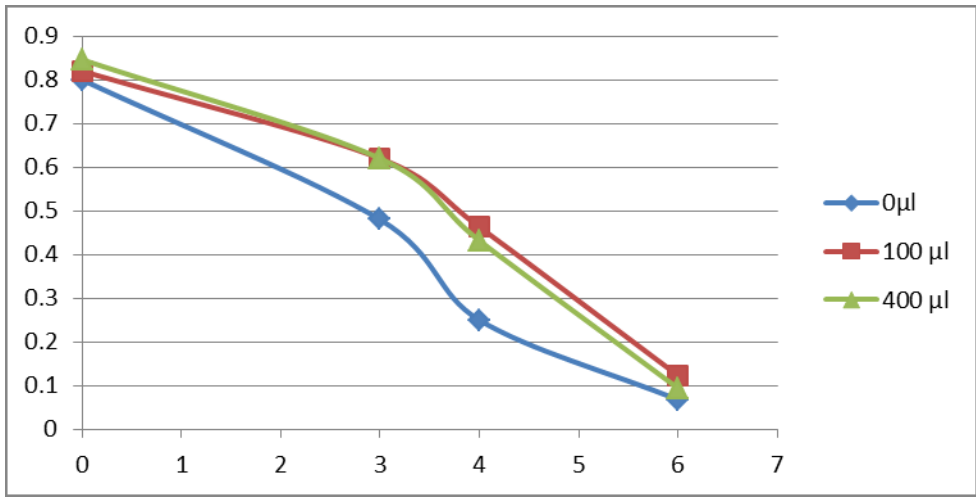


Figure 3.21 Effects of UVB and folinic acid on cell survival with 1 minute UVB exposure

Table 3.22 Effects of UVB and folinic acid on cell proliferation with 10 minute UVB exposure

5FTHF	0	3	4	6
0 µg/ml	1.3	0	0	0
100 µg/ml	1.4	0.005	0.005	0
400 µg/ml	1.44	0.015	0.01	0

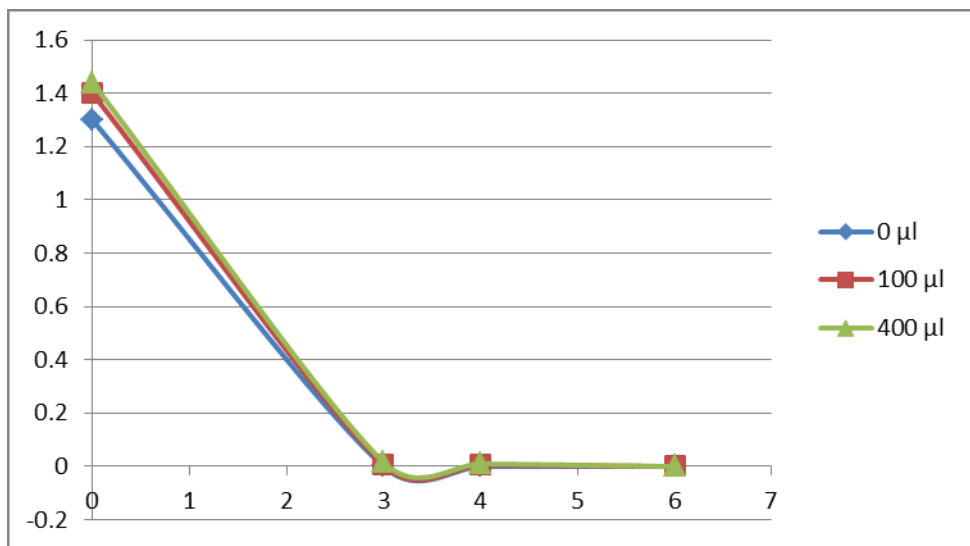


Figure 3.22 Effects of UVB and folinic acid on cell proliferation with 10 minute UVB exposure

Table 3.23 Effects of UVB and folic acid on cell survival with 10 minutes UVB exposure

5FTHF	0	3	4	6
0µg/ml	0.726	0	0	0
100 µg/ml	0.81	0.002	0.002	0
400 µg/ml	0.847	0.008	0.005	0

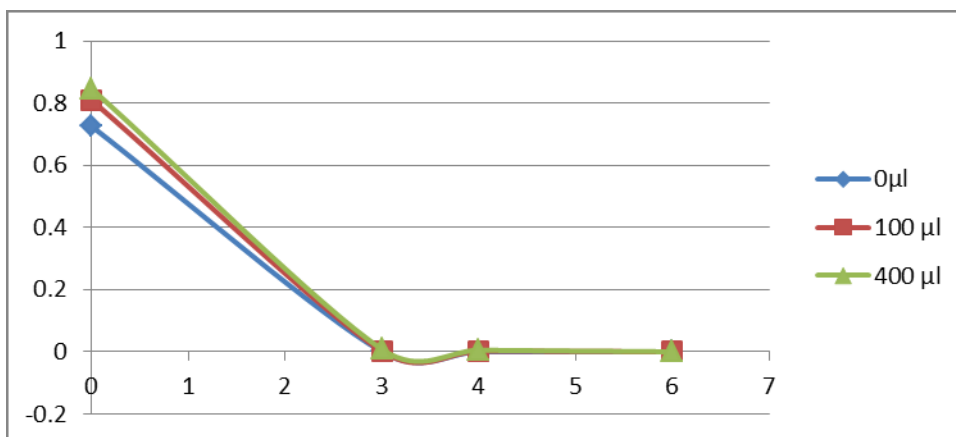


Figure 3.23 Effects of UVB and folic acid on cell survival with 10 minutes UVB exposure

3.5.2 5FTHF doses on UVB-treated HL-60 cells

to determine which is the 5FTHF dose that prevents apoptosis after 1 min UV-B exposure. Cells were starved overnight in Iscove serum free medium. Next day before the culture being prepared both cell count and viability were checked. Then cells plated at 5×10^6 cells in 5 ml(6x35 mm)Iscove serum free medium. Then different doses of folic acid were added namely 0, 5, 10, 25, 50 and 100 µg/ml. then plates were exposed to UVB for 1 minute. Cells harvested at 2h and 3 days post- radiation where cell count and viability were checked.

3.5.2.1 Result:

Folic acid seems to reinvigorate cells against toxicity such as UVB light. Apart from folic acid restriction cell, all folic acid supplemental cell continued proliferating

proportionately with varying degrees or directly proportional to folic acid concentration. Supraphysiologic dose 100 $\mu\text{g/ml}$ is impeccably perfect for inducing proliferation since cells nearly double its number as shown in table and figure

Table 3.24 cell proliferation using haemocytometer:

5FTHF	0	3
0 $\mu\text{g/ml}$	1.035	0.97
5 $\mu\text{g/ml}$	0.86	1.6
10 $\mu\text{g/ml}$	1.07	1.615
25 $\mu\text{g/ml}$	1.295	1.735
50 $\mu\text{g/ml}$	1.265	1.7
100 $\mu\text{g/ml}$	1.2225	1.86

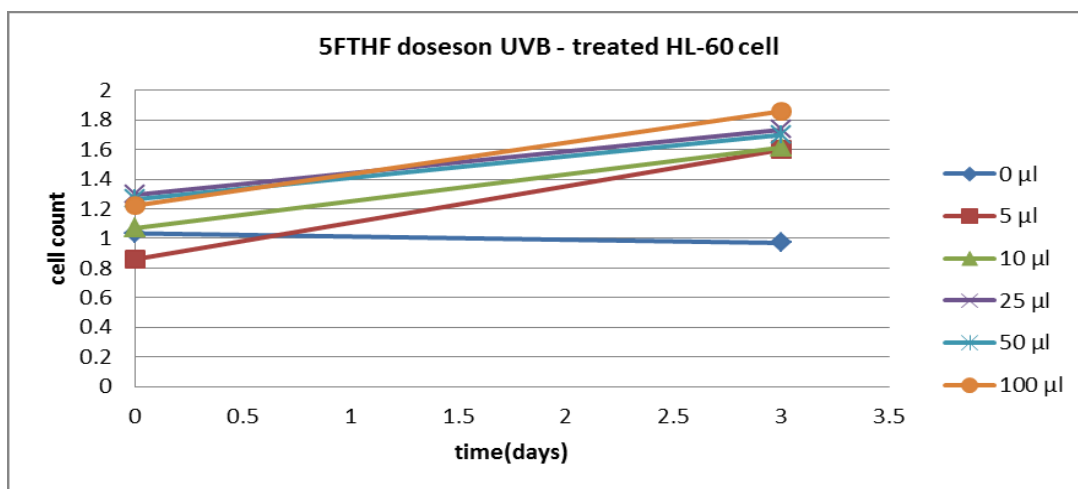


Figure 3.24 cell proliferation using haemocytometer

Table 3.25 Cell survival using trypan blue exclusion

5FTHF	0	3
0 $\mu\text{g/ml}$	0.73	0.42
5 $\mu\text{g/ml}$	0.77	0.53
10 $\mu\text{g/ml}$	0.8	0.56
25 $\mu\text{g/ml}$	0.88	0.61
50 $\mu\text{g/ml}$	0.89	0.64

100 µg/ml	0.85	0.72
-----------	------	------

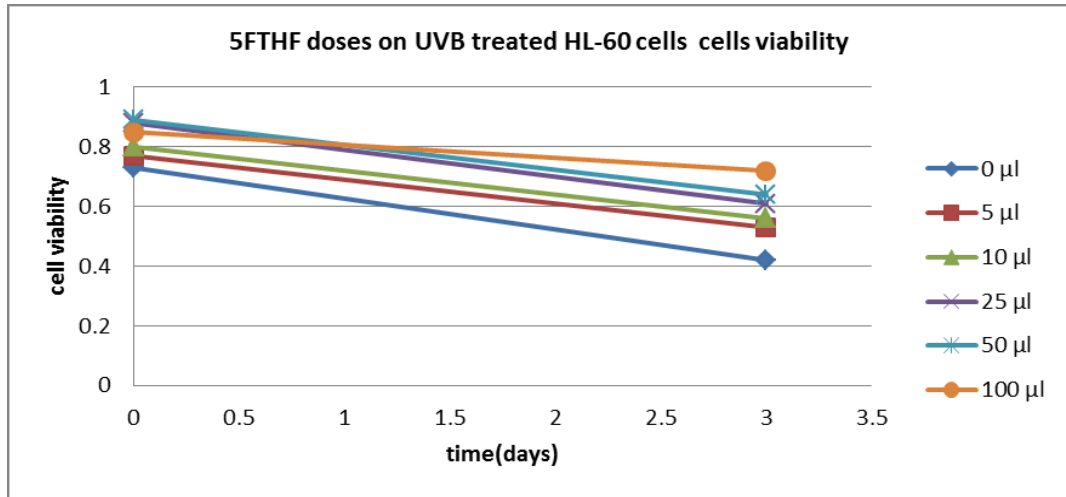


Figure 3.25 Cell survival using trypan blue dye exclusion

3.5.3 UVB dose exposure of HL-60 cells treated with 5FTHF (cell count)

Cells were starved overnight and maintained in Iscove serum free medium, thereafter plated into six dishes($5 \times 10^6/5\text{ml}$) for each. Next day supplemented with 100 µg/ml, then exposed to different doses of UVB(312 nm) namely, 0, 0.5, 1, 2, 5, 10 minutes respectively. Cells harvested after 2h and 3 days post- irradiation treatment, where both cell count and viability were done.

3.5.3.1 Result:

Folinic acid tremendously, bolster up and sustain cellular proliferation. Nevertheless it is functioning well with low- doses of UVB specifically with 0.5 and 1 minute UVB as found out in the present study. With regard to relatively low- dose and high- dose as well, supraphysiologic dose fails to keep cells safe and sound, instead cells underwent apoptosis en masse

Table 3.26 cell proliferation using haemocytometer

time	0	3
0 min	1.085	1.63
0.5 min	1.03	1.12
1 min	1.03	1.45
2 min	0.975	0.045
5 min	0.925	0.02
10 min	0.905	0.015

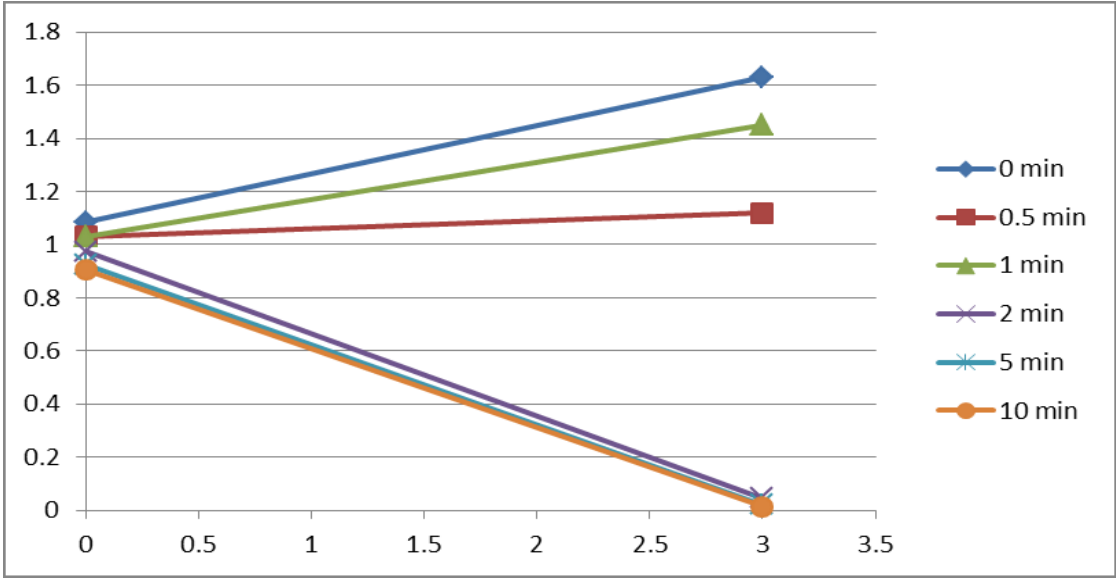


Figure 3.26 cell proliferation using haemocytometer

Table 3.27 % Cell survival using trypan blue dye exclusion:

time	0	3
0 min	0.86	0.64
0.5 min	0.84	0.54
1 min	0.8	0.52
2 min	0.72	0.02
5 min	0.68	0.009
10 min	0.62	0.007

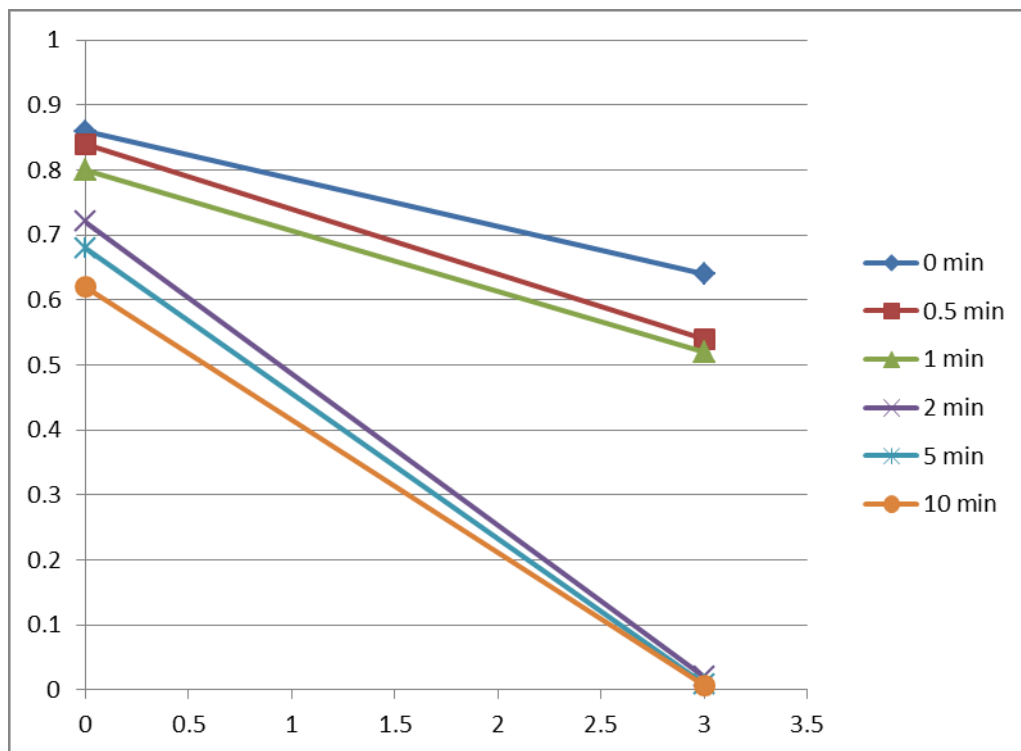


Figure 3.27 Cell survival using trypan blue dye exclusion:

3.5.4 UVB dose exposure of HL-60 cells treated with 5FTHF (cell count)

to determine which is the maximum UV-B exposure for which 5FTHF (100ug/ml) prevents apoptosis, thereby cells were starved overnight and maintained in Iscove serum free medium, thereafter plated into six dishes($5 \times 10^6/5\text{ml}$) for each. Next day supplemented with 100 $\mu\text{g/ml}$, then exposed to different doses of UVB(312 nm) namely, 0, 0.5, 1, 2, 5, 10 minutes respectively. Cells harvested after 2h and 3 days post- irradiation treatment, where both cell count and viability were done, and cell fixed with formaldehyde(), permeabilized with cold methyl alcohol and analysed using flow cytometry.

3.6 Cell cycle protocol with propidium iodide PI:

Cells($2 \times 10^6/2\text{ml}$) were harvested, and washed in 1x phosphate buffered saline(PBS) at 1200 rpm for 3 minutes. then supernatant was discarded, and pellet was resuspended in 2 ml of 1x PBS. 6 ml of formaldehyde were added dropwise while vortexing, and incubated at room temperature for 10 minutes. then centrifuged at 1200 rpm for 5 minutes. Cells were permeabilized with cold absolute methyl alcohol solution for at least 1 hour at - 20°C. Then cells were washed twice in 1x PBS at 1200 rpm for 5 minutes. Supernatant was discarded and cells were resuspended in PI at final concentration 50 $\mu\text{g/ml}$ (a combination of 450 μl PBS and 25 μl of propidium iodide) for 30 minutes on ice. Then cells were washed twice in 1x PBS at 1200 rpm for 5 minutes. The supernatant was discarded the pellet was resuspended in 300 μl of 1x PBS. Then the DNA content was analysed by using cytometer(FACScan flow cytometer; Becton Dickinson, San Jose, CA) at an excitation wavelength of 488 nm. The data were analysed using the software program(Cell Quest, Becton Dickinson).

3.5.4.1 Result:

Folinic acid nicely enable and further untreated cells to proliferate thrice by day 3 as well as cells that treated with low doses of UVB(0.5 min and 1 min) appears. Intriguingly, UVB treated cells that treated with relatively low dose(2 minute), more likely, there is initial hiatus of cell cycle and therefore cells underwent apoptosis en masse. The same phenomenon observed in UVB treated cells which exposed to high doses (5 and 10 min). UVB dose for 2 minutes is a potent and killing dose, mount same effects of high doses(5 & 10) min, as cells underwent apoptosis. During cell proliferation the flow cytometric analysis shows that,

increasing number of cells in the S and G2/M phases and decreasing number of cells in sub G1 phase which is evident in UVB untreated cells and UVB treated with low doses. Whereas in UVB treated with relatively and high doses there are low percentage in S and G2/M phase and high cell percentage in sub G1 cells.

Table 3.28 UVB dose exposure HL-60 supplemented with 5FTHF (cell count) using haemocytometer

time	0	3
0 min	1.69	3.685
0.5 min	1.59	3.27
1 min	2	3.17
2 min	1.46	0.09
5 min	1.45	0.045
10 min	1.165	0.025

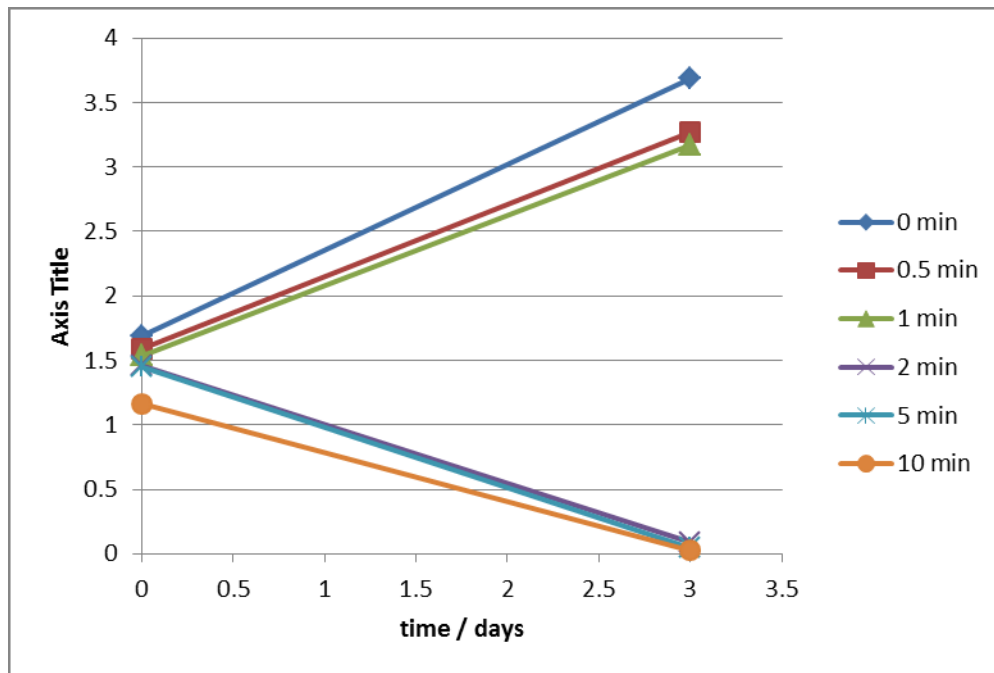


Figure 3.28 UVB dose exposure HL-60 supplemented with 5FTHF (cell count) using haemocytometer

Table 3.29 % UVB dose exposure HL-60 supplemented with 5FTHF (cell survival) using Trypan blue dye exclusion

time	0	3
0 min	0.938	0.9
0.5 min	0.913	0.847
1 min	0.889	0.828
2 min	0.848	0.027
5 min	0.798	0.0157
10 min	0.685	0.0068

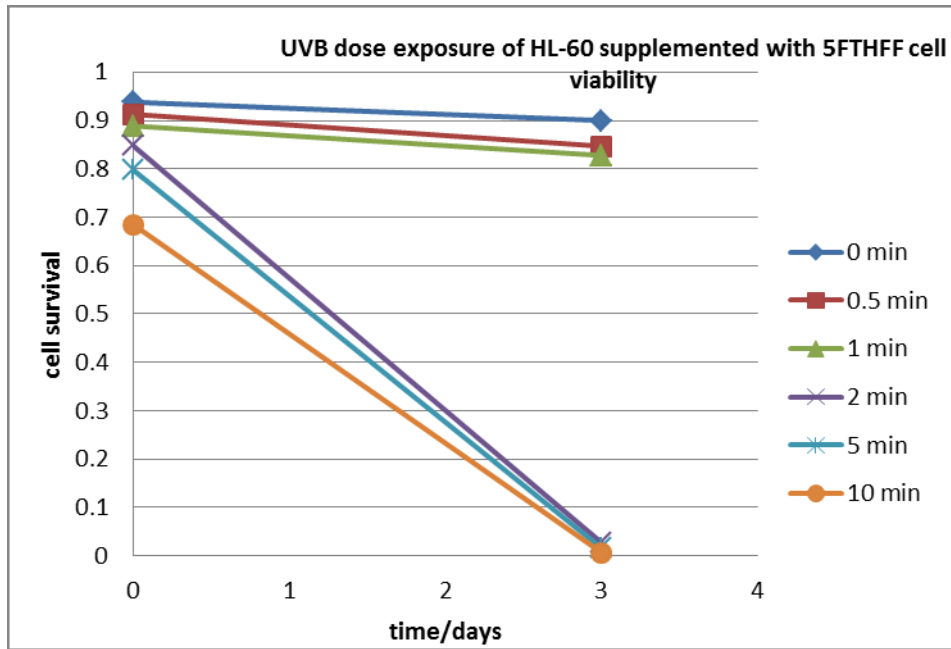
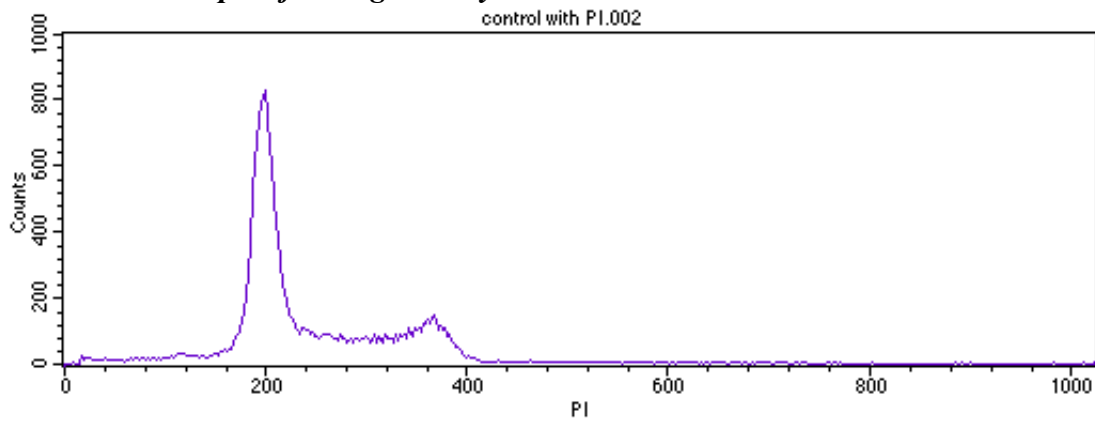


Figure 3.29 % UVB dose exposure HL-60 supplemented with 5FTHF (cell survival) using Trypan blue dye exclusion

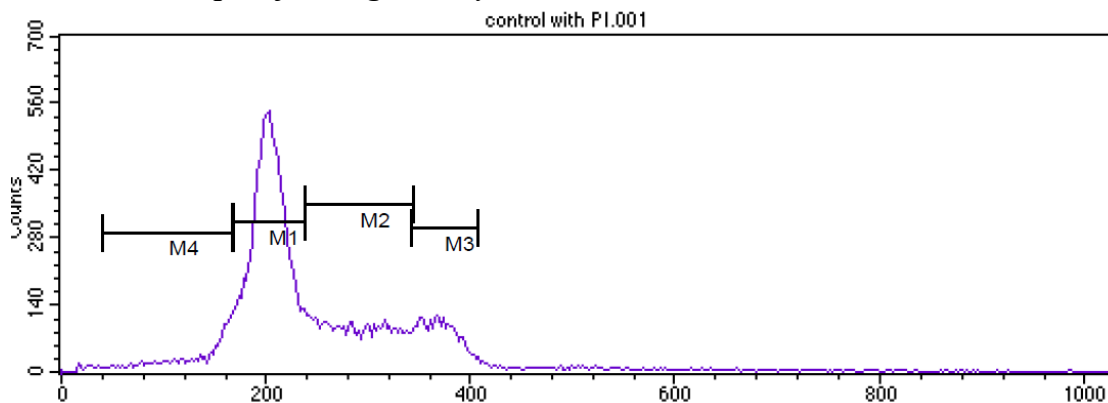
3.6.1 Flow cytometric analysis

3.6.1.1 control proliferating cell day 1



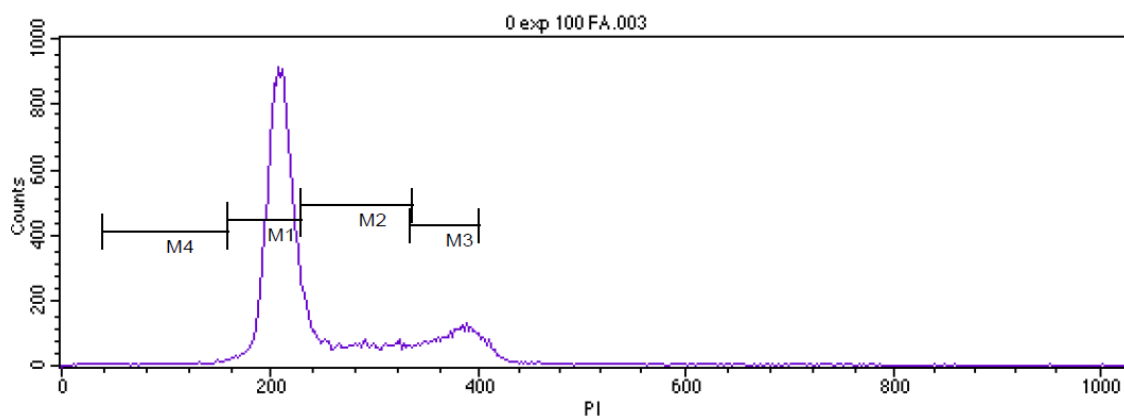
Marker	Left, Right	Events	% Gated	% Total	Mean	Geo Mean	CV	Median	Peak Ch
All	0, 1023	38630	100.00	96.58	238.00	225.03	33.11	207.00	199
M1	161, 231	22822	59.08	57.05	199.05	198.62	6.50	199.00	199
M2	231, 337	7977	20.65	19.94	281.48	279.67	11.35	280.00	237
M3	335, 401	5488	14.21	13.72	363.28	362.92	4.42	363.00	366
M4	40, 161	1897	4.91	4.74	114.24	108.29	29.30	118.00	159

3.6.1.2 control proliferating cell day 3



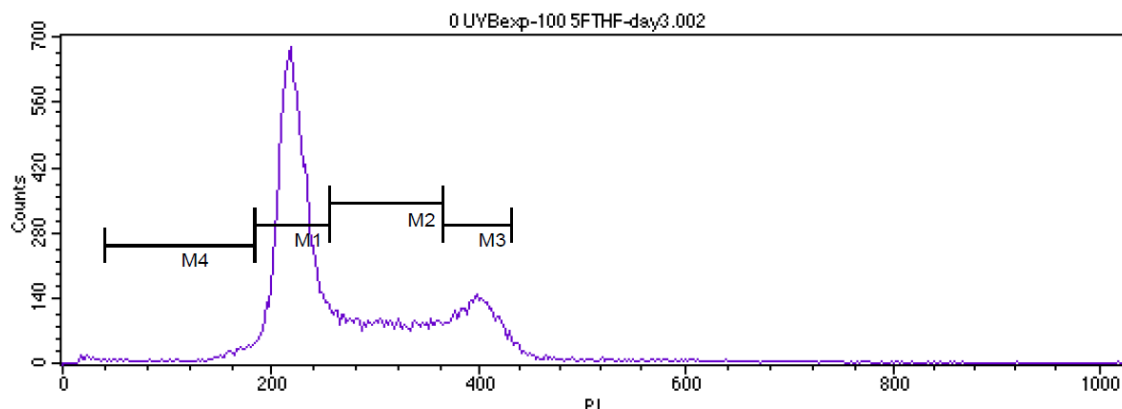
Marker	Left, Right	Events	% Gated	% Total	Mean	Geo Mean	CV	Median	Peak Ch
All	0, 1023	38663	100.00	96.66	247.82	233.07	35.88	216.00	203
M1	167, 237	20469	52.94	51.17	202.70	202.07	7.84	203.00	203
M2	237, 343	9194	23.78	22.98	287.40	285.68	10.94	286.00	238
M3	341, 407	5048	13.06	12.62	369.14	368.75	4.58	368.00	367
M4	40, 168	3149	8.14	7.87	132.81	127.01	25.96	147.00	167

3.6.1.3 0 UVB exposure – 100 µg/ml 5FTHF day 0



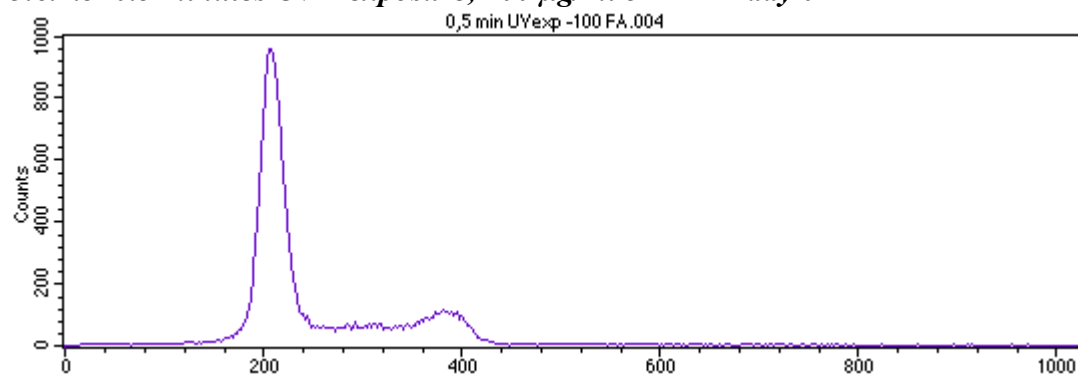
Marker	Left, Right	Events	% Gated	% Total	Mean	Geo Mean	CV	Median	Peak Ch
All	0, 1023	39513	100.00	98.78	251.90	242.36	29.82	218.00	208
M1	161, 231	25095	63.51	62.74	209.22	208.89	5.60	210.00	208
M2	231, 337	7339	18.57	18.35	274.55	272.53	12.22	271.00	231
M3	335, 401	5427	13.73	13.57	371.99	371.52	5.00	374.00	390
M4	40, 161	382	0.97	0.95	121.67	114.98	29.30	133.50	158

3.6.1.4 0 UVB exposure – 100 µg/ml 5FTHF day 3



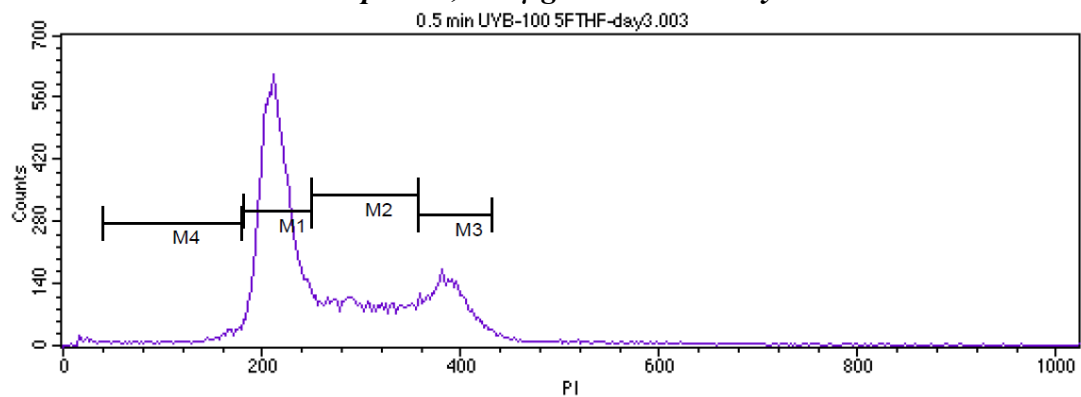
Marker	Left, Right	Events	% Gated	% Total	Mean	Geo Mean	CV	Median	Peak Ch
All	0, 1023	39486	100.00	98.72	277.90	264.41	31.68	238.00	220
M1	185, 258	21768	55.13	54.42	222.87	222.40	6.50	222.00	220
M2	257, 366	8827	22.35	22.07	309.36	307.64	10.53	308.00	258
M3	366, 432	6510	16.49	16.28	397.73	397.36	4.32	398.00	399
M4	41, 185	1158	2.93	2.90	148.28	140.38	26.91	164.00	185

3.6.1.5 0.5 minutes UVB exposure, 100 µg/ml 5FTHF- day 0



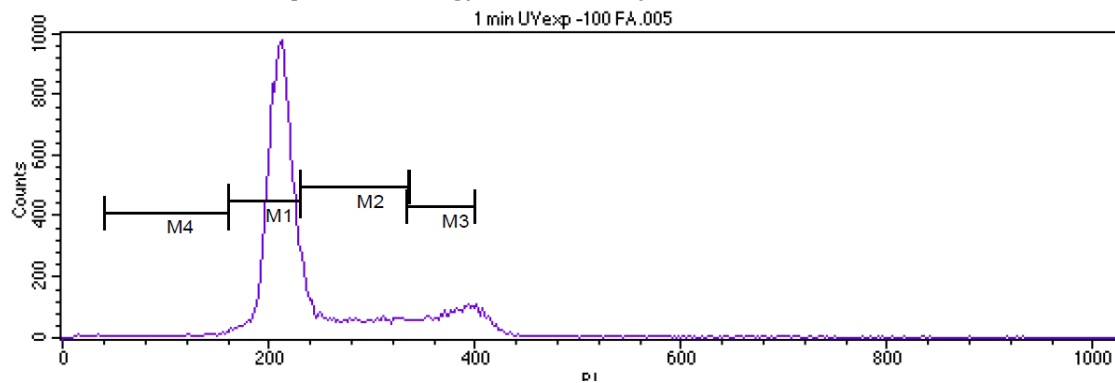
Marker	Left, Right	Events	% Gated	% Total	Mean	Geo Mean	CV	Median	Peak Ch
All	0, 1023	39312	100.00	98.28	247.36	237.98	29.92	215.00	206
M1	161, 231	25992	66.12	64.98	208.01	207.67	5.62	209.00	206
M2	231, 337	6625	16.85	16.56	277.39	275.40	12.00	276.00	231
M3	335, 401	5207	13.25	13.02	371.49	371.03	4.99	374.00	382
M4	40, 161	527	1.34	1.32	120.35	113.75	29.30	130.00	160

3.6.1.6 0.5 minute UVB exposure, 100 µg/ml 5FTHF- day 3



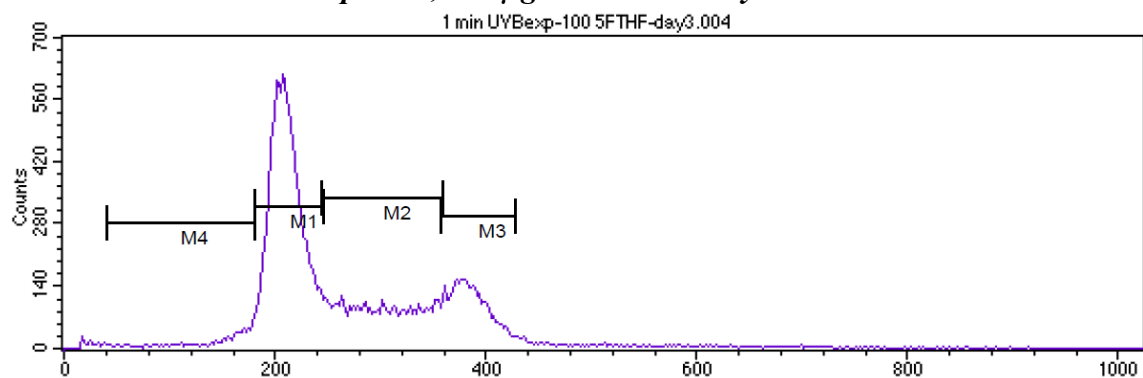
Marker	Left, Right	Events	% Gated	% Total	Mean	Geo Mean	CV	Median	Peak Ch
All	0, 1023	39423	100.00	98.56	273.46	259.13	32.79	235.00	213
M1	182, 251	20633	52.34	51.58	215.63	215.13	6.86	214.00	213
M2	251, 358	9255	23.48	23.14	302.53	300.89	10.42	301.00	251
M3	357, 433	7116	18.05	17.79	389.13	388.68	4.79	388.00	382
M4	40, 180	1220	3.09	3.05	139.52	131.52	28.74	156.00	179

3.6.1.7 1 minute UVB exposure, 100 µg/ml 5FTHF- day 0



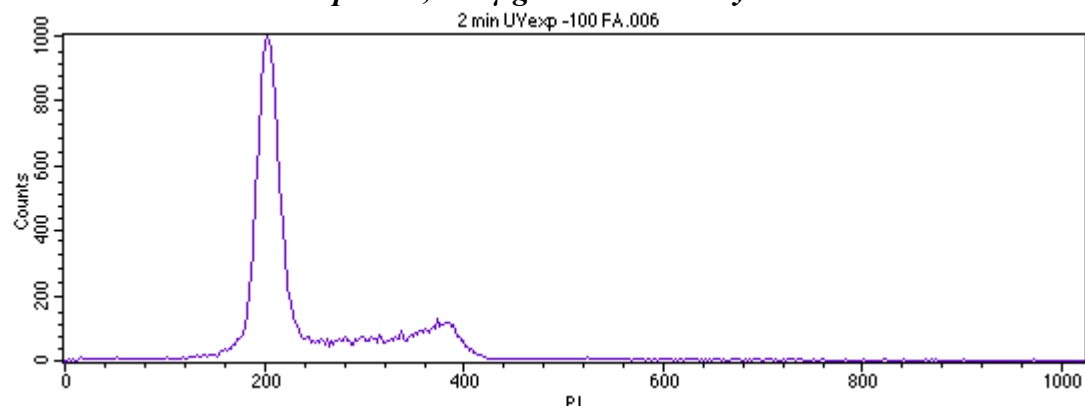
Marker	Left, Right	Events	% Gated	% Total	Mean	Geo Mean	CV	Median	Peak Ch
All	0, 1023	39455	100.00	98.64	249.44	240.26	29.33	218.00	213
M1	161, 231	25726	65.20	64.31	210.19	209.86	5.52	211.00	213
M2	231, 337	7166	18.16	17.91	273.62	271.56	12.36	268.00	232
M3	335, 401	4785	12.13	11.96	372.11	371.61	5.18	375.00	401
M4	40, 161	439	1.11	1.10	120.00	113.17	30.00	131.00	161

3.6.1.8 1 minute UVB exposure, 100 µg/ml 5FTHF- day 3



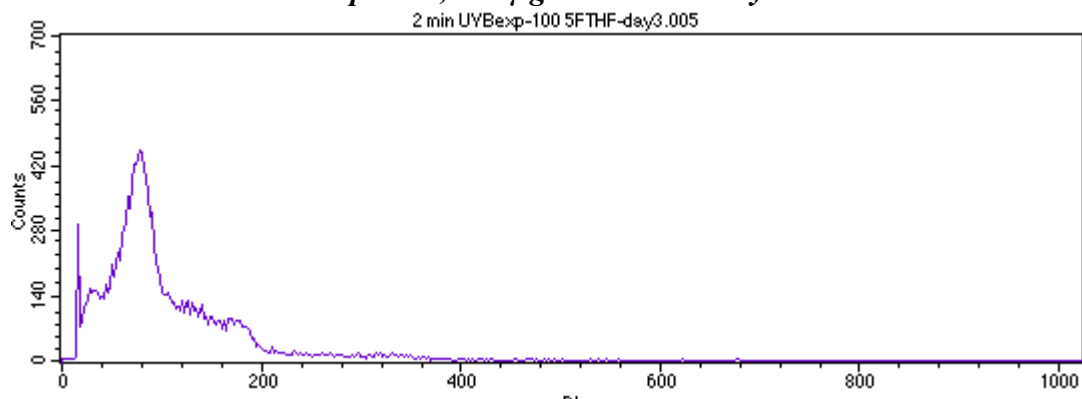
Marker	Left, Right	Events	% Gated	% Total	Mean	Geo Mean	CV	Median	Peak Ch
All	0, 1023	39287	100.00	98.22	267.30	253.33	32.83	229.00	207
M1	181, 246	20762	52.85	51.91	211.31	210.84	6.75	210.00	207
M2	244, 360	9915	25.24	24.79	300.62	298.57	11.66	300.00	244
M3	358, 429	6573	16.73	16.43	385.72	385.34	4.47	384.00	377
M4	40, 181	1427	3.63	3.57	145.19	138.06	26.13	161.00	179

3.6.1.9 2 minute UVB exposure, 100 µg/ml 5FTHF- day 0



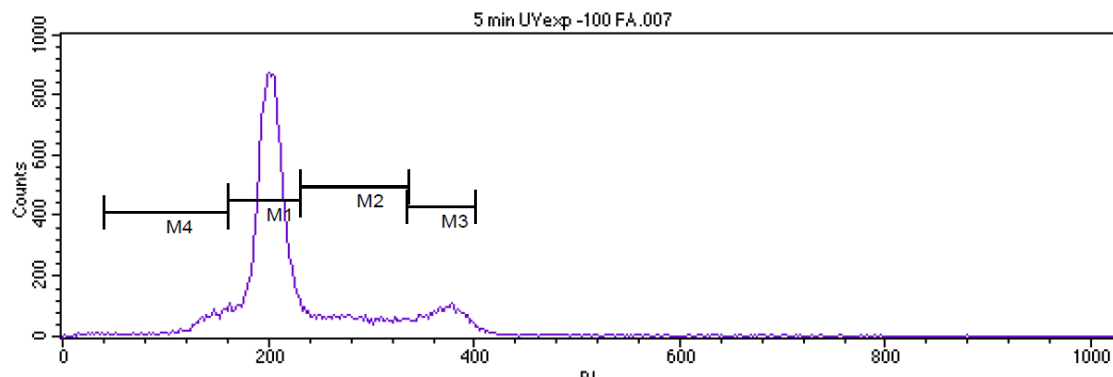
Marker	Left, Right	Events	% Gated	% Total	Mean	Geo Mean	CV	Median	Peak Ch
All	0, 1023	39443	100.00	98.61	243.03	233.25	30.59	211.00	204
M1	161, 231	26452	67.06	66.13	204.10	203.74	5.81	204.00	204
M2	231, 337	6219	15.77	15.55	282.59	280.74	11.39	283.00	231
M3	335, 401	5466	13.86	13.66	369.27	368.83	4.82	371.00	374
M4	40, 161	690	1.75	1.73	124.80	118.57	27.41	137.00	160

3.6.1.10 2 minute UVB exposure, 100 µg/ml 5FTHF- day 3



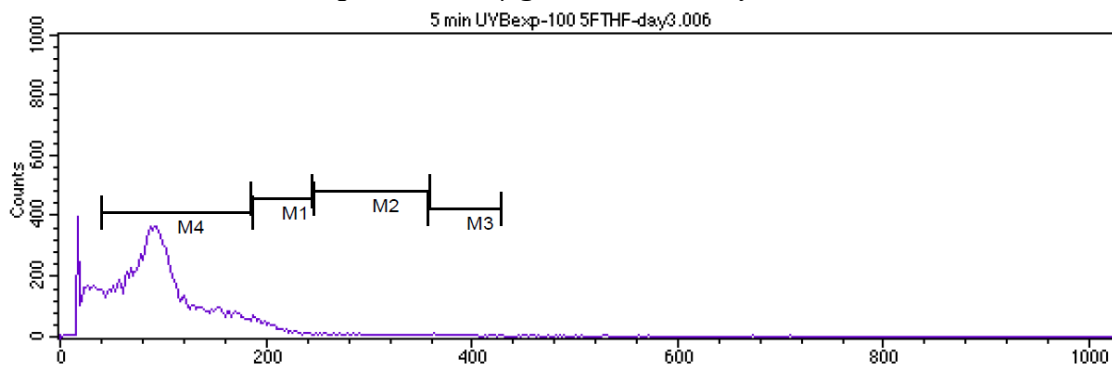
Marker	Left, Right	Events	% Gated	% Total	Mean	Geo Mean	CV	Median	Peak Ch
All	0, 1023	29297	100.00	73.24	100.19	85.48	59.90	84.00	80
M1	185, 246	1331	4.54	3.33	204.86	204.12	8.65	199.00	185
M2	244, 360	901	3.08	2.25	297.89	296.05	11.12	298.00	261
M3	358, 429	84	0.29	0.21	377.11	376.68	4.86	371.00	364
M4	40, 187	24338	83.07	60.85	95.21	88.92	37.99	85.00	80

3.6.1.11 5 minute UVB exposure, 100 µg/ml 5FTHF- day 0



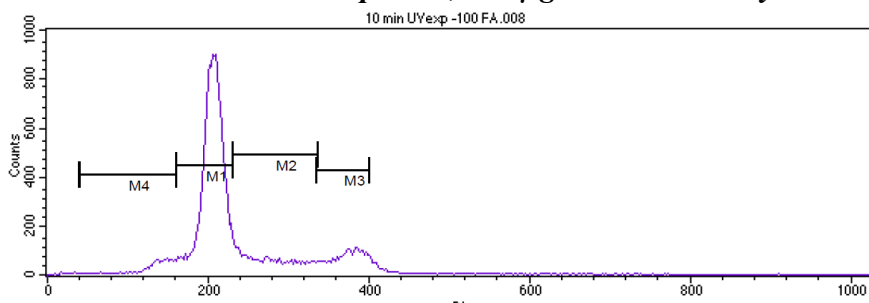
Marker	Left, Right	Events	% Gated	% Total	Mean	Geo Mean	CV	Median	Peak Ch
All	0, 1023	39117	100.00	97.79	229.82	220.07	30.55	207.00	201
M1	161, 231	25898	66.21	64.74	201.35	200.88	6.73	202.00	201
M2	231, 337	6009	15.36	15.02	279.10	277.34	11.25	277.00	231
M3	335, 401	4290	10.97	10.72	368.68	368.26	4.71	370.00	379
M4	40, 161	2617	6.69	6.54	135.12	131.56	19.25	143.00	147

3.6.1.12 5 minute UVB exposure, 100 µg/ml 5FTHF- day 3



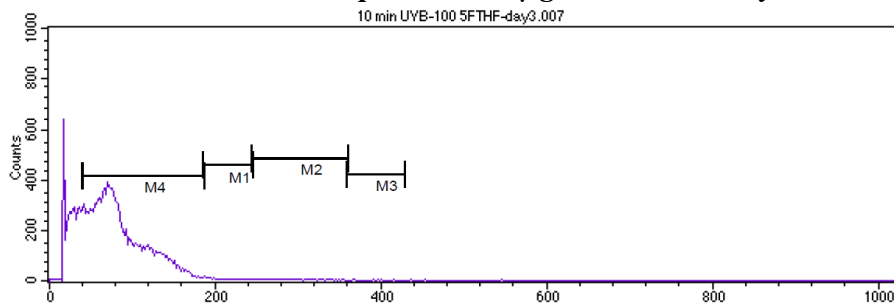
Marker	Left, Right	Events	% Gated	% Total	Mean	Geo Mean	CV	Median	Peak Ch
All	0, 1023	27676	100.00	69.19	99.55	84.89	56.78	91.00	18
M1	185, 246	1518	5.48	3.79	203.87	203.35	7.29	200.00	187
M2	244, 360	425	1.54	1.06	292.52	290.51	11.86	284.00	257
M3	358, 429	108	0.39	0.27	384.63	384.15	5.07	381.50	363
M4	40, 187	22452	81.12	56.13	98.46	92.41	35.43	94.00	94

3.6.1.13 10 minute UVB exposure, 100 µg/ml 5FTHF- day 0



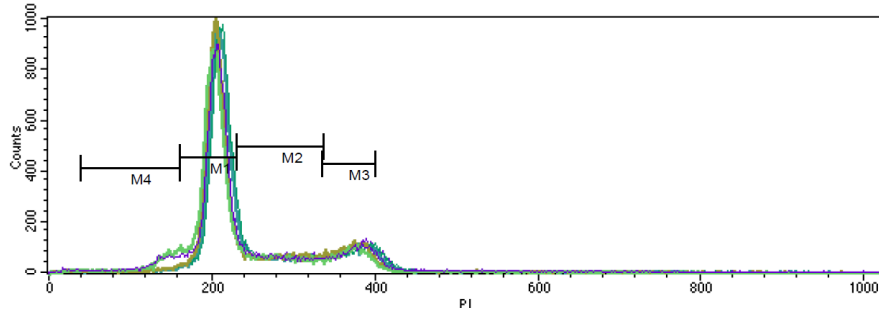
Marker	Left, Right	Events	% Gated	% Total	Mean	Geo Mean	CV	Median	Peak Ch
All	0, 1023	39148	100.00	97.87	238.13	227.88	30.84	212.00	209
M1	161, 231	25311	64.65	63.28	205.31	204.87	6.40	206.00	209
M2	231, 337	6069	15.50	15.17	277.05	275.18	11.68	274.00	231
M3	335, 401	4785	12.22	11.96	371.97	371.52	4.92	374.00	383
M4	40, 161	2200	5.62	5.50	134.71	131.60	18.20	141.00	149

3.6.1.14 10 minute UVB exposure, 100 µg/ml 5FTHF- day 3



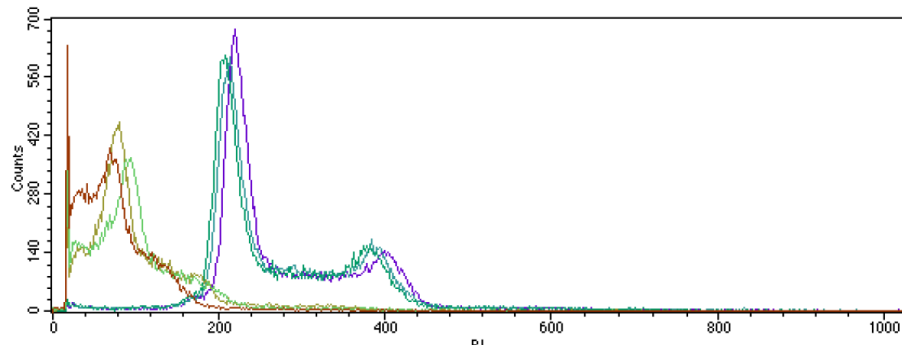
Marker	Left, Right	Events	% Gated	% Total	Mean	Geo Mean	CV	Median	Peak Ch
All	0, 1023	29021	100.00	72.55	75.51	64.86	55.00	69.00	18
M1	185, 246	236	0.81	0.59	208.86	208.08	8.76	204.50	187
M2	244, 360	118	0.41	0.29	287.54	285.93	10.76	280.00	270
M3	358, 429	8	0.03	0.02	386.88	386.48	4.83	393.00	365
M4	40, 187	22806	78.58	57.02	85.23	79.54	38.04	77.00	70

3.6.1.15 Overlay day 0



Key	Name	Parameter	Gate
—	0 exp 100 FA.003	FL2-H	G2
—	0,5 min UVexp -100 FA.004	FL2-H	G2
—	1 min UVexp -100 FA.005	FL2-H	G2
—	2 min UVexp -100 FA.006	FL2-H	G2
—	5 min UVexp -100 FA.007	FL2-H	G2
—	10 min UVexp -100 FA.008	FL2-H	G2

3.6.1.16 Overlay day 3



Key	Name	Parameter	Gate
—	0 UVBexp-100 5FTHF-day3.002	FL2-H	G2
—	0.5 min UVB-100 5FTHF-day3.003	FL2-H	G2
—	1 min UVBexp-100 5FTHF-day3.004	FL2-H	G2
—	2 min UVBexp-100 5FTHF-day3.005	FL2-H	G2
—	5 min UVBexp-100 5FTHF-day3.006	FL2-H	G2
—	10 min UVB-100 5FTHF-day3.007	FL2-H	G2

3.5.5 5FTHF doses on UVB treated HL-60

to determine which is the 5FTHF dose that might prevent apoptosis after 1 min UV-B exposure. Therefore, cells were starved and maintained overnight in Iscove serum free medium. Then plated in 8 dishes Next day. increasing concentrations(0,1.25, 2.5, 5, 10,25, 50 and 100 µg/ ml) of folic acid were added to each plate, then all dishes were exposed to UVB for 1 minute using transilluminator UV gene™, then cells were harvested, cell count using haemocytometer, cell viability using trypan blue dye exclusion and flow cytometry using propidium iodide(PI) were performed.

3.5.5.1 Results:

Folic acid strongly support cell proliferation, in this context folic acid deficient cells failed to proliferate and underwent cell cycle arrest and subsequently, apoptosis en masse by day 3. Whereas the folic acid supplemental cells had proliferated and increased their number proportionately more according to increasing folic doses as well evident in cells supplemented with relatively high doses(25,50 and 100 µg/ml) of folic acid managed to double their number. The flow cytometric analysis reveals that high doses promote proliferation as there is high percentage of cells in S and G2/M phases, and low percentage of cells in sub G1.

1. **Table 3.30 shows 5FTHF doses on UVB treated HL-60 cell (cell proliferation) by Haemocytometer:**

5FTHF	0	3
0 µg/ml	1.285	0.695
1.25 µg/ml	1.1	0.685
2.5 µg/ml	1.125	0.685
5 µg/ml	1.235	0.725
10 µg/ml	1.22	1.45
25 µg/ml	1.35	1.99
50 µg/ml	1.42	2.24
100 µg/ml	1.45	2.67

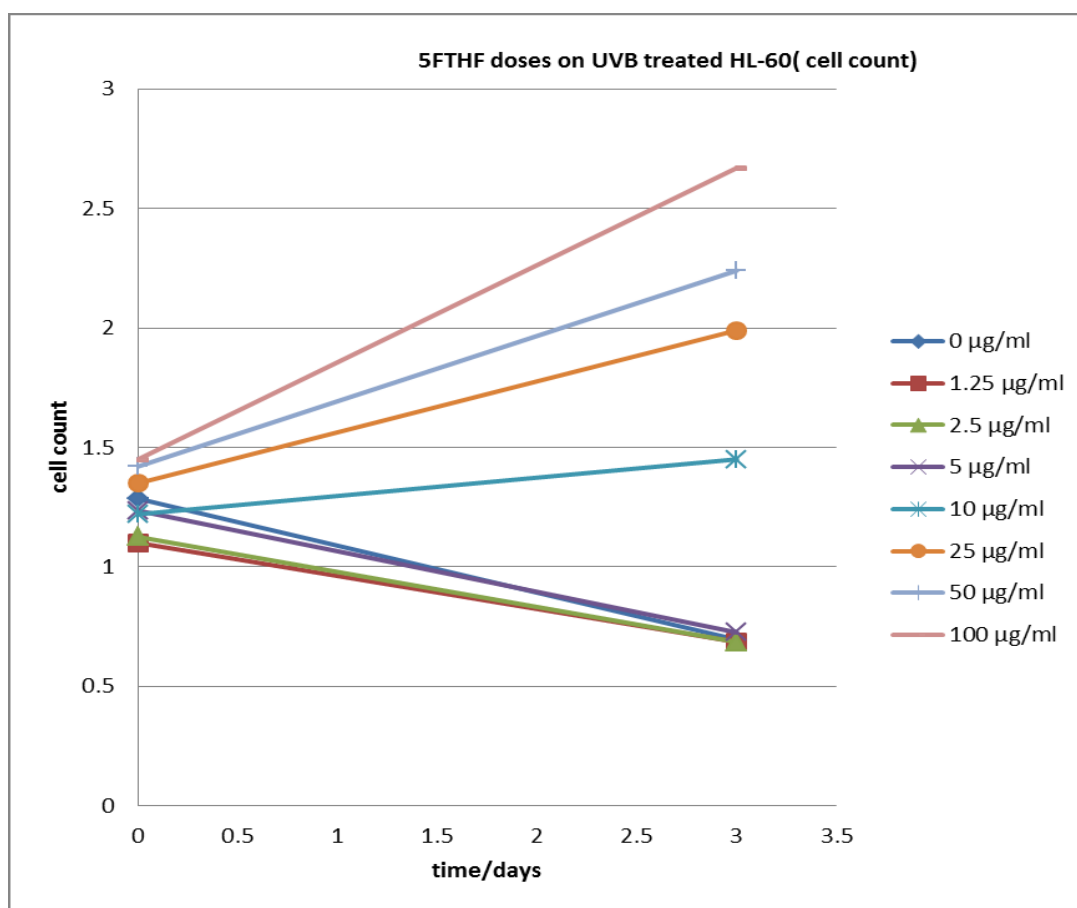


Figure 3.30 shows 5FTHF doses on UVB treated HL-60 cell (cell proliferation) by Haemocytometer:

2. Table 3.31 shows 5FTHF doses on UVB treated HL-60 cell (cell survival) by (% of Trypan blue dye exclusion):

5FTHF	0	3
0 $\mu\text{g/ml}$	0.892	0.262
1.25 $\mu\text{g/ml}$	0.905	0.314
2.5 $\mu\text{g/ml}$	0.929	0.293
5 $\mu\text{g/ml}$	0.925	0.348
10 $\mu\text{g/ml}$	0.917	0.481
25 $\mu\text{g/ml}$	0.945	0.742
50 $\mu\text{g/ml}$	0.965	0.78
100 $\mu\text{g/ml}$	0.97	0.78

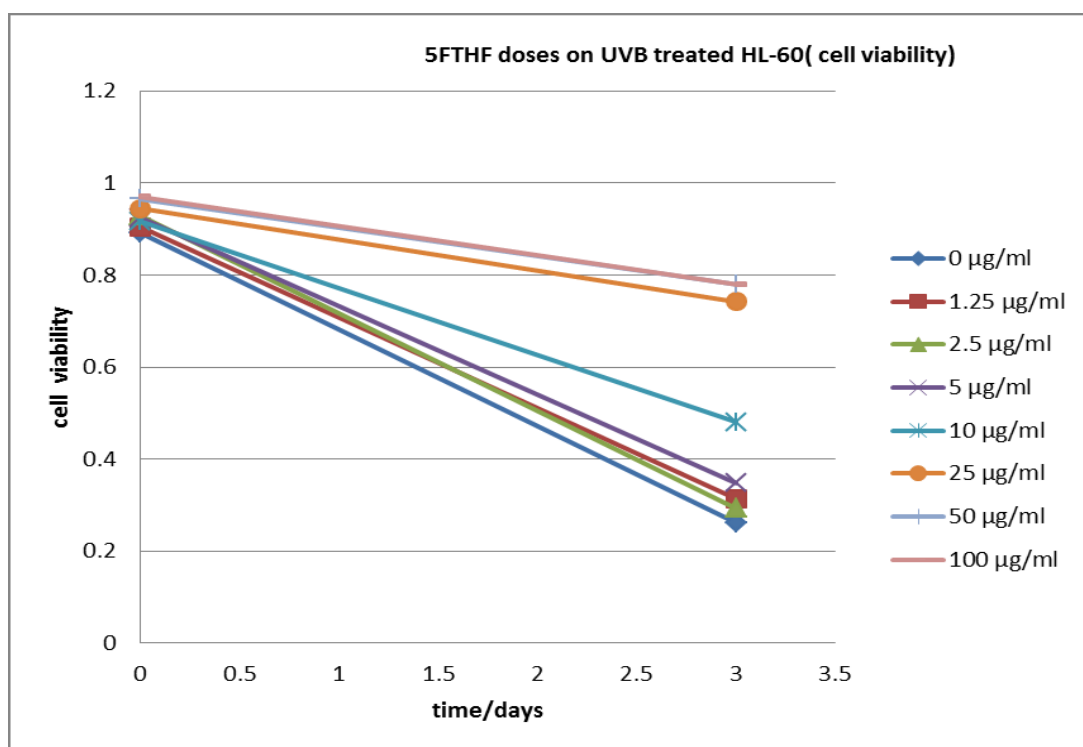
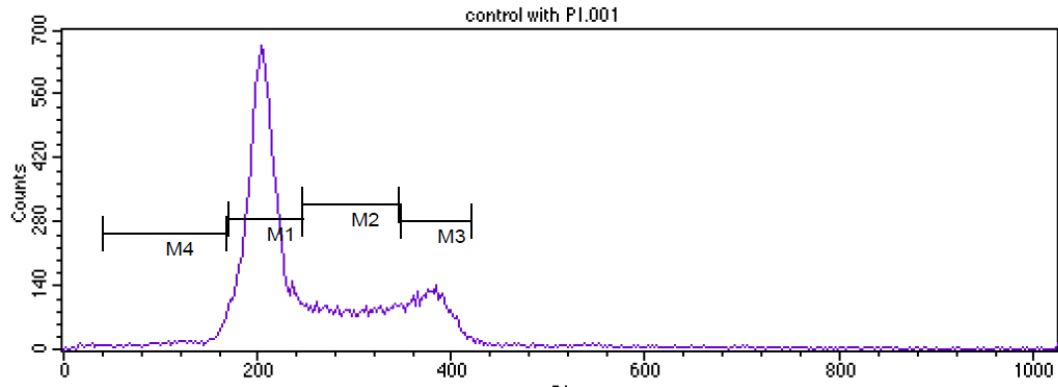


Figure 3.31 shows 5FTHF doses on UVB treated HL-60 cell (cell survival) by (% of Trypan blue dye exclusion):

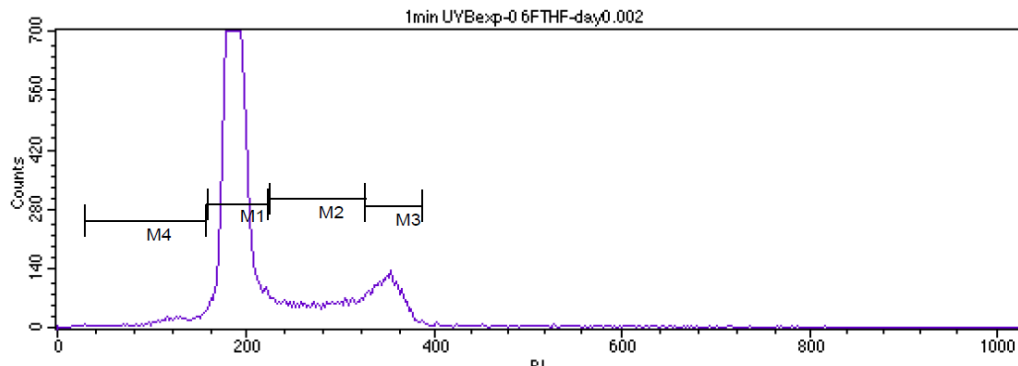
3.5.5.2 PI of stained cells by FACS:

3.5.5.2.1 Control: proliferating cells (no UVB exposure)



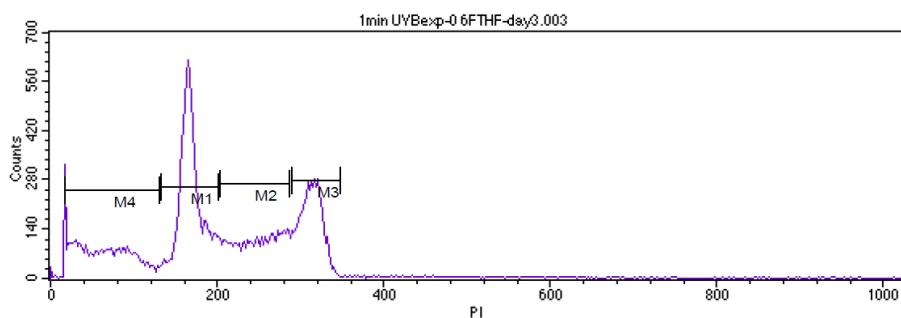
Marker	Left, Right	Events	% Gated	% Total	Mean	Geo Mean	CV
All	0, 1023	39186	100.00	97.97	259.49	244.59	36.40
M1	170, 246	22178	56.60	55.45	205.86	205.25	7.67
M2	246, 346	7934	20.25	19.84	295.70	294.19	10.08
M3	348, 419	6032	15.39	15.08	378.20	377.79	4.63
M4	40, 168	1517	3.87	3.79	126.69	120.03	28.85

3.5.5.2.2 1 min UVB exposure; 0 µg/ml 5FTHF; day0



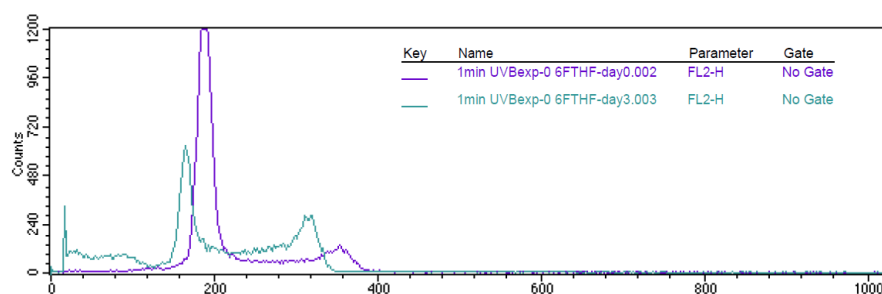
Marker	Left, Right	Events	% Gated	% Total	Mean	Geo Mean	CV
All	0, 1023	39633	100.00	99.08	219.32	211.31	29.38
M1	159, 225	28508	71.93	71.27	189.63	189.34	5.62
M2	226, 327	5368	13.54	13.42	277.14	275.44	11.02
M3	327, 388	4358	11.00	10.90	351.21	350.93	3.97
M4	30, 158	1131	2.85	2.83	122.88	117.55	24.61

3.5.5.2.3 1 min UVB exposure; 0 µg/ml 5FTHF; day3

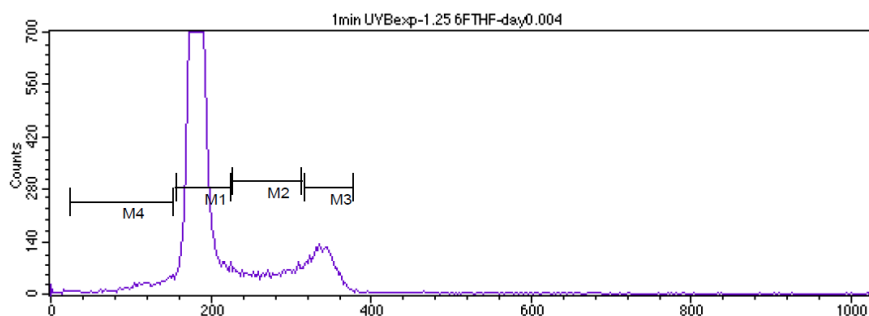


Marker	Left, Right	Events	% Gated	% Total	Mean	Geo Mean	CV
All	0, 1023	40000	100.00	100.00	202.56	171.31	48.11
M1	133, 202	14180	35.45	35.45	169.39	168.84	8.08
M2	204, 287	8424	21.06	21.06	247.55	246.29	10.04
M3	290, 348	8707	21.77	21.77	313.01	312.78	3.86
M4	18, 131	7695	19.24	19.24	64.93	56.47	48.11

3.5.5.2.4 Overlay:

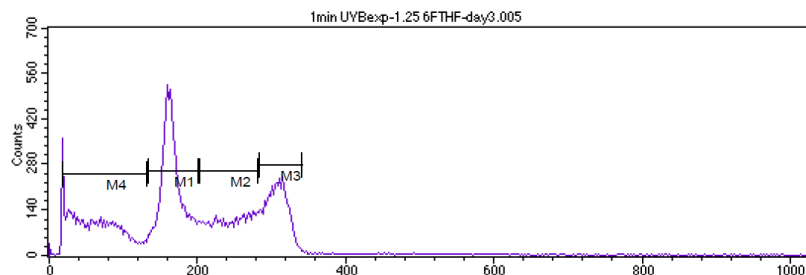


3.5.5.2.5 1 min UVB exposure; 1.25 µg/ml 5FTHF; day0



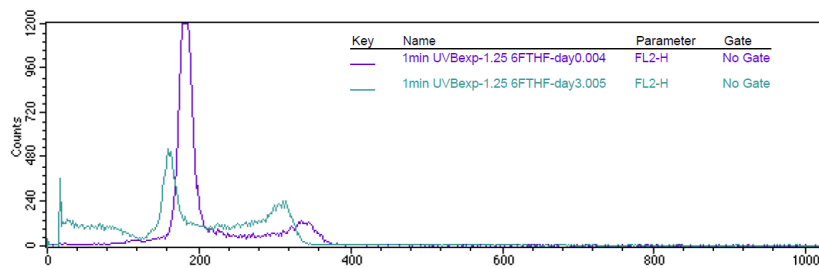
Marker	Left, Right	Events	% Gated	% Total	Mean	Geo Mean	CV
All	0, 1023	40000	100.00	100.00	211.27	201.77	31.62
M1	157, 225	28737	71.84	71.84	184.73	184.40	6.04
M2	227, 314	4396	10.99	10.99	271.53	270.21	9.80
M3	317, 378	4402	11.00	11.00	340.20	339.94	3.95
M4	24, 152	1679	4.20	4.20	114.12	107.50	28.22

3.5.5.2.5 1 min UVB exposure; 1.25 µg/ml 5FTHF; day3

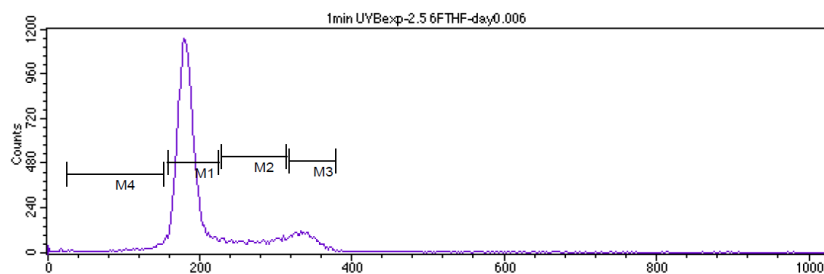


Marker	Left, Right	Events	% Gated	% Total	Mean	Geo Mean	CV
All	0, 1023	40000	100.00	100.00	191.12	157.49	52.82
M1	133, 202	13675	34.19	34.19	166.15	165.49	9.00
M2	204, 281	7746	19.36	19.36	244.48	243.40	9.37
M3	282, 340	8160	20.40	20.40	306.70	306.41	4.36
M4	18, 131	9541	23.85	23.85	63.98	55.77	48.33

3.5.5.2.7 Overlay:

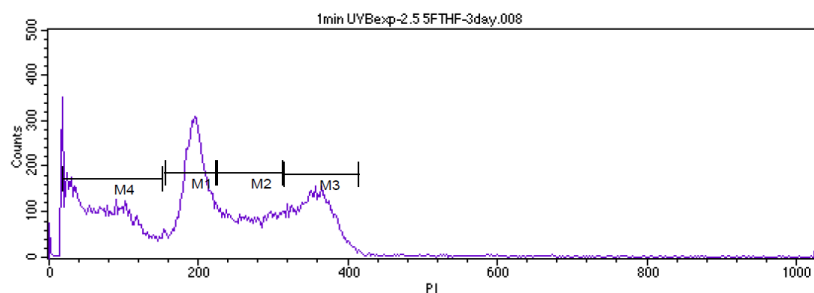


3.5.5.2.8 1 min UVB exposure; 2.5 µg/ml 5FTHF; day0



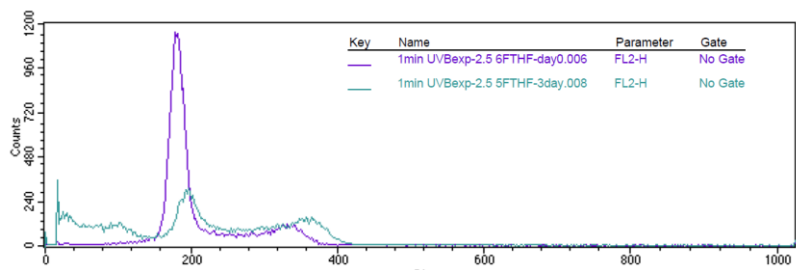
Marker	Left, Right	Events	% Gated	% Total	Mean	Geo Mean	CV
All	0, 1023	40000	100.00	100.00	210.06	200.00	32.41
M1	157, 225	28873	72.18	72.18	183.08	182.69	6.68
M2	227, 314	4927	12.32	12.32	271.26	269.94	9.81
M3	317, 378	3854	9.63	9.63	338.54	338.26	4.10
M4	24, 152	1366	3.42	3.42	114.37	105.93	31.26

3.5.5.2.9 1 min UVB exposure; 2.5 µg/ml 5FTHF; day3

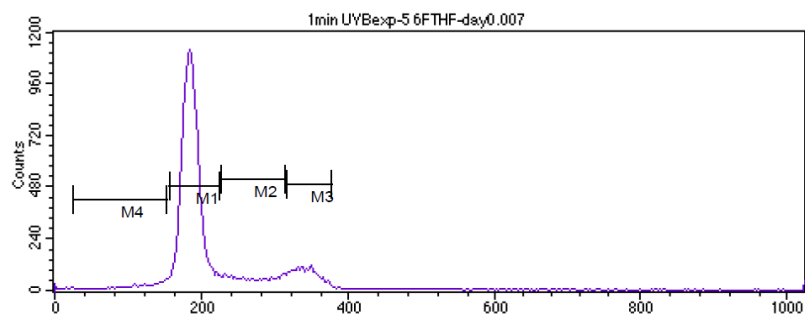


Marker	Left, Right	Events	% Gated	% Total	Mean	Geo Mean	CV
All	0, 1023	40000	100.00	100.00	209.15	162.61	57.53
M1	155, 224	10698	26.75	26.75	194.70	194.07	7.90
M2	225, 312	7131	17.83	17.83	268.36	267.07	9.78
M3	314, 414	8786	21.96	21.96	354.92	354.17	6.54
M4	18, 151	12285	30.71	30.71	71.46	61.21	51.03

3.5.5.2.10 Overlay:

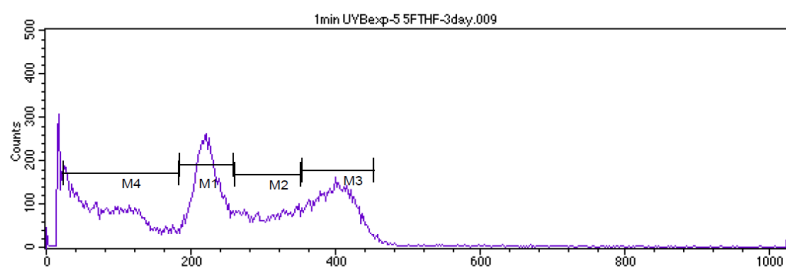


3.5.5.2.11 1 min UVB exposure; 5 µg/ml 5FTHF; day0



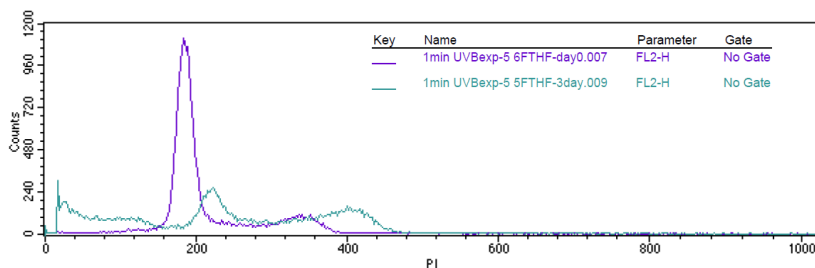
Marker	Left, Right	Events	% Gated	% Total	Mean	Geo Mean	CV
All	0, 1023	40000	100.00	100.00	214.81	204.19	34.00
M1	157, 225	28829	72.07	72.07	186.59	186.22	6.38
M2	227, 314	4294	10.73	10.73	270.20	268.88	9.89
M3	317, 378	4353	10.88	10.88	342.98	342.63	4.54
M4	24, 152	1463	3.66	3.66	112.06	104.54	30.44

3.5.5.2.12 1 min UVB exposure; 5 µg/ml 5FTHF; day3

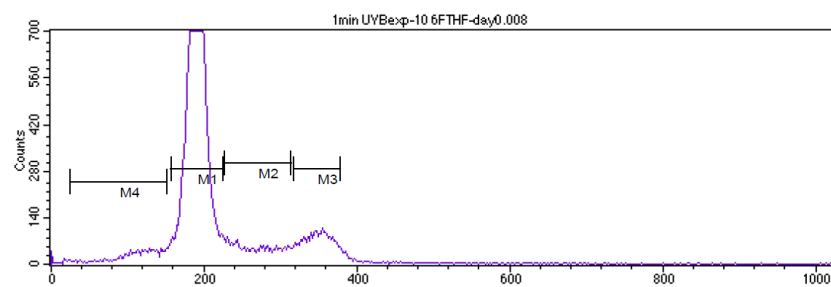


Marker	Left, Right	Events	% Gated	% Total	Mean	Geo Mean	CV
All	0, 1023	40000	100.00	100.00	236.68	180.67	57.73
M1	184, 258	10173	25.43	25.43	222.45	221.81	7.59
M2	260, 351	6275	15.69	15.69	306.48	305.23	8.98
M3	353, 453	9537	23.84	23.84	398.42	397.65	6.21
M4	24, 182	11838	29.59	29.59	85.29	73.34	51.30

3.5.5.2.13 Overlay:

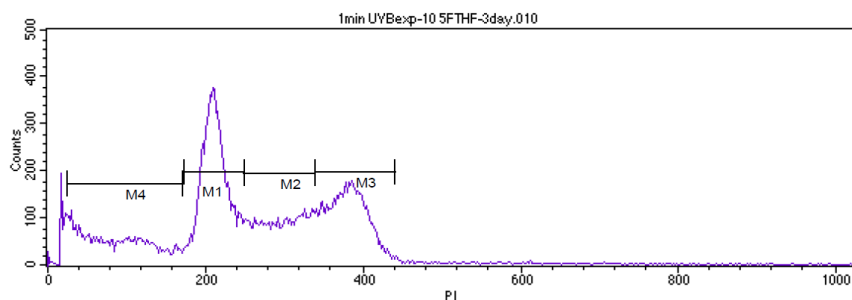


3.5.5.2.14 1 min UVB exposure; 10 µg/ml 5FTHF; day0



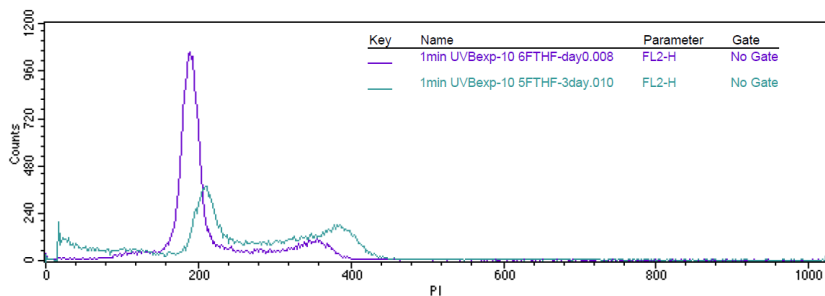
Marker	Left, Right	Events	% Gated	% Total	Mean	Geo Mean	CV
All	0, 1023	40000	100.00	100.00	215.84	204.32	34.38
M1	157, 225	28099	70.25	70.25	190.29	189.90	6.35
M2	227, 314	3925	9.81	9.81	267.91	266.58	9.98
M3	317, 378	4315	10.79	10.79	347.87	347.48	4.71
M4	24, 152	2359	5.90	5.90	112.37	106.49	27.18

3.5.5.2.15 1 min UVB exposure; 10 µg/ml 5FTHF; day3

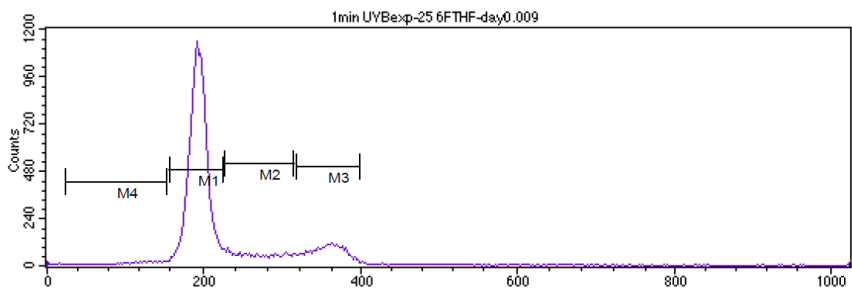


Marker	Left, Right	Events	% Gated	% Total	Mean	Geo Mean	CV
All	0, 1023	40000	100.00	100.00	252.90	210.98	47.63
M1	172, 249	13375	33.44	33.44	212.40	211.77	7.67
M2	249, 339	7945	19.86	19.86	295.68	294.45	9.07
M3	340, 440	10236	25.59	25.59	380.67	379.98	6.03
M4	24, 171	6956	17.39	17.39	84.48	72.87	50.21

3.5.5.2.16 Overlay:

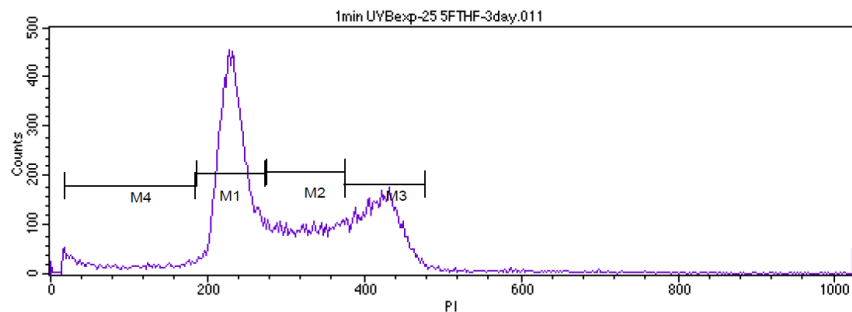


3.5.5.2.17 1 min UVB exposure; 25 µg/ml 5FTHF; day0



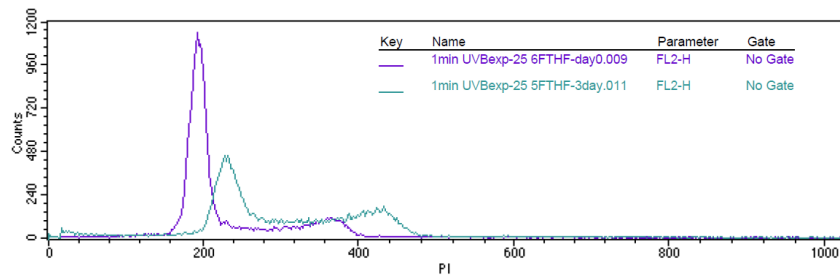
Marker	Left, Right	Events	% Gated	% Total	Mean	Geo Mean	CV
All	0, 1023	40000	100.00	100.00	226.70	216.01	33.33
M1	157, 225	28290	70.73	70.73	193.13	192.79	5.91
M2	227, 314	4298	10.75	10.75	268.24	266.92	9.95
M3	317, 398	5546	13.87	13.87	356.25	355.68	5.68
M4	24, 152	954	2.38	2.38	111.80	104.29	29.88

3.5.5.2.18 1 min UVB exposure; 25 µg/ml 5FTHF; day3

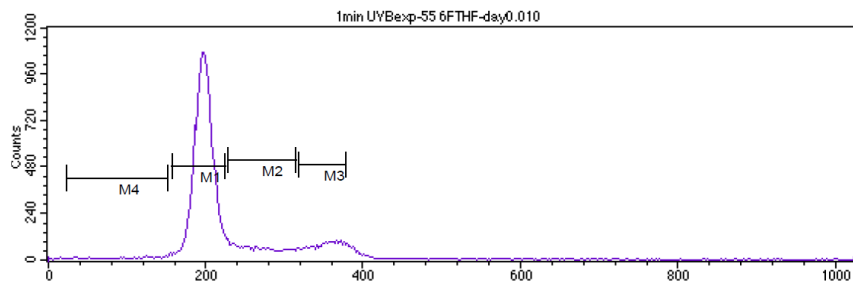


Marker	Left, Right	Events	% Gated	% Total	Mean	Geo Mean	CV
All	0, 1023	40000	100.00	100.00	302.22	275.86	37.87
M1	187, 274	17756	44.39	44.39	233.47	232.81	7.54
M2	275, 375	8600	21.50	21.50	325.36	324.01	9.10
M3	374, 477	10172	25.43	25.43	418.03	417.31	5.85
M4	18, 185	2415	6.04	6.04	95.04	76.40	57.61

3.5.5.2.19 Overlay:

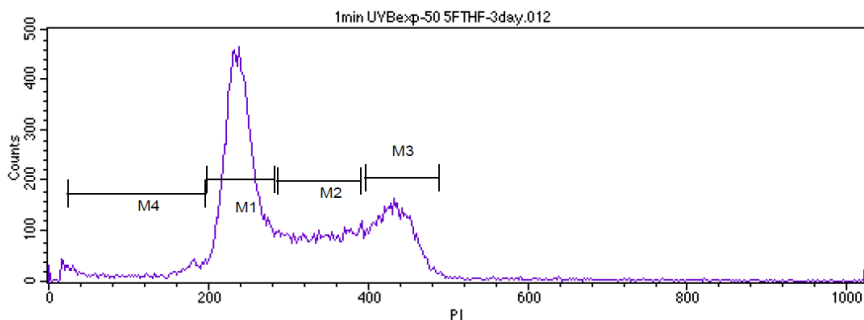


3.5.5.2.20 1 min UVB exposure; 50 µg/ml 5FTHF; day0



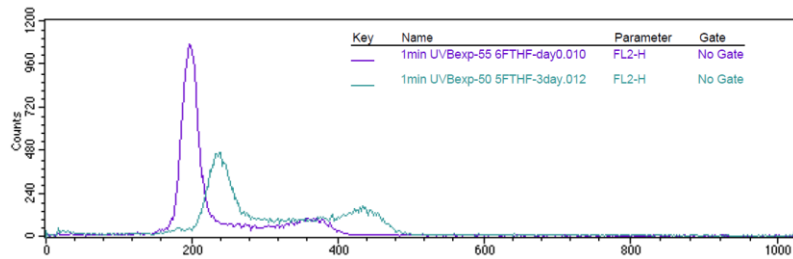
Marker	Left, Right	Events	% Gated	% Total	Mean	Geo Mean	CV
All	0, 1023	40000	100.00	100.00	230.04	220.13	32.24
M1	157, 225	28326	70.81	70.81	197.33	197.00	5.78
M2	227, 314	4758	11.89	11.89	265.42	264.15	9.83
M3	317, 378	4289	10.72	10.72	350.77	350.34	4.92
M4	24, 152	695	1.74	1.74	105.09	95.13	36.77

3.5.5.2.21 1 min UVB exposure; 50 µg/ml 5FTHF; day3

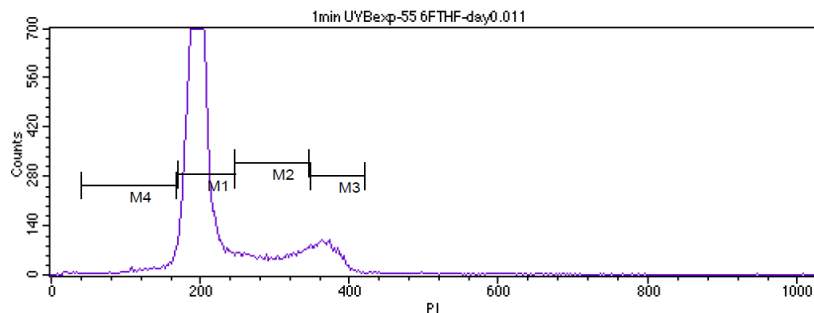


Marker	Left, Right	Events	% Gated	% Total	Mean	Geo Mean	CV
All	0, 1023	40000	100.00	100.00	305.99	283.18	35.17
M1	199, 283	18869	47.17	47.17	240.48	239.82	7.41
M2	287, 392	8699	21.75	21.75	340.46	339.02	9.17
M3	397, 489	8545	21.36	21.36	433.98	433.45	4.94
M4	24, 197	2210	5.53	5.53	125.57	106.41	46.79

3.5.5.2.22 Overlay:

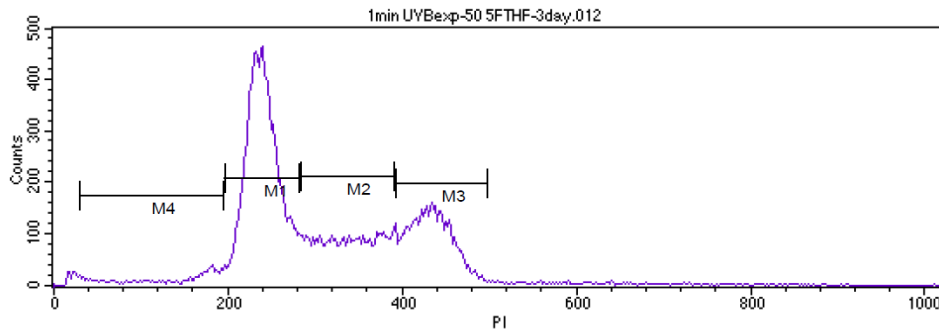


3.5.5.2.23 1 min UVB exposure; 100 µg/ml 5FTHF; day0



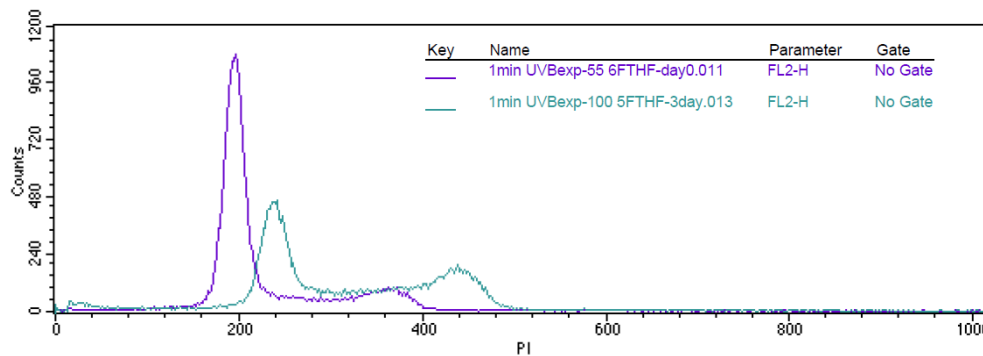
Marker	Left, Right	Events	% Gated	% Total	Mean	Geo Mean	CV
All	0, 1023	39577	100.00	98.94	226.77	218.35	29.89
M1	170, 246	29198	73.78	73.00	197.90	197.45	6.83
M2	246, 346	4987	12.60	12.47	297.76	296.13	10.40
M3	348, 419	3580	9.05	8.95	371.32	371.00	4.15
M4	40, 168	1342	3.39	3.36	138.34	134.34	21.08

3.5.5.2.24 1 min UVB exposure; 100 µg/ml 5FTHF; day3



Marker	Left, Right	Events	% Gated	% Total	Mean	Geo Mean	CV
All	0, 1023	39222	100.00	98.06	307.49	288.85	32.62
M1	197, 281	18700	47.68	46.75	239.98	239.34	7.31
M2	283, 390	8786	22.40	21.96	337.00	335.50	9.41
M3	392, 497	9031	23.03	22.58	432.46	431.85	5.35
M4	30, 195	1598	4.07	4.00	135.79	120.64	39.44

3.5.5.2.25 Overlay:



3.5.6 5FTHF doses on UVB-treated HL-60 cells :

To describe the time course of apoptosis in starved HL-60 cells, and depending on 5FTHF doses. Cells were washed twice in 1x PBS, and after being starved by seeding for two consecutive days in Iscove serum free medium, cells were supplemented with/no increasing doses of folic acid in a dose- dependent manner namely 0, 5, 10, 25 and 50 µg/ml and incubated at 37° C in an atmosphere of 95% air and 5% CO₂. Afterwards cells were exposed

to UVB for 1 minute and then incubated. One day later cells were harvested after 1,2, 3 and 6 days where cell count , viability and PI were performed.

3.5.6.1 Result:

Concerning the cell that has maintained in serum free medium and 5FTHF deficient there is a transient arrest of replication by 24 h post-irradiation as evidenced by reduction in cell number, then one day later the cell re-entering the cell cycle by 48 h post- radiation then levelled off by day 3. Folinic acid was crucial and remarkable in promoting cells proliferation and rescuing cells from apoptosis($p>0.05$). The results confirmed latter by flow cytometric analysis which shows increase in phase S and G2/M2 cells With regard to cells that grown in Iscove serum free media which supplemented with 5FTHF continued proliferating in dose-dependent manner, and levelled off by day 3. The flow cytometric analysis show increase in subG1 cell and decrease in S and G2/M cells respectively.

Table 3.32 shows 5FTHF doses on UVB-treated HL-60 cells(cell proliferation) using haemocytometer

5FTHF	0	1	2	3	6
0 µg/ml	1	0.985	1.195	1.185	1.06
5 µg/ml	1	1.21	1.435	1.575	1.12
10 µg/ml	1	1.385	1.69	1.84	1.465
25 µg/ml	1	1.385	2.03	1.975	1.765
50µg/ml	1	1.565	2.07	2	1.955

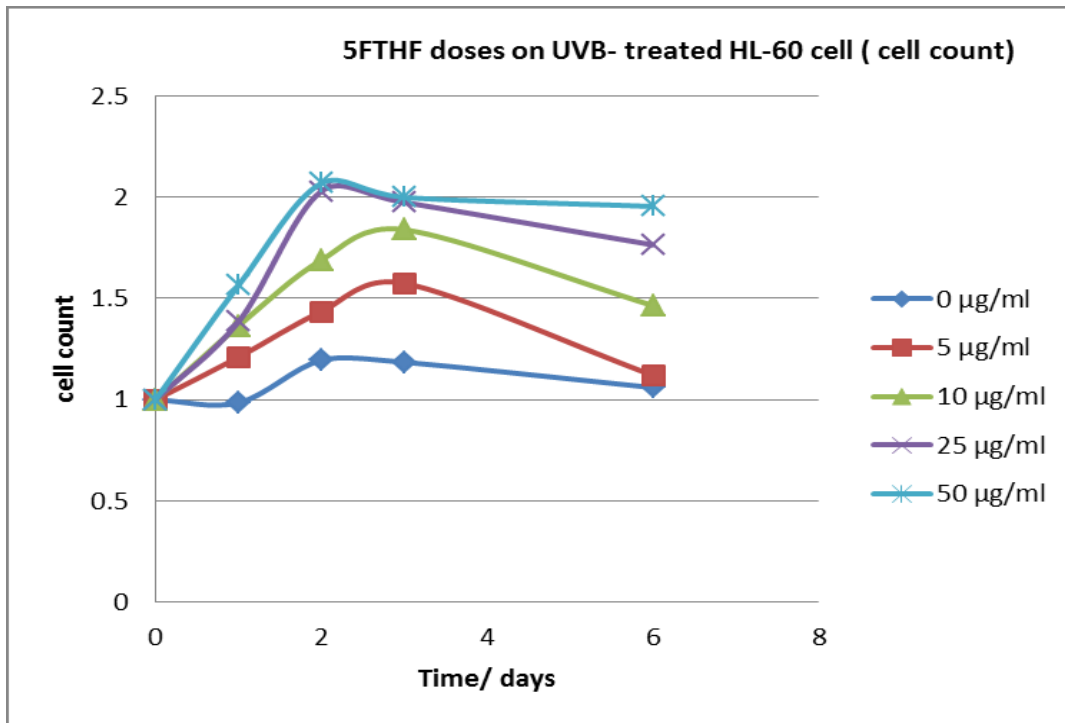


Figure 3.32 shows 5FTHF doses on UVB-treated HL-60 cells(cell proliferation) using haemocytometer

Table 3.33 shows 5FTHF doses on UVB-treated HL-60 cells(cell proliferation)

5FTHF	0	1	2	3	6
0 µg/ml	1	0.985	1.195	1.185	1.06
5 µg/ml	1	1.21	1.435	1.575	1.12
10 µg/ml	1	1.365	1.69	1.84	1.465
25 µg/ml	1	1.385	2.03	1.975	1.765
50 µg/ml	1	1.565	2.07	2	1.955

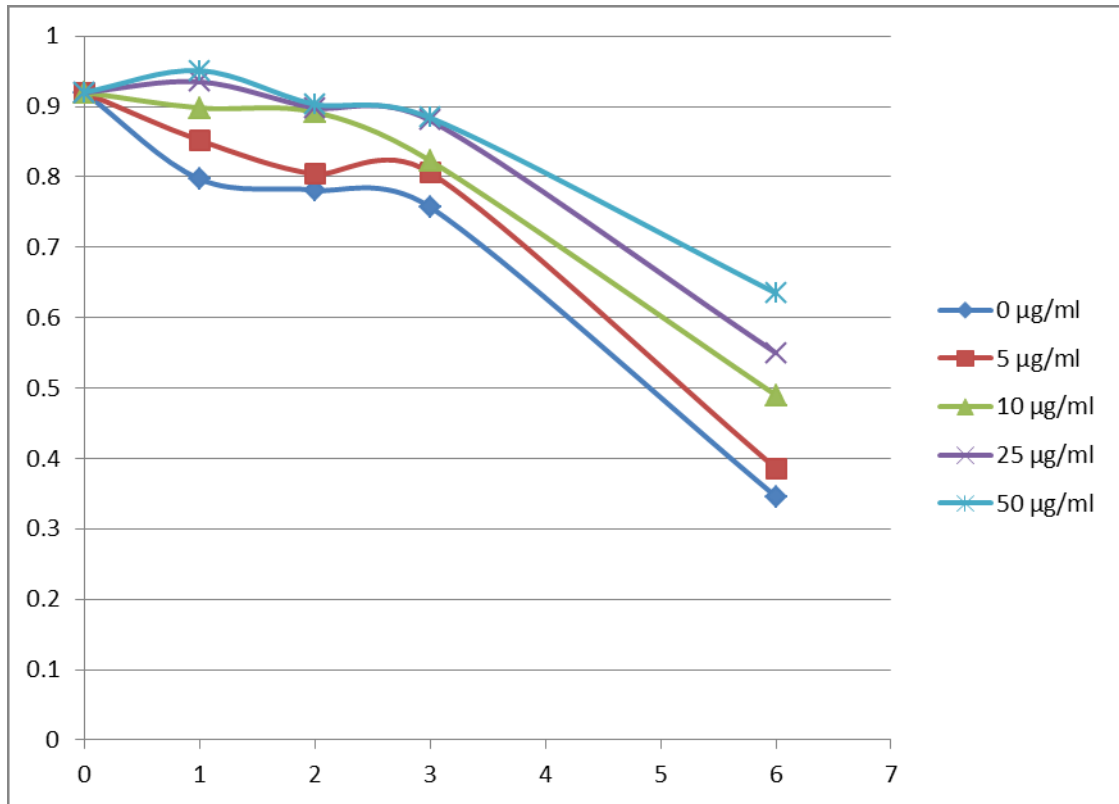
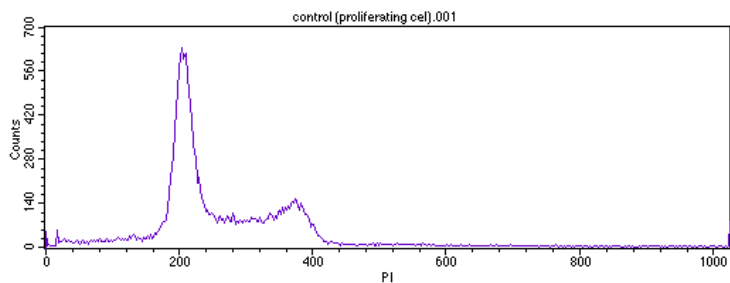


Figure 3.33 shows 5FTHF doses on UVB-treated HL-60 cells (cell proliferation)

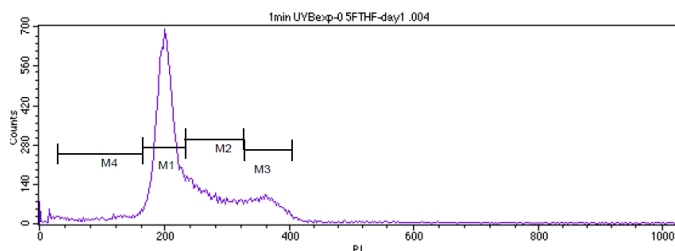
3.5.6.2 Flow cytometric analysis:

3.5.6.2.1 Control proliferating cell



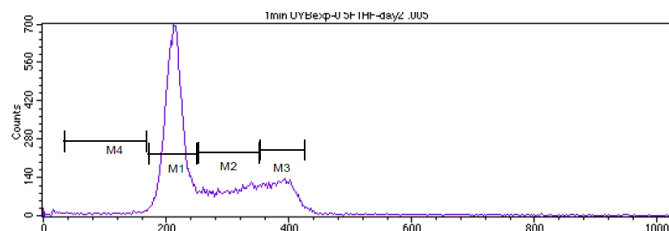
Marker	Left, Right	Events	% Gated	% Total	Mean	Geo Mean	CV
All	0, 1023	40000	100.00	100.00	259.13	237.70	40.70
M1	168, 246	21191	52.98	52.98	208.23	207.65	7.46
M2	246, 342	7833	19.58	19.58	293.24	291.85	9.73
M3	340, 413	6892	17.23	17.23	372.06	371.63	4.81
M4	40, 168	2453	6.13	6.13	115.86	109.12	31.26

3.5.6.2.2 1 minute UVB exposure - 0µl 5FTHF- day 1



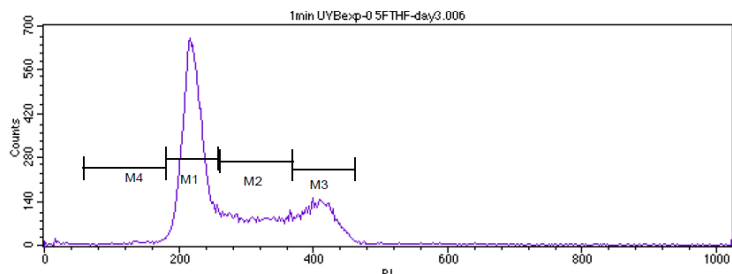
Marker	Left, Right	Events	% Gated	% Total	Mean	Geo Mean	CV
All	0, 1023	40000	100.00	100.00	247.35	226.01	44.15
M1	166, 234	21986	54.96	54.96	202.29	201.79	6.98
M2	234, 327	8974	22.43	22.43	273.60	272.26	9.97
M3	329, 405	5152	12.88	12.88	362.52	361.96	5.54
M4	30, 166	2234	5.58	5.58	109.73	99.41	38.28

3.5.6.2.3 1 minute UVB exposure - 0µl 5FTHF- day 2



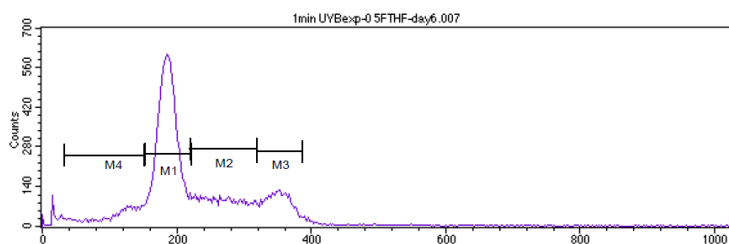
Marker	Left, Right	Events	% Gated	% Total	Mean	Geo Mean	CV
All	0, 1023	40000	100.00	100.00	268.97	254.06	33.80
M1	172, 250	22508	56.27	56.27	213.93	213.44	6.74
M2	253, 352	8419	21.05	21.05	304.83	303.40	9.61
M3	354, 427	6961	17.40	17.40	386.27	385.82	4.88
M4	34, 168	706	1.76	1.76	111.26	101.12	38.29

3.5.6.2.1 1 minute UVB exposure - 0µl 5FTHF- day 3



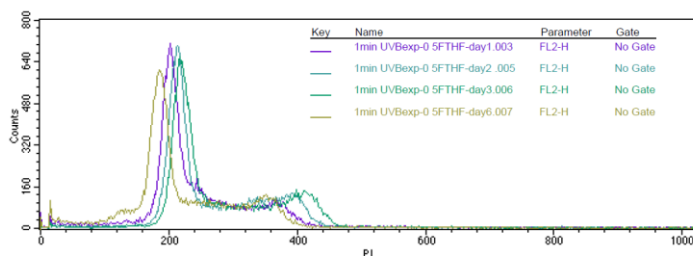
Marker	Left, Right	Events	% Gated	% Total	Mean	Geo Mean	CV
All	0, 1023	40000	100.00	100.00	282.05	268.48	32.14
M1	181, 259	22321	55.80	55.80	222.23	221.72	6.76
M2	261, 370	8573	21.43	21.43	314.03	312.35	10.34
M3	370, 462	7849	19.62	19.62	408.88	408.31	5.29
M4	58, 181	534	1.33	1.33	145.06	141.09	21.19

3.5.6.2.2 1 minute UVB exposure - 0µl 5FTHF- day 6

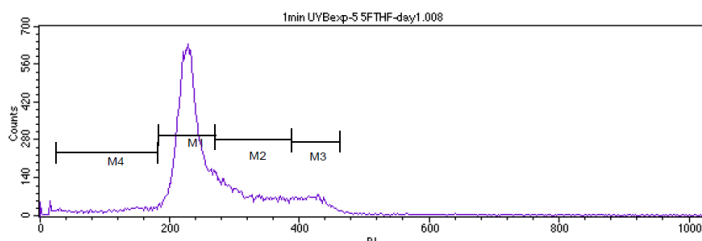


Marker	Left, Right	Events	% Gated	% Total	Mean	Geo Mean	CV
All	0, 1023	40000	100.00	100.00	225.81	205.22	41.68
M1	154, 222	20605	51.51	51.51	187.08	186.54	7.62
M2	220, 319	8539	21.35	21.35	267.39	265.84	10.77
M3	319, 386	5794	14.49	14.49	350.19	349.77	4.86
M4	33, 150	3682	9.21	9.21	108.05	100.98	31.39

3.5.6.2.3 1 minute UVB exposure – 0 µl 5FTHF- overlay:

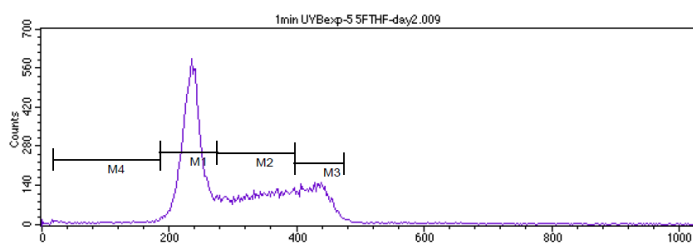


3.5.6.2.4 1 minute UVB exposure - 5µl 5FTHF- day 1



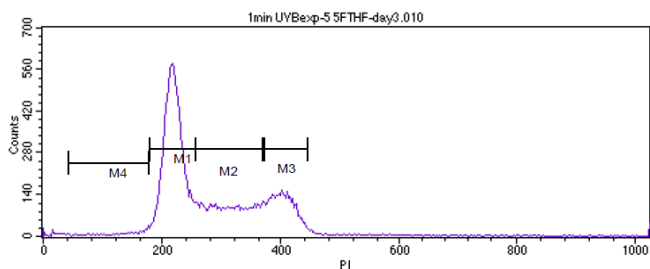
Marker	Left, Right	Events	% Gated	% Total	Mean	Geo Mean	CV
All	0, 1023	40000	100.00	100.00	267.60	247.98	37.98
M1	182, 270	24258	60.65	60.65	229.65	228.98	7.69
M2	270, 388	8773	21.93	21.93	319.18	317.29	11.00
M3	387, 461	3641	9.10	9.10	418.60	418.16	4.60
M4	24, 180	2398	6.00	6.00	112.46	99.45	41.75

3.5.6.2.5 1 minute UVB exposure - 5 μ l 5FTHF- day 2



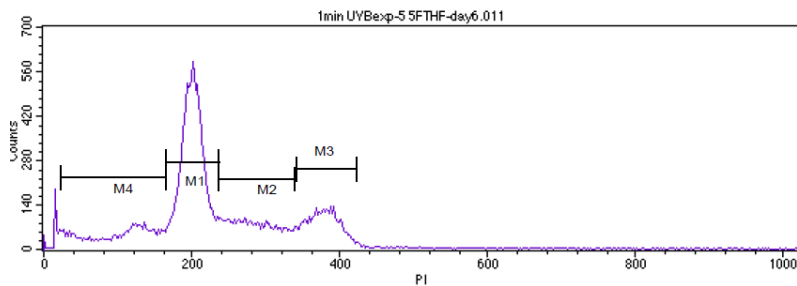
Marker	Left, Right	Events	% Gated	% Total	Mean	Geo Mean	CV
All	0, 1023	40000	100.00	100.00	307.25	290.34	33.00
M1	185, 276	19425	48.56	48.56	235.55	234.97	7.02
M2	275, 396	11564	28.91	28.91	339.08	337.21	10.40
M3	396, 474	7435	18.59	18.59	428.50	428.08	4.46
M4	18, 185	887	2.22	2.22	111.19	93.55	47.82

3.5.6.2.6 1 minute UVB exposure - 5 μ l 5FTHF- day 3



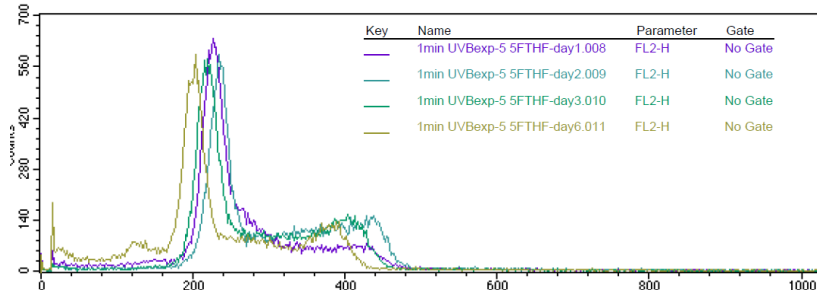
Marker	Left, Right	Events	% Gated	% Total	Mean	Geo Mean	CV
All	0, 1023	40000	100.00	100.00	283.14	268.32	32.13
M1	180, 257	20516	51.29	51.29	220.55	220.01	6.97
M2	257, 370	10336	25.84	25.84	312.89	311.10	10.66
M3	374, 447	7314	18.29	18.29	404.53	404.12	4.51
M4	42, 178	695	1.74	1.74	135.36	128.12	28.37

3.5.6.2.7 1 minute UVB exposure - 5µl 5FTHF- day 6

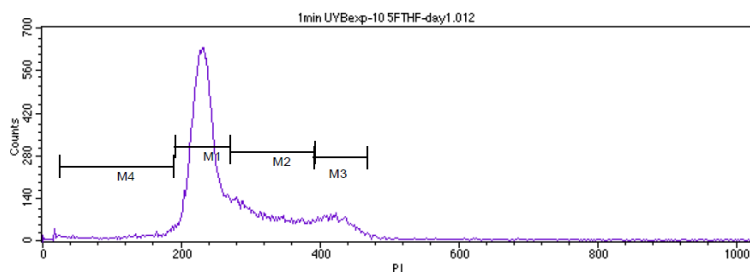


Marker	Left, Right	Events	% Gated	% Total	Mean	Geo Mean	CV
All	0, 1023	40000	100.00	100.00	236.00	207.20	45.96
M1	165, 237	18983	47.46	47.46	201.63	201.09	7.32
M2	237, 340	7474	18.68	18.68	284.30	282.79	10.36
M3	342, 423	6389	15.97	15.97	378.29	377.79	5.17
M4	23, 165	6010	15.02	15.02	101.51	89.42	42.19

3.5.6.2.8 1 minute UVB exposure - 5µl 5FTHF- overlay:

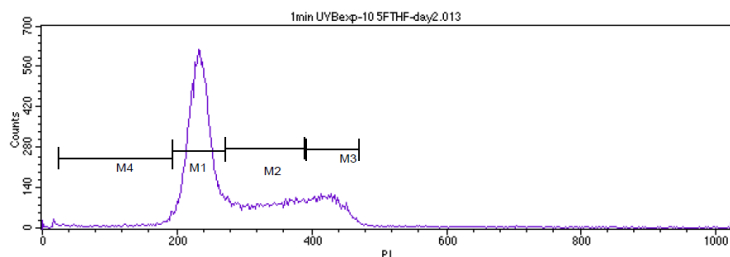


3.5.6.2.9 1 minute UVB exposure – 10 µl 5FTHF- day 1



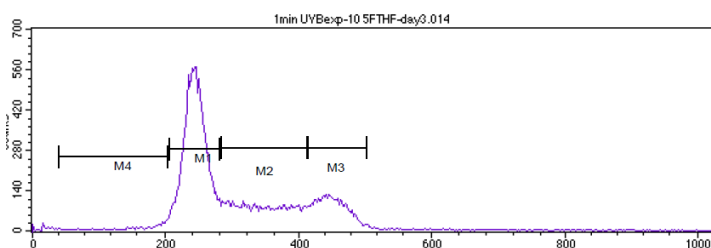
Marker	Left, Right	Events	% Gated	% Total	Mean	Geo Mean	CV
All	0, 1023	40000	100.00	100.00	276.97	261.08	35.11
M1	191, 270	23836	59.59	59.59	231.94	231.38	6.95
M2	270, 393	9595	23.99	23.99	321.65	319.63	11.30
M3	391, 468	4172	10.43	10.43	423.36	422.90	4.69
M4	24, 189	1640	4.10	4.10	126.84	111.56	41.08

3.5.6.2.10 1 minute UVB exposure – 10 µl 5FTHF- day 2



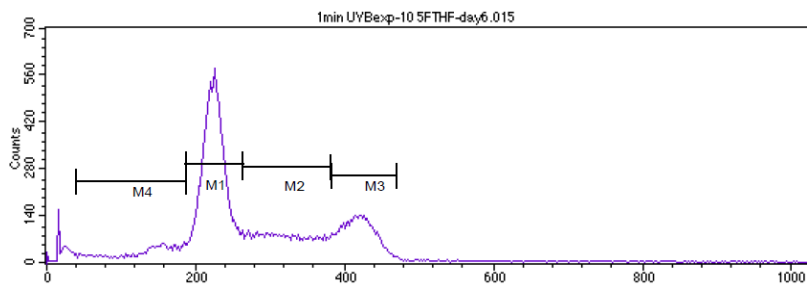
Marker	Left, Right	Events	% Gated	% Total	Mean	Geo Mean	CV
All	0, 1023	40000	100.00	100.00	289.25	273.68	32.55
M1	193, 272	22717	56.79	56.79	233.75	233.21	6.80
M2	272, 390	9210	23.03	23.03	331.99	330.08	10.68
M3	392, 470	6108	15.27	15.27	424.48	424.03	4.66
M4	24, 193	1172	2.93	2.93	134.92	118.48	40.49

3.5.6.2.11 1 minute UVB exposure – 10 µl 5FTHF- day 3

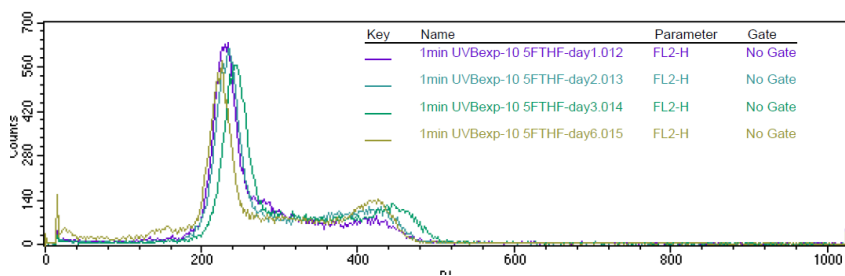


Marker	Left, Right	Events	% Gated	% Total	Mean	Geo Mean	CV
All	0, 1023	40000	100.00	100.00	308.64	292.78	32.15
M1	205, 281	21317	53.29	53.29	244.29	243.77	6.50
M2	283, 411	9803	24.51	24.51	344.77	342.67	11.02
M3	414, 502	6860	17.15	17.15	449.57	449.07	4.74
M4	39, 203	910	2.27	2.27	159.02	149.58	28.57

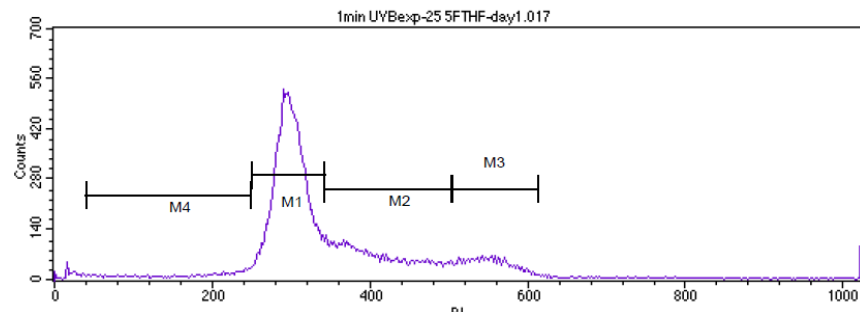
3.5.6.2.12 1 minute UVB exposure – 10 µl 5FTHF- day 6



Marker	Left, Right	Events	% Gated	% Total	Mean	Geo Mean	CV
All	0, 1023	40000	100.00	100.00	275.62	248.01	40.72
M1	187, 263	18945	47.36	47.36	224.85	224.33	6.80
M2	263, 381	8440	21.10	21.10	319.99	318.15	10.71
M3	383, 469	7384	18.46	18.46	418.97	418.50	4.76
M4	39, 187	3722	9.30	9.30	131.18	122.16	32.41

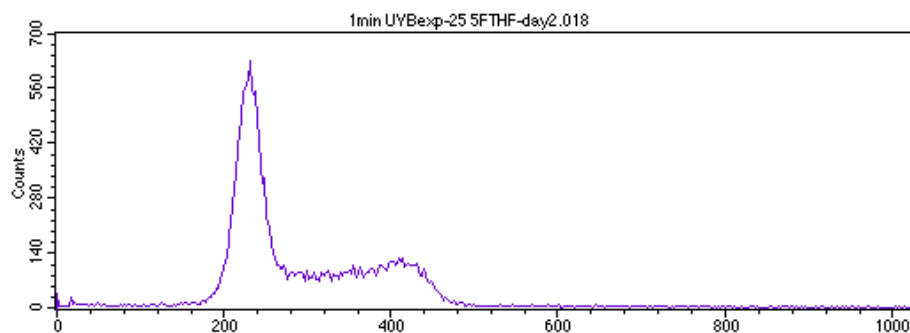


3.5.6.2.13 1 minute UVB exposure – 25 µl 5FTHF- day 1



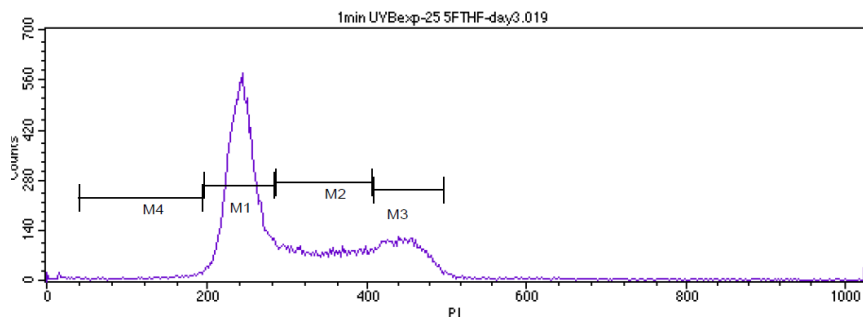
Marker	Left, Right	Events	% Gated	% Total	Mean	Geo Mean	CV
All	0, 1023	40000	100.00	100.00	355.24	332.34	34.34
M1	251, 343	23259	58.15	58.15	299.46	298.85	6.38
M2	343, 503	9699	24.25	24.25	408.60	406.01	11.38
M3	505, 614	4137	10.34	10.34	550.01	549.35	4.92
M4	40, 249	1700	4.25	4.25	169.19	152.15	38.80

3.5.6.2.14 1 minute UVB exposure – 25 µl 5FTHF- day 2



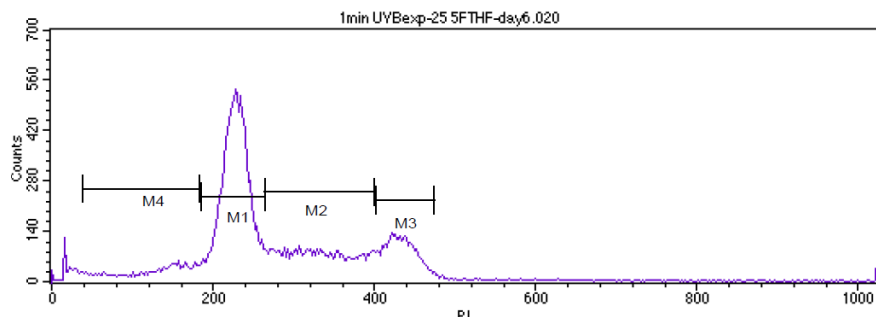
Marker	Left, Right	Events	% Gated	% Total	Mean	Geo Mean	CV
All	0, 1023	40000	100.00	100.00	287.14	271.78	32.80
M1	189, 267	22508	56.27	56.27	230.52	230.00	6.76
M2	267, 376	8576	21.44	21.44	321.31	319.66	10.11
M3	376, 469	7381	18.45	18.45	414.40	413.78	5.50
M4	40, 189	917	2.29	2.29	140.08	130.42	32.28

3.5.6.2.15 1 minute UVB exposure – 25 µl 5FTHF- day3



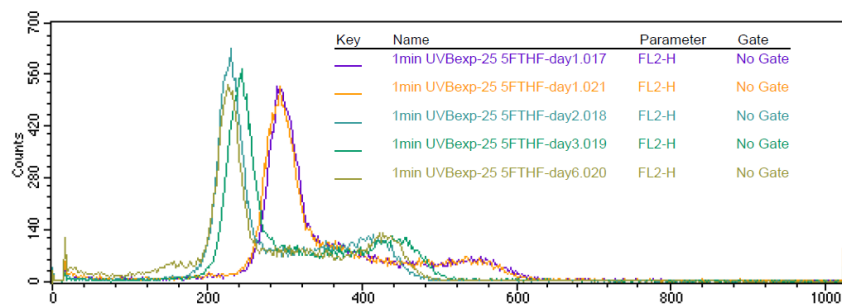
Marker	Left, Right	Events	% Gated	% Total	Mean	Geo Mean	CV
All	0, 1023	40000	100.00	100.00	309.05	293.14	32.49
M1	197, 284	22045	55.11	55.11	244.39	243.79	6.99
M2	286, 407	9015	22.54	22.54	344.82	342.92	10.49
M3	409, 497	7131	17.83	17.83	446.92	446.37	4.98
M4	41, 195	660	1.65	1.65	144.00	134.35	31.38

3.5.6.2.16 1 minute UVB exposure – 25 µl 5FTHF- day6

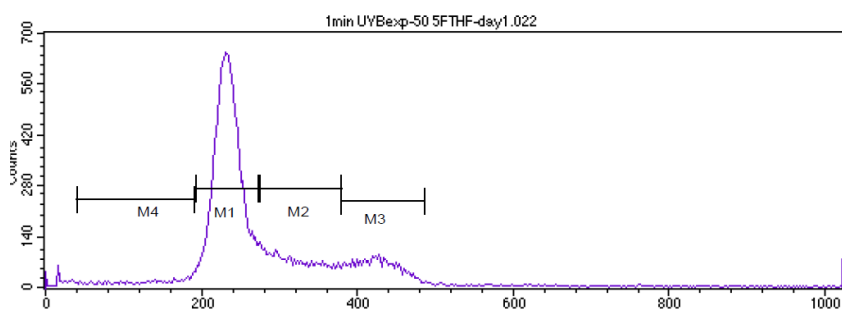


Marker	Left, Right	Events	% Gated	% Total	Mean	Geo Mean	CV
All	0, 1023	40000	100.00	100.00	279.21	253.02	39.73
M1	186, 265	19500	48.75	48.75	228.38	227.82	6.96
M2	265, 400	9496	23.74	23.74	330.26	327.90	11.95
M3	402, 475	6076	15.19	15.19	433.03	432.67	4.13
M4	38, 184	3453	8.63	8.63	128.06	118.93	33.02

3.5.6.2.17 Overlay:

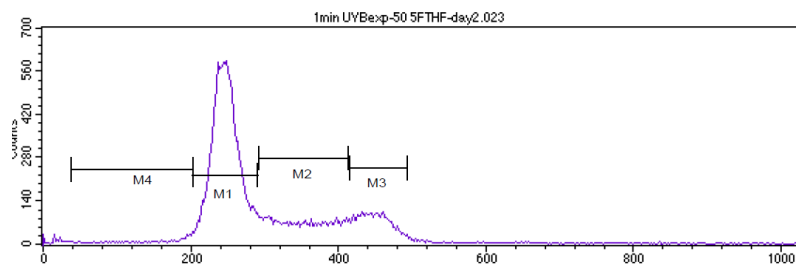


3.5.6.2.18 1 minute UVB exposure – 50 µl 5FTHF- day1



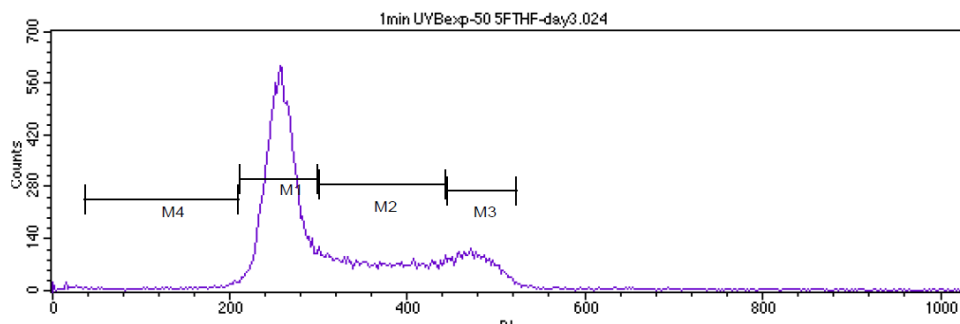
Marker	Left, Right	Events	% Gated	% Total	Mean	Geo Mean	CV
All	0, 1023	40000	100.00	100.00	280.43	260.35	38.59
M1	193, 273	24461	61.15	61.15	234.42	233.86	6.90
M2	275, 380	7045	17.61	17.61	321.23	319.76	9.60
M3	380, 486	5388	13.47	13.47	424.98	424.16	6.23
M4	40, 191	1622	4.06	4.06	128.66	118.63	35.82

3.5.6.2.19 1 minute UVB exposure – 50 µl 5FTHF- day2



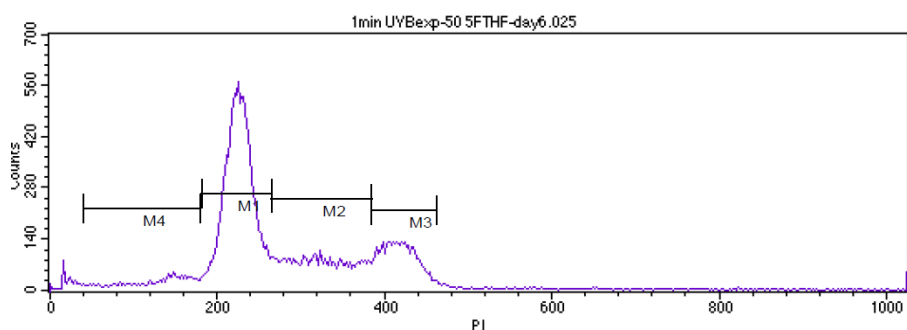
Marker	Left, Right	Events	% Gated	% Total	Mean	Geo Mean	CV
All	0, 1023	40000	100.00	100.00	303.44	285.93	35.01
M1	203, 291	24370	60.92	60.92	247.58	246.96	7.07
M2	293, 413	7810	19.53	19.53	351.49	349.61	10.33
M3	415, 493	5529	13.82	13.82	448.40	447.96	4.44
M4	38, 203	943	2.36	2.36	149.12	137.62	33.78

3.5.6.2.20 1 minute UVB exposure – 50 µl 5FTHF- day3



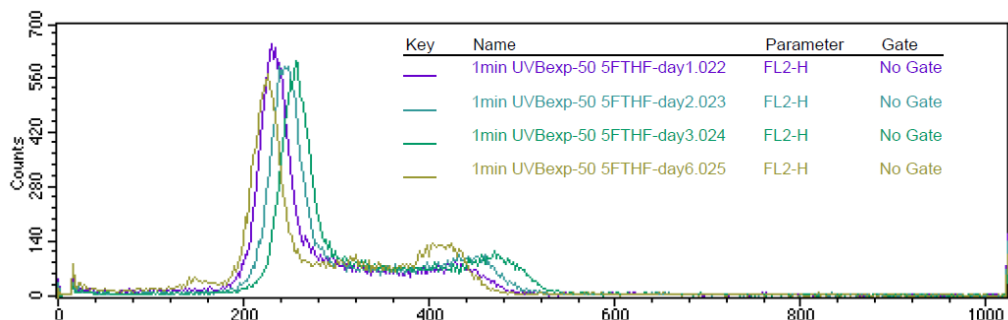
Marker	Left, Right	Events	% Gated	% Total	Mean	Geo Mean	CV
All	0, 1023	40000	100.00	100.00	320.34	304.03	32.10
M1	211, 298	22802	57.00	57.00	257.60	257.04	6.59
M2	300, 443	9897	24.74	24.74	368.56	366.07	11.60
M3	444, 522	5528	13.82	13.82	476.71	476.30	4.17
M4	36, 209	746	1.86	1.86	153.05	140.14	34.25

3.5.6.2.21 1 minute UVB exposure – 50 µl 5FTHF- day6



Marker	Left, Right	Events	% Gated	% Total	Mean	Geo Mean	CV
All	0, 1023	40000	100.00	100.00	280.50	257.78	38.89
M1	181, 266	20680	51.70	51.70	225.89	225.29	7.30
M2	265, 384	8634	21.58	21.58	322.87	321.00	10.74
M3	384, 462	6979	17.45	17.45	416.87	416.43	4.60
M4	40, 179	2503	6.26	6.26	125.93	118.24	30.88

3.5.6.2.22 overlay 1 minute UVB exposure – 50 µl 5FTHF



3.5.7 Serum free medium(SFM) - 5FTHF doses – 1-12 days kinetics:

For modulation of 5 folinic acid 70×10^6 cells were washed extensively in 1x PBS, resuspended in Iscove serum free medium, aliquoted into 5 dishes (14×10^6 in each 100mm), and incubated overnight. Next day cell count and viability were checked. then cells were supplemented with or no assigned increasing doses of folinic acid namely (5, 10, 25 and 50 µg/ml. cells harvested after 1, 2, 3, 6, 9 and 12 days where cell count using haemocytometer, cell viability using trypan blue dye exclusion and staining with PI for FACS analysis were performed.

3.5.7.1 Results:

The results show that , HL-60 cells double in number at 3 days, and later decrease in number, until completely die at 12 days. Furthermore, administration of 5FTHF increased cell growth in SFM, up to 9 days (50ug/ml), while cell death starts at day 6. Proliferation compensates death up to day 9. Later death prevails, so the cell number decreases. There is a dose dependence of 5FTHF in both proliferation and survival. The findings show that administration of 5FTHF is specific and target only to the temporary growth in SFM($p > 0.05$). The results confirmed by flow cytometric analysis, with high- doses of folinic acid there is a reduction in sub G1, increase the number of S phase by day 3 and G2 phase indicating, however, as time went by there are increase in sub G1, decrease in S and G2 phases indicating depletion of folinic acid, whereas, with low- doses of folinic acid there are elevation in sub G1 compared with high- doses folinic acid($p < 0.05$).

Table 3.34 5FTHF doses -1 -12 doses kinetics (cell proliferation)

5FTHF	0	1	2	3	6	9	12
0µg/ml	1.015	1.34	1.34	1.865	1.845	1.12	0.05
5 µg/ml	1.015	1.325	1.55	1.87	2.11	1.555	0.625
10 µg/ml	1.015	1.51	1.665	1.88	2.33	1.61	0.7
25 µg/ml	1.015	1.555	1.735	2.09	2.48	2.16	1.31
50 µg/ml	1.015	1.665	1.76	2.59	2.955	3.38	1.69

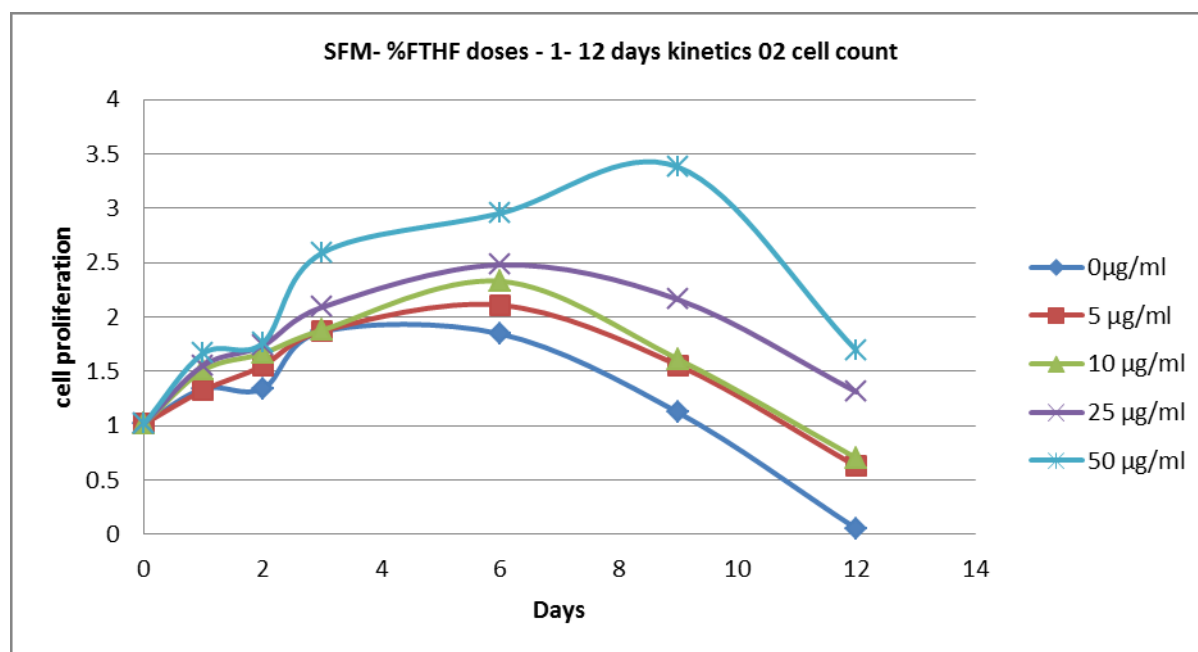


Figure 3.34 5FTHF doses -1 -12 doses kinetics (cell proliferation)

Table 3.35 5FTHF doses -1 -12 doses kinetics (cell survival)

5FTHF	0	1	2	3	6	9	12
0µg/ml	0.92	0.905	0.87	0.88	0.59	0.29	0.0064
5 µg/ml	0.92	0.93	0.93	0.92	0.73	0.41	0.13
10 µg/ml	0.92	0.92	0.93	0.93	0.75	0.44	0.17
25 µg/ml	0.92	0.93	0.95	0.94	0.79	0.52	0.3

50 µg/ml	0.92	0.95	0.954	0.94	0.81	0.64	0.37
----------	------	------	-------	------	------	------	------

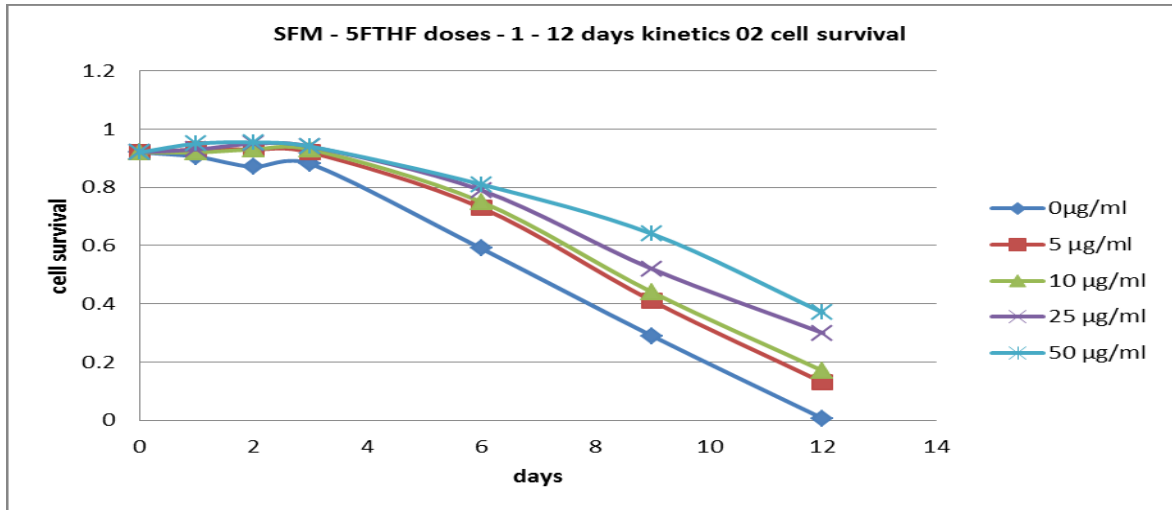
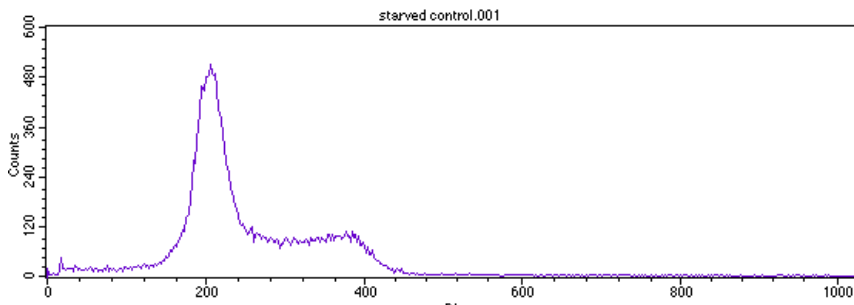


Figure 3.35 5FTHF doses -1 -12 doses kinetics (cell survival)

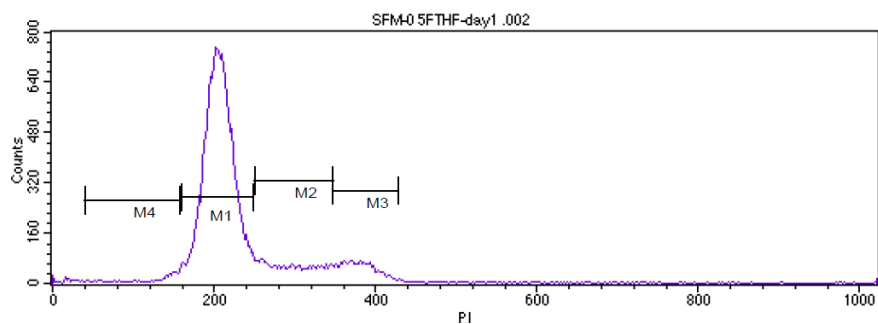
3.5.7.2 Flow cytometry analysis:

3.5.7.2.1 Starved cells (control)



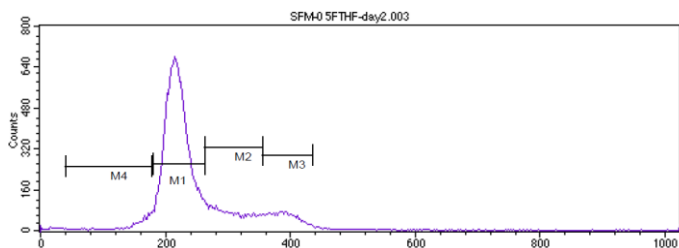
Marker	Left, Right	Events	% Gated	% Total	Mean	Geo Mean	CV
All	0, 1023	40000	100.00	100.00	247.71	230.60	36.21
M1	164, 249	22945	57.36	57.36	207.58	206.73	9.01
M2	249, 343	7710	19.28	19.28	293.75	292.41	9.56
M3	345, 427	5802	14.51	14.51	379.22	378.63	5.56
M4	41, 162	2423	6.06	6.06	117.36	110.38	31.06

3.5.7.2.2 SFM- 0 µg/ml – day 1



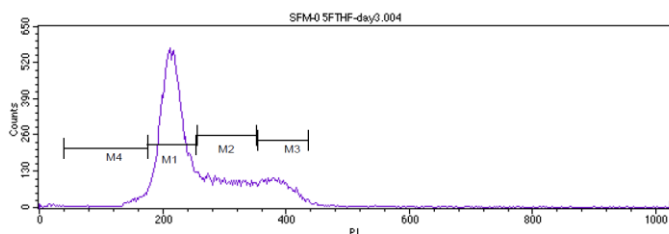
Marker	Left, Right	Events	% Gated	% Total	Mean	Geo Mean	CV
All	0, 1023	40000	100.00	100.00	233.05	223.33	30.39
M1	160, 249	30347	75.87	75.87	206.75	206.03	8.30
M2	251, 348	4781	11.95	11.95	297.42	295.94	9.97
M3	347, 429	3549	8.87	8.87	379.52	379.00	5.25
M4	41, 158	847	2.12	2.12	126.05	119.75	26.98

3.5.7.2.2 SFM- 0 µg/ml – day 2



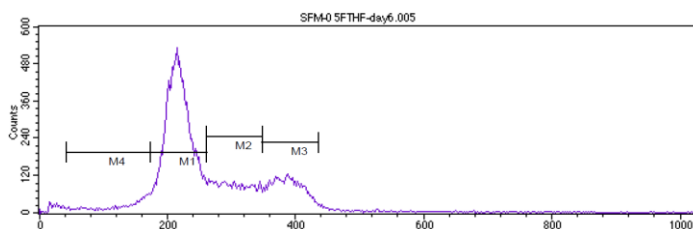
Marker	Left, Right	Events	% Gated	% Total	Mean	Geo Mean	CV
All	0, 1023	40000	100.00	100.00	249.22	239.67	28.36
M1	182, 263	27946	69.86	69.86	219.93	219.24	7.95
M2	263, 356	6126	15.32	15.32	304.10	302.86	9.09
M3	355, 437	4035	10.09	10.09	389.58	389.01	5.41
M4	41, 179	1433	3.58	3.58	154.02	149.30	19.89

3.5.7.2.3 SFM- 0 $\mu\text{g}/\text{ml}$ – day 3



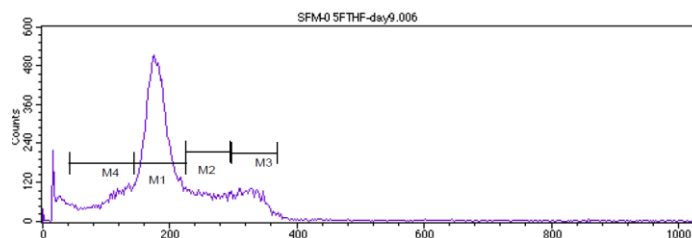
Marker	Left	Right	Events	% Gated	% Total	Mean	Geo Mean	CV
All	0	1023	40000	100.00	100.00	262.36	250.91	30.91
M1	175	254	23426	58.56	58.56	215.66	214.99	7.89
M2	256	352	8707	21.77	21.77	301.50	300.17	9.38
M3	354	436	5818	14.54	14.54	387.67	387.11	5.40
M4	41	176	1247	3.12	3.12	150.72	146.61	19.16

3.5.7.2.4 SFM- 0 $\mu\text{g}/\text{ml}$ – day 6



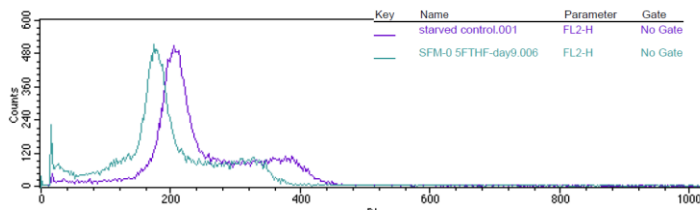
Marker	Left	Right	Events	% Gated	% Total	Mean	Geo Mean	CV
All	0	1023	40000	100.00	100.00	262.33	244.67	35.98
M1	173	260	22385	55.96	55.96	216.75	215.94	8.66
M2	260	348	7203	18.01	18.01	302.23	301.13	8.55
M3	347	435	7082	17.71	17.71	386.29	385.63	5.83
M4	41	173	2278	5.70	5.70	129.26	121.67	29.97

3.5.7.2.5 SFM- 0 $\mu\text{g}/\text{ml}$ – day 9

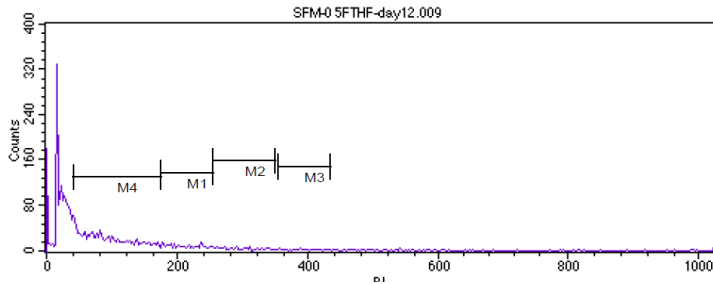


Marker	Left, Right	Events	% Gated	% Total	Mean	Geo Mean	CV
All	0, 1023	40000	100.00	100.00	201.54	175.02	53.24
M1	144, 225	21290	53.23	53.23	181.07	180.17	10.03
M2	225, 295	5364	13.41	13.41	258.47	257.63	8.03
M3	297, 368	4776	11.94	11.94	326.64	326.15	5.45
M4	41, 143	5961	14.90	14.90	102.42	97.28	28.91

3.5.7.2.6 Starved control vs. SFM- 0 µg/ml – day 9

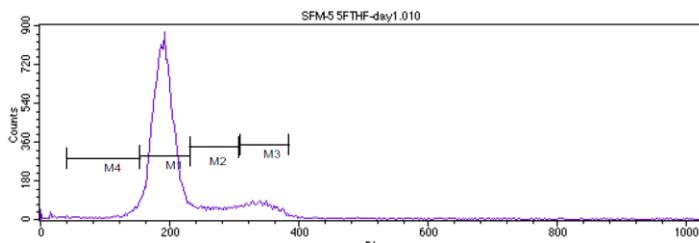


3.5.7.2.7 SFM- 0 µg/ml – day 12



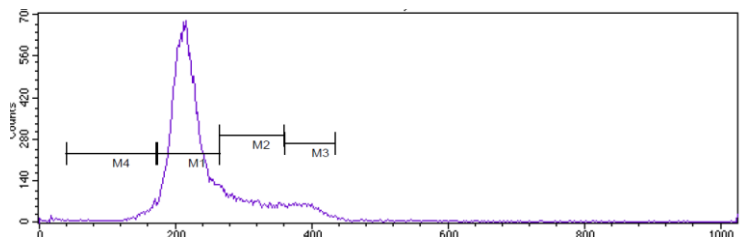
Marker	Left, Right	Events	% Gated	% Total	Mean	Geo Mean	CV
All	0, 1023	5580	100.00	100.00	91.57	51.22	122.95
M1	175, 254	431	7.72	7.72	211.08	209.74	11.34
M2	256, 352	192	3.44	3.44	294.19	292.89	9.54
M3	354, 436	67	1.20	1.20	391.28	390.66	5.70
M4	41, 176	2377	42.60	42.60	90.22	82.56	41.88

3.5.7.2.8 SFM- 5 µg/ml – day 1



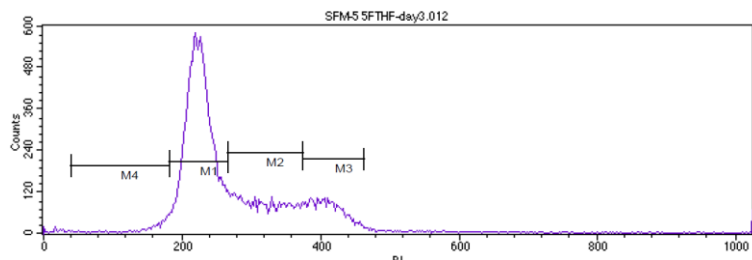
Marker	Left, Right	Events	% Gated	% Total	Mean	Geo Mean	CV
All	0, 1023	40000	100.00	100.00	215.53	204.57	34.31
M1	153, 231	30087	75.22	75.22	190.37	189.76	8.04
M2	231, 307	3665	9.16	9.16	268.07	267.08	8.57
M3	308, 384	4163	10.41	10.41	341.41	340.83	5.80
M4	41, 153	1317	3.29	3.29	124.42	118.86	25.33

3.5.7.2.9 SFM- 5 µg/ml – day 2



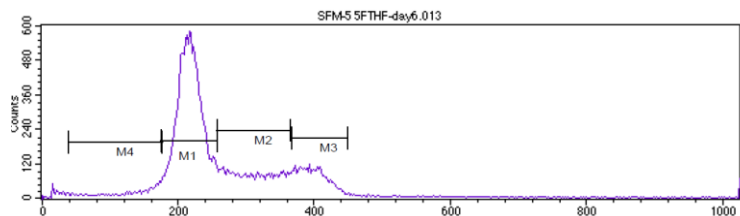
Marker	Left, Right	Events	% Gated	% Total	Mean	Geo Mean	CV
All	0, 1023	40000	100.00	100.00	243.24	234.03	28.77
M1	173, 264	29100	72.75	72.75	215.96	215.12	8.90
M2	264, 359	6175	15.44	15.44	304.71	303.42	9.27
M3	361, 435	2932	7.33	7.33	390.84	390.39	4.82
M4	39, 171	1224	3.06	3.06	146.68	142.10	20.39

3.5.7.2.10 SFM- 5 µg/ml – day 3



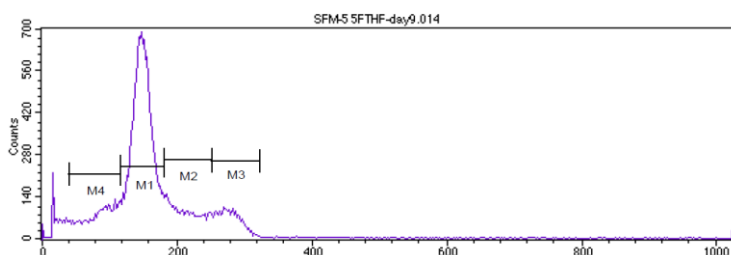
Marker	Left, Right	Events	% Gated	% Total	Mean	Geo Mean	CV
All	0, 1023	40000	100.00	100.00	274.77	262.10	31.98
M1	182, 266	24026	60.07	60.07	225.03	224.32	7.93
M2	266, 375	8874	22.18	22.18	316.96	315.29	10.27
M3	375, 463	5634	14.09	14.09	409.87	409.28	5.37
M4	39, 182	954	2.38	2.38	156.44	151.04	20.86

3.5.7.2.11 SFM- 5 µg/ ml – day 6



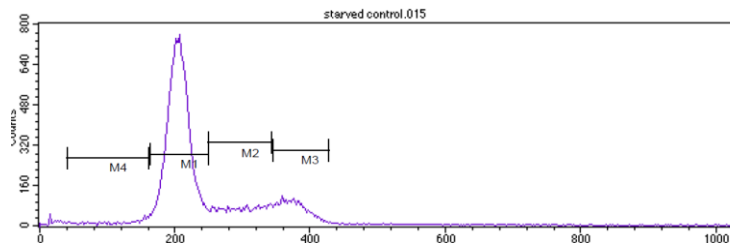
Marker	Left, Right	Events	% Gated	% Total	Mean	Geo Mean	CV
All	0, 1023	40000	100.00	100.00	262.60	245.85	35.95
M1	174, 257	23389	58.47	58.47	216.73	216.03	7.98
M2	257, 363	8081	20.20	20.20	308.46	306.82	10.30
M3	365, 448	5645	14.11	14.11	397.20	396.70	5.09
M4	39, 176	1975	4.94	4.94	131.04	122.51	31.16

3.5.7.2.12 SFM- 5 µg/ ml – day 9



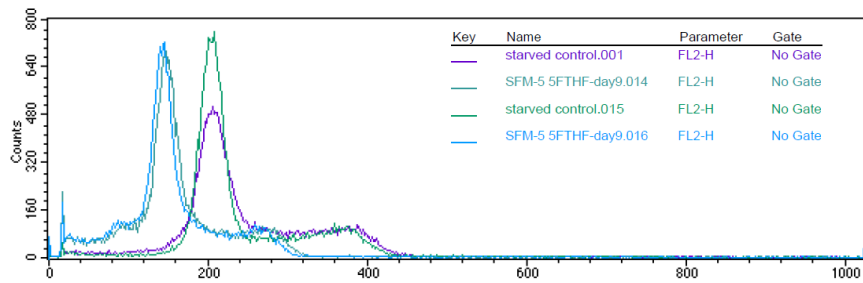
Marker	Left, Right	Events	% Gated	% Total	Mean	Geo Mean	CV
All	0, 1023	40000	100.00	100.00	161.98	144.55	47.28
M1	116, 181	22801	57.00	57.00	148.79	148.10	9.54
M2	181, 251	5953	14.88	14.88	212.30	211.26	9.95
M3	251, 322	4099	10.25	10.25	277.38	276.91	5.89
M4	39, 116	5647	14.12	14.12	84.05	80.73	26.25

3.5.7.2.13 Starved (control):

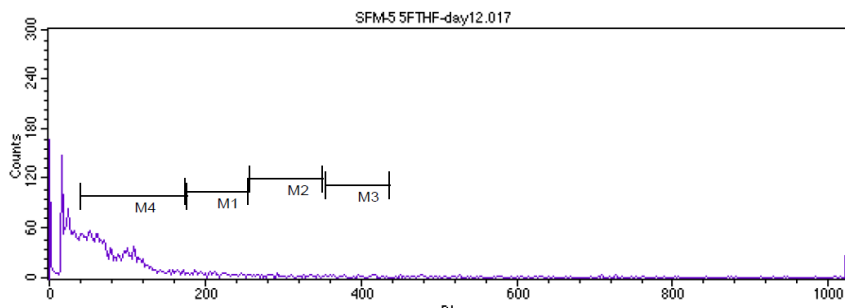


Marker	Left, Right	Events	% Gated	% Total	Mean	Geo Mean	CV
All	0, 1023	40000	100.00	100.00	242.76	229.07	35.25
M1	164, 249	27097	67.74	67.74	205.63	205.02	7.69
M2	249, 343	5797	14.49	14.49	297.45	296.12	9.43
M3	345, 427	4944	12.36	12.36	376.19	375.69	5.18
M4	41, 162	1128	2.82	2.82	117.13	109.50	32.45

3.5.7.2.14 Starved control 001 & 015 vs. SFM- 5 $\mu\text{g}/\text{ml}$ – day 9 014 and 016

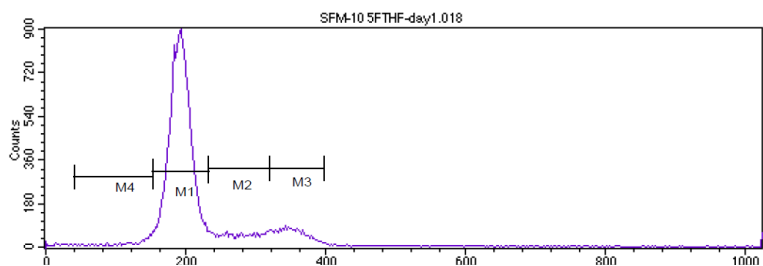


3.5.7.2.16 SFM- 5 $\mu\text{g}/\text{ml}$ – day 12



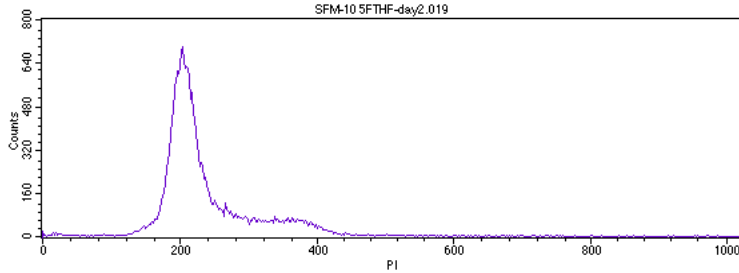
Marker	Left, Right	Events	% Gated	% Total	Mean	Geo Mean	CV
All	0, 1023	4860	100.00	100.00	94.23	53.06	149.18
M1	175, 254	197	4.05	4.05	206.27	205.20	10.35
M2	256, 352	75	1.54	1.54	296.49	295.09	9.84
M3	354, 436	43	0.88	0.88	387.81	387.02	6.50
M4	41, 176	2781	57.22	57.22	82.03	76.36	38.85

3.5.7.2.17 SFM- 10 $\mu\text{g}/\text{ml}$ – day 1



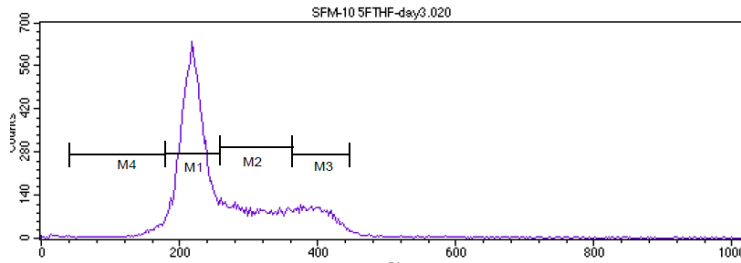
Marker	Left, Right	Events	% Gated	% Total	Mean	Geo Mean	CV
All	0, 1023	40000	100.00	100.00	218.65	208.16	34.59
M1	153, 232	30536	76.34	76.34	192.56	191.99	7.67
M2	234, 321	3826	9.56	9.56	278.09	276.85	9.42
M3	320, 398	3851	9.63	9.63	351.96	351.42	5.57
M4	41, 153	1093	2.73	2.73	121.31	115.40	26.85

3.5.7.2.18 SFM- 10 µg/ml – day 2



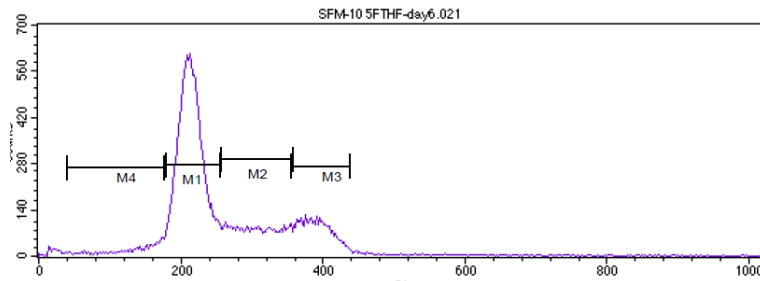
Marker	Left, Right	Events	% Gated	% Total	Mean	Geo Mean	CV
All	0, 1023	40000	100.00	100.00	235.29	226.36	29.13
M1	164, 249	28772	71.93	71.93	207.52	206.76	8.57
M2	249, 341	6380	15.95	15.95	288.14	286.86	9.48
M3	343, 427	3334	8.33	8.33	375.90	375.32	5.63
M4	41, 164	1116	2.79	2.79	142.06	138.47	18.40

3.5.7.2.19 SFM- 10 µg/ml – day 3



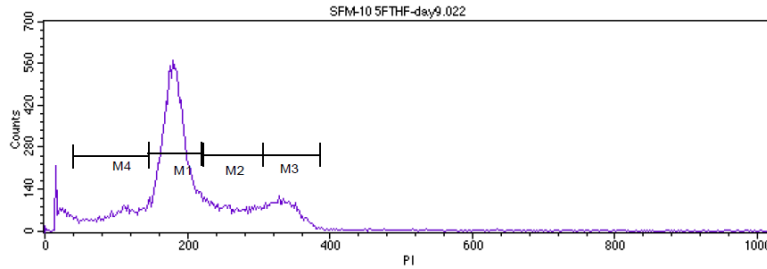
Marker	Left, Right	Events	% Gated	% Total	Mean	Geo Mean	CV
All	0, 1023	40000	100.00	100.00	269.48	257.29	31.68
M1	180, 260	23617	59.04	59.04	220.27	219.63	7.62
M2	260, 364	8733	21.83	21.83	309.66	308.10	10.06
M3	363, 447	5982	14.95	14.95	398.74	398.15	5.48
M4	41, 180	1158	2.90	2.90	155.22	151.16	18.64

3.5.7.2.20 SFM- 10 µg/ml – day 6



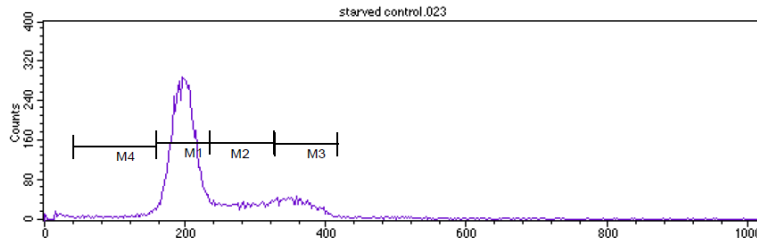
Marker	Left, Right	Events	% Gated	% Total	Mean	Geo Mean	CV
All	0, 1023	40000	100.00	100.00	260.85	245.53	35.14
M1	178, 255	23414	58.54	58.54	214.47	213.87	7.54
M2	257, 358	7622	19.05	19.05	306.81	305.36	9.70
M3	355, 439	6380	15.95	15.95	389.99	389.42	5.40
M4	40, 176	1769	4.42	4.42	133.16	125.70	28.91

3.5.7.2.21 SFM- 10 µg/ ml – day 9



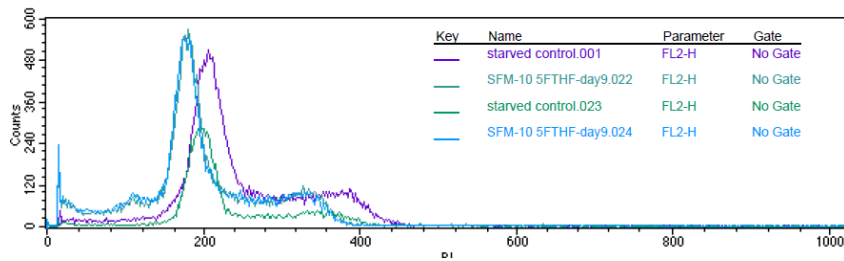
Marker	Left, Right	Events	% Gated	% Total	Mean	Geo Mean	CV
All	0, 1023	40000	100.00	100.00	206.16	180.51	49.97
M1	145, 220	21195	52.99	52.99	182.20	181.46	9.02
M2	222, 306	6319	15.80	15.80	261.78	260.56	9.66
M3	306, 386	5086	12.72	12.72	336.28	335.77	5.55
M4	40, 145	5189	12.97	12.97	100.44	95.08	30.13

3.5.7.2.22 Starved (Control)

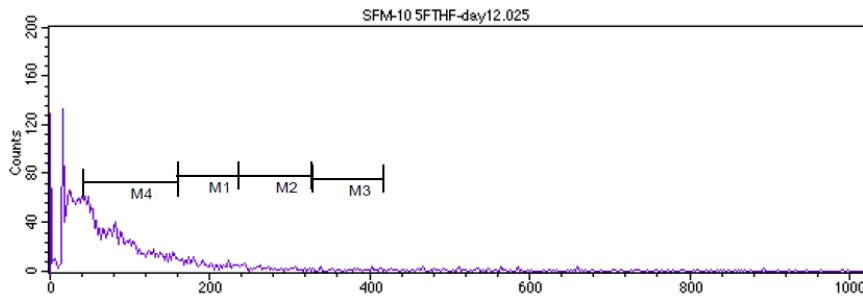


Marker	Left, Right	Events	% Gated	% Total	Mean	Geo Mean	CV
All	0, 1023	16614	100.00	100.00	234.89	220.67	36.51
M1	159, 235	11028	66.38	66.38	197.92	197.33	7.72
M2	235, 326	2427	14.61	14.61	280.21	278.87	9.76
M3	328, 417	2187	13.16	13.16	361.82	361.18	5.98
M4	41, 159	518	3.12	3.12	117.75	110.88	30.71

3.5.7.2.23 Starved control 001 & 023 vs. SFM- 10 µg/ ml – day 9 022 and 024

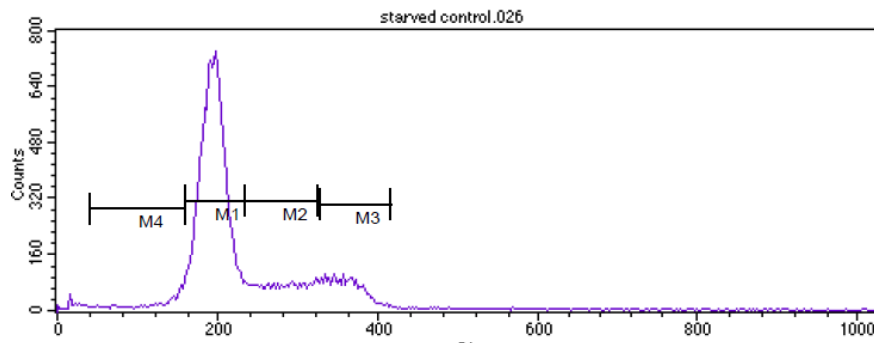


3.5.7.2.24 SFM- 10 µg/ml – day 12



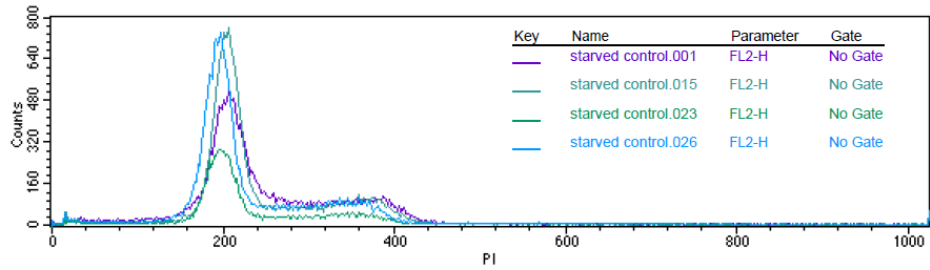
Marker	Left, Right	Events	% Gated	% Total	Mean	Geo Mean	CV
All	0, 1023	5020	100.00	100.00	97.85	57.52	137.97
M1	159, 235	304	6.06	6.06	188.91	187.58	12.08
M2	235, 326	124	2.47	2.47	271.64	270.34	9.89
M3	328, 417	50	1.00	1.00	374.92	374.06	6.77
M4	41, 159	2775	55.28	55.28	81.06	75.32	39.05

3.5.7.2.25 Starved (control)

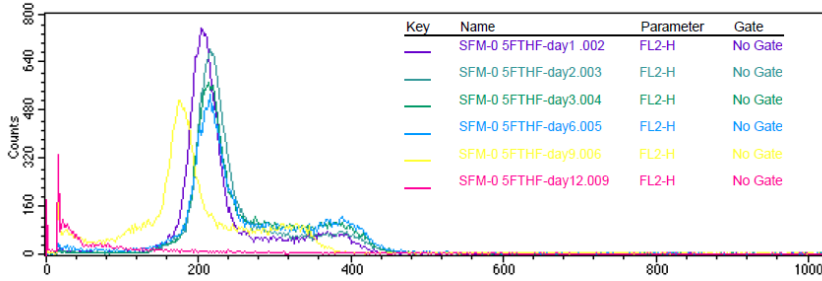


Marker	Left, Right	Events	% Gated	% Total	Mean	Geo Mean	CV
All	0, 1023	40000	100.00	100.00	230.44	216.56	36.65
M1	159, 235	26585	66.46	66.46	195.44	194.84	7.85
M2	235, 326	5963	14.91	14.91	281.25	279.93	9.63
M3	328, 417	4849	12.12	12.12	359.95	359.36	5.79
M4	41, 159	1638	4.09	4.09	122.08	115.22	29.36

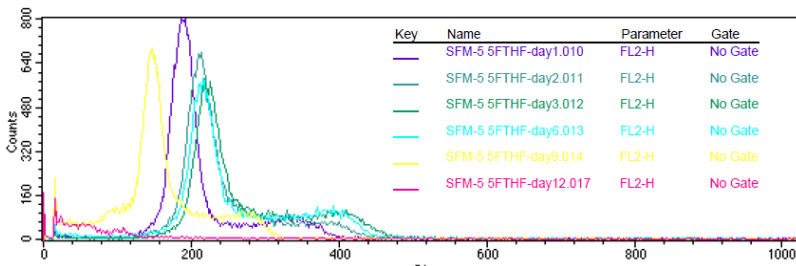
3.5.7.2.26 Starved control overlay:



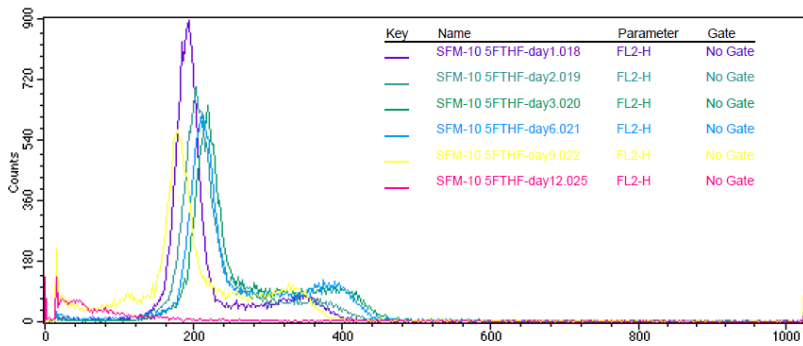
3.5.7.2.27 SFM- 0 µg/ ml – overlay



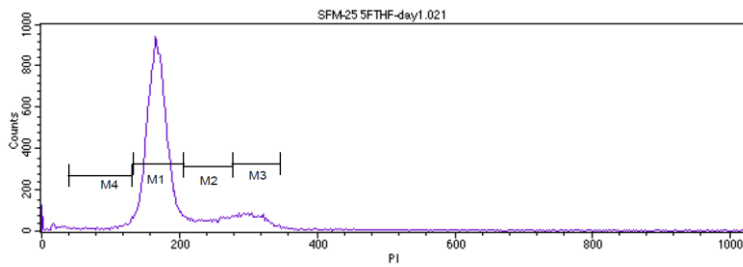
3.5.7.2.28 SFM- 5 µg/ ml – overlay



3.5.7.2.29 SFM- 10 µg/ ml – overlay

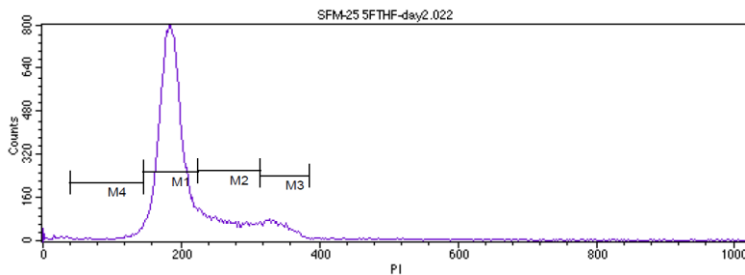


3.5.7.2.30 serum free medium SFM- 25 µg/ ml – day 1



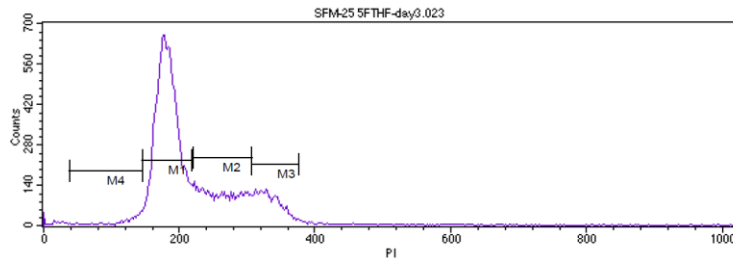
Marker	Left, Right	Events	% Gated	% Total	Mean	Geo Mean	CV
All	0, 1023	40000	100.00	100.00	194.31	179.05	44.03
M1	133, 206	29737	74.34	74.34	168.30	167.74	8.20
M2	206, 277	3625	9.06	9.06	241.83	240.85	9.01
M3	277, 347	3936	9.84	9.84	305.83	305.31	5.84
M4	39, 131	1159	2.90	2.90	98.58	93.38	29.23

3.5.7.2.31 serum free medium SFM- 25 µg/ ml – day 2



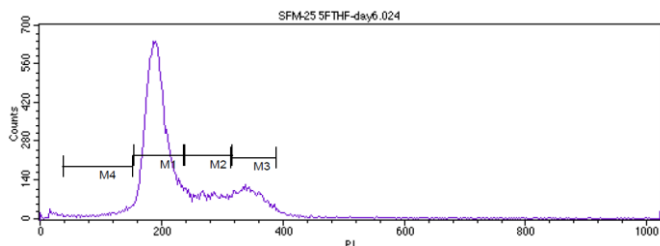
Marker	Left, Right	Events	% Gated	% Total	Mean	Geo Mean	CV
All	0, 1023	40000	100.00	100.00	213.98	202.38	36.56
M1	145, 224	29010	72.52	72.52	185.37	184.71	8.38
M2	224, 315	6212	15.53	15.53	264.36	262.95	10.37
M3	315, 384	2963	7.41	7.41	340.95	340.53	4.99
M4	39, 145	923	2.31	2.31	115.76	110.17	26.70

3.5.7.2.32 serum free medium SFM- 25 µg/ ml – day 3



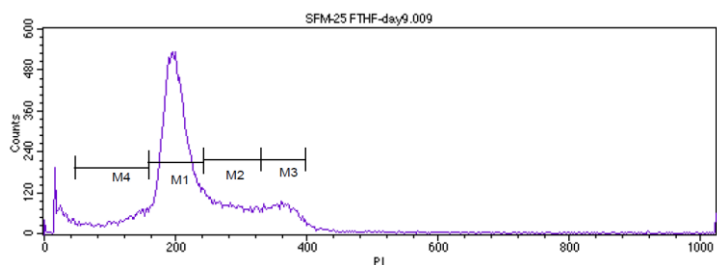
Marker	Left, Right	Events	% Gated	% Total	Mean	Geo Mean	CV
All	0, 1023	40000	100.00	100.00	221.81	210.51	32.41
M1	145, 218	24190	60.48	60.48	182.34	181.70	8.39
M2	220, 307	9008	22.52	22.52	262.08	260.78	9.97
M3	307, 376	5124	12.81	12.81	332.84	332.41	5.08
M4	39, 145	867	2.17	2.17	119.88	115.56	22.75

3.5.7.2.33 serum free medium SFM- 25 µg/ ml – day 6



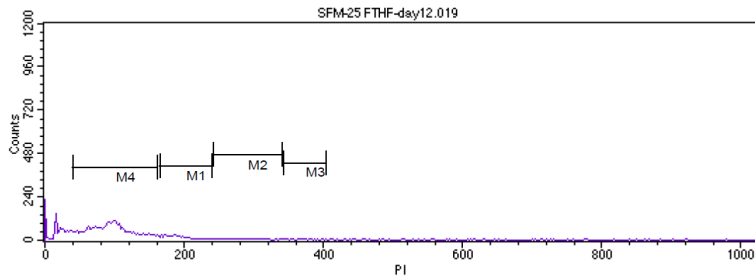
Marker	Left, Right	Events	% Gated	% Total	Mean	Geo Mean	CV
All	0, 1023	40000	100.00	100.00	231.23	216.68	36.43
M1	155, 237	25338	63.34	63.34	193.30	192.54	8.91
M2	239, 317	6006	15.02	15.02	276.98	276.01	8.36
M3	315, 389	5766	14.41	14.41	347.28	346.74	5.59
M4	39, 152	1480	3.70	3.70	114.49	108.51	28.46

3.5.7.2.34 serum free medium SFM- 25 µg/ ml – day 9



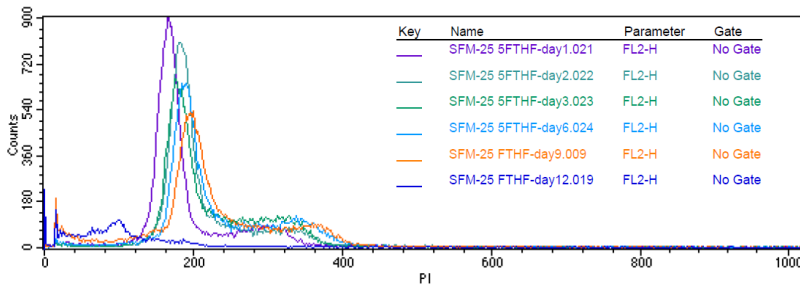
Marker	Left, Right	Events	% Gated	% Total	Mean	Geo Mean	CV
All	0, 1023	40000	100.00	100.00	224.80	200.32	42.54
M1	159, 243	22987	57.47	57.47	200.91	200.08	9.09
M2	244, 331	6556	16.39	16.39	283.24	282.07	9.11
M3	331, 398	4379	10.95	10.95	361.37	360.93	4.98
M4	47, 159	3620	9.05	9.05	114.71	108.86	29.27

3.5.7.2.35 serum free medium SFM- 25 µg/ ml – day 12

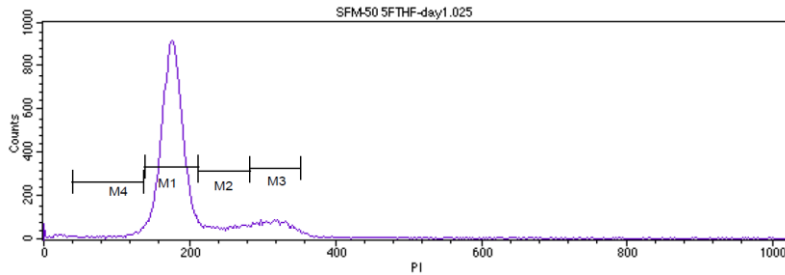


Marker	Left, Right	Events	% Gated	% Total	Mean	Geo Mean	CV
All	0, 1023	8540	100.00	100.00	100.97	72.99	81.07
M1	166, 240	821	9.61	9.61	191.63	190.87	9.07
M2	242, 341	137	1.60	1.60	280.54	279.22	9.82
M3	343, 405	33	0.39	0.39	369.88	369.37	5.32
M4	41, 162	5904	69.13	69.13	94.39	89.65	31.12

3.5.7.2.36 serum free medium SFM- 25 µg/ ml Overlay

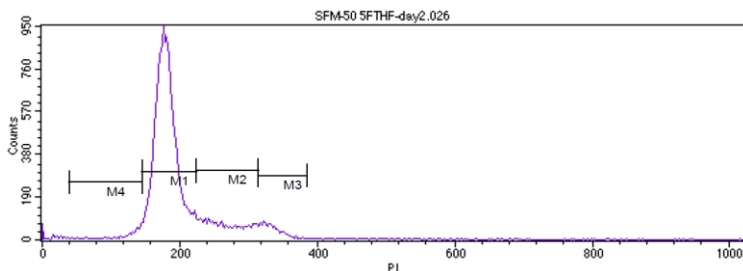


3.5.7.2.37 serum free medium SFM- 50 µg/ ml – day 1



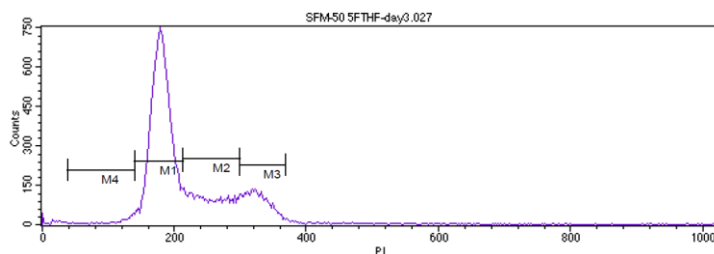
Marker	Left, Right	Events	% Gated	% Total	Mean	Geo Mean	CV
All	0, 1023	40000	100.00	100.00	200.18	189.31	34.94
M1	139, 212	30256	75.64	75.64	176.72	176.17	7.85
M2	212, 283	3560	8.90	8.90	247.14	246.19	8.76
M3	283, 352	4285	10.71	10.71	315.60	315.06	5.85
M4	39, 137	925	2.31	2.31	105.20	99.66	28.76

3.5.7.2.38 serum free medium SFM- 50 µg/ ml – day 2



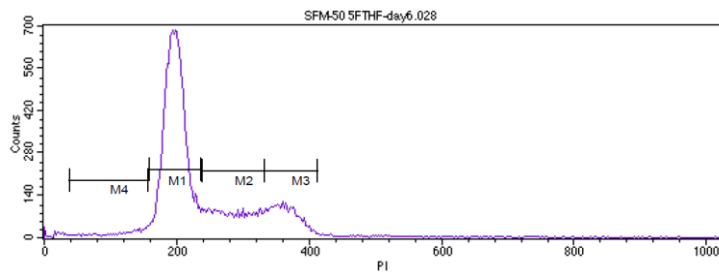
Marker	Left, Right	Events	% Gated	% Total	Mean	Geo Mean	CV
All	0, 1023	40000	100.00	100.00	200.32	191.34	29.47
M1	145, 224	30721	76.80	76.80	180.64	179.99	8.56
M2	224, 315	5736	14.34	14.34	265.71	264.28	10.41
M3	315, 384	2132	5.33	5.33	334.33	334.03	4.27
M4	39, 145	1099	2.75	2.75	121.36	116.85	22.94

3.5.7.2.39 serum free medium SFM- 50 µg/ ml – day 3



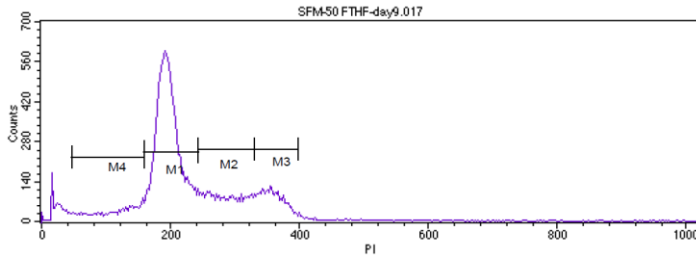
Marker	Left, Right	Events	% Gated	% Total	Mean	Geo Mean	CV
All	0, 1023	40000	100.00	100.00	217.92	206.65	32.97
M1	140, 213	25016	62.54	62.54	179.94	179.37	7.97
M2	213, 299	8106	20.27	20.27	254.13	252.81	10.19
M3	299, 369	5617	14.04	14.04	326.08	325.64	5.25
M4	39, 140	655	1.64	1.64	115.94	111.25	23.92

3.5.7.2.40 serum free medium SFM- 50 µg/ ml – day 6



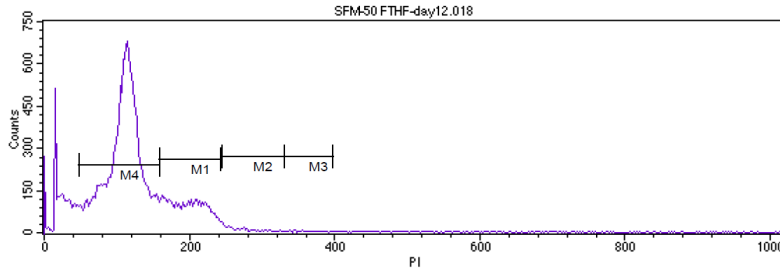
Marker	Left, Right	Events	% Gated	% Total	Mean	Geo Mean	CV
All	0, 1023	40000	100.00	100.00	238.40	224.63	34.67
M1	158, 237	25233	63.08	63.08	197.86	197.28	7.64
M2	239, 333	7125	17.81	17.81	285.02	283.64	9.83
M3	333, 413	5539	13.85	13.85	364.11	363.60	5.32
M4	39, 156	1177	2.94	2.94	115.60	109.27	29.33

3.5.7.2.41 serum free medium SFM- 50 µg/ ml – day 9



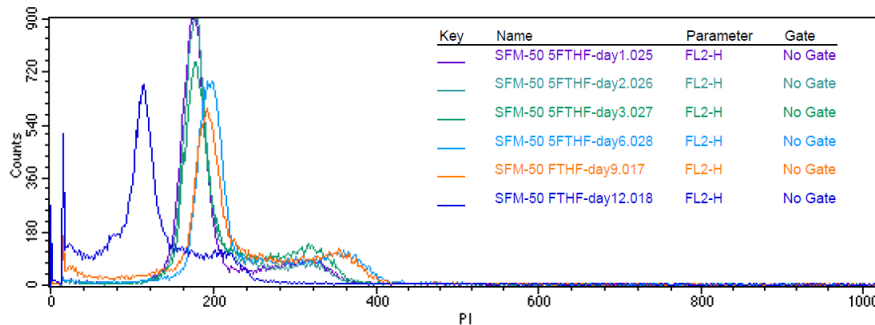
Marker	Left, Right	Events	% Gated	% Total	Mean	Geo Mean	CV
All	0, 1023	40000	100.00	100.00	226.80	204.11	41.05
M1	159, 243	22735	56.84	56.84	197.25	196.46	9.05
M2	244, 331	6931	17.33	17.33	286.58	285.40	9.05
M3	331, 398	5041	12.60	12.60	358.49	358.09	4.72
M4	47, 159	3311	8.28	8.28	113.71	107.81	29.66

3.5.7.2.42 serum free medium SFM- 50 µg/ ml – day 12



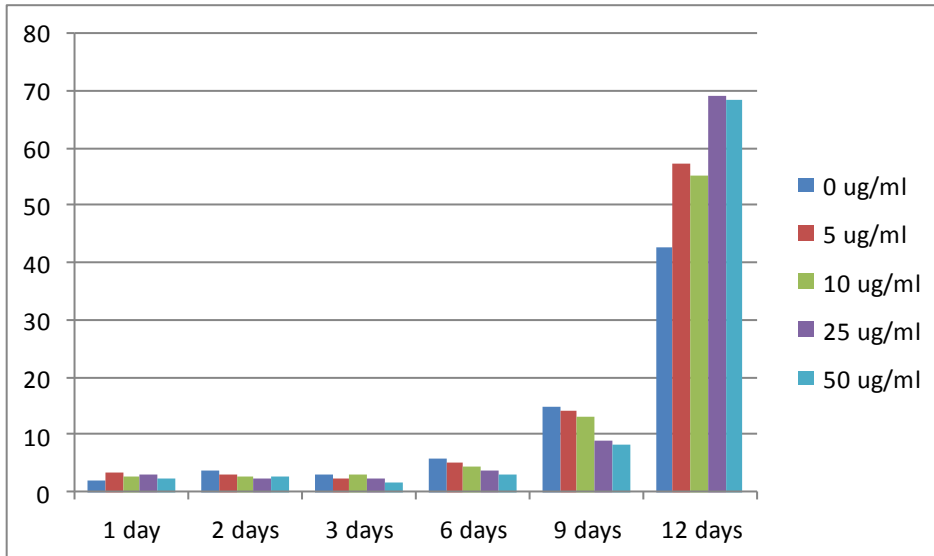
Marker	Left, Right	Events	% Gated	% Total	Mean	Geo Mean	CV
All	0, 1023	39820	100.00	100.00	125.34	104.71	60.08
M1	159, 243	7514	18.87	18.87	197.18	195.79	11.86
M2	244, 331	686	1.72	1.72	269.66	268.67	8.76
M3	331, 398	128	0.32	0.32	360.17	359.70	5.18
M4	47, 159	27276	68.50	68.50	109.34	106.29	22.01

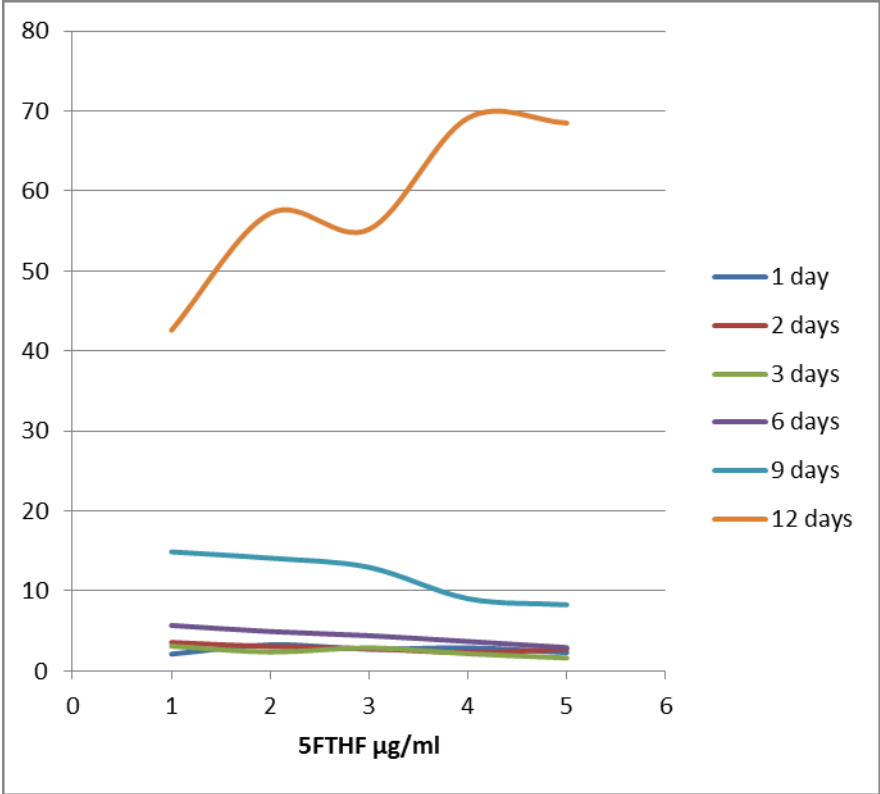
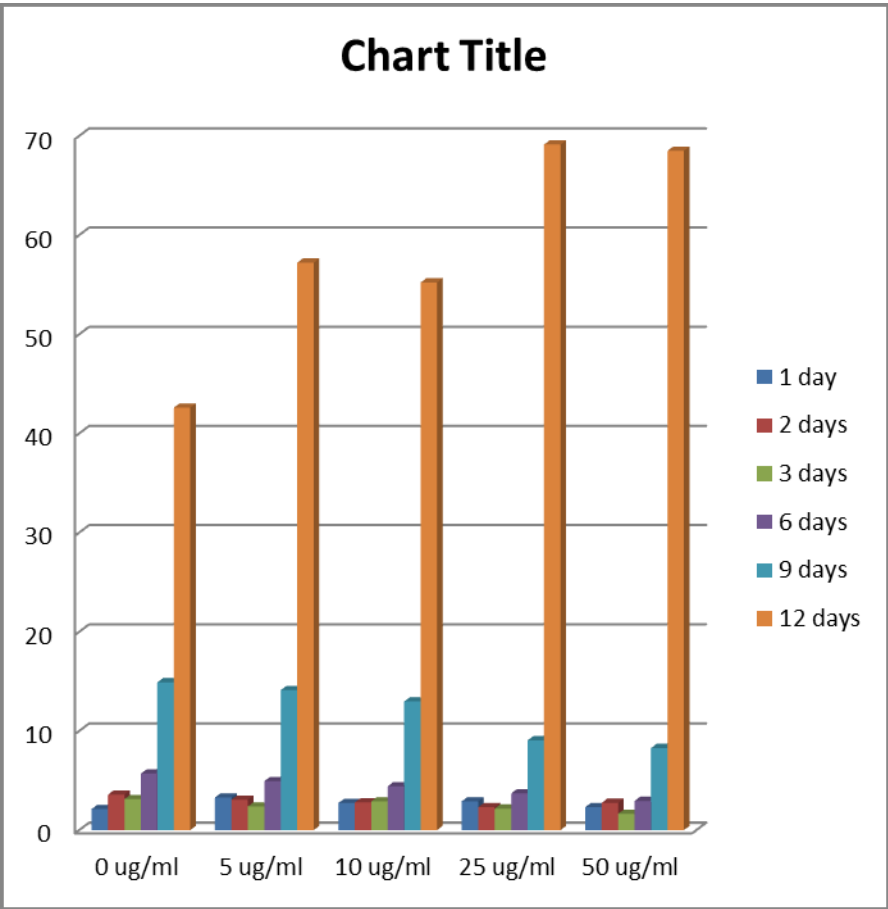
3.5.7.2.43 serum free medium SFM- 50 µg/ ml overlay



3.5.7.2.44 Elaboration of FACS result

3.5.7.2.45 Serum medium and 5FTHF doses- 1 -12 days free





3.5.8 SFM 5FTHF 10x5 vs 50 9-15 days

To check if the decreased proliferation observed after day 9 is due to actual degradation and depletion of 5FTHF, or rather to exhaustion of proliferative potential. This was assessed by testing if a single dose of 50µg/ml of 5FTHF at day 0 provides similar result to multiple administration of 10 µg/ml 5THF from day 0 and given every 2 days. In this context 42×10^6 cells were washed thoroughly in 1x PBS, resuspended in serum free medium, after that plated into three dishes(100x15 diameter) and incubated overnight. Next day doses of folic acid were added namely 0, 50 and 10x5 µg/ml to each plate. Cell number and viability were checked. Cells were harvested after 9, 12 and 15 days where cell count and viability were performed.

3.5.8.1 Result:

Cells have ceased its proliferation after day 9 much likely due to depletion of folic acid as well as exhaustion of its proliferative potentiality, as no significant difference between administering single dose of 50 µg/ml and multiple doses of 10x5 µg/ml($p < 0.05$). Nonetheless, cells supplemented with single dose of 50 µg/ml have successfully doubled their number by day 9 then gradually underwent apoptosis compared to the cell that supplemented with multiple doses (5x10 µg/ml) which have epic failed to complete one complete one cycle by day 9 then gradually underwent apoptosis en masse.

5FTHF	0	9	12	15
0 $\mu\text{g/ml}$	0.995	1.095	0.815	0.12
5x10 $\mu\text{g/ml}$	0.995	1.665	1.375	0.455
50 $\mu\text{g/ml}$	0.995	2.1	1.255	0.455

Table 3.36 shows SFM 5FTHF 10x5 vs 50 9-15 days(cell proliferation)

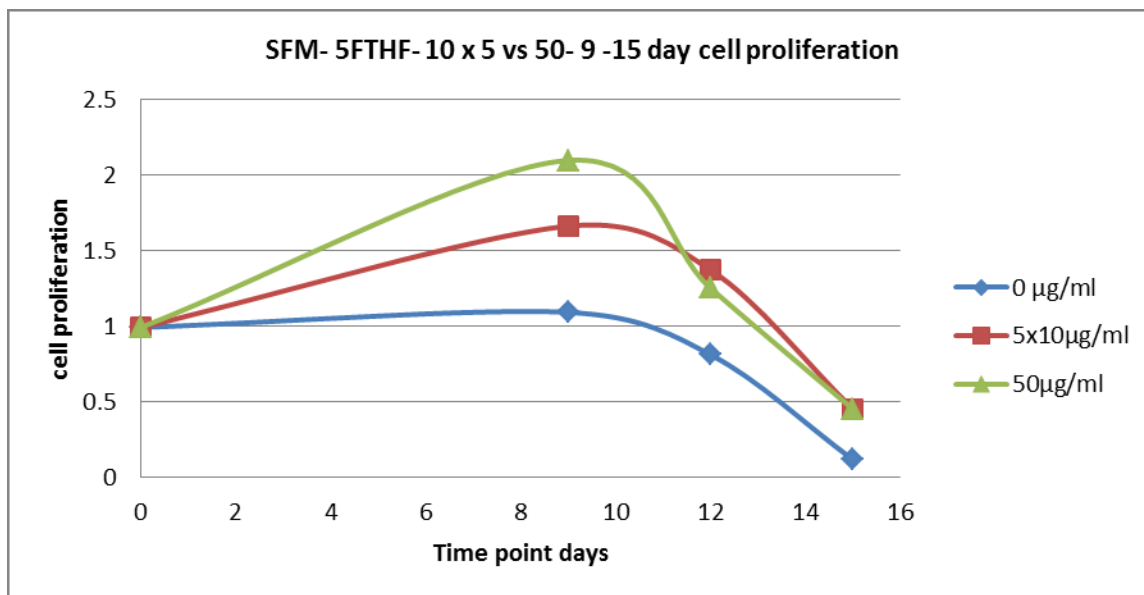


Figure 3.36 shows SFM 5FTHF 10x5 vs 50 9-15-days(cell proliferation)

Table 3.37 shows s SFM 5FTHF 10x5 vs 50 9-15-days (cell survival)

5FTHF	0	9	12	15
0 µg/ml	0.85	0.33	0.2	0.02
5x10µg/ml	0.85	0.58	0.38	0.1
50µg/ml	0.85	0.7	0.39	0.1

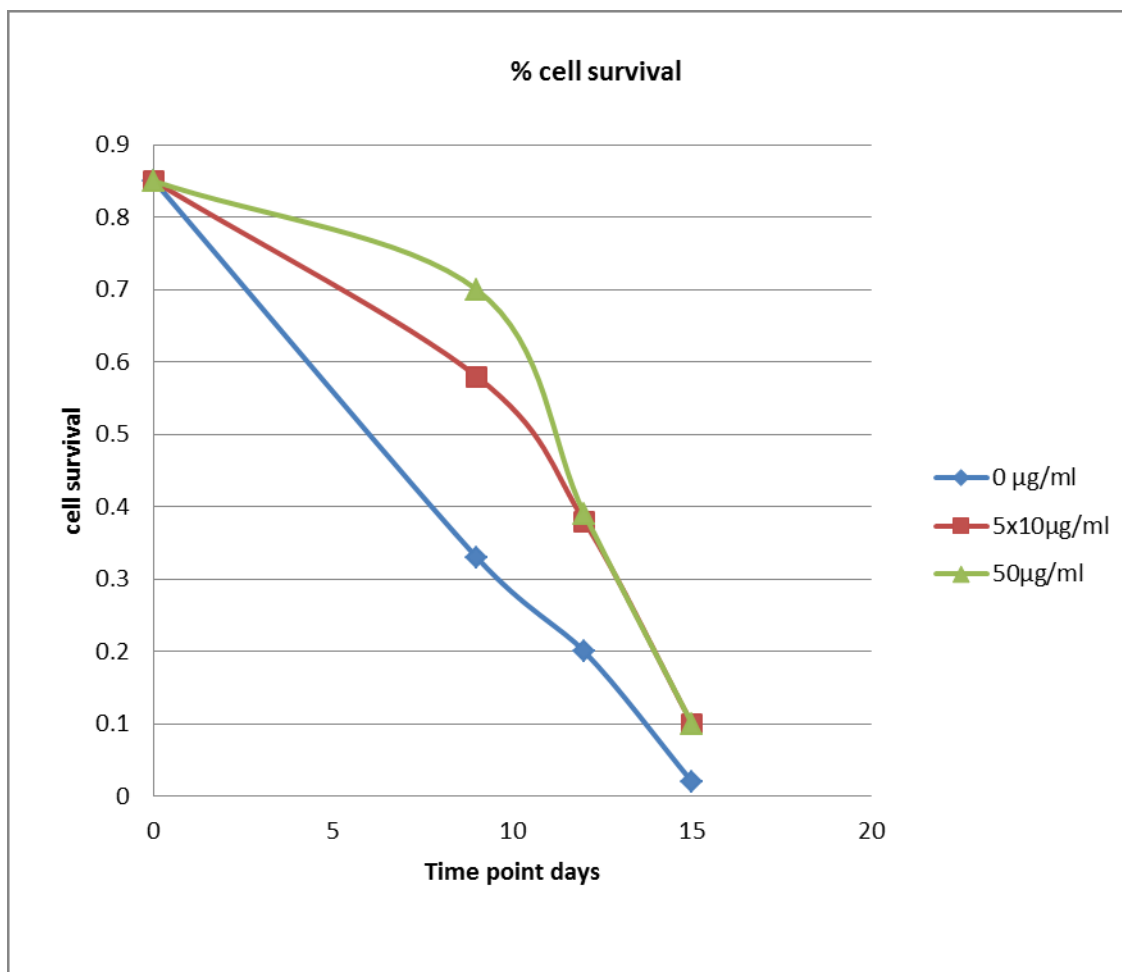


Figure 3.37 shows Table shows s SFM 5FTHF 10x5 vs 50 9-15-days (cell survival)

3.5.9 PBMC SFM 5FTHF doses 1-12 days

3.5.9.1 Peripheral Blood mononuclear cells PBMCs preparation

3.5.9.1.1 PBMCs isolation:

PBMCs were isolated from buffy-coat bag obtained from S.I.T. FERRARA 2013015692 (Ferrara hospital Blood bank) by using standard density gradient centrifugation Ficoll 1077. The blood was subsequently diluted by adding 260 ml of sterile 1x PBS to the buffy-coat(40 ml). 36 ml of the buffy coat/saline mixture was carefully layered over 12 ml of Lympholyte^R- H (CEDARLANE CANADA) in a universal falcon 50 ml tube (8 tubes were used) ensuring that a distinct interface between the two layers was maintained. The blood was then centrifuged at 1500 rpm for 30 minutes at 4°C with no brake applied, to ensure separation of the PBMCs from the denser Ficoll/erythrocyte layer below, and the less dense dilute plasma layer above. The top plasma level was siphoned off and discarded, while the peripheral blood mononuclear cell layer was then gently removed with a sterile micro pipette and placed in a sterile falcon tube. The PBMCs were further washed twice with 50 ml of 1x PBS and centrifuged at 1500 rpm for 10 minutes with brake applied. Supernatant was siphoned off, and the pellet was washed twice with 1x PBS. The cell pellet was finally resuspended in 2-3mls of 1x PBS. The freshly isolated PBMCs were counted by adding 1 ml of cell suspension to 9 ml of 1x PBS. 10µl of this mixture was thoroughly mixed, and loaded in a haemocytometer (Neubauer). Cells were counted and resuspended in Iscove serum free medium overnight(modified from Lan et al., 2007)

3.5.9.1.2 Cells culture and 5FTHF doses:

Cells were grown in serum- starved Iscove medium. Next day cells were plated into 4 duplicates 50x10⁶/15 ml per each. First duplicate supplemented with or no 1% foetal bovine serum(400 µl/15 ml). Second duplicate in addition to presence or absence of serum they further treated with phytohaemagglutinin PHA375 µl/15 ml). Third duplicate in addition to presence or absence of serum they were treated with PHA and 50 µg/ml of folic acid. The last duplicate supplemented with or no serum in addition 50 µg/ml of folic acid. Cells were incubated overnight at humidified atmosphere.. cells were harvest cell at day 1, 2, 3, 6, 9 and 12 thereby cell count and viability were performed.

3.5.9.1.2.1 Results:

According to its baseline cells grown in 1% serum increase their number by day 2 then steadily levelled off their number compared to cells that grown in serum deprived condition, however no significant difference($p < 0.05$). stimulating cells with PHA in presence of serum is crucial as it leads cells to proliferate as shown herein cells increase a bit their number by day 6 ($p > 0.05$). Whereas cells grown in absence of serum their growth was abrogated and thus underwent apoptosis. Folinic acid supplemental doesn't induce profuse proliferation since cells supplemented with serum and folinic acid doubled its number by day 2 then began to level off its number, whereas cells maintained in serum free medium its number increased a bit and afterward underwent apoptosis *en masse*($p < 0.05$). Cells supplemented with serum and folinic acid and later activated with PHA increased its number by day 6. Nonetheless, its number is far from the baseline. while its counterpart which grown in absence of serum underwent apoptosis *en masse*($p > 0.05$).

Table 3.38 shows cells proliferation in absence of serum

	1	2	3	6	9	12
0 % FBS	0.785	1.532	0.73	0.665	0.4	0.28
PHA/ 0%FBS	0.18	0.045	0.04	0.035	0.04	0.005
0% FBS+ 5FTHF	1.08	1.325	1.11	0.64	0.615	0.28
PHA/0% FBS+5FTHF	0.06	0.075	0.05	0.03	0.045	0.04

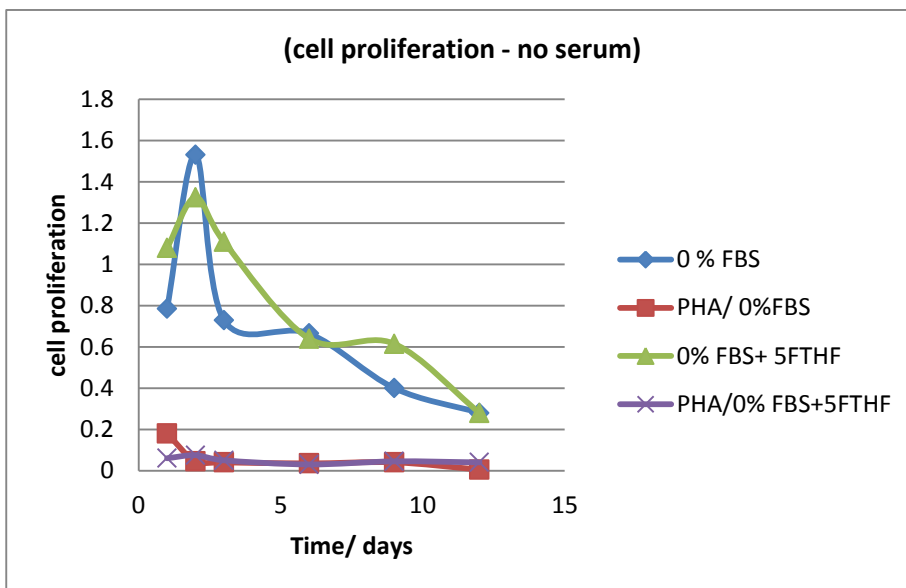


Figure 3.38 shows cells proliferation in absence of serum

Table 3.39 cell survival in absence of serum

	1	2	3	6	9	12
0 % FBS	0.31	0.36	0.23	0.16	0.06	0.06
PHA/ 0%FBS	0.31	0.05	0.03	0.013	0.011	0.007
0% FBS+ 5FTHF	0.23	0.31	0.28	0.08	0.08	0.03
PHA/0% FBS+5FTHF	0.08	0.06	0.04	0.014	0.015	0.01

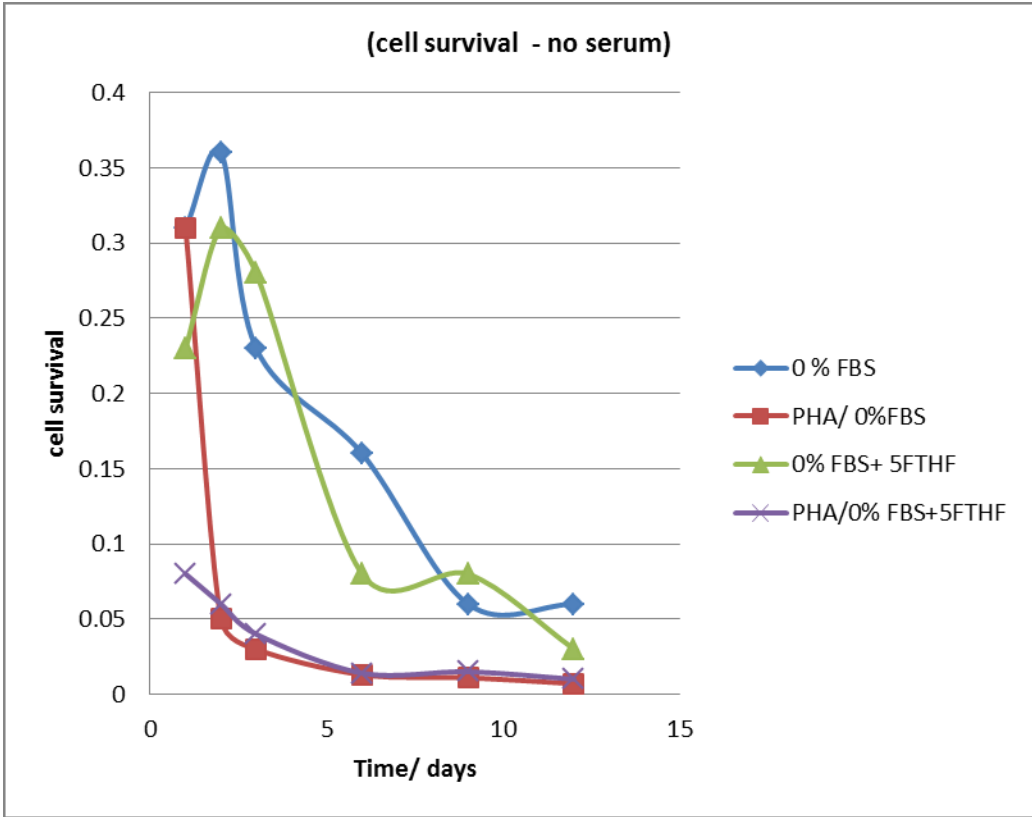


Figure 3.39 shows cell survival in absence of serum

Table 3.40 shows cell proliferation in presence of (1% serum)

	1	2	3	6	9	12
1 % FBS	1.55	2	1.91	1.27	0.8	0.53
PHA/ 1%FBS	0.32	0.335	0.31	0.525	0.48	0.305
1% FBS+ 5FTHF	1.825	2.505	2.1	1.585	0.957	0.54
PHA/1% FBS+5FTHF	0.46	0.32	0.565	0.59	0.845	0.285

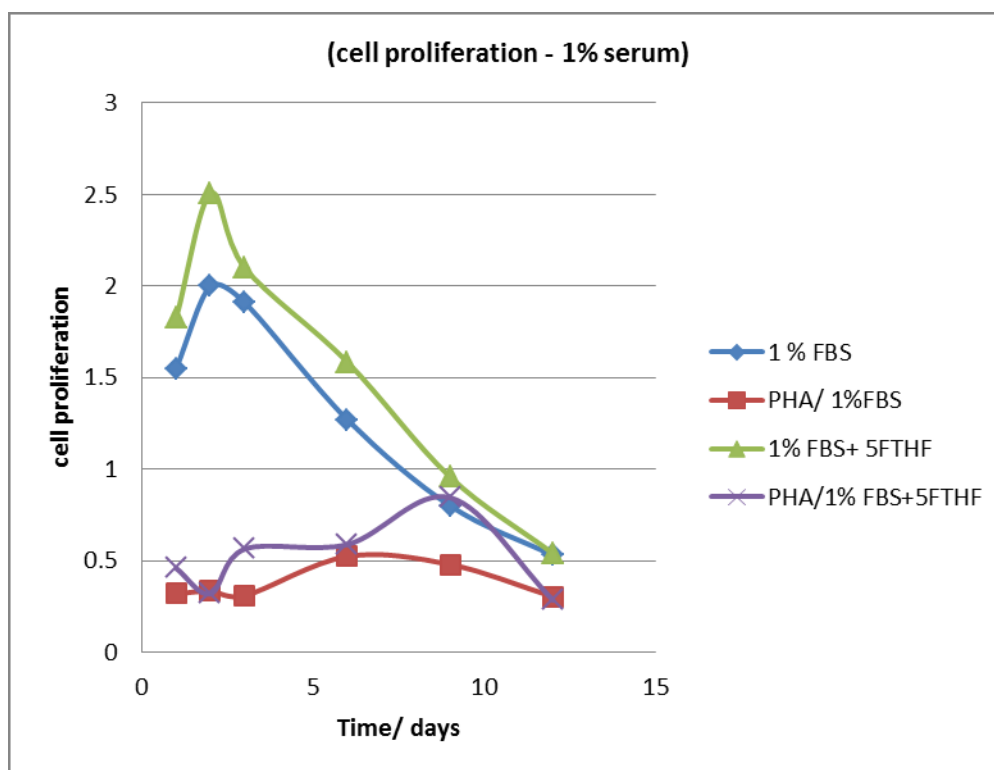


Figure 3.40 shows Cell proliferation in presence of 1% serum

Table 3.41 shows cell survival in presence of 1% serum)

	1	2	3	6	9	12
1 % FBS	0.34	0.43	0.43	0.31	0.15	0.11

PHA/ 1%FBS	0.36	0.25	0.2	0.16	0.113	0.04
1% FBS+ 5FTHF	0.34	0.51	0.42	0.24	0.13	0.06
PHA/1% FBS+5FTHF	0.35	0.21	0.24	0.15	0.12	0.05

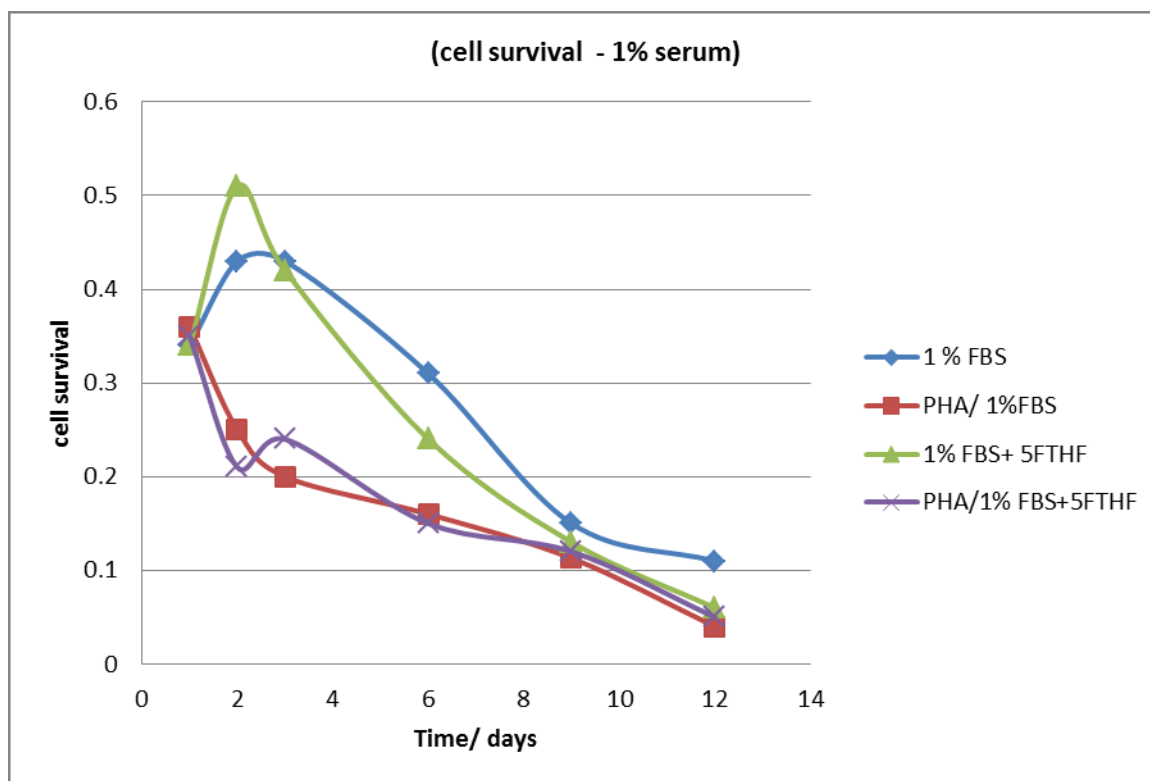


Figure 3.41 shows cell survival in presence of 1% serum

3.5.10 SFM 5FTHF maximal effective dose

To determine which is the minimal doses that produces maximal proliferating response at 9-15 days of culture. After being washed extensively in 1x PBS, HL- 60 cells cultured in serum free medium grew comparably with cells supplemented with different concentration of folic acid 0, 50, 10, 200 and 400 $\mu\text{g}/\text{ml}$ respectively. Cells were harvested after 6, 9, 12 and 15 days thereby cell count and viability were performed,

3.5.10.1 Results:

Folic acid effectively induces cellular proliferation in absence of growth factor ($p > 0.05$). In this context cells seeded in 5FTHF restriction Iscove serum free medium proliferate but nearly complete one cycle, where-upon their numbers sharply, began

declining by day 9. whereas cells maintained in Iscove serum free media and supplemented with varying concentration of 5FTHF they more or less double their number twice indicating they have entered two cycles. Then their number steadily reduced by day 12 in dose dependently manner implying degradation and consuming of folate. . Moreover 50 µg/ml could be the minimal dose that could induce maximum proliferation Surprisingly, No much difference between administering 100 and 200 µg/ml($p < 0.05$).

Table 3.42 shows - SFM- 5FTHF maximal effective dose (cell proliferation)

5FTHF	0	6	9	12	15
0 µg/ml	1.075	1.93	1.805	1.445	0.83
50 µg/ml	1.075	2.535	2.965	2.13	1.565
100 µg/ml	1.075	2.67	3.35	2.62	2.37
200 µg/ml	1.075	2.66	3.34	2.605	2.375
400µg/ml	1.075	3.03	3.69	2.875	2.55

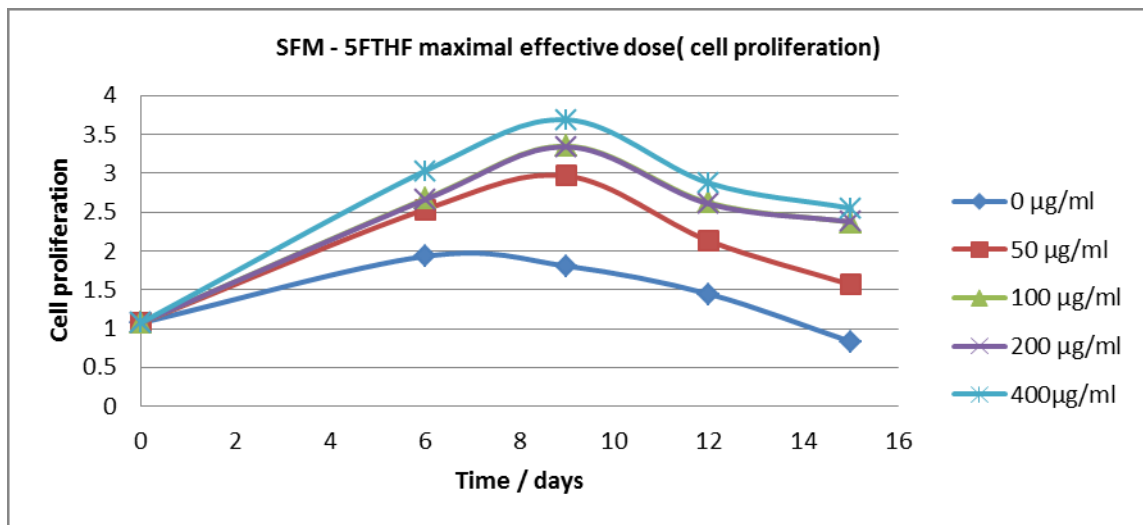


Figure 3.42 shows Table shows - SFM- 5FTHF maximal effective dose (cell proliferation)

Table 3.43 shows SFM- 5FTHF - maximal effective dose (% cell survival) using trypan blue exclusion

5FTHF	0	6	9	12	15
0 µg/ml	0.92	0.7	0.39	0.23	0.1

50 µg/ml	0.92	0.78	0.6	0.41	0.22
100 µg/ml	0.92	0.8	0.64	0.47	0.29
200 µg/ml	0.92	0.82	0.66	0.52	0.3
400µg/ml	0.92	0.82	0.68	0.52	0.33

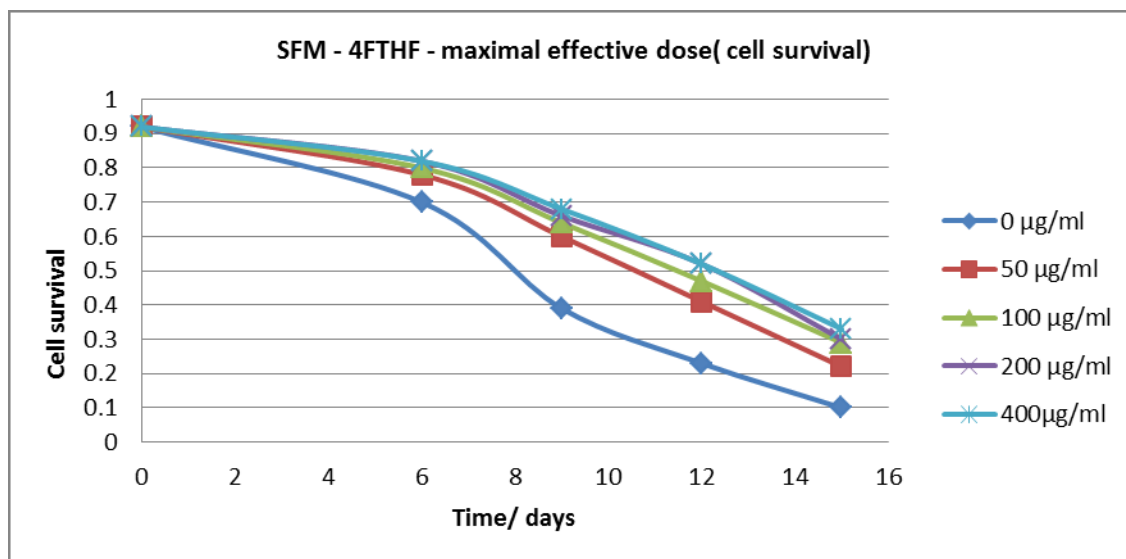


Figure 3.43 shows SFM- 5FTHF - maximal effective dose (% cell survival) using trypan blue exclusion

3.5.11 Effect of 5FTHF supplemental on cell proliferation using HL-60:

To determine therefore, whether 5FTHF supplemental might involve in inducing changes in proliferation among HL- 60. Thereby cells were maintained in Iscove medium supplemented with 5% foetal bovine serum, then plated into two dishes namely 5FTHF supplemental (supplemented with 50 µg/ ml), and 5FTHF deprived, then incubated overnight at 37°C in an atmosphere of 95% air and 5% CO₂. Cells were harvested after 1,2 and 3 days where cell count and viability were performed.

3.5.11.1 Results:

cells which grown in absence of 5FTHF exponentially quadrupled their number by 48h then its nearly proliferate to complete one cycle. Whereas 5FTHF supplemental cells slowly quadrupled their number by 72 but they didn't reach the number of its counterpart(p<. Considering cell survival cells grown in absence of 5FTHF steadily increase in cell survival then began to decline a bit by 72h, whereas cells seeded in presence of 5FTHF slow decline by

24h then began to increase by 72h might it needs time to acclimatize to toxicity induced by folinic acid.

Table 3.44 shows effect of 5FTHF supplemental on HL- 60 (Cell proliferation using haemocytometer

	0	1	2	3
5FTHF(-ve)	1	2.56	4.165	4.94
5FTHF(+ve)	1	1.695	2.78	4.395

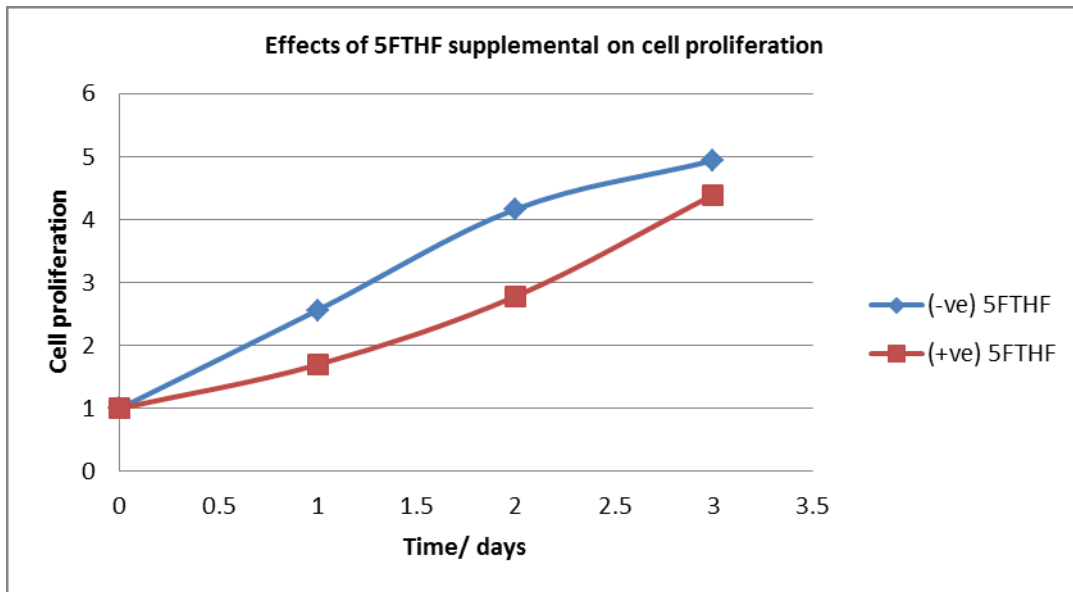


Figure 3.44 shows table shows effect of 5FTHF supplemental on HL-60 (cell proliferation)

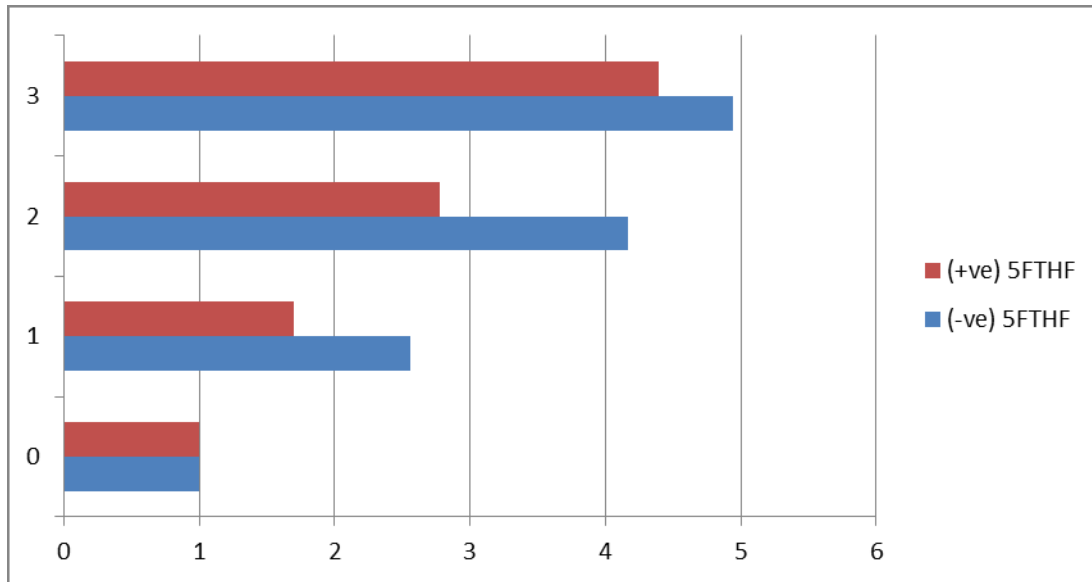


Figure 3.45 shows table shows effect of 5FTHF supplemental on HL-60 (cell proliferation)

Table 3.45 illustrate Effect of 5FTHF supplemental on HL-60 (cell survival) using trypan blue exclusion

	0	1	2	3
5FTHF(-ve)	0.85	0.88	0.89	0.87
5FTHF(+ve)	0.85	0.8	0.84	0.86

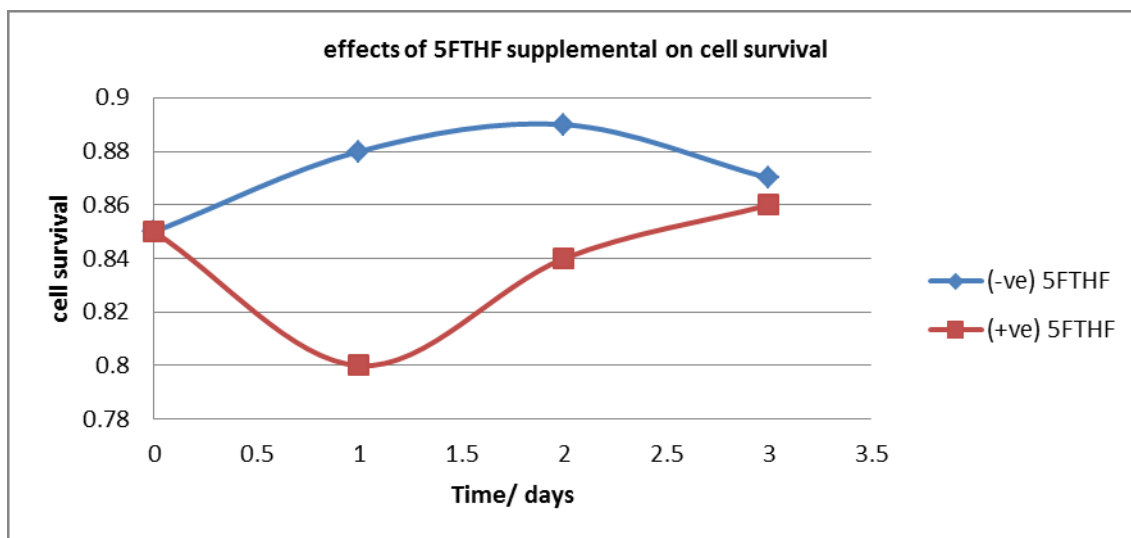


Figure 3.46 illustrate Effect of 5FTHF supplemental on HL-60 (cell survival) using trypan blue exclusion:

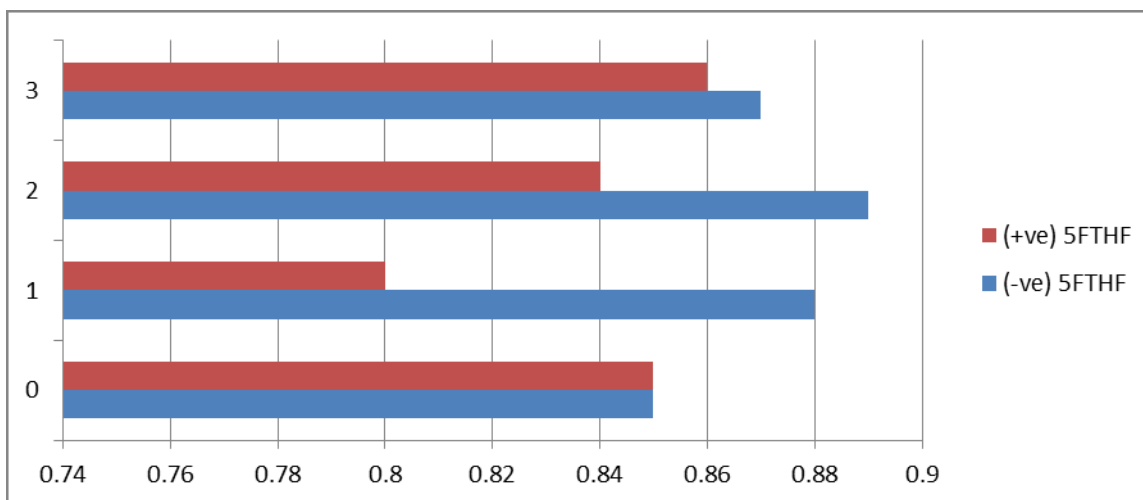


Figure 3.47 illustrate Effect of 5FTHF supplemental on HL-60 (cell survival) using trypan blue exclusion

3.5.12 Effect of 5FTHF supplemental on cell proliferation using MCF-7 cell:

To determine therefore, whether 5FTHF supplemental might involve in inducing changes in proliferation among MCF-7 cell lines. 3×10^6 were maintained in Iscove medium, supplemented with 5% foetal bovine serum. Then aliquoted into 6 dishes (35x10 mm), three dishes among them further supplemented with 50 $\mu\text{g/ml}$ hence described as folic acid supplemental while the other 3 dishes described as folic acid restriction cell. Cells were incubated in humidified atmosphere and cell harvested at day 1, 2 and three (each dish represent a day).

3.5.12.1 Results:

Folic acid restriction cells exponentially proliferate culminating its proliferative capacity by day 3. Whereas the folic acid supplemental cell decrease its number by day 1 and nearly reach the baseline by day 2 and nearly doubled their number by day 3 ($p < 0.05$).

Table 3.46 shows effects of 5FTHF supplemental on cell proliferation using MCF-7:

status	0	1	2	3
FA(+)	0.5	0.29	0.455	0.96
FA(-)	0.5	0.615	0.9	1.874

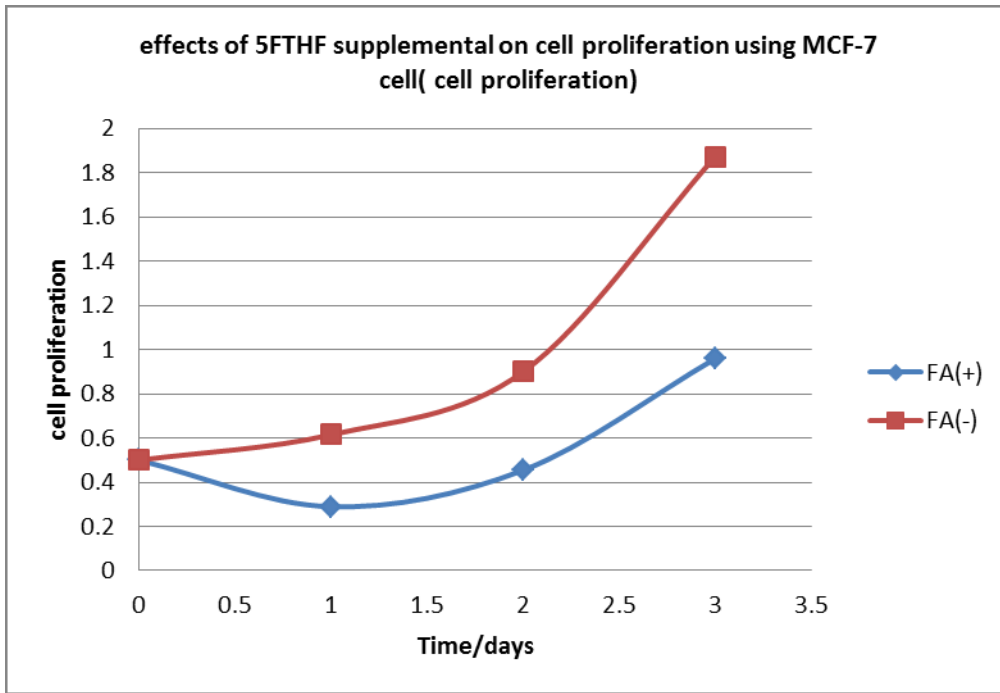


Figure 3.48 describes Effect of 5FTHF supplemental on cell proliferation using MCF-7 cell

Table 3.47 shows the effects of 5FTHF supplemental on cell proliferation using MCF-7 (cell survival)

status	0	1	2	3
FA(+)	0.93	0.84	0.84	0.9
FA(-)	0.93	0.94	0.98	0.95

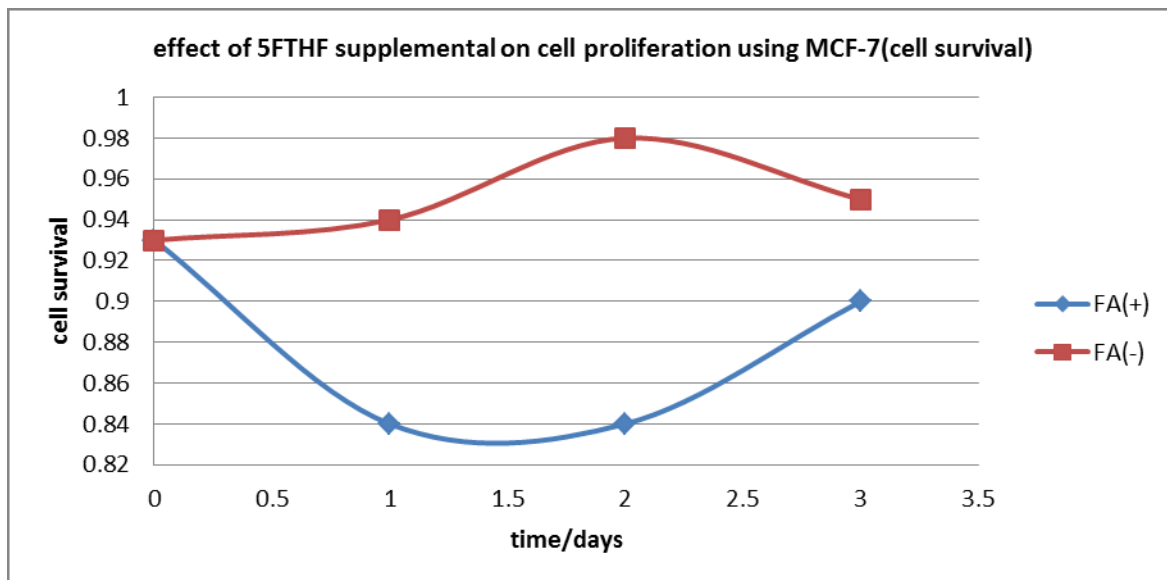


Figure 3.49 shows **effects of 5FTHF supplemental on cell proliferation using MCF-7 (cell survival)**

3.5.13 c-Myc inhibition and rescue with 5FTHF:

20x10⁶ cells were grown in Iscove Modified Dulbecco's Medium, supplemented with 5% foetal bovine serum, then cells were plated into 4 dishes, the first two dishes treated with c-myc inhibitor 10058-F4(sigma) and supplemented with or no folic acid. Whereas the other two dishes supplemented with DMSO(Fischer life sciences) with or no folic acid. Cells were harvested at day 1,2 and 3 whereby cell count and viability were performed, and cells were fixed and permeabilized for flow cytometric analysis.

3.5.13.1 Result:

Cells treated with c-Myc inhibitor 10058-F4 with no folic acid supplementation there is tremendous drop in its number and viability as well and the drop reached its nadir by day 3(p>0.05). Whereas folic acid partially bypass the effect of c-Myc inhibitor in cells treated with c-Myc inhibitor 10058-F4(p<0.05), however, the cell number is far from the baseline. There is a proliferative inhibition in The folic acid supplemental cell compare to folic acid restriction cells(p<0.05), at day for cells that treated with 10058-F4, the flow cytometric analysis shows peak sub G1 indicating apoptosis, supplementation of folic acid has no real effect at day 3 as indicated by accumulation of cells at sub G1. Folic acid supplementation slightly inhibits cell proliferation compare to folic acid deficient cells.

Table 3.48 shows the effect c-Myc inhibition and rescue with 5FTHF(cell proliferation) using haemocytometer:

	0	1	2	3
FBS/10058/FA	1	1.365	0.815	0.3`
FBS	1	0.89	0.455	0.125
FBS/FA/DMSO	1	1.56	2.22	2.805
FBS/DMSO	1	1.88	2.395	3.615

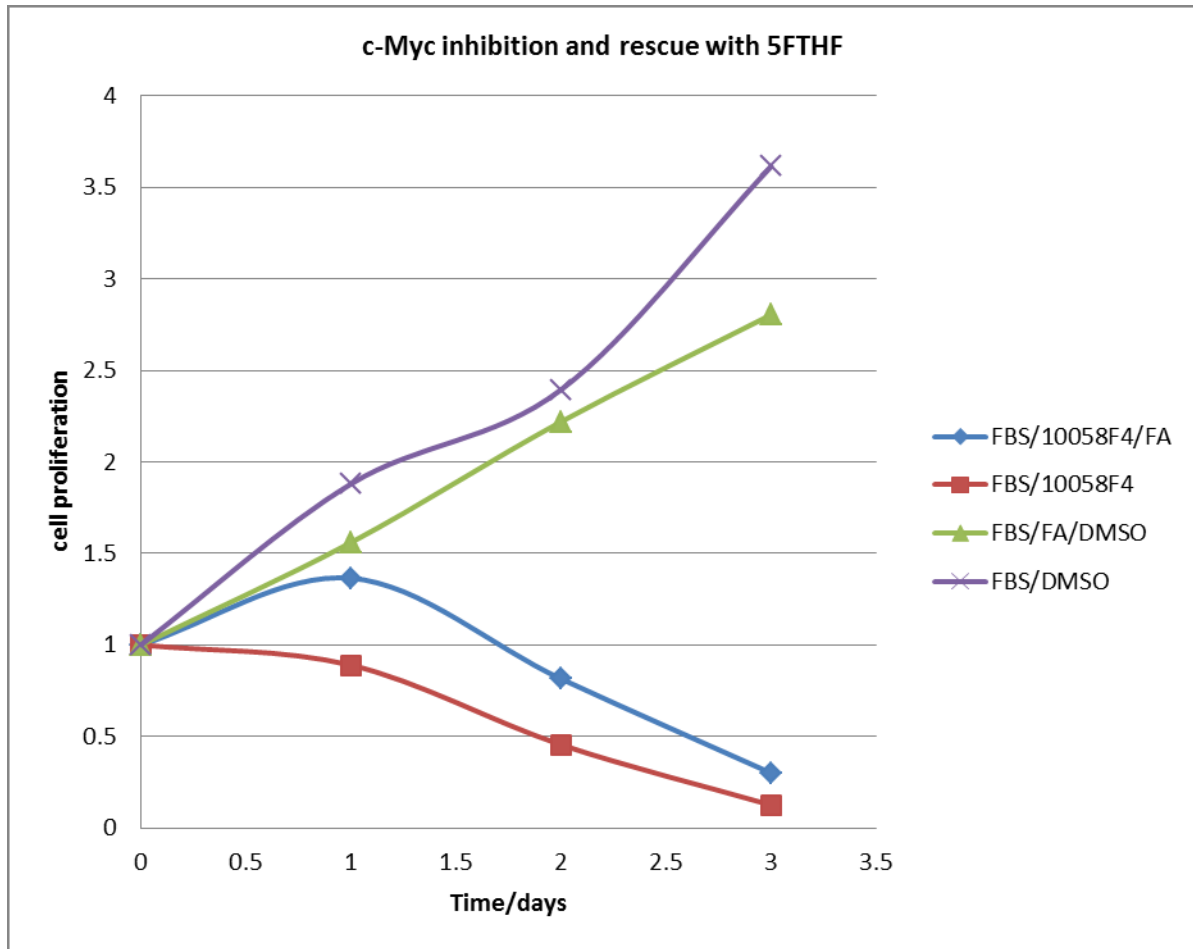


Figure 3.50 shows c-Myc inhibition and rescue with 5FTHF(cell proliferation) using haemocytometer

Table 3.49 shows c-myc inhibition and rescue with 5FTHF Cell survival) using trypan blue dye exclusion:

	0	1	2	3
FBS/10058F4/FA	0.96	0.64	0.34	0.11
FBS/10058F4	0.96	0.48	0.21	0.04
FBS/FA/DMSO	0.96	0.89	0.85	0.84
FBS/DMSO	0.96	0.92	0.89	0.9

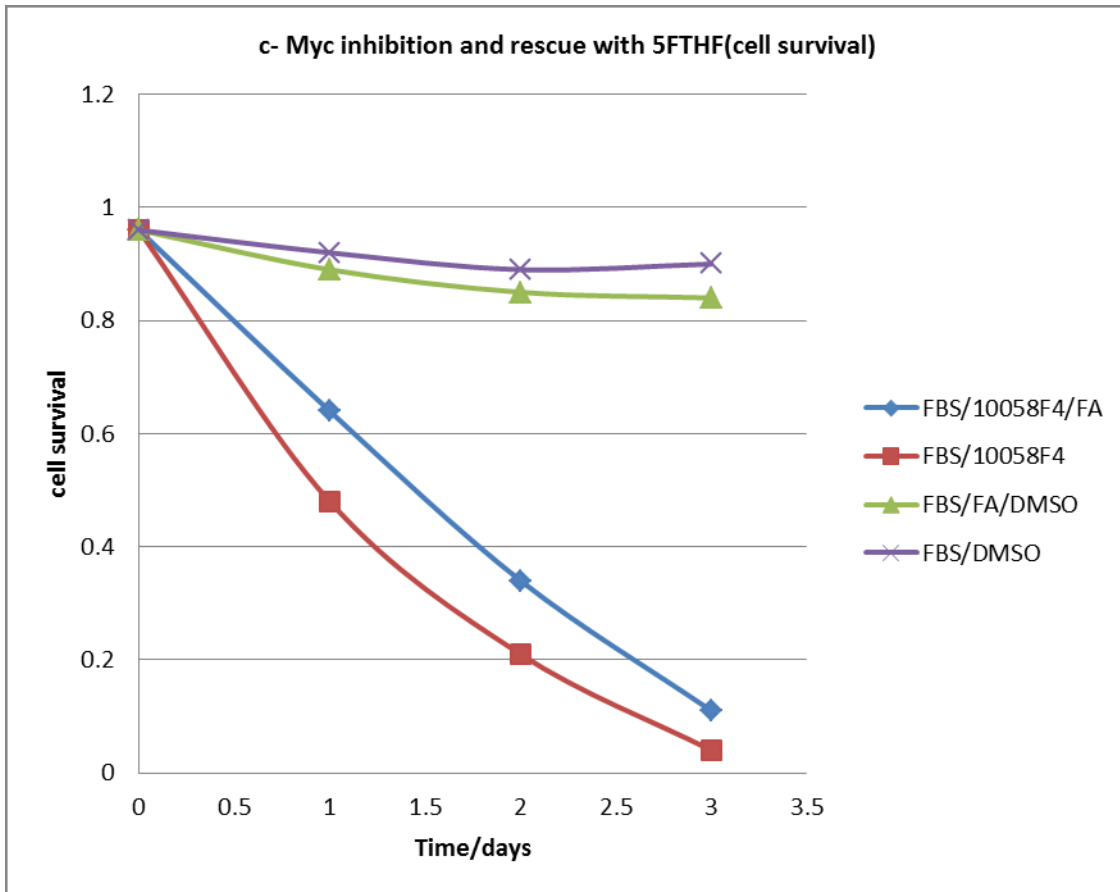
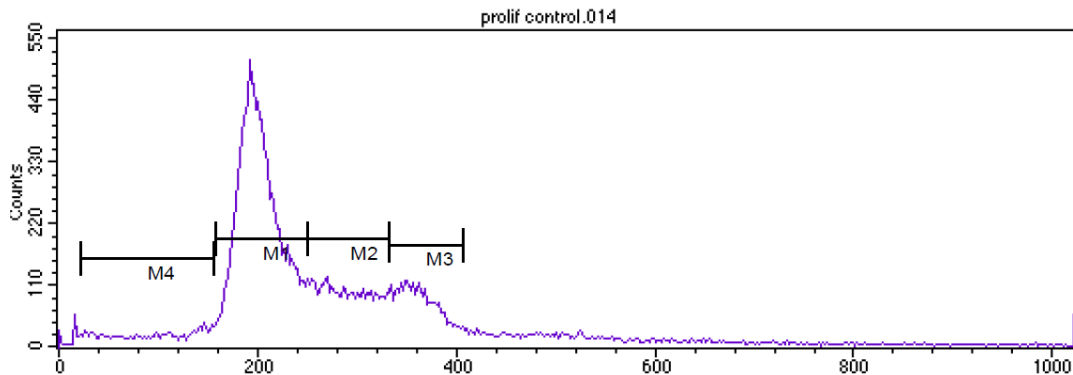


Figure 3.51 shows Table shows c-myc inhibition and rescue with 5FTHF Cell survival) using trypan blue dye exclusion:

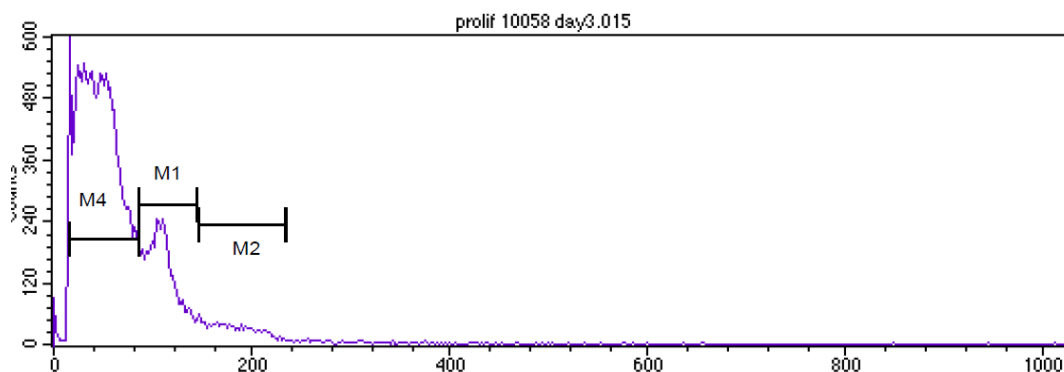
3.3.13.2 Flow cytometric analysis:

3.5.13.2.1 stained proliferating control:



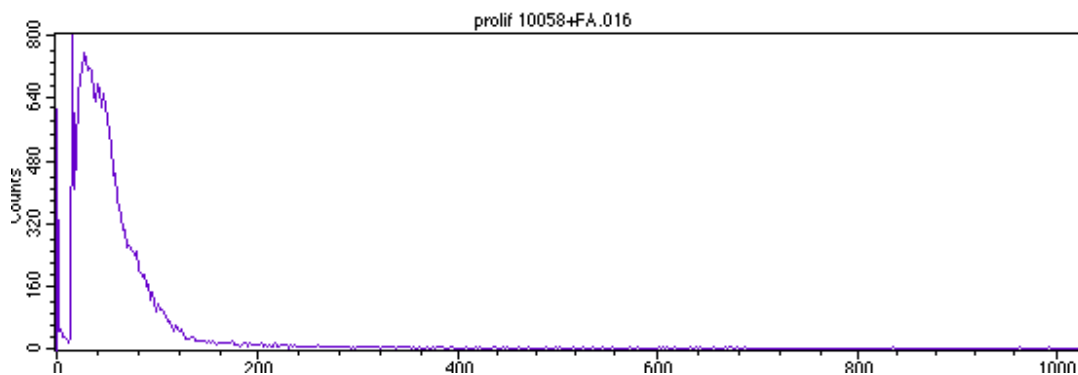
Marker	Left, Right	Events	% Gated	% Total	Mean	Geo Mean	CV	Median	Peak Ch
All	0, 1023	40000	100.00	100.00	270.00	242.12	48.70	225.00	193
M1	158, 251	20924	52.31	52.31	202.68	201.66	10.14	200.00	193
M2	251, 333	7543	18.86	18.86	290.53	289.52	8.34	289.00	270
M3	333, 407	5390	13.48	13.48	363.01	362.50	5.33	361.00	348
M4	22, 156	2202	5.50	5.50	93.51	81.92	44.89	98.00	147

3.5.13.2.2 proliferating cells treated with anti c-myc 10058-F4- day 3:



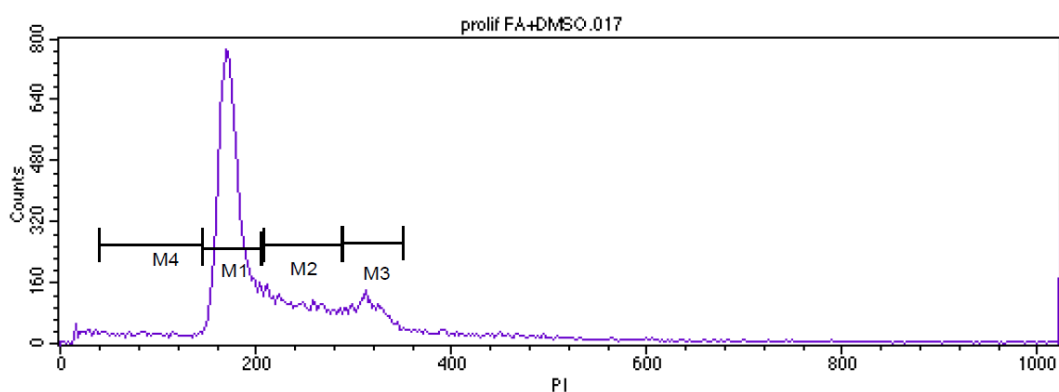
Marker	Left, Right	Events	% Gated	% Total	Mean	Geo Mean	CV	Median	Peak Ch
All	0, 1023	40000	100.00	100.00	68.67	55.51	71.00	56.00	17
M1	86, 145	8233	20.58	20.58	108.97	108.01	13.40	108.00	104
M2	148, 235	2218	5.54	5.54	182.07	180.66	12.58	180.00	148
M4	16, 86	29113	72.78	72.78	46.43	42.35	40.44	46.00	17

3.5.13.2.3 proliferating cells treated with anti c-myc 10058-F4 and folinic acid- day 3:



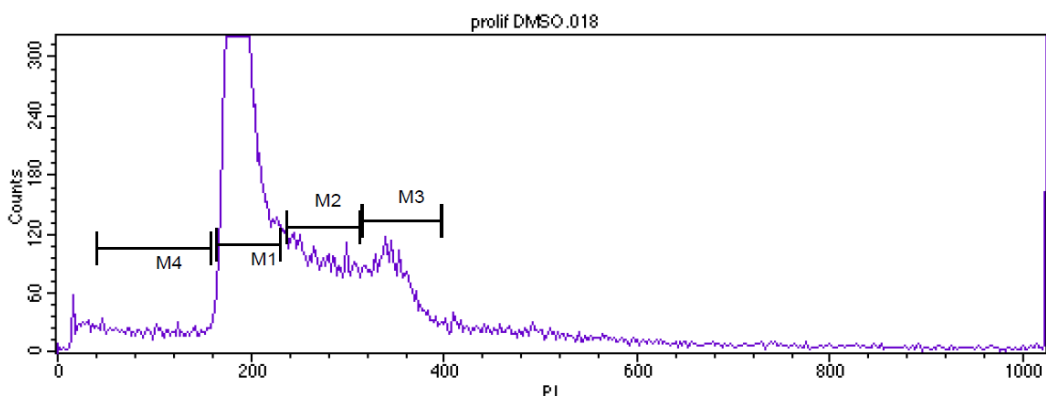
Marker	Left, Right	Events	% Gated	% Total	Mean	Geo Mean	CV	Median	Peak Ch
All	0, 1023	40000	100.00	100.00	52.36	41.86	75.98	44.00	17
M1	154, 240	541	1.35	1.35	186.31	184.86	12.73	181.00	156
M2	242, 341	128	0.32	0.32	279.05	277.68	10.11	271.00	262
M3	343, 405	23	0.06	0.06	366.39	365.97	4.93	363.00	345
M4	29, 150	29924	74.81	74.81	57.90	53.60	41.66	52.00	29

3.5.13.2.4 proliferating cells treated with folinic acid and DMSO- day 3:



Marker	Left, Right	Events	% Gated	% Total	Mean	Geo Mean	CV	Median	Peak Ch
All	0, 1023	40000	100.00	100.00	246.42	216.17	58.73	192.00	170
M1	146, 206	19617	49.04	49.04	175.53	175.13	6.84	174.00	170
M2	208, 289	7773	19.43	19.43	244.84	243.69	9.69	243.00	213
M3	288, 352	5055	12.64	12.64	316.40	315.96	5.28	315.00	313
M4	41, 146	1976	4.94	4.94	92.91	87.38	33.22	93.00	43

3.5.13.2.5 proliferating cells treated with DMSO- day 3:



Marker	Left, Right	Events	% Gated	% Total	Mean	Geo Mean	CV	Median	Peak Ch
All	0, 1023	40000	100.00	100.00	269.58	235.97	57.90	213.00	185
M1	166, 231	19719	49.30	49.30	192.53	191.97	7.74	189.00	185
M2	237, 314	6887	17.22	17.22	272.82	271.88	8.32	271.00	238
M3	315, 398	5375	13.44	13.44	348.19	347.56	6.05	345.00	340
M4	41, 159	1957	4.89	4.89	98.51	91.58	36.05	98.00	47

3.5.13.3 Mitotic index:

100 µl of Colcemid(Gibco) was added to a flask containing 10 ml of cell culture for 90 minutes. Then solution was transferred into 15 ml falcon tube. Then centrifuged at 2040 rpm for 10 minutes. Then supernatant was siphon off leaving only 2 ml. The pellet was vortexed and hypotonic solution(0.47 g potassium chloride K Cl was dissolved in 100 ml distilled water DW and kept in water path at 37°C), was added dropwise until 4ml then the volume completed to 14 ml. Then the falcon tube was put in water path at 37°C for 22 minutes. After that centrifuged at 2000 rpm for 10 minutes, and at the same time fixative solution (3 volumes of ethyl alcohol were added to 1 volume of acetic acid) was prepared. The supernatant was siphon off leaving only 2 ml. The was resuspended, and fixative solution was added dropwise while vortexing first to 3 ml then the volume completed to 14 ml, and left for 45 minutes at room temperature RT. Then centrifuged at 2040 rpm for 10 minutes. The supernatant was siphon off leaving only 1.5 ml. Then the pellet was resuspended and 3:1 fixative solution was added dropwise while vortexing and volume completed to 10 ml. Then centrifuged at 2040 rpm for 10 minutes. The supernatant was siphon off leaving only 1 ml. Then the pellet was resuspended and fixative solution was added dropwise and the volume completed to 10 ml. Then centrifuged at 2040 rpm for 10 minutes. The slide was prepared by dropping the swollen fixed cells onto microscopic slide and left to dry. Then the slide was stained using Giemsa stain(20 ml of Giemsa diluted in 80 ml of disodium hydrogen phosphate Na₂ HPO₄, pH 6.8).the mitotic indices were calculated using the following equation

$$\text{Mitotic index MI} = \frac{\text{Number of metaphase HL-60 cells}}{2 \times \text{Total number of cells}} \times 100$$

Wherefore the number of examined metaphase cells represented the mitotic division since the Colcemid substance blocked the mitotic division at metaphase.

3.5.13.3.1 Mitotic index of cells treated with c-myc inhibitor and rescue with folinic acid:

To determine the mitotic index, 15×10^6 cells were seeded in Iscove medium, supplemented with 5% Fetal bovine serum. Cells were equally plated into three dishes 5×10^6 per each. Then treated with Colcemid ($50 \mu\text{l}/5\text{ml}$) for three hours. The first dish was treated with c-myc inhibitor (10058-F4). The second treated with c-myc inhibitor in addition to folic acid. The last one was left untreated (control). Then incubated overnight. Next day cell treated as mentioned above.

3.5.13.3.1.1 Result:

Cells that has been treated with c-myc inhibitor has shown low mitotic activity compared to same cells which has been supplemented with folic acid. Confirming that folic acid may bypass the effect of anti c-Myc as shown in the figure below.

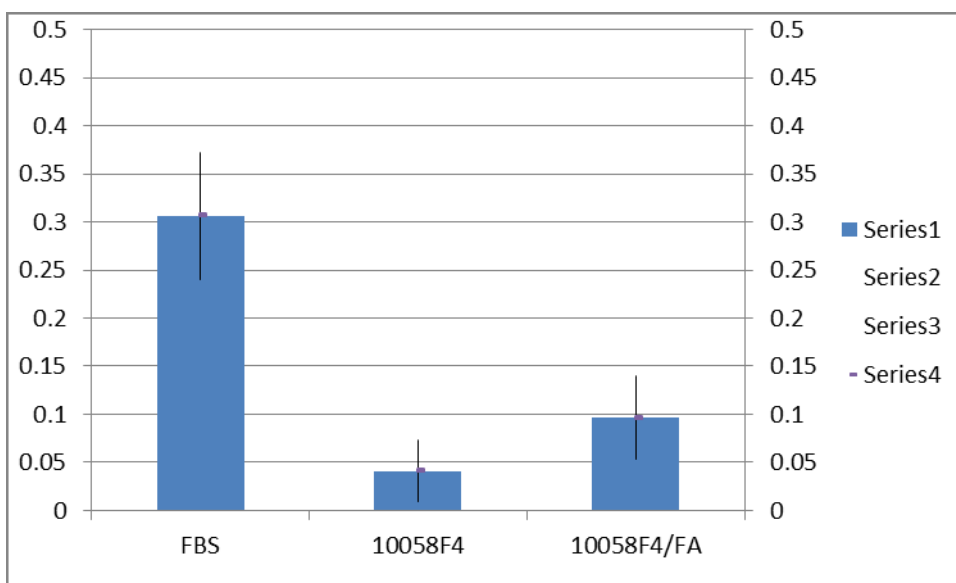


Figure 3.52 describes the mitotic activity

3.5.13.4 synchronization of cells with methotrexate and treatment with c-myc inhibitor:

30×10^6 cells were maintained in Iscove medium, supplemented with 5% fetal bovine serum. Then plated into six dishes (5×10^6 per each), 3 dishes represent one group that released from the block after 3 hours. and rest represent another group that released from the block after 5 hours. Each dish was treated with $257 \mu\text{l}$ of methotrexate (lederle) for 16 hours. Next day cell were washed with sterile 1x PBS, resuspended in Iscove medium supplemented with 5% FBS. 3h and 5 h latter cells were released from the block by adding $50 \mu\text{l}$ of

Colcemid(Colchicine). Then treated with c-myc inhibitor, c-myc inhibitor and folinic acid and untreated cells, and incubated overnight, next day cells were treated as mentioned above.

3.5.13.4.1 Results:

With regard to cells that have being released from the block after 3 hours, the obtained results show that, the mitotic activity has shown reduction in c-Myc inhibitor treated cell, while administration of folinic acid has increased the mitotic activity in c-Myc inhibitor treated cell, generally speaking there are a reduction in both cells compare to control. Concerning cells that have being released from the block after 5 hours. Intriguingly there is a reduction in the mitotic activity.

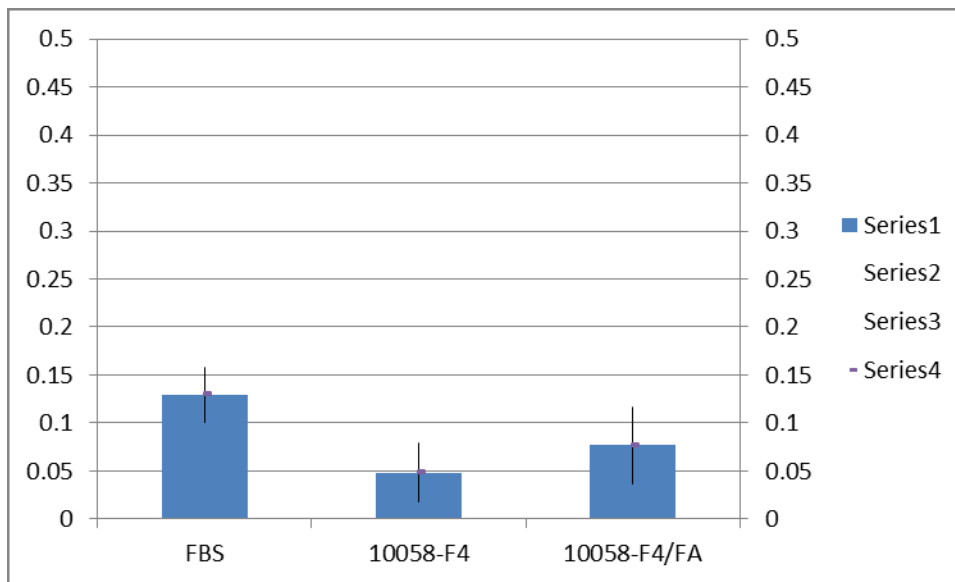


Figure 3.53 shows mitotic activity of cells that has been released from the block after 3 hours

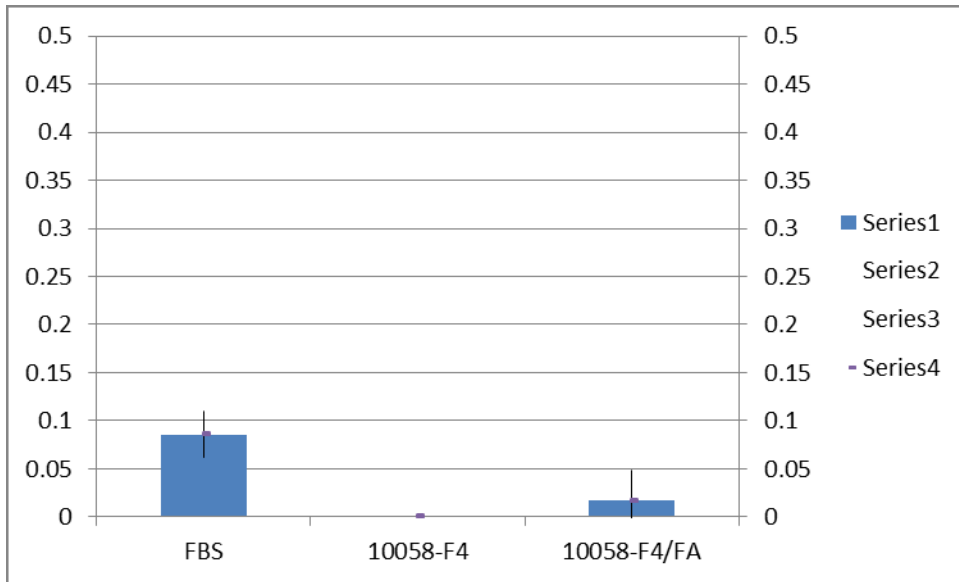


Figure 3.54 shows mitotic activity of cells that has been released from the block after 5 hours

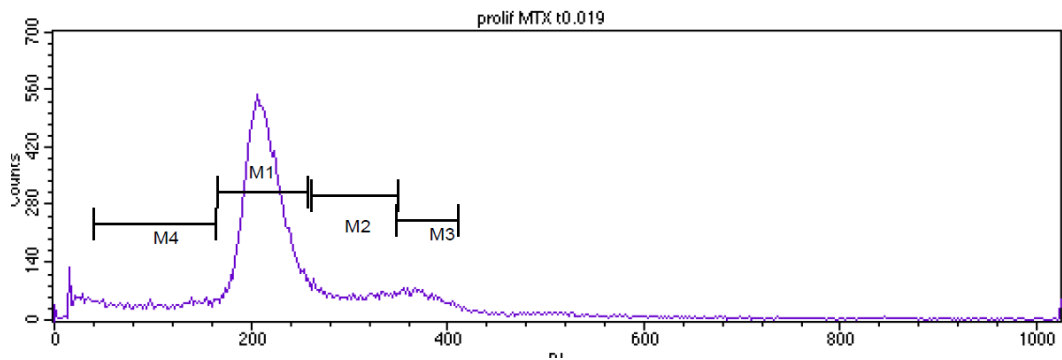
3.5.13.5 Flow cytometric analysis for synchronization of cells with methotrexate and treatment with c-Myc inhibitor

Cells were seeded at density of 40×10^6 cells and maintained in Iscove medium, supplemented with 5% foetal bovine serum. Then plated into six dishes (5×10^6 per each), 3 dishes represent one group that released from the methotrexate block after 3 hours. And the rest represent another group that released from the methotrexate block after 5 hours. In addition to control group that treated with methotrexate. Each dish was treated with (0.1 mM) $257 \mu\text{l}$ of methotrexate (lederle) for 16 hours. Next day cell were washed with sterile 1x PBS, resuspended in Iscove medium supplemented with 5% FBS. 3h and 5 h later cells were released from the block by. Treating it with c-myc inhibitor, c-myc inhibitor and folinic acid and untreated cells, afterward adding $50 \mu\text{l}$ of Colcemid. The cells were prepared for flow cytometric analysis using the protocol.

3.5.13.5.1 Results:

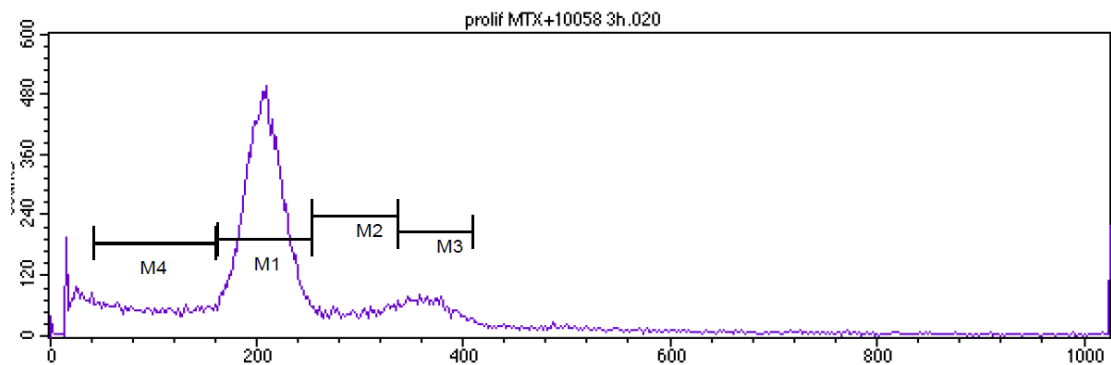
We intended to synchronize cells in S phase, then determine the effect of anti-c-Myc, moreover, to determine the capacity of folinic acid to rescue cells. By serendipity We added high amount of methotrexate 0.mM which results in trapping and freezing cells at G₀/G₁, however this treatment abrogate the action of anti c-Myc. Meanwhile administration of folinic acid helps cell a bit to traverse the S- phase and continued the cell cycle

3.5.13.5.1.1 MTX synchronized cell(control):



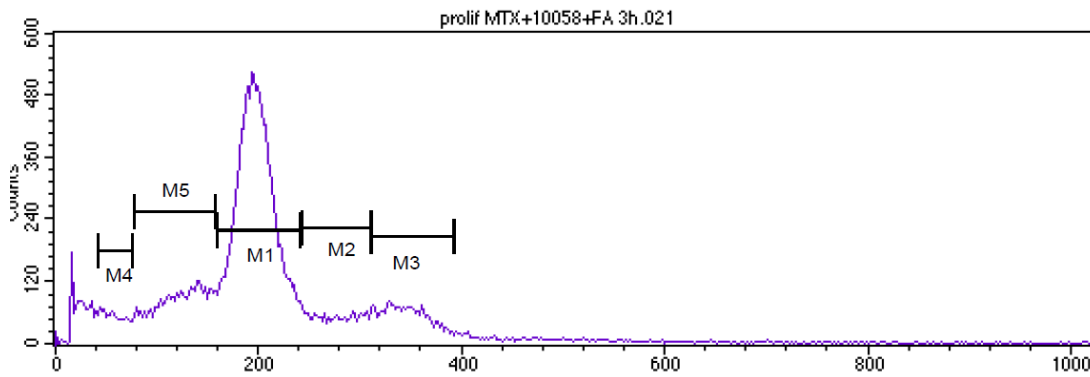
Marker	Left, Right	Events	% Gated	% Total	Mean	Geo Mean	CV	Median	Peak Ch
All	0, 1023	40000	100.00	100.00	243.77	213.48	48.48	218.00	206
M1	166, 258	23838	59.59	59.59	213.50	212.67	8.84	212.00	206
M2	262, 351	4929	12.32	12.32	305.09	303.89	8.88	305.00	264
M3	348, 411	3269	8.17	8.17	375.42	375.02	4.64	374.00	356
M4	41, 164	3973	9.93	9.93	103.87	96.26	36.16	105.00	141

3.5.13.5.1.2 MTX synchronized cells that have being treated with anti c-Myc(10058-F4)- 3h after the block:



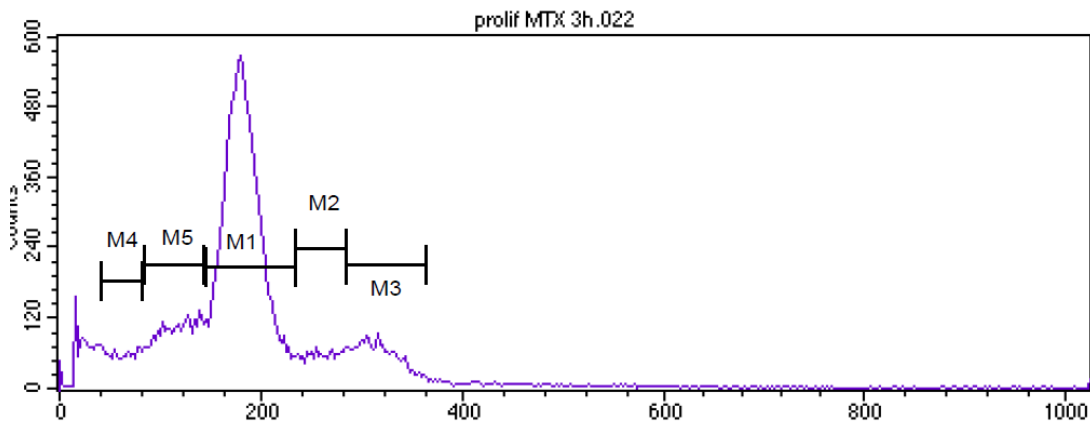
Marker	Left, Right	Events	% Gated	% Total	Mean	Geo Mean	CV	Median	Peak Ch
All	0, 1023	40000	100.00	100.00	239.43	196.51	61.78	210.00	209
M1	161, 252	21413	53.53	53.53	206.62	205.74	9.18	207.00	209
M2	252, 337	3649	9.12	9.12	295.95	294.81	8.75	297.00	335
M3	336, 409	3925	9.81	9.81	368.28	367.77	5.32	367.00	356
M4	41, 159	5730	14.32	14.32	97.43	90.53	36.43	96.00	41

3.5.13.5.1.3 MTX synchronized cells that have being treated with anti c-Myc(10058-F4) and FA- 3h after the block:



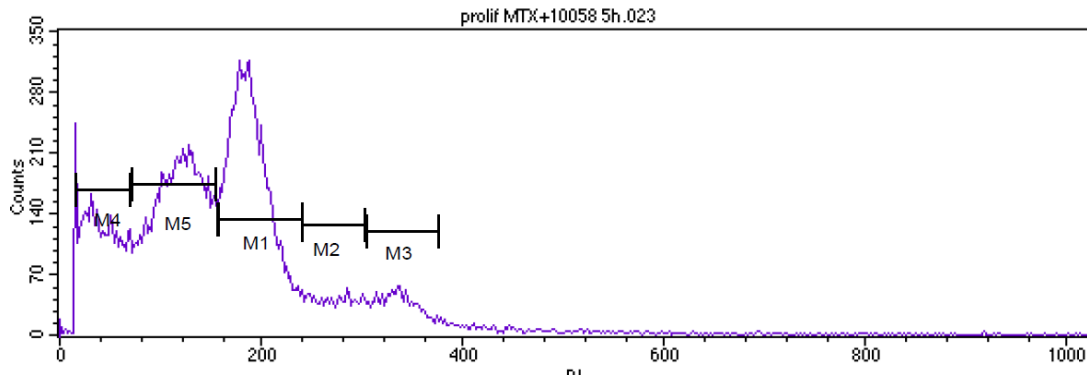
Marker	Left, Right	Events	% Gated	% Total	Mean	Geo Mean	CV	Median	Peak Ch
All	0, 1023	40000	100.00	100.00	202.59	175.54	48.34	195.00	193
M1	159, 241	21753	54.38	54.38	197.32	196.53	8.95	197.00	193
M2	243, 310	3103	7.76	7.76	276.68	275.94	7.30	277.00	310
M3	311, 392	4036	10.09	10.09	345.35	344.72	6.04	344.00	329
M4	41, 76	1655	4.14	4.14	57.31	56.37	18.03	57.00	44
M5	78, 157	6185	15.46	15.46	122.15	120.03	18.10	124.00	139

3.5.13.5.1.3 MTX synchronized cells- 3h after the block:



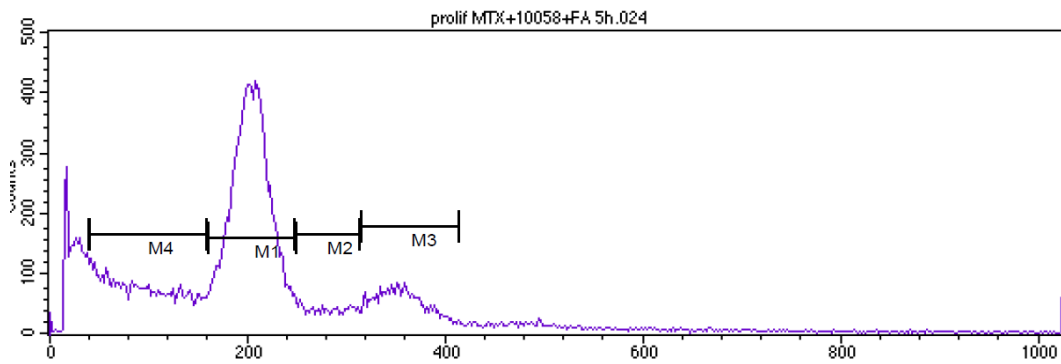
Marker	Left, Right	Events	% Gated	% Total	Mean	Geo Mean	CV	Median	Peak Ch
All	0, 1023	40000	100.00	100.00	184.86	161.42	46.95	179.00	180
M1	146, 236	22860	57.15	57.15	183.14	182.23	10.04	182.00	180
M2	235, 285	2620	6.55	6.55	260.79	260.37	5.68	261.00	254
M3	285, 365	4015	10.04	10.04	317.08	316.45	6.34	316.00	317
M4	41, 82	2190	5.47	5.47	61.60	60.27	20.47	62.00	41
M5	84, 144	5551	13.88	13.88	116.51	115.21	14.72	118.00	140

3.5.13.5.1.4 MTX synchronized cells that have being treated with anti c-myc(10058-F4)- 5h after the block:



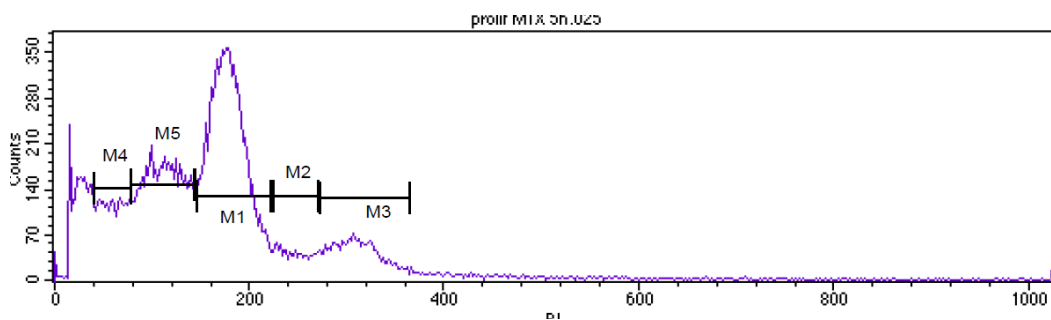
Marker	Left, Right	Events	% Gated	% Total	Mean	Geo Mean	CV	Median	Peak Ch
All	0, 1023	40000	100.00	100.00	161.41	131.79	60.38	156.00	179
M1	157, 241	14371	35.93	35.93	189.90	188.92	10.27	188.00	179
M2	240, 303	2277	5.69	5.69	271.18	270.52	6.95	271.00	285
M3	305, 377	2344	5.86	5.86	336.22	335.70	5.56	335.00	338
M4	16, 70	6573	16.43	16.43	41.11	37.77	38.79	40.00	17
M5	72, 155	13204	33.01	33.01	116.85	114.59	19.12	118.00	128

3.5.13.5.1.5 MTX synchronized cells that have being treated with anti c-myc(10058-F4) and FA- 5h after the block:



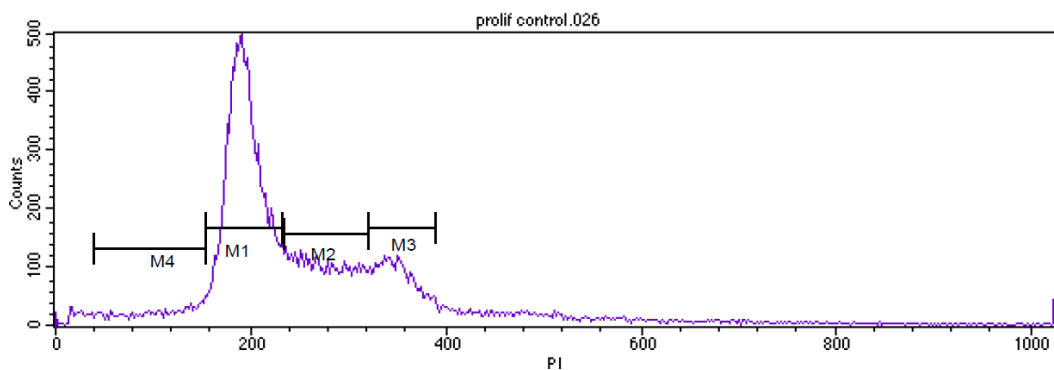
Marker	Left, Right	Events	% Gated	% Total	Mean	Geo Mean	CV	Median	Peak Ch
All	0, 1023	40000	100.00	100.00	210.51	163.79	65.93	200.00	207
M1	161, 249	19018	47.55	47.55	203.68	202.81	9.22	204.00	207
M4	40, 159	8307	20.77	20.77	93.16	86.26	37.69	90.00	42
M2	247, 313	2310	5.78	5.78	279.16	278.42	7.31	279.00	247
M3	315, 413	4514	11.29	11.29	356.09	355.25	6.90	354.00	350

3.5.13.5.1.6 MTX synchronized cell- 5h after the block:



Marker	Left, Right	Events	% Gated	% Total	Mean	Geo Mean	CV	Median	Peak Ch
All	0, 1023	40000	100.00	100.00	158.31	128.61	60.86	159.00	176
M1	146, 224	16012	40.03	40.03	178.57	177.71	9.90	177.00	176
M2	222, 270	1786	4.46	4.46	245.15	244.73	5.86	245.00	228
M3	271, 364	3594	8.98	8.98	309.69	308.84	7.41	308.00	306
M4	41, 79	4231	10.58	10.58	60.16	59.06	18.89	60.00	68
M5	79, 144	9832	24.58	24.58	111.99	110.47	16.32	112.00	100

3.5.13.5.1.7 proliferating cells control:



Marker	Left, Right	Events	% Gated	% Total	Mean	Geo Mean	CV	Median	Peak Ch
All	0, 1023	40000	100.00	100.00	260.77	235.29	47.75	218.00	191
M1	154, 232	19705	49.26	49.26	194.20	193.44	8.85	193.00	191
M2	234, 320	8311	20.78	20.78	274.90	273.72	9.27	274.00	237
M3	320, 390	5575	13.94	13.94	349.71	349.22	5.29	348.00	337
M4	39, 154	2035	5.09	5.09	105.70	99.03	32.75	110.00	150

4- Discussion

It is well-known that, short wavelength UV radiation (UVC) elicits predominantly DNA damage to cells by forming pyrimidine dimers and 6-4 photoproducts. These DNA lesions can cause cytotoxicity by activating death pathways or inhibiting transcription and replication which consequently result in apoptosis(Ljungman et al., 1999; Gentile et al., 2003). The results obtained in the present study show that UVC can induce prominent apoptosis in HL-60 as easily identified by trypan blue dye exclusion. However, the manner and modality of action and the sequel of the event seem to be dose – dependent. As reported by Latonen et al., (2001), that in response to low dose of UV radiation, DNA replication is repressed and the cells undergo a transient arrest re-entering the cell cycle by 24 hours. Instead, a high dose of UV damage results in initial replicative arrest followed by death of the cells via apoptosis. Our findings consistently agree with this, since after supplementing cells with fetal bovine serum 2 hours post radiation, cells that were exposed to low dose of UVC awesomely restored and reverted their proliferative capacity nearly to untreated one($p < 0.05$). Nevertheless cells that were exposed to high dose of UVC underwent apoptosis en masse. Additionally, UV irradiation may induce apoptosis by activating cell surface death receptor CD-95. Lu et al., (1996), reported activation of p36 myelin basic protein(MBP) kinase specifically associated with cells undergoing apoptosis. Furthermore this finding could be imputed to the supplementation of fetal bovine serum which contains growth factors(GFs), which are not only implicated in survival signaling, cell migration, metastasis formation and angiogenesis, but also confer a reduction in the response of tumour cells to cytotoxic compounds. Also growing amount of evidence has indicated that the intracellular redox state plays a paramount role in the mechanism action of GFs. Particularly, GFs have been reported to produce reactive oxygen species (ROS), which may function such as proliferation and programmed cell death(Thannickal and Fanburg, 2000; Melisi et al., 2004).

5-formyltetrahydrofolate is an ubiquitous member of folate biological pool, usually constituting about 10- 25% of total cellular folates(Cossins, 1984; Horne et al., 1989). It is long- established as a nutrient supplement, and is capable of inhibiting cytotoxicity and chromosomal damage elicited by chemicals. The results presented in our study show that folic acid induce cell proliferation in UVC untreated cells, however, in UVC treated cells 10 and 25 µg/ml of folic acid had no real effects on UVC treated cells probably the amount of folic acid not instrumental enough to rescue inflicted cells, while cells supplemented with hyper-physiologic dose(400 µg/ml) can sparsely out compete the cytotoxicity induced by UVC and sustains cell viability without restoring the proliferative capacity. This finding is in an accord with study conducted by Keshava et al., (1996), who pointed out that folic acid had minimal effect in reversing the cytotoxicity induced by UVC and X-rays radiations. The most likely explanation for the inhibition of radiation induced chromosome aberrations could be a reduction in the number of single strand breaks(SSBs)prior to their conversion into double strand breaks(DSBs). Furthermore, several lines of evidence indicate that folate depletion alone accounting for DNA strand breaks equal to 26 cGy of radiation, as following 400 cGy of irradiation folate depleted cells exhibited strand breaks to a dose of 710 cGy. These observations suggest that, folate deficiency acts synergistically with carcinogen to magnify the genetic damage((Branda and Blickensderfer, 1993). Nonetheless, in the present study no folate deficiency, UVC inflicted severe damage that minimally reversed by supplementing folic acid which might impact the synthesis and repair of DNA after damage. Following DNA damage slight amount of DNA repair occurs inside the cell utilizing the nucleotide pool exist in the cell. Since UVC radiation causes excessive breaks which could result in shortage and run out of nucleotide pool resulting in a defect of repair mechanism. In contrary supplementation of folic acid could assist in generation of the *de novo* nucleotide pool. Thanks to Dihydrofolate reductase well recognize to mediate the reduction of dihydrofolate into tetrahydrofolate, a known cofactor needed for synthesizing thymidylate, important for DNA synthesis. Needless to say that, Folic acid is important in DNA synthesis and repair and may play an important role in preventing DNA mutations that lead to cancer. Additionally, deficiencies in micronutrients including folate have been indicated as a major cause of DNA damage, as shown in normal lymphocytes grown in low folate medium exhibit excessive DNA strands breaks and increased uracil misincorporation even at folate concentrations within the normal range observed in human plasma. In humans, folate

depletion causes both massive incorporation of uracil into DNA and chromosome breaks, which can be reversed by administering folate (Wei et al., 2003). Concerning the effects of pre and post- treatment and UVC on cell proliferation. We found no marked difference between pre and post treatment($p < 0.05$), despite there is evolving body of evidence that exposure to UV irradiation might result in folate depletion(Williams and Jacobson, 2010).

Ultraviolet B(UVB) radiation is a potent apoptotic trigger in many cell types, in tumour and normal cells as well. Many studies have described that UVB- induced cell death via the generation of reactive oxygen species, which consequently result in the impairment of cellular antioxidants, induction of DNA damage and eventually occurrence of apoptosis(Salucci et al., 2012). The data presented in this study demonstrate that, UVB can induce irrefutably noticeable damage on HL-60. Nevertheless, the interplay and modus operandi are dose- dependent. Low dose of UVB(1 minute), elicits minimal adverse effect, while high-dose(10 minutes) cause apoptosis in medias res. Our findings are reasonable concordance with Al-Mohanna et al., (2001). The minimal adverse effects induced by low dose of UVB is attributed to the behavior of UVB in inducing cyclobutane pyrimidine dimers CPDs. These bulky DNA lesions are removed by nucleotide excision repair. Accordingly, temporary arrest at diverse phases of cell cycle is occurred. This process is needed for coherent repair of DNA lesions. The genomic custodian guard p53 plays fundamental role in the cellular response to DNA damage. Moreover , p53 protein has a tremendous role in the γ -ray-induced cell cycle delay in G1 phase. Surprisingly, HL-60 is p53 deficient cells thus indicating that there is an alternative p53- independent pathway causes the delay in G1. Study by Al-Mohanna et al., (2001), reported that HL-60 undergo p53 independent cell cycle arrest. Regarding UVB high dose, HL-60 underwent p53- independent apoptosis en masse likewise UVC proving that it might be a killing dose. Folic acid is indispensable for nucleotide excision repair, a mechanism used to eliminate the detrimental consequences of DNA damage induced by cyclobutane pyrimidine dimers and photoproduct adducts. Folic acid mitigate the adverse effects produced by CPDs notably in low- dose UVB treated cells. While in high-dose UVB treated cells which triggers excessive DNA bulky lesions, folic acid supplementation minimally protect cells from apoptosis most probably to the excessive amount of CPDs. Intriguingly folic acid at concentration 100 $\mu\text{g/ml}$ was found to modulate cell growth for untreated cells, additionally, maintain proliferation, protect cells from apoptosis as well as survival of low- dose UVB treated cells(0.5 and 1 minute), indicating dose

dependence is premised on dose of UVB exposure. Interestingly, low- dose UVB(2 minutes exposure) seems to be detrimental dose with same effect of 10 minutes, it is hard to identify exactly the mechanism behind that, since in theory no much difference between 1 and 2 minutes. Unfortunately folic acid fails to reverse the damage induced relatively low- dose UVB suggesting that the excessive underlying damage is beyond the capacity of the repair system. However, HL-60 is well known as sensitive cells against apoptosis inducing agents such as UV irradiation(Sonoda et al., 2000), implying that folic acid has minimal protection effect against relatively low- doses as well as high- doses UVB. Moreover, HL-60 is a malignant cells having a reduced rate of folic acid transport, and therefore, are preferentially harmed by high doses of chemotherapy (Golan et al., 2011). Surprisingly the corollary low- dose UVB synergistically has been enhanced and promoted cell proliferation in cells supplemented with high- doses of folic acid. However, we couldn't substantiate this process, thankfully, It has observed that UV could induce Unscheduled DNA synthesis (UDS) in human lymphocyte(Mohankumar et al., 1998). Huang et al., (1996), reported that UV activates growth factor via reactive oxygen intermediate(ROI). Furthermore, several mechanism can be considered to explain the swift EGF receptor activation by UV, one is that UV elevates the secretion of EGF- like ligands or other factors that consequently activate the receptor. A second likelihood is that UV brings about the production of ROI that trigger the UV signal pathway. Alternatively, damaged DNA produces an effect on EGF receptor protein (Huang et al., 1996).

The term serum starvation, serum deprivation, depletion, removal, restriction, withdrawal as well as serum limitation have been used to denote different procedures that include growing cells in either reduced serum, serum free(SFM), or serum and protein- free medium(Pirkmajer and Chibalin, 2011). The data presented in this study suggest that the administration of 5FTHF has effect on temporary proliferation of HL-60 cells in SFM (that is dose-dependently prolonged), whereas has limited effect on cell survival (that is just partially reduced in slope) and no effect on UVB resistance. However, our findings are in contrast with findings of Balk et al., (1978), they found that, the normal and Rous sarcoma virus- infected fibroblast has proliferated at maximal, again nearly identical rates in in medium containing a physiological concentration(10 ng/ml). similar results reported by Chello and Bertino, (1973) who found that physiological concentration of 5- methyltetrahydrofolate would support maximal proliferation of L-5178Y mouse leukemia cells in culture. Furthermore, no increase

in the rate of proliferation was noticed in media containing supra-physiologic concentration (100ng/ml). Nevertheless, in regard to sub-physiological concentration(0.1ng/ml), a reduced proliferative rate was observed which in tantamount with our finding, this difference may ascribed to cell type specific behaviour. Folate deficiency has been found to slow down the proliferation of varied cell types, not surprisingly cells devoid folates accumulate in the S phase possibly due to impaired nucleotide excision repair and slow DNA synthesis, increased uracil misincorporation and DNA damage. However when folate is replenished to folate-deprived cells, reversal of the S phase accumulation and proliferation is revived. Folate deficiency is more likely to affect proliferative cells, which have a higher nucleotides requirement (Choi et al., 1998; Courtemanche et al., 2004). It is well- observed that cells cease proliferation after day 9 and sub G1 peak was evident, this possibly maybe either due to actual depletion of folic acid. In this context we found no significant difference between administering single dose of 50 µg/ml, and replenishing cells with 10 µg/ml every 2 days($p < 0.05$), or would rather limitation of the proliferative capability, it is well-recognized that a novel mode of apoptosis induction observed in human leukemic HL-60 cells. These cells spontaneously underwent apoptosis in the course of proliferation when the cell density become higher than $1 \times 10^6 / \text{ml}$ (Saeki et al., 2000). HL-60 is unique human leukemic cell line capable of seemingly infinite proliferation in suspension culture (Collins et al. 1977). And the consequential DNA replication and cell division occur at an accelerated rate, folate depletion results in an ineffective DNA synthesis, leading to repression of cell growth(Kamen, 1997).

To verify the proliferative response to folic acid in starved HL-60. We check the proliferative response to 5-FTHF in normal peripheral blood mononuclear cell(PBMCs), under different stringent conditions. The data presented show that, Folic acid had a beneficial effects particularly when combined with serum as it synergistically enhanced cell proliferation. However the number of cells haven't reverted to baseline level($p < 0.05$). Not surprisingly the results show that serum is crucial for cell proliferation. Furthermore, it is well evident when cells have been stimulated with mitogen like PHA as in absence of serum intriguingly, PHA seems acting as apoptotic trigger. It has been published that mitogen as phytohaemagglutinin may induce lymphocyte to mitogenesis (DNA synthesis) and cytotoxicity(lysis of target cell)(Dawkins and Zilko, 1975. Furthermore, activation of PBMCs with mitogen leads to proliferation. Nevertheless, under certain conditions, principally when

cells are quiescent and restimulated, it can result in the induction of apoptosis. This type of cell death in PBMCs has been called activation-induced cell death(AICD)(Pahlavani and Vargas, 2001). PHA involved activation of caspase-3 and the anti-apoptotic protein Bcl-2 in addition to PARP cleavage, suggesting that PHA induces apoptosis via different pathways(Nielsen et al., 2007). PHA might work as double-edged sword in presence of growth factor enhances cell proliferation while in absence of growth factor accelerates cell apoptosis, Hypothesizing that deficient of folate may result in uracil misincorporation and as a consequence cells undergo apoptosis. Alternatively maybe imputed to the cell type specific and the amount of serum, we used 1% which considered by others as serum free medium.

Supplementation of cells with high doses of 5FTHF dramatically affect cells in terms of proliferation and survival as cells proliferate steadily compared to cells grown in 5FTHF restriction. We observed that folic acid at concentration 50 µg/ml could be the minimal dose to elicit maximal proliferating response by expanding folate pool in malignant cells; however this finding seemingly in discordance with the hypothesis hypothesizing that malignant cells have a reduced rate of folic acid transport (Golan and Tashjian, 2011). In contrast it has been published recently that excessive folate supplementation may also diminish the activity of antifolate drugs that influenced by influenced by a higher intracellular folate content(Chattopadhyay et al., 2007).

It is widely accepted that folic acid preferentially rescues normal cells but does not rescue cancer cells; however, this selective rescue is not well elucidated. Leucovorin competes with MTX for DHFR binding sites allowing for enzyme reactivation and restoration of reduced folate stores preconditioned for DNA/RNA synthesis(Suh-Lailam et al., 2013). Intriguingly, in the present study We noticed that the simultaneous supplementation of folic acid and FBS inhibit the proliferation of HL-60 cells particularly in the first two days, same finding corroborated by testing MCF-7, which exhibit similar phenomenon, suggesting that it is not a cell type specific phenomenon. Consistently, it has been recently suggested that folic acid which works in similar way as folic acid that Folic acid and its metabolite 5-MTHF inhibit EGFR promoter activity in colon cancer cells by promoting and enhancing methylation of the promoter. This could partly be accounting for folic acid mediated inhibition of growth – related processes in colorectal neoplasia(Nagothu et al., 2004). Furthermore, it has been evidenced that folic acid governs and control IGF-1R gene expression in colon cancer cells via mechanism(s) involving transcriptional suppression of IGF-1R promoter(Attias et al., 2006).

The latter finding in harmony with concept that the chemopreventive functionalized via folic acid maybe linked to its capacity to inhibit IGF-1R levels. Below a certain IGF-1R threshold level. The capability of most cells to engage in mitogenic activity is significantly impaired(Rubini et al., 1997).

Global hypomethylation results in activation of oncogene, transposition of repetitive elements, chromosomal instability commonly observed in solid tumours. Among these hypomethylated sequences is c-Myc(Mani and Herceg, 2011). C-Myc, a proto-oncogene encodes a protein that regulates cellular proliferation and differentiation. Alteration in the stability of c-Myc mRNA may lead to overexpression of the gene, and eventually resulting in uncontrolled cell growth(Coulis et al., 2000). In the present study we abrogate the activity of c-Myc using anti- c-Myc inhibitor 10058-F4, has been known to preclude the dimerization of c-Myc to its client Max, and an a priori and inevitability suppression of cells proliferation and triggering of apoptosis. 10058-F4 has been found to be instrumental in inhibiting cell proliferation.it has been published that, c-Myc not only can increase the cell cycle regulators such as cyclin D1, cyclin D2, CDK4, but also can decrease the expression of p21 and p27(Roussel et al., 1995).. Importantly, it has been observed that, 10058-F4 arrests the cell cycle at (G0/G1 phase)and triggers apoptosis upon expanded treatment most probably by increasing cyclin dependent kinase inhibitor, p21WAF1 And decreasing cyclin D3 levels, additionally, 10058-F4 also remarkably decreases the Alpha- fetoprotein levels, an indicator for hepatocellular carcinoma(Lin et al., 2007). Furthermore, it has been shown that, 10058-F4 upregulate p21 via p53- independent. In accordance as HL-60 lacks p53(Huang et al., 2006). Also Zirath et al., (2013), have demonstrated that 10058-F4 inhibits MYCN signaling in NB cells, resulting in cell cycle arrest, apoptosis and/or differentiation as well as reduction of tumour growth in aggressive mouse models of NB. Interestingly We observed that Folinic acid administration could partially bypass and reverse the adverse effects of anti- c-Myc($p < 0.05$). possibly by reviving and restoring the growth capacity of c-Myc. It is well recognized that folinic acid is synthesized from 5,10-methenyltetrahydrofolate by both mitochondrial and cytoplasmic isoform SHMT(Stover and Schirch, 1990). Hypothesizing that folinic acid can functionalize and mimic same role as mSHMT. Intriguingly. It has been published that mSHMT was found to be capable of partial complementation of the growth defects of c-Myc null cells, accounting on its role as a major source for the biosynthesis of nucleotide and amino acids(Nikiforov et al., 2002),

Methotrexate(MTX) is one of the most powerful anticancer agent, especially for human leukemia. Moreover, it considered to kill cells in the S- phase by means of binding to irreversibly to the enzyme DHFR(Yamauchi et al., 2005). In the present study We used MTX to synchronize cells in S- phase however, by serendipity we use high doses of MTX, which results in the accumulation in G0/G1 implying that either freezing or apoptosis. Nevertheless few cell thanks to folinic acid traverse the S- phase, indicating that folinic acid in optimal doses could reverse the effect of MTX.

5- Conclusion and recommendations

Folinic acid is a powerful and indispensable drug. It is found to minimally reverse the adverse effects that triggered by UV irradiation, possibly by increasing the nucleotide pool. Importantly it acts as a double-edged sword in treating cancer cells, as it behaves synergistically by abrogating and inhibiting growth factor such as EGFR and IGF-1R. while in absence of growth factor it works differently as growth factor to cancer cells or by lowering the efficacy of anti- folate drug especially when administered in hyper physiologic doses. Additionally, folinic acid could partially revert and restore the growth activity of c-Myc deprived cell this could crucially impact the potential new regimen for the treatment of tumour driven by c-Myc.

Bibliography

Abella JV, & Park M (2009). Breakdown of endocytosis in the oncogenic activation of receptor tyrosine kinases. *American Journal of Physiology-Endocrinology And Metabolism*, 296(5), E973-E984.

Adams TE et al (2000) Structure and function of the type 1 insulin-like growth factor receptor. *Cell Mol Life Sci* 57(7):1050–1093

Adhikary S, Eilers M(2005). Transcriptional regulation and transformation by Myc proteins. *Nat Rev Mol Cell Biol*.6:635-45.

Alberts SR, Horvath WL, Sternfeld WC, et al(2005). Oxaliplatin, fluorouracil, and leucovorin for patients with unresectable liver-only metastases from colorectal cancer: a North Central Cancer Treatment Group Phase II Study. *J Clin Oncol*, 23:9243^9.

Aleksic T, Chitnis MM, Perestenko OV, Gao S, Thomas PH, Turner GD, Protheroe AS, Howarth M, Macaulay VM (2010). Type 1 insulin-like growth factor receptor translocates to the nucleus of human tumor cells. *Cancer Res*; 70:6412-9

Al-Mohanna MA, Al-Khodairy FM, Krezolek Z, Bertilsson PA, Al-Houssein KA, & Aboussekhra A (2001). p53 is dispensable for UV-induced cell cycle arrest at late G1 in mammalian cells. *Carcinogenesis*, 22(4), 573-578.

Amati B, Frank SR, Donjerkovic D, Taubert S(2001). Function of the c-Myc oncoprotein in chromatin remodeling and transcription, *Biochim. Biophys. Acta* 1471 (2001) M135–M145.

Ameisen JC(1994). Programmed cell death(apoptosis) and cell survival regulation: relevance to AIDS and cancer. *AIDS*.8:1197-1213.

Andersson S (2009). The many faces of IGF-1R from cell surface to the nucleus. Institutionen för onkologi-patologi/Department of Oncology-Pathology.

Angier R.B et al.,(1946). The Structure and Synthesis of the Liver *L. casei* factor. *Science*,1032683):p. 667 -669.

Appling DR(1991). *FASEB J.* 5, 2645–2651

Ashkenazi A, Dixit VM(1998). Death receptors: signaling and modulation. *Science*. ;281:1305–1308

Attias Z, Werner H, & Vaisman N (2006). Folic acid and its metabolites modulate IGF-I receptor gene expression in colon cancer cells in a p53-dependent manner. *Endocrine-related cancer*, 13(2), 571-581.

Bach LA, Fu P, & Yang Z (2013). Insulin-like growth factor-binding protein-6 and cancer. *Clinical Science*, 124(4), 215-229

Bach LA, Headey SJ and Norton RS (2005). IGF-binding proteins: the pieces are failing into place. *Trends Endocrinol. Metab.* 16, 228–234

Baggott J E (2000) *Biochemistry* 39, 14647–14653

Balk SD, LeStourgeon D, & Mitchell RS (1978). 5-methyltetrahydrofolic acid, 5-formyltetrahydrofolic acid (folinic acid), and folic acid requirements of normal and Rous sarcoma virus-infected chicken fibroblasts. *Cancer research*, 38(11 Part 1), 3966-3968.

Baserga R, Hongo A, Rubini M, Prisco M and Valentini B (1997). The IGF-I receptor in cell growth, transformation and apoptosis. *Biochimica et Biophysica Acta* 1332 F105–F126.

Bender FC, Reymond MA, Bron C, Quest AF (2000). Caveolin-1 levels are down-regulated in human colon tumors, and ectopic expression of caveolin-1 in colon carcinoma cell lines reduces cell tumorigenicity. *Cancer Res*;60:5870-8

Bennett A, Wilson DM, Liu F, et al (1983). Levels of insulin-like growth factors I and II in human cord blood. *J Clin Endocrinol Metab*; 57: 609–612.

Bertrand R, Beauchemin M, Dayan A, Ouimet M, Jolivet J (1995)*Biochim. Biophys. Acta* 1266, 245- 249

Bohula EA, Playford MP & Macaulay VM (2003). Targeting the type 1 insulin-like growth factor receptor as anticancer treatment. *Anticancer Drugs* 14 669–682.

Botz J, Zerfass-Thome K, Spitkovsky D, et al (1996). Cell cycle regulation of the murine cyclin E gene depends on an E2F binding site in the promoter. *Mol Cell Biol* 16:3401-3409

Branda RF and Blickensderfer DB (1993). Folate deficiency increases genetic damage caused by alkylating agents and γ -irradiation in Chinese hamster ovary cells, *Cancer Res.*, 53, 5401-5408.

Brazil DP, Yang ZZ and Hemmings BA (2004). Advances in protein kinase B signalling: AKTion on multiple fronts. *Trends in Biochemical Sciences* 29 233–242

Cassidy J, Tabernero J, Twelves C (2004). et al. XELOX (capecitabine plus oxaliplatin): active first-line therapy for patients with metastatic colorectal cancer. *J Clin Oncol* 2004;22:2084-91.

Chambers AF, Matrisian LM (1997) Changing views of the role of matrix metalloproteinase in metastasis. *J Natl Cancer Inst* 89: 1260–1270.

Chan KL, Guan XY, Ng IO (2004). High-throughput tissue microarray analysis of c-myc activation in chronic liver diseases and hepatocellular carcinoma. *Hum Pathol*; 35: 1324-1331

Chandarlapaty S, Sawai A, Scaltriti M, et al (2011). AKT inhibition relieves feedback suppression of receptor tyrosine kinase expression and activity. *Cancer Cell*; 19: 58-71.

Chattopadhyay S, Tamari R, Min SH, Zhao R, Tsai E, & Goldman ID (2007). Commentary: a case for minimizing folate supplementation in clinical regimens with pemetrexed based on the marked sensitivity of the drug to folate availability. *The oncologist*, 12(7), 808-815.

Chello PL, & Bertino JR (1973). Dependence of 5-methyltetrahydrofolate utilization by L5178Y murine leukemia cells in vitro on the presence of hydroxocobalamin and transcobalamin II. *Cancer research*, 33(8), 1898-1904.

Chen YNP, Sharma SK, Ramsey TM, et al(1999). Selective killing of transformed cells by cyclin/cyclin- dependent cyclin kinases 2 antagonists. *Proc Natl Acad Sci U S A* 96:4325-4329

Chen YW, Boyartchuk V, & Lewis BC (2009). Differential roles of insulin-like growth factor receptor-and insulin receptor-mediated signaling in the phenotypes of hepatocellular carcinoma cells. *Neoplasia* (New York, NY), 11(9), 835

Chiba T, Ochiai A (2004). Matrix metalloproteinase-7 facilitates insulin-like growth factor bioavailability through its proteinase activity on insulin-like growth factor binding protein 3. *Cancer Research*, Vol. 64, pp. 665-671, ISSN 0008-5472

Choi SW, Kim YI, Weitzel JN, and Mason JB (1998). Folate depletion impairs DNA excision repair in the colon of the rat. *Gut*, 43: 93–99.

Clemmons DR (1998). Role of insulin-like growth factor binding proteins in controlling IGF actions. *Mol Cell Endocrinol* 140(1-2): 19-24.

Cohen JJ (1991). Programmed cell death in the immune system. *Adv. Immunol.* 50:55-85.

Collins SJ, Gallo RC, and Galloagher RE (1977). Continuous growth and differentiation of myeloid leukaemic human cells in suspension culture. *Nature, Lond* 270, 347-349.

Couet J, Li S, Okamoto T, Ikezu T, Lisanti MP (1997). Identification of peptide and protein ligands for the caveolin-scaffolding domain. Implications for the interaction of caveolin with caveolae-associated proteins, *J. Biol. Chem.* 272 6525–6533

Coulis CM, Lee C, Nardone V, & Prokipcak RD (2000). Inhibition of c-myc expression in cells by targeting an RNA-protein interaction using antisense oligonucleotides. *Molecular pharmacology*, 57(3), 485-494

Courtemanche C, Elson-Schwab I, Mashiyama ST, Kerry N, & Ames BN (2004). Folate deficiency inhibits the proliferation of primary human CD8+ T lymphocytes in vitro. *The Journal of Immunology*, 173(5), 3186-3192.

Cowin GJ, Willgoss DA, Bartley J, Endre ZH(1996) *Biochim.Biophys. Acta* 1310, 32- 40

Croxtton R, Ma Y, Song L, et al(2002). Direct repression of the Mcl-1 promoter by E2F1. *Oncogene* 21:1359-1369

Cuatrecasas M, et al (2011). Expression patterns of p-IGF-1R and assessment of p-IGF-1R and MMP7 positive expression as predictive marker of chemo-resistance in wild type K-RAS metastatic colorectal carcinoma treated with panitumumab and mFOLFOX6. The PULSE trial. European Pathology Congress

Dang CV (1999). c-Myc target genes involved in cell growth, apoptosis and metabolism. *Mol Cell Biol*;19:1–11.

Danial NN, & Korsmeyer SJ (2004). Cell death: critical control points. *Cell*, 116(2), 205-219.

Dawkins RL, & Zilko PJ (1975). Separation of cells involved in phytohaemagglutinin-induced mitogenesis and cytotoxicity.

de Laurentiis A, Donovan, L, Arcaro A (2007). Lipid rafts and caveolae in signaling by growth factor receptors. *The open biochemistry journal*, 1, 12.

Debnath J, Baehrecke EH, and Kroemer G (2005). Does autophagy contribute to cell death? *Autophagy* 1, 66-74.

Denault JB and Salvesen GS (2002). "Caspases: keys in the ignition of cell death." *Chem Rev* 102(12): 4489-500.

Deng H, Lin Y, Badin M, Vasilcanu D, Strömberg T, Jernberg-Wiklund H, ... & Larsson O (2011). Over-accumulation of nuclear IGF-1 receptor in tumor cells requires elevated expression of the receptor and the SUMO-conjugating enzyme Ubc9. *Biochemical and biophysical research communications*, 404(2), 667-671.

Desoize B, Madoulet C (2002) Particular aspects of platinum compounds used at present in cancer treatment. *Crit Rev Oncol Hematol* 42:317

Doherty GJ, McMahon HT (2009) Mechanisms of endocytosis. *Annu Rev Biochem* 78: 857-902

Donnelly JG (2001). *Crit. Rev. Clin. Lab. Sci.*, 38, 183- 223.

Dunkern TR. & Kaina B (2002). Cell proliferation and DNA breaks are involved in ultraviolet light-induced apoptosis in nucleotide excision repair-deficient Chinese hamster cells. *Molecular biology of the cell*, 13(1), 348-361.

Dynlacht BD, Flores O, Lees JA, et al (1994). Differential regulation of E2F transactivation by cyclin^{cdk2} complexes. *Genes Dev* 8:1772-1786

Earnshaw WC, Martins LM and Kaufmann SH (1999). "Mammalian caspases: structure, activation, substrates, and functions during apoptosis." *Annu Rev Biochem* 68: 383-424.

Eilers M, Eisenman RN (2008). Myc's broad reach. *Genes Dev.* 2008;22: 2755-66.

El Ghissassi F, Baan R, Straif K, Grosse Y, Secretan B, Bouvard V, Benbrahim-Tallaa L, Guha N., Freeman C, Galichet L. et al. (2009) A review of human carcinogens? Part D: radiation. *Lancet Oncol.*, 10, 751–752.

Eng C, Van Cutsem E, Nowara E, et al (2011). A randomized, phase Ib/II trial of rilotumumab (AMG102;ril) or ganitumab (AMG479;gan) with panitumumab (pmab) versus pmab alone in patients (pts) with wild-type (WT) KRAS metastatic colorectal cancer (mCRC): primary and biomarker analyses. *ASCO Proc* 3500.

Fernandez PC, Frank SR, Wang L, Schroeder M, Liu S, Greene J, Cocito A, Amati B (2003). Genomic targets of the human c-Myc protein. *Genes Dev.* 17:1115-29.

Fielding CJ, Bist A, Fielding PE (1997). *Proc. Natl. Acad. Sci., USA*, 1997, 94, 3753-8.

Fischer U, Jänicke RU, & Schulze-Osthoff K (2003). Many cuts to ruin: a comprehensive update of caspase substrates. *Cell Death & Differentiation*, 10(1), 76-100.

Formigli L, Papucci L, Tani A, Schiavone N, Tempestini A, Orlandini GE, Capaccioli S, and Orlandini S.Z (2000). Aponecrosis; morphological and biochemical exploration of a syncretic process of cell death sharing apoptosis and necrosis. *J Cell Physiol* 182, 41-9.

Foti M, Moukil MA, Dudognon P, Carpentier JL (2004). Insulin and IGF-1 receptor trafficking and signalling. Novartis Foundation Symposium 262 125–141.

Fowlkes JL, Enghild JJ, Suzuki K, and Nagase H (1994). Matrix metalloproteinases degrade insulin-like growth factor-binding protein-3 in dermal fibroblast cultures. *J. Biol. Chem.* 269:25742–25746.

Fowlkes JL, Suzuki K, Nagase H, and Thrailkill KM (1994). Proteolysis of insulin-like growth factor binding protein-3 during rat pregnancy: a role for matrix metalloproteinases. *Endocrinology* 135:2810–2813.

French AR, Tadaki DK, Niyogi SK, Lauffenburger DA (1995). Intracellular trafficking of epidermal growth factor family ligands is directly influenced by the pH sensitivity of the receptor/ligand interaction. *J Biol Chem* 270: 4334–4340, 1995.

Friesen C, Herr I, Krammer PH and Debatin KM (1996). Involvement of the CD95(APO-1/Fas) receptor/ ligand system in drug induced apoptosis in leukemia cells. *Nat.*2:574-577.

Fürstenberger G and Senn HJ (2002). Insulin-like growth factors and cancer. *Lancet Oncol*; 3: 298–302.

Gallego R, Codony-Servat J, García-Albéniz X, Carcereny E, Longarón R, Oliveras A, Tosca M, Augé JM, Gascón P, Maurel J (2009). Serum IGF-I, IGFBP-3 and MMP-7 levels and acquired chemo-resistance in advanced colorectal cancer. *Endocr Relat Cancer*;16:311-7

Gareau JR, & Lima CD (2010). The SUMO pathway: emerging mechanisms that shape specificity, conjugation and recognition. *Nature Reviews Molecular Cell Biology*, 11(12), 861-871.

Gauguin L, Klaproth B, Sajid W, et al (2008). Structural basis for the lower affinity of the insulin-like growth factors for the insulin receptor. *J Biol Chem*; 283: 2604–2613.

Gehri R, Hahn S, Rothenm M, Steuerwald M, Nuesch R, and Erb P(1996). The Fas receptor in HIV infection: expression on peripheral blood lymphocytes and role in the depletion of T cells. *AIDS*. 10:9-16.

Geng Y, Eaton EN, Picon M, et al (1996). Regulation of cyclin E transcription by E2Fs and retinoblastoma protein. *Oncogene* 12:1173-1180

Gentile M, Latonen L, & Laiho M (2003). Cell cycle arrest and apoptosis provoked by UV radiation-induced DNA damage are transcriptionally highly divergent responses. *Nucleic acids research*, 31(16), 4779-4790.

Girgis S, Suh JR, Jolivet J, & Stover PJ (1997). 5-Formyltetrahydrofolate regulates homocysteine remethylation in human neuroblastoma. *Journal of Biological Chemistry*, 272(8), 4729-4734.

Girnita L, Worrall C, Takahashi SI, Seregard S, & Girnita A (2013). Something old, something new and something borrowed: emerging paradigm of insulin-like growth factor type 1 receptor (IGF-1R) signaling regulation. *Cellular and Molecular Life Sciences*, 1-25.

Golan DE, Tashjian AH, & Armstrong EJ (Eds.). (2011). Principles of pharmacology: the pathophysiologic basis of drug therapy. Lippincott Williams & Wilkins.

Gorman AM, Orrenius S, & Ceccatelli S (1998). Apoptosis in neuronal cells: role of caspases. *Neuroreport*, 9(10), R49-R55.

Gourdier I, Del Rio M, Crabbé L, Candeil L, Copois V, Ychou M, ... & Pau B (2002). Drug specific resistance to oxaliplatin is associated with apoptosis defect in a cellular model of colon carcinoma. *FEBS letters*, 529(2), 232-236.

Grandori C, Cowley SM, James L.P, Eisenman RN (2000). The Myc/ Max/Mad network and the transcriptional control of cell behavior, Max/Mad network and the transcriptional control of cell behavior, *Annu. Rev. Cell. Dev. Biol.* 16: 653–699.

Green JM, Ballou DP, Matthews RG (1988). Examination of the role of methylenetetrahydrofolate reductase incorporation of methyltetrahydrofolate into cellular metabolism. *Faseb J*, 2(1): p. 42-7.

Gropper S, Smith J, and Groff J (2005). Advanced nutrition and human metabolism. Fourth ed.: Thomson Wadworth.

Guix M, Faber AC, Wang SE, Olivares MG, Song Y, Qu S, Rinehart C, Seidel B, Yee D, Arteaga CL, Engelman JA (2008). Acquired resistance to EGFR tyrosine kinase inhibitors in cancer cells is mediated by loss of IGF-binding proteins. *J Clin Invest*; 118:2609-19

Guo Y, Srinivasula SM, Druilhe A, Fernandes- Alnemri T, Alnemri ES (2002). Caspase-2 induces apoptosis by releasing proapoptotic proteins from mitochondria. *J Biol Chem*;277:13430-7.

Gupta S (2000). Molecular steps of cell suicide: An insight into immune senescence. *J Clin Immunol*, 20, 229-39.

Hacker G (2000). The morphology of apoptosis. *Cell Tissue Res* 301, 5–17.

Hall M, Peters G (1996). Genetic alterations of cyclins, cyclin-dependent kinases, and cdk inhibitors in human cancer. *Adv Cancer Res* 68:67-108

Harbour JW, Dean DC (2000). The Rb/E2F pathway: Expanding roles and emerging paradigms. *Genes Dev* 14:2393-2409

Harbour JW, Luo RX, Santi AD, Postigo AA, & Dean DC (1999). Cdk phosphorylation triggers sequential intramolecular interactions that progressively block Rb functions as cells move through G1. *Cell*, 98(6), 859-869.

Harper JW, Elledge SJ (1998). The role of Cdk7 in CAK function, a retro- retrospective, *Genes Dev* 12: 285- 289

Hartwell L (1992). Defects in a cell cycle checkpoint may be responsible for the genomic instability of cancer cells. *Cell*, 71:543–546

Heald AH, Kaushal K, Siddals KW, Rudenski AS, Anderson SG, Gibson JM (2006). Insulin-like growth factor binding protein-2(IGFBP-2) is a marker for the metabolic syndrome. *Exp Clin Endocrinol Diabetes* 114(7): 371-6.

Hellawell GO, Turner GD, Davies DR, Poulosom R, Brewster SF & Macaulay VM (2002). Expression of the type 1 insulin-like growth factor receptor is up-regulated in primary prostate cancer and commonly persists in metastatic disease. *Cancer Research* 62 2942–2950.

Hengartner MO (1997). Programmed Cell Death. In: *C. elegans* II. Riddle, DL. Et al. eds. 383-496.(Cold Spring Harbor Laboratory Press, Plainview, N.Y)

Hengartner MO (1999). "Programmed cell death in the nematode *C. elegans*." *Recent Prog Horm Res* 54: 213-22; discussion 222-4

Hengst L, Dulic V, Slingerland JM, Lees E, Reed SI (1994). A cell cycle regulated inhibitor of cyclin- dependent kinases. *Proc Natl Acad Sci USA*, 91: 5291- 5295

Hoffman B, Amanullah A, Shafarenko M, Liebermann DA (2002). The protooncogene c-myc in hematopoietic development and leukemogenesis. *Oncogene*.;21:3414-21.

Holmes WB, & Appling DR (2002). Cloning and characterization of methenyltetrahydrofolate synthetase from *Saccharomyces cerevisiae*. *Journal of Biological Chemistry*, 277(23), 20205-20213.

Hörndler C, Gallego R, García-Albeniz X, Alonso-Espinaco V, Alonso V, Escudero P, Jimeno M, Ortego J, Codony-Servat J, Fernández-Martos C, Calatrava A, Marín-Aguilera M, Muñoz J, Castellví-Bel S, Castells A, Rubini M, Gascón P, Maurel J (2011). Co-expression of matrix metalloproteinase-7 (MMP-7) and phosphorylated insulin growth factor receptor I (pIGF-1R) correlates with poor prognosis in patients with wild-type KRAS treated with cetuximab or panitumumab: A GEMCAD study. *Cancer Biol Ther*;11:177-183.

Horvitz HR (1999). Genetic control of programmed cell death in the nematode *Caenorhabditis elegans*. *Cancer Res* 59, 1701-1706s.

Howard A, Pelc SR (1953). Synthesis of deoxyribonucleic acid in normal and irradiated cells and its relation to chromosome breakage. *Heridity*, 6(Suppl): 261- 273

Huang MJ, Cheng YC, Liu CR, Lin S, Liu HE. (2006). A small-molecule c-Myc inhibitor, 10058-F4, induces cell-cycle arrest, apoptosis, and myeloid differentiation of human acute myeloid leukemia. *Experimental hematology*, 34(11), 1480-1489

Huang RP, Wu JX, Fan Y, & Adamson ED (1996). UV activates growth factor receptors via reactive oxygen intermediates. *The Journal of cell biology*, 133(1), 211-220.

Ichihashi M, Ueda M, Budiyanoto A, Bito T, Oka M, Fukunaga M, ... & Horikawa T (2003). UV-induced skin damage. *Toxicology*, 189(1), 21-39.

Ifergan I, Jansen G, Assaraf, YG (2008). The reduced folate carrier(RFC) is cytotoxic to cells under conditions of severe folate deprivation. RFC as a double edged sword in folate homeostasis. *J Biol Chem*, 283(30): p. 20687- 95.

Ishizaki Y, Cheng L, Mudge AW and Raff MC (1995). "Programmed cell death by default in embryonic cells, fibroblasts, and cancer cells." *Mol Biol Cell* 6(11): 1443-58.

Jacobson MD, Weil M, and Raff MC (1997). Programmed cell death in animal development. *Cell*.88::347-354.

Jensen M , De Meyts P (2009). Molecular mechanisms of differential intracellular signaling from the insulin receptor. *Vitamins and Hormones* 80 51–75. (doi:10.1016/S0083-6729(08)00603-1)

Jiang H, Chou HS, Zhu L (1998). Requirement of cyclin E-cdk2 inhibition in p16INK4a-mediated growth suppression. *Mol Cell Biol* 18:5284-5290

Jiang X, Wang X (2004). Cytochrome C-mediated apoptosis. *Annu Rev Biochem*;73:87-106.

Jo MC (2005). Ultraviolet (UV) Radiation Safety. Environmental Health and Safety University of Nevada Reno, pp. 3

Kamen B (1997) Folate and antifolate pharmacology. *Semin. Oncol.*, 24, S18—S30; S39.

Kerr JFR, Winterford CM, and Harmon BV (1994). Apoptosis: its significance in cancer and cancer therapy. *Cancer*. 73:2013-2026. in cancer and cancer therapy. *Cancer*. 73:2013-2026.

Kerr JF (2002). History of the events leading to the formulation of the apoptosis concept. *Toxicology* 181- 182, 471-4.

Kerr JF, Wyllie AH, and Currie AR (1972). Apoptosis: a basic biological phenomenon with wide ranging implications in tissue kinetics. *Br J Cancer* 26, 239-57.

Keshava C, Nagalakshmi R, Ong T, & Nath J (1996). Inhibitory effect of folic acid on radiation-induced micronuclei and chromosomal aberrations in V79 cells. *Mutation Research/Fundamental and Molecular Mechanisms of Mutagenesis*, 352(1), 123-134.

Khandwala HM, McCutcheon IE, Flyvbjerg A & Friend KE (2000). The effects of insulin-like growth factors on tumorigenesis and neoplastic growth. *Endocrine Reviews* 21 215–244.

Kim YI (2007). Folate and colorectal cancer: an evidence-based critical review. *Mol Nutr Food Res*, 51(3): p. 267-92.

- Kitagawa M**, Higashi H, Suzuki-Takahashi I, et al (1995). Phosphorylation of E2F-1 by cyclin A-cdk2. *Oncogene* 10:229-236
- Kompis IM**, Islam K, Then, RL (2005). DNA and RNA synthesis: antifolates. *Chem Rev*, 105(2): p. 593- 620.
- Krek W**, Ewen ME, Shirodkar S, et al (1994). Negative regulation of the growth-promoting transcription factor E2F-1 by a stably bound cyclin A-dependent protein kinase. *Cell* 78:161-172
- Kulik G**, Weber MJ (1998). Akt-dependent and -independent survival signaling pathways utilized by Insulin-Like growth factor I. *Mol Cell Biol*; 18:6711-6718
- Kusiak JW**, Izzo JA, and Zhao B (1996). Neurodegeneration in Alzheimer disease. Is apoptosis involved? *Mol. Chem. Neuropathol.*28:153-162.
- Lassus P**, Opitz-Araya X, Lazebnik Y (2002). Requirement for caspase-2 in stress-induced apoptosis before mitochondrial permeabilization. *Science*;297: 1352-4.
- Latonen L**, Taya Y. and Laiho M (2001) UV-radiation induces dose dependent regulation of p53 response and modulates p53-HDM2 interaction in human fibroblasts. *Oncogene*, 20, 6784-6793.
- Lee H**, Volonte D, Galbiati F, Iyengar P, Lublin DM, Bregman DB , ... & Lisanti MP (2000). Constitutive and growth factor-regulated phosphorylation of caveolin-1 occurs at the same site (Tyr-14) in vivo: identification of a c-Src/Cav-1/Grb7 signaling cassette. *Molecular Endocrinology*, 14(11), 1750-1775.
- Leist M** and Jäättelä M (2001). Four deaths and a funeral: From caspases to alternative mechanisms. *Nat. Rev. Mol. Cell Biol.*2, 589-98
- Levens DL** (2003). Reconstructing MYC. *Genes Dev*, 17:1071-7.
- Li J**, & Yuan J (2008). Caspases in apoptosis and beyond. *Oncogene*, 27(48), 6194-6206.
- Li S**, Couet J, Lisanti MP (1996). Src tyrosine kinases, Ga subunits, and H-Ras share a common membrane-anchored scaffolding protein, caveolin. Caveolin binding negatively regulates the auto-activation of Src tyrosine kinases, *J. Biol. Chem.* 271, 29182–29190.

Lin CP, Liu JD, Chow JM, Liu CR, & Liu HE (2007). Small-molecule c-Myc inhibitor, 10058-F4, inhibits proliferation, downregulates human telomerase reverse transcriptase and enhances chemosensitivity in human hepatocellular carcinoma cells. *Anti-cancer drugs*, 18(2), 161-170.

Lindahl T, Wood RD (1999). Quality control by DNA repair. *Science*, 286:1897–1905.

Liu JP, Baker J, Perkins AS, Robertson EJ & Efstratiadis A(1993). Mice carrying null mutations of the genes encoding insulin-like growth factor I (Igf-1) and type 1 IGF receptor (Igf1r). *Cell* 75 59–72.

Ljungman M, Zhang F, Chen F, Rainbow AJ, & McKay BC (1999). Inhibition of RNA polymerase II as a trigger for the p53 response. *Oncogene*, 18(3).

Lomeli H, & Vázquez M (2011). Emerging roles of the SUMO pathway in development. *Cellular and Molecular Life Sciences*, 68(24), 4045-4064.

Lu ML, Sato M, Cao B, & Richie JP (1996). UV irradiation-induced apoptosis leads to activation of a 36-kDa myelin basic protein kinase in HL-60 cells. *Proceedings of the National Academy of Sciences*, 93(17), 8977-8982

Lucock M (2000). Folic acid: nutritional biochemistry, molecular biology, and role in disease processes. *Mol Genet Metab*, 71(1-2): p. 121- 38.

Lundberg AS, Weinberg RA (1998). Functional inactivation of the retinoblastoma protein requires sequential modification by at least two distinct cyclin-cdk complexes. *Mol Cell Biol*, 18:753-761

Lüscher B, Larsson LG (1999). The basic region/helix-loop-helix/leucine zipper domain of Myc proto-oncoproteins: function and regulation. *Oncogene*, 18:2955-2966.

Maggi D, Biedi, C, Segat, D, Barbero D, Panetta D, Cordera R (2002). IGF-I induces caveolin 1 tyrosine phosphorylation and translocation in the lipid rafts. *Biochemical and biophysical research communications*, 295(5), 1085-1089.

Mani S, & Herceg Z (2011). DNA Methylation Changes in Cancer. *Epigenetics: A Reference Manual*, 195

- Maras** B, Stover P, Valiante S, Barra D, Schirch V (1994) *J. Biol.Chem.* 269, 18429- 18433
- Martin** SJ, Cotter TG (1991). Ultraviolet B irradiation of human leukemia HL-60 cells in vitro induces apoptosis. *Int. J. Radiat. Biol.* 59, 1001–1016.
- Martins** AS, Ordo'n~ ez JL, Amaral AT, Prins F, Floris G, et al. (2011) IGF1R Signaling in Ewing Sarcoma Is Shaped by Clathrin-/Caveolin-Dependent Endocytosis. *PLoS ONE* 6(5): e19846. doi:10.1371/journal.pone.0019846
- Mateyak** MK, Obaya AJ, Adachi S, Sedivy JM (1997). Phenotype of c-Myc- deficient Rat Fibroblasts isolated by targeted homologous recombination. *Cell growth and differentiation*(8): 1039- 1048
- Matthews** RG, Baugh CM (1980). Interactions of pig liver methylenetetrahydrofolate reductase with methylenetetrahydropteroylpolyglutamate substrates and with dihydropteroylpolyglutamate inhibitors. *Biochemistry*, 19(10): p. 2040-5
- Meinhart** A, Kamenski T, Hoepfner S, et al (2005). A perspective of CTD function. *Genes Dev structural*, 19:1401-1415
- Melisi** D, Troiani T, Damiano V, Tortora G and Ciardiello F (2004). Therapeutic integration of signal transduction targeting agents and conventional anticancer treatments. *Endocr Relat Cancer* 11: 51-68
- Meyerhardt** JA, Mayer RJ (2005). Systemic therapy for colorectal cancer. *NEngl JMed* ,352:476-87.
- Meyerson** M, Enders GH, Wu CL, et al (1992). A family of human cdc2- related protein kinases. *EMBOJ*, 11: 2909- 2917
- Mishima** M, Samimi G, Kondo A, Lin X, & Howell SB (2002). The cellular pharmacology of oxaliplatin resistance. *European Journal of Cancer*, 38(10), 1405-1412.
- Mitchell** HK, Snell EE, Williams R.J (1941). The Concentration of "Folic Acid". *Journal of the American Chemical Society*, 63: p. 2284.

Miyamoto S, Yano K, Sugimoto S, Ishii G, Hasebe T, Endoh Y, et al (2004). Matrix metalloproteinase-7 facilitates insulin-like growth factor bioavailability through its proteinase activity on insulin-like growth factor binding protein 3. *Cancer Res*; 64, 665-671.

Mohankumar MN, Paul SF, Venkatachalam P, & Jeevanram RK (1998). Influence of in vitro low-level gamma-radiation on the UV-induced DNA repair capacity of human lymphocytes—analysed by unscheduled DNA synthesis (UDS) and comet assay. *Radiation and environmental biophysics*, 37(4), 267-275.

Moschos SJ & Mantzoros CS (2002). The role of the IGF system in cancer: from basic to clinical studies and clinical applications. *Oncology* 63 317–332.

Mukherjee S, Tessema M and Wandinger-Ness A (2006). Vesicular trafficking of tyrosine kinase receptors and associated proteins in the regulation of signaling and vascular function. *Circulation research*, 98(6), 743-756

Murray AW (1992). Creative blocks: cell-cycle checkpoints and feedback controls. *Nature*, 359:599–604

Nagothu KK, Rishi AK, Jaszewski R, Kucuk O, & Majumdar AP (2004). Folic acid-mediated inhibition of serum-induced activation of EGFR promoter in colon cancer cells. *American Journal of Physiology-Gastrointestinal and Liver Physiology*, 287(3), G541-G546

Narkewicz MR, Sauls S D, Tjoa SS, Fennessey PV(1996). *Biochem. J.* 313,991-996

Nicholson DW (1999). Caspase structure, proteolytic substrates, and function during apoptotic cell death. *Cell Death Differ*; 6:1028– 1042.

Nicholson DW, Thornberry NA (1997). Caspases: Killer proteases. *Trends Biochem Sci*, 22, 299-306.

Nielsen CH, Albertsen L, Bendtzen K, & Baslund B (2007). Methotrexate induces poly (ADP-ribose) polymerase-dependent, caspase 3-independent apoptosis in subsets of proliferating CD4+ T cells. *Clinical & Experimental Immunology*, 148(2), 288-295.

Nikiforov MA, Chandriani, S, O'Connell B, Petrenko O, Kotenko I, Beavis A, ... & Cole MD (2002). A functional screen for Myc-responsive genes reveals serine

hydroxymethyltransferase, a major source of the one-carbon unit for cell metabolism. *Molecular and cellular biology*, 22(16), 5793-580

Nolan CM, Kyle JW, Watanabe H and Sly WS (1990). Binding of insulin-like growth factor II (IGF-II) by human cation-independent mannose 6-phosphate receptor/IGF-II receptor expressed in receptor-deficient mouse L cells. *Cellular Regulation* 1 197–213.

Pahlavani MA, & Vargas DA (2001). Activation-induced apoptosis in T cells: effect of age and caloric restriction. *Iranian Biomedical Journal*, 5(1), 1-9.

Palancade B, Bensaude O (2003). Investigating RNA polymerase II carboxyl-terminal domain (CTD) phosphorylation *Eur J Biochem* 270:3859-3870

Panetta D, Biedi C, Repetto S, Cordera R, & Maggi D (2004). IGF-I regulates caveolin 1 and IRS1 interaction in caveolae. *Biochemical and biophysical research communications*, 316(1), 240-243.

Paweletz N (2001). Walther Flemming: pioneer of mitosis research. *Nat Rev Mol Cell Biol* 2,72-5.

Pelley RJ (2001). Oxaliplatin: a new agent for colorectal cancer. *Current oncology reports*, 3(2), 147-155.

Peruzzi F, Prisco M, Dews M, Salomoni P, Grassilli E, Romano G, Calabretta Band Baserga R (1999). Multiple signaling pathways of the insulin-like growth factor 1 receptor in protection from apoptosis. *Molecular and Cellular Biology* 19 7203–7215.

Phillips A, Ernst M, Bates S, et al (1999). E2F-1 potentiates cell death by blocking antiapoptotic signaling pathways. *Mol Cell* 4:771-781

Phillips AC, & Vousden KH (2001). E2F-1 induced apoptosis. *Apoptosis*, 6(3), 173-182.

Pines J (1991). Cyclins: wheels within wheels. *Cell growth & differentiation: the molecular biology journal of the American Association for Cancer Research*, 2(6), 305-310.

Pirkmajer S, & Chibalin AV (2011). Serum starvation: caveat emptor. *American Journal of Physiology-Cell Physiology*, 301(2), C272-C279.

Playford MP, Bicknell D, Bodmer WF and Macaulay VM (2000). Insulin-like growth factor 1 regulates the location stability, and transcriptional activity of beta-catenin. *PNAS* 97 12103–12108.

Pollak MN, Schernhammer ES & Hankinson SE (2004). Insulin-like growth factors and neoplasia. *Nature Reviews. Cancer* 4 505–518.

Prelich G (2002). RNA polymerase II carboxy terminal domain kinases: Emerging clues to their function. *Eukaryot Cell* 1: 153- 162

Ravid D, Maor S, Werner H, Liscovitch M (2005). Caveolin-1 inhibits cell detachment-induced p53 activation and anoikis by upregulation of insulin-like growth factor-I receptors and signaling. *Oncogene*;24:1338-47-

Razani B, Woodman SE, Lisanti (2002). MP Caveolae: from cell biology to animal physiology, *Pharmacol. Rev.* 54 431–467.

Reed SI (1992). The role of p34 kinases in the G1 to S-phase transition. *Annu Rev Cell Biol*, 8: 529- 561

Reed SI, Bailly E, Dulic, V, Hengst L, Resnitzky D, Slingerland J (1994). G1 control in mammalian cells. *J Cell Sci* 1994, 18:69–73

Reidy DL, Vakiani E, Fakhri MG, Saif MW, Hecht JR, Goodman-Davis N, et al (2010). Randomized, phase II study of the insulin-like growth factor-1 receptor inhibitor IMC-A12, with or without cetuximab, in patients with cetuximab- or panitumumab-refractory metastatic colorectal cancer. *J Clin Oncol*; 28:4240-6.

Reiss K, Wang JY, Romano G, Furnari FB, Cavenee WK, Morrione A, Tu X and Baserga R (2000). IGF-I receptor signaling in a prostatic cancer cell line with a PTEN mutation. *Oncogene* 19 2687–2694.

Remacle-Bonnet MM, Garrouste FL, Heller S, André F, Marvaldi JL, Pommier GJ (2007). Insulin-like growth factor-I protects colon cancer cells from death factor-induced apoptosis by potentiating tumor necrosis factor alpha-induced mitogen-activated protein kinase and nuclear factor kappaB signaling pathways. *Cancer Res*; 60:2007-

- Renneville A**, Roumier C, Biggio V, et al (2008). Cooperating gene mutations in acute myeloid leukemia: a review of the literature. *Leukemia*.;22:915-31.
- Richardson H** and Kumar S(2002). "Death to flies: Drosophila as a model system to study programmed cell death." *J Immunol Methods* 265(1-2): 21-38
- Roje S**, Janave MT, Ziemak M J, Hanson AD (2002). *J. Biol. Chem.*277, 42748- 42754.
- Romanelli RJ**, LeBeau AP, Fulmer CG, Lazzarino DA, Hochberg A, Wood TL (2007). Insulin-like Growth Factor Type-I Receptor Internalization and Recycling Mediate the Sustained Phosphorylation of Akt. *J. Biol. Chem.* 282:22513-22524. doi: 10.1074/jbc.M704309200
- Roussel MF**, Theodoras AM, Pagano M, Sherr CJ (1995). Rescue of defective mitogenic signaling by D-type cyclins. *Proc Natl Acad Sci U S A*;92:6837–6841.
- Rubini M**, D'Ambrosio C, Carturan S, Yumet G, Catalano E, Shan S, ... & Baserga R (1999). Characterization of an antibody that can detect an activated IGF-I receptor in human cancers. *Experimental cell research*, 251(1), 22-32.
- Rubini M**, Hongo A, D'Ambrosio C & Baserga R (1997). The IGF-I receptor in mitogenesis and transformation of mouse embryo cells: role of receptor number. *Experimental Cell Research* 230 284 292.
- Saeki K**, Yuo A, Okuma E, Yazaki Y, Susin SA, Kroemer G, & Takaku F (2000). Bcl-2 down-regulation causes autophagy in a caspase-independent manner in human leukemic HL60 cells. *Cell Death & Differentiation*, 7(12).
- Salani B**, Passalacqua M, Maffioli S, Briatore L, Hamoudane M, et al (2010). IGF-IR Internalizes with Caveolin-1 and PTRF/Cavin in Hacat Cells. *PLoS ONE* 5(11): e14157. doi:10.1371/journal.pone.0014157
- Salucci S**, Burattini S, Battistelli M, Baldassarri V, Maltarello MC, & Falcieri E (2012). Ultraviolet B (UVB) Irradiation-Induced Apoptosis in Various Cell Lineages in Vitro. *International journal of molecular sciences*, 14(1), 532-546.
- Salvesen GS** and Rønsbo M (2002). "Apoptosome: the seven-spoked death machine." *Dev Cell* 2(3): 256-7.

- Sancar** A, Lindsey-Boltz LA, Ünsal-Kaçmaz K, & Linn S (2004). Molecular mechanisms of mammalian DNA repair and the DNA damage checkpoints. *Annual review of biochemistry*, 73(1), 39-85.
- Saraste** A and Pulkki K (2000). "Morphologic and biochemical hallmarks of apoptosis." *Cardiovasc Res* 45(3): 528-37.
- Sartorius** U, Schmitz I and Krammer PH (2001). "Molecular mechanisms of death-receptor-mediated apoptosis." *Chembiochem* 2(1): 20-9.
- Sausville** EA (2002). Complexities in the development of cyclin- dependent kinase inhibitor drugs. *Trends Mol Med*8: S32- S37
- Scheving** LE (1984). Chronobiology of cell proliferation in mammals: implications for basic research and cancer chemotherapy. *Cell cycle clocks*, 455-500.
- Schmidt** W, Chaney SG (1993). Role of carrier ligand in platinum resistance of human carcinoma cell lines. *Cancer Res*, 53:799–805.
- Sciacca** L, Mineo R, Pandini G, Murabito A, Vigneri R, & Belfiore A (2002). In IGF-I receptor-deficient leiomyosarcoma cells autocrine IGF-II induces cell invasion and protection from apoptosis via the insulin receptor isoform A. *Oncogene*, 21(54)
- Sehat** B (2007). SUMO and ubiquitin: The Yin and Yang of IGF-1R function. Institutionen för onkologi-patologi/Department of Oncology-Pathology.
- Sehat** B, Tofigh A, Lin Y, Trocme E, Liljedahl U, Lagergren J, Larsson O (2010). SUMOylation mediates the nuclear translocation and signaling of the IGF-1 receptor, *Sci. Signal.* 3 ra10.
- Serini** G, Sigismund S, Lanzetti L (2012). Endocytosis and Exocytosis in Signal Transduction and in Cell Migration, Crosstalk and Integration of Membrane Trafficking Pathways, Dr. Roberto Weigert (Ed.), ISBN: 978-953-51-0515-2, InTech, Available from: <http://www.intechopen.com/books/crosstalk-andintegration-of-membrane-trafficking-pathways/endocytosis-and-exocytosis-in-signal-transduction-and-in-cellmigration>
- Shane** B (1989). Folylpolyglutamate synthesis and role in the regulation of one- carbon metabolism. *Vitam Horm.* 45: p. 263- 335.

Shane B (1995). Folate chemistry and metabolism. In Bailey, L.B. (ed.) Folate in Health and Disease. Marcel Dekker. New York, pp. 1 – 22.

Sharma SV, Lee DY, Li B, Quinlan MP, Takahashi F, Maheswaran S, McDermott U, Azizian N, Zou L, Fischbach MA, Wong KK, Brandstetter K, Wittner B, Ramaswamy S, Classon M, Settleman J (2010). A chromatin-mediated reversible drug-tolerant state in cancer cell subpopulations. *Cell*; 141:69-80.

Sheaff RJ, Groudine M, Gordon M, et al (1997). Cyclin E-cdk2 is a regulator of p27Kip1. *Genes Dev* 11:1464-1478

Sherr CJ (1994).: G1 phase progression: cycling on cue. *Cell* , 79:551– 555

Sherr CJ (1996). Cancer cell cycles. *Science* 274: 1672- 1677

Sherr CJ (1993). Mammalian G1 cyclins. *Cell* , 73:1059–1065

Sherr CJ, and Roberts JM (1995). Inhibitors of mammalian G1 cyclin- dependent kinases. *Genes Dev* 9: 1149- 1163

Sherr CJ, Roberts JM (1999). CDK inhibitors: Positive and negative regulators of G1-phase progression. *Genes Dev* 13:1501-1512

Simons K, Toomre D (2000) Lipid rafts and signal transduction. *Nat Rev Mol Cell Biol* 1: 31– 39.

Sinha RP, Ha¨der D-P (2002). UV-induced DNA damage and repair: A review. *Photochem*

Solomon MJ(1993). Activation of the various cyclin/cdk2 protein kinases. *Curr Opin Cell Biol*, 5: 180- 186

Sonoda Y, Matsumoto Y, Funakoshi M, Yamamoto D, Hanks SK, & Kasahara T (2000). Anti-apoptotic role of focal adhesion kinase (FAK) Induction of inhibitor-of-apoptosis proteins and apoptosis suppression by the overexpression of FAK in a human leukemic cell line, HL-60. *Journal of Biological Chemistry*, 275(21), 16309-16315.

Sperandio S, de Belle I, and Bredesen DE (2000). An alternative, non- apoptotic form of programmed cell death. *Proc Natl Acad Sci USA* 97, 14376-81.

Stokstad EL, Koch J (1967). Folic acid metabolism. *Physiol Rev*,47(1): p. 83- 116

Stover P, Schirch V (1993). *Trends Biochem. Sci* 18, 102- 106

Stover P, and Schirch V (1990) *J. Biol. Chem.* 265, 14227–14233

Suh-Lailam B, Juenke J, Thompson C, & Johnson-Davis KL (2013, October). Performance Characteristics of Three Assays for the Therapeutic Drug Monitoring of Methotrexate. In *THERAPEUTIC DRUG MONITORING* (Vol. 35, No. 5, pp. 720-720). 530 WALNUT ST, PHILADELPHIA, PA 19106-3621 USA: LIPPINCOTT WILLIAMS & WILKINS.

Thannickal VJ and Fanburg BL(2000). Reactive oxygen species in cell signaling. *Am J Physiol Lung Cell Mol Physiol* 279: 1005- 1028

Tozluog˘ lu M, Karaca E, Nussinov R, Halilog˘ lu T (2010). A Mechanistic View of the Role of E3 in Sumoylation. *PLoS Comput Biol* 6(8): e1000913. doi:10.1371/journal.pcbi.1000913

Tyrrell RM, & Pidoux M (1986). ENDOGENOUS GLUTATHIONE PROTECTS HUMAN SKIN FIBROBLASTS AGAINST THE CYTOTOXIC ACTION OF UVB, UVA AND NEAR-VISIBLE RADIATIONS. *Photochemistry and photobiology*, 44(5), 561-564.

Ullrich A, Gray A, Tam AW, Yang-Feng T, Tsubokawa M, Collins C, Henzel W, Le Bon T, Kathuria S, Chen E et al (1986). Insulin-like growth factor I receptor primary structure composition with insulin with insulin receptor suggests structural determinants that define functional specificity. *EMBO Journal* 5 2503–2512.

Vakifahmetoglu H, Olsson M, Orrenius S, Zhivotovsky B(2006). Functional connection between p53 and caspase-2 is essential for apoptosis induced by DNA damage. *Oncogene*;25:5683-92.

Valentinis B, Navarro M, Zanocco-Marani T, Edmonds P, McCormick J, Morrione A, Sacchi A, Romano G, Reiss K and Baserga R (2000). Insulin receptor substrate-1, p70S6K, and cell size in transformation and differentiation of hemopoietic cells. *Journal of Biological Chemistry* 27525451–25459.

Vandel L, Kouzarides T (1999). Residues phosphorylated by TFIIH are required for E2F-1 degradation during S-phase. *EMBO J* 18:4280-4291

Villanueva J, Vultur A, Lee JT, et al (2010). Acquired resistance to BRAF inhibitors mediated by a RAF Kinase switch in melanoma can be overcome by cotargeting MEK and IGF-1R/PI3K. *Cancer Cell* ;18: 683-695.

Vlach J, Hennecke S, Amati B (1997). Phosphorylation dependent degradation of the cyclin-dependent kinase inhibitor p27. *EMBO J* 16:5334-5344, 1997

Wagner C, Briggs WT, Cook RJ (1985). Inhibition of glycine N- methyltransferase activity by folate derivatives: implications for regulation of methyl group metabolism. *Biochem Biophys Res Commu*, 127(3): p. 746- 52.

Watkins DJ, Taberero J, Schmoll H, et al (2011). A randomized phase II/III study of the antibody MK-0646 (dalotuzumab) in combination with cetuximab (Cx) and irinotecan (Ir) in the treatment of chemorefractory metastatic colorectal cancer (mCRC) with wild-type (wt) KRAS status. *ASCO Proc* 3501.

Wei Q, Shen H, Wang LE, Duphorne CM, Pillow PC, Guo Z, ... & Spitz MR (2003). Association between low dietary folate intake and suboptimal cellular DNA repair capacity. *Cancer Epidemiology Biomarkers & Prevention*, 12(10), 963-969.

Weil M, Jacobson MD, Coles HS, Davies TJ, Gardner RL, Raff KD and Raff MC (1996). "Constitutive expression of the machinery for programmed cell death." *J Cell Biol* 133(5): 1053-9.

Weinberg RA (1995). The retinoblastoma protein and cell cycle control. *Cell* 81:323-330

Williams JD, & Jacobson MK (2010) Photobiological implications of folate depletion and repletion in cultured human keratinocytes. *Journal of Photochemistry and Photobiology B: Biology*, 99(1), 49-61.

Williamson P, et al. (2000). Phosphatidylserine exposure and phagocytosis of apoptotic cells. *Meth. Cell Biol.* 66,339-64.

Willis L(1931) Treatment of Pernicious Anaemia of Pregnancy and Tropical Anaemia with special Reference to yeast Extract as curative Agent. *British Journal of medicine*, 1: p. 1059 – 1064.

Wyllie AH (1980). Glucocorticoid-induced thymocyte apoptosis is associated with endogenous endonuclease activation. *Nature* 284, 555-6.

Xu M, Sheppard KA, Peng CY, et al (1994). Cyclin A/Cdk2 binds directly to E2F-1 and inhibits the DNA-binding activity of E2F-1/DP-1 by phosphorylation. *Mol Cell Biol* 14:8420-8431

Yakar S, Pennisi P, Wu Y, Zhao H, LeRoith D (2005). Clinical relevance of systemic and local IGF-I. *Endocr Dev* 9: 11-6.

Yamauchi A, Ichimiya T, Inoue K, Taguchi Y, Matsunaga N, Koyanagi S, ... & Ohdo S (2005). Cell-cycle-dependent pharmacology of methotrexate in HL-60. *Journal of pharmacological sciences*, 99(4), 335-341.

Yang AD, Fan F, Camp ER, van Buren G, Liu W, Somcio R, ... & Ellis LM (2006). Chronic oxaliplatin resistance induces epithelial-to-mesenchymal transition in colorectal cancer cell lines. *Clinical Cancer Research*, 12(14), 4147-4153.

Zirath H, Frenzel A, Oliynyk G, Segerström L, Westermark UK, Larsson K, ... & Henriksson MA (2013). MYC inhibition induces metabolic changes leading to accumulation of lipid droplets in tumor cells. *Proceedings of the National Academy of Sciences*, 110(25), 10258-10263.

Zou H, Li YC, Liu HS, Wang XD(1999). An APAF-1 center dot cytochrome c multimeric complex is a Functiona apoptosome that activates procaspase-9. *J Biol Chem*;274:11549-56.